UNIVERSITY OF STRATHCLYDE

THE STRATHCLYDE INSTITUTE OF PHARMACY AND BIOMEDICAL SCIENCES

EFFECTS OF OESTROGEN ON NEURAL STEM CELL SUCCESS IN A STROKE MODEL

Shalmali Patkar

A THESIS PRESENTED IN FULFILMENT OF THE REQUIREMENTS FOR THE DEGREE OF DOCTOR OF PHILOSOPHY

2010

COPYRIGHT STATEMENT

Signed: Date: 18th February 2011

ACKNOWLEDGMENTS

I would like to thank everybody who was important to the successful realisation of this thesis, as well as expressing my apology at first for not being able to mention personally one by one.

Firstly, I want to thank my supervisor Dr. Hilary Carswell. It has been an honour to be her first Ph.D. student here at SIPBS. She has taught me, both consciously and unconsciously, how good experimental science is done. I appreciate all her contributions of time, ideas and funding to make my Ph.D. experience productive and stimulating. Her support from the initial to the final level enabled me to develop an understanding of the subject and gain further interest. The joy and enthusiasm she has for her research was contagious and motivational for me, even during tough times in the Ph.D. pursuit. I am also thankful for the excellent example she has provided as a successful female scientist and working mother.

Secondly, Prof. Robin Plevin, my second supervisor (the so-so artist) with his truly scientist intuition has made him as a constant oasis of ideas and his passion in science which exceptionally inspires and enriches my growth as a student, a researcher and a scientist want to be. I am indebted to him more than he knows. Robin, I hope to keep up our collaboration in the future not only in science but also in art.

I would like to thank Dr. Rothwelle Tate for his advice and crucial contribution, his involvement has triggered my intellectual maturity in the molecular side of the project that I will benefit from, for a long time to come.

During this work I have collaborated with many colleagues for whom I have great regard, and I wish to extend my warmest thanks to all those. Especially to Katie Chapman, Ph.D. student of Dr. McColl, University of Manchester for her continuous support and advice while establishing the stroke model here in Strathclyde. Special thanks are due to Dr. Mike Modo from King's College London for providing the neural stem cells and his continuous constructive comments and support through this work. I must also acknowledge Dr. Dafe Uwanogho's efforts that went into generating the Dax1 knockdown and aromatase over-expression MHP36 lines without which this project wouldn't have attained its novelty. I also benefited by the outstanding support and advice time to time from Stephano Fumagilli from Mario-Negri Institute, Italy.

Special thanks to the University of Strathclyde for funding my studies and Strathclyde Institute of Pharmacy and Biomedical Sciences (SIPBS) who provided the support and equipment I have needed to produce and complete my thesis and. It is my pleasure to extend my thanks also to all members of the Integrative Mammalian Biology group at SIPBS. I would personally like to thank David Blatchford for his time and guidance devoted under the confocal microscope to

achieve the images. In addition, to the Biological Procedure Unit (BPU) staff members Stevie, Kevin and Lee for their constant help with taking care of animals and during the in vivo experiments. Special thanks are in order to Dr. David Young and Dr. Louise Kelly from the Department of Mathematics and Statistics at the University of Strathclyde who have advised me at a very short notice on using the appropriate statistical model for my behavioural study. Appreciation also goes out to Gillian and Selina from the IMB group at SIPBS for lending a hand at the behavioural testing.

The members of the Plevin & Paul group have contributed immensely to my personal and professional time at Strathclyde. The group has been a source of friendships as well as good advice and collaboration. Many thanks go in particular to my fellow brothers Sameer, Muhannad and Ahmed who have been there as my batch mates and gone through long hours in cell culture together. All the past and present group members that I have had the pleasure to work with or alongside of are Carly, Gary, Julianna, Katy, Margaret, Mary, Mashael, Rebecca and Yuen and of course the summer students who have come through the lab. I can't forget to thank all my 407 write-up roomies, Satirah, Gillian, Selina, Tamara, Jennifer and Ejaife for the endless discussions on practically anything from science to music, conferences to holidays, lab-duties to cooking delicious food. It is a pleasure to convey my gratitude to them all in my humble acknowledgment.

My time in Glasgow was made enjoyable in large part due to the many good friends that became a part of my life. I am grateful for time spent with flatmates and family who visited for the many adventurous and memorable trips and get-togethers all over the UK. Special thanks to Abhay and Diana for their hospitality and keeping calm, as flatmates, as I worked long hours in the lab and while I finished my thesis and for many other people with whom good times were spent.

Lastly and most importantly, where would I be without my family? I owe my loving thanks to my parents for their inseparable support and prayers. My Father, "Pappi", in the first place, is the person showing me the joy of intellectual pursuit ever since I was a child. My Mother, "Maa", is the one who sincerely raised me with her caring, gentle and unconditional love. Sarthak thanks for being a supportive and kind brother.

Words fail me to express my appreciation to my loving, sympathetic, encouraging and patient friend and husband Aditya during the stages of my Ph.D. Thank you dearest! I would also like to extend my thanks to my new family Daddy, Aai, Daa and Mahua for accepting me as a member of the family, warmly.

Thank you!!!

PUBLICATIONS

Oral and Poster presentations

Patkar S., Tate R., Modo M., Plevin R., Carswell H.V.O. (2010) Conditionally Immortalised Neural Stem Cells Improve Behavioural Recovery After Transient Focal Cerebral Ischaemia In Mice. VIth International Symposium On Neuroprotection And Neurorepair, Germany, PP III-8.

Patkar S., Tate R., Modo M., Uwanogho D., Plevin R., Carswell H.V.O. (2010) Stem Cell Based Therapy For Stroke: Potential For Oestrogen. Scottish Neuroscience Group (SNG) Meeting, O-6.

Patkar S., Tate R., Modo M., Plevin R., Carswell H.V.O. (2009) Characterisation Of Neural Stem Cells For Oestrogen: Stem Cell Based Therapy For Stroke. SNG Meeting, St. Andrews, Poster presentation.

Patkar S., Tate R., Modo M., Plevin R., Carswell H.V.O. (2009) Characterisation Of Neural Stem Cells For Oestrogen: Stem Cell Based Therapy For Stroke. The XXIVth International Symposium On Cerebral Blood Flow, Metabolism, & Function, And The IXth International Conference On Quantification Of Brain Function With PET, *J Cereb Blood Flow Metab* 29: S544-S552, P-223.

Patkar S., Tate R., Modo M., Plevin R., Carswell H.V.O. (2008) Stem Cell Based Therapy For Promoting Brain Repair After Stroke: Potential Of Oestrogen. SNG Meeting, Glasgow, Poster Presentation.

Research papers

S. Patkar, T. D. Farr, E. Cooper, F. J. Dowell, H. V. O. Carswell (2010), Differential Vasoactive Effects Of Oestrogen, Oestrogen Receptor Agonists And Selective Oestrogen Receptor Modulators In Rat Middle Cerebral Artery. *Neuroscience Research*. (Submitted, under review)

S. Patkar, R. Tate, M. Modo, R. Plevin, H. V. O. Carswell (2010), Conditionally Immortalised Neural Stem Cells Improves Behavioural Recovery In Transient Model Of Ischaemia In Mice. *Neuroscience*. (Submitted, under review)

S. Patkar, R. Tate, D. Uwanogho, M. Modo, R. Plevin, H. V. O. Carswell (2010), Neural Stem Cells Genetically Modified To Over-Express Oestrogen Enhance Neuronal Differentiation And Restore Functional Deficits In A Mouse Stroke Model. (In preparation to be submitted to PNAS)

A B S T R A C T

Stroke is a problem for the ageing population. The ageing population is increasing but there is no licensed therapy for chronic stages of the disease. Cell replacement has enormous potential to restore neurological function after stroke. Since evidence suggests that oestrogen may improve integration of neural stem cells *in vivo*. The study tested the hypothesis that transplantation of murine Maudsley hippocampal stem cell line clone 36 (MHP36) over-expressing oestrogen (Dax-1KD-MHP36), into mouse brain after a transient middle cerebral artery occlusion (MCAO), would promote functional recovery and improve integration and differentiation *in vivo*. Before the hypothesis could be addressed, the MHP36 cells were fully characterised for oestrogen, the *in vivo* murine model of stroke was established and since this is the first time the cells have been used in murine stroke model, the efficacy of these cells to restore functional recovery was established.

The expression of the enzyme that synthesises oestrogen (aromatase), oestrogen receptors (ERα, ERβ) and GPR30 protein in the MHP36 stem cells was investigated by immunofluorescence, Western blotting and reverse transcriptase PCR (RT-PCR). A lentiviral vector was used to silence dosage-sensitive sex reversal adrenal hypoplasia congenita region on X-chromosome gene 1 (Dax-1), to over-express oestrogen in MHP36 cells (Dax-1KD-MHP36). Adult C57BL/6 (male, 12-14 week old, weighing between 25 and 30 g) mice underwent transient MCAO and two days post-MCAO vehicle, oestradiol (E2), MHP36, Dax-1KD-MHP36 and MHP36 cells suspended in oestradiol (MHP36+E2) were transplanted into the brain ipsilateral to the injury. Sensorimotor function was assessed using cylinder and ladder rung tests at pre-MCAO and 2, 7, 14 and 28 days post-MCAO. Mice were perfusion fixed at 28 days post-MCAO for measurement of lesion (tissue loss) and histology.

Undifferentiated MHP36 cells were shown to express aromatase, ERβ and GPR30. ERα was absent in the MHP36 cells when compared to positive control (breast cancer) MCF-7 cells. Moreover, the genetically modified Dax-1KD-MHP36 cells were successfully characterised for over-expressing oestrogen with significantly reduced Dax-1, increased aromatase and oestrogen production when compared to MHP36 cells *in vitro*. Transplantation of Dax-1KD-MHP36

completely restored the sensorimotor function to pre-MCAO scores in both the ladder rung and cylinder test 28 days after transplantation post-MCAO. Function was not completely restored in any of the other treatment groups to pre-MCAO baseline scores and MHP36 and MHP36+E2 actually induced a significant bias towards the impaired limb in the cylinder test. In the ladder rung test, significant acceleration in recovery was observed by 14 days in the Dax-1KD-MHP36 group but not in any of the other groups. A significant increase in MAP-2 positive neurons and synaptophysin was observed in Dax-1KD-MHP36 when compared to vehicle. Lesion volume was significantly reduced only in Dax-1KD-MHP36 group when compared to vehicle.

In conclusion, the MHP36 cells express ERβ, GPR30 and aromatase, but do not express ERα. Aromatase and oestrogen production were significantly increased after genetic modification of the MHP36 cells. *In vivo* Dax-1KD-MHP36 cells completely restored functional recovery, which was not observed in any other group. This may be mediated via reduced tissue loss, improved synaptic plasticity and/or improved neuronal differentiation. Our approach therefore has great potential to improve the clinical application of cell replacement therapy, as well as gene therapy in patients suffering from stroke.

ABBREVIATIONS

17β-oestradiol	E2
2', 3'-Cyclic Nucleotide 3'-Phosphodiesterase	CNPase
3,3' Diaminobenzidine	DAB
α-amino-3-hydroxyl-5-methyl-4-isoxazole-propionate	AMPA
Adenylyl cyclase	AC
Aromatase knock-out	ArKO
Basic fibroblast growth factor	bFGF
Basilar artery	BA
Blood brain barrier	BBB
Bone marrow stromal cells	BMSCs
Bovine serum albumin	BSA
Brain derived neurotrophic factor	BDNF
Cerebral blood flow	CBF
Cerebrospinal fluid	CSF
c-Jun N-terminal protein kinase activation	JNK
Common carotid artery	CCA
Common carotid artery occlusion	CCAO
Complementary DNA	cDNA
Computational tomography	CT
Contralateral	C
Cyclic-AMP-responsive-element-binding protein	CREB
Dax-1knock-down Maudsley hippocampal stem cell lines clone 36	Dax-1KD-MHP36
DNA-binding domain	DBD
Dosage-sensitive sex reversal adrenal hypoplasia congenita region on X-chromosome gene 1	Dax-1
Embryonic stage 14	E14
Embryonic stem cells	ES cells
Endothelial progenitor cells	EPCs
Enzyme-linked immunosorbent assay	ELISA
Epidermal growth factor	EGF
Epidermal growth factor	EGF
External carotid artery	ECA
Extracellular-signal-regulated kinase 1/2	Erk1/2
Fibroblast growth factor-2	FGF-2
Fluorescein isothiocyanate	FITC
G protein-coupled receptor 30	GPR30
Glial fibrillary acidic protein	GFAP
Glycogen synthase kinase-3β	GSK-3β

Hanks Balanced salt solution	HBSS
Hemisphere volume	HV
Hormone-replacement therapy	HRT
Human umbilical cord blood cells	HUCBCs
Human umbilical cord blood cell neural progenitors	HUCBCNP
Hypoxia inducible factor-1α subunit	HIF-1α
Inducible nitric oxide synthases	iNOS
Insulin-like growth factor 1	IGF-1
Interferon- gamma	IFNγ
Internal carotid artery	ICA
Intracerebral haemorrhage	ICH
Intraluminal thread	ILT
Ionized calcium binding adaptor molecule 1	IBA-1
Ipsilateral	I
Large vessel disease	LVD
Lesion volume	LV
Ligand binding domain	LBD
Krueppel-like factor 4	Klf4
Magnetic resonance imaging	MRI
Maudsley hippocampal stem cell lines clone 36	MHP36
Mesenchymal stem cells	MSCs
Microtubule-associated protein 2	MAP-2
Middle cerebral artery occlusion	MCAO
Middle cerebral artery	MCA
Mitogen-activated protein kinase	MAPK
Multiple Outcomes of Raloxifene Evaluation	MORE
Neural progenitor cells	NPCs
Neural stem cells	NSCs
N-methyl-D-aspartic acid	NMDA
Octamer-binding transcription factor 4	Oct4
Oestrogen receptor alpha	ERα
Oestrogen receptor beta	ERβ
Oestrogen receptors	ERs
Oestrogen response element	ERE
Open reading frame	ORF
Ovariectomised	OVX
Oxygen-glucose deprivation	OGD
Phosphate buffered saline	PBS
Phosphatidylinositol 3-kinase	PI3K
Protein kinase A	PKA
Protein kinase C	PKC

Rapidly accelerated fibrosarcoma	Raf
Rat sarcoma	Ras
Recombinant tissue plasminogen activator	rtPA
Reverse transcriptase polymerase chain reaction	RT-PCR
Selective oestrogen receptor modulator	SERMs
Steroid receptor co-activator 1	SRC-1
SRY (sex determining region Y)-box 2	Sox2
Simian virus 40	SV40
Small vessel disease	SVD
Spontaneously hypertensive stroke prone	SHRSP
Standard mean error	SEM
Steroidogenic factor-1	SF-1
Stroke Therapy Academic Industry Roundtable	STAIR
Sub ventricular zone	SVZ
Subarachnoid haemorrhage	SAH
Sub-granular zone	SGZ
Synaptophysin	Syn
Tissue plasminogen activator	tPA
Transient ischaemic attack	TIA
Tumour antigen	TAg
Vascular endothelial growth factor	VEGF
Wild-type	WT
Wilms' tumor suppressor gene	WT1
Women's Estrogen for Stroke Trial	WEST
Women's Health Initiative	WHI

Table of Content

Table of Figures

CHAPTER 1

GENERAL INTRODUCTION

1.1 | Introduction to Stroke

Stroke, now also called brain attack (an analogy with heart attack (myocardial infarction)), is the clinical designation for a rapidly developing loss of brain function due to an interruption in the blood supply to a part of the brain (Kumar et al., 2005). This interruption in the blood supply to the brain, results in a depletion of oxygen and glucose in the affected area, immediately reducing or abolishing neuronal function (Kumar et al., 2005).

Stroke is the second leading cause of death after ischaemic heart disease (Donnan et al., 2008) and in 2004 overall death rate for stroke was 50 % in industrialized countries. The number of patients is predicted to rise due to the rapidly ageing population since almost 90 % of the deaths attributed to stroke are among people aged over 65 years (Bonita, 1992). Stroke is also the major cause of severe long-term disability (Lloyd-Jones et al., 2010) and has potentially enormous emotional and socioeconomic consequences for patients and their families. According to World Health Organisation estimates, 15 million people each year suffer from stroke and 5 million are left permanently disabled (Lloyd-Jones et al., 2010).

Men's stroke incidence rates are greater than women's at younger ages but not at older ages. The male/female incidence is 1.25 at ages 55-64 years; 1.50 for ages 65-74 years; 1.07 at 75-84 years and 0.76 at 85 years and older (Adams et al., 2007). Worldwide, stroke consumes about 2-4% of total health-care costs, and in industrialised countries stroke accounts for more than 4% of direct

health-care costs. The total costs to society are variously estimated at £8.9 billion in the UK at 2009 prices (Saka et al., 2009), AUS$ 2.14 billion in Australia at 2009 prices (Cadilhac et al., 2009) and US$ 63·0 billion in USA at 2007 prices (Adams et al., 2007) which represents about US$ 100 per head of population per year. Nevertheless, the proportion of research funds directed towards stroke remains disproportionately and disappointingly low (Rothwell, 2001).

1.1.1 | Subtypes and Pathophysiology of Stroke

Strokes are either ischaemic or haemorrhagic. In the UK, approximately 85% of strokes are due to cerebral ischaemia, the remainder due to intracerebral and subarachnoid haemorrhage (Bamford et al., 1990, Thrift et al., 2001). Because the management of these subtypes is so different, the clinical distinction between the subtypes is one of the most important and urgent steps in stroke management. This distinction has been revolutionised by the introduction of computational tomography (CT) and Magnetic resonance Imaging (MRI) (Fiebach et al., 2002). The aetiology of a stroke, when it can be determined, affects treatment decisions, including therapy for secondary stroke prevention. For example, oral anticoagulation is a primary recommended treatment for cardioembolism, antiplatelet therapy is recommended for non-cardioembolic ischaemic stroke and transient ischaemic attack (TIA) and carotid endarterectomy is recommended for recent TIA or minor stroke occurring with severe carotid artery stenosis (Fisher, 2008).

Unlike brain haemorrhage, which originates from blood collecting in the extra vascular space, ischaemic stroke involves the occlusion of blood vessels. In the core zone of ischaemia, where blood flow is within a range, or lower than a threshold, irreversible neuronal damage can occur within minutes (Kaufmann et al., 1999, Fisher, 2008). In contrast in the ischaemic penumbra

neurons can remain viable for several hours. Rapid restoration of reperfusion in this region can save penumbral cells (Fisher, 2008, van der Worp and van Gijn, 2007).

1.1.1.1 | Ischaemic Subtypes

Ischaemic strokes occur in two ways embolic and thrombotic stroke and investigators have used several systems to classify them (Fisher, 2008, Onal and Fisher, 1997). Systems based primarily on the clinical features of the stroke syndrome (most commonly the Oxfordshire Community Stroke Project (OCSP) classification) are usually refined by the results of brain imaging (Bamford et al., 1991). Other studies have used clinical and imaging features of the presenting stroke but also included risk factors in their ischaemic stroke subtype definitions (most commonly the Trial of Org 10172 in Acute Stroke Treatment (TOAST) classification) (Adams et al., 1993). A few studies relied on imaging findings alone to classify ischaemic stroke subtypes regardless of the patients' symptoms (Jackson and Sudlow, 2005).

Embolic stroke results from blood clots that develop in the heart or elsewhere in the body. Embolic sources include fat emboli often produced after long bone fractures for example and particulate emboli often found after intravenous drug abuse. The principal causes of cardioembolism are atrial fibrillation, acute myocardial infarction (MI), valve disease, cardiomyopathy, and endocarditis (Brickner, 1996).

In the second type of ischaemic stroke, blood flow is impaired because of a blockage to one or more of the arteries supplying blood to the brain. The process leading to this blockage is known as thrombosis and strokes caused in this way are called thrombotic strokes. Two types of thrombosis can cause stroke: large vessel disease (LVD) and small vessel disease (or lacunar infarction) (SVD). Thrombotic stroke occurs most often in the large arteries, so large vessel

disease is the most common and best understood type of thrombotic stroke. In LVD mainly slowly developing atherosclerosis narrows and obstructs blood flow making major blood vessels in the body thick and stiff (**Figure 1.1**) (Adams et al., 1993). Other LVD strokes are caused by occlusion of a main artery or stenosis, which leads to ischaemic injury at the farthest branches of the artery (Bogousslavsky and Regli, 1986).

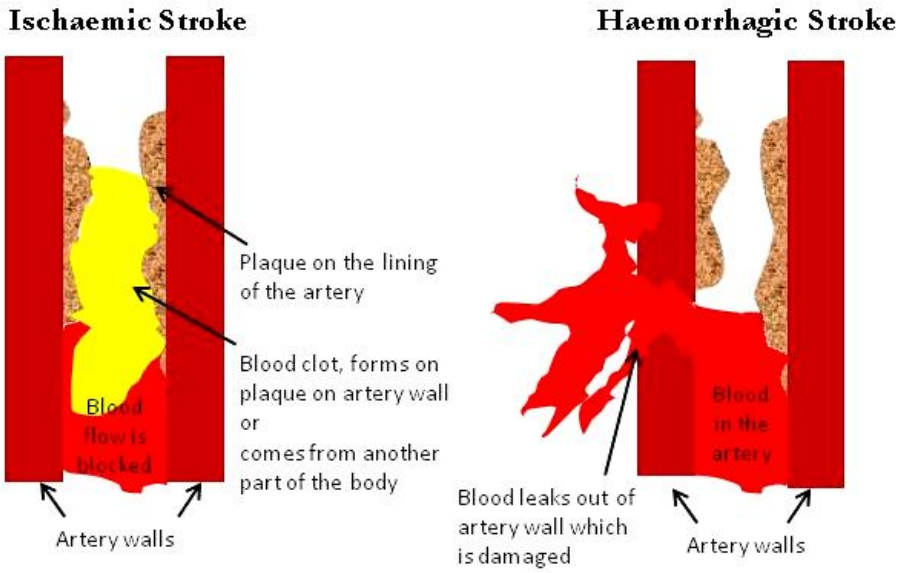

Figure 1.1: Illustration of different types of stroke.

Ischaemic stroke (thrombotic) which occurs when an artery to the brain is blocked due to plaque and intracerebral haemorrhagic stroke which is caused when a diseased vessel ruptures due to sudden increased pressure in the brain (modified from Adams et al., 1993).

SVD typically involve small areas of infarction and can occur when disease develops in the smaller penetrating arteries - usually lipohyalinosis, a degeneration that forms glassy substances which block arteries (Jackson and Sudlow, 2005, Kolominsky-Rabas et al., 2001).

1.1.1.2 | Haemorrhagic Subtypes

Intracerebral Haemorrhage (ICH) is the presence of blood within the main cellular mass of the brain and accounts for ~10% of all strokes (Donnan et al., 2008). The incidence of ICH due to the use of oral anticoagulants has increased as these therapies have become more prevalent (Flaherty et al., 2007). In elderly individuals, the deposition of amyloid protein into blood vessel walls may cause haemorrhage (Thanvi and Robinson, 2006). In most cases of ICH however, chronic hypertension leads to the degeneration of smaller brain arteries and micro aneurysms in which bleeding originates from tears at the bifurcation between the vessels (**Figure 1.1**).

Subarachnoid haemorrhage (SAH) is the second haemorrhagic subtype and accounts for 5% of all strokes (Donnan et al., 2008). SAH is most prevalent among middle-aged women and has a high mortality rate (Suarez et al., 2006). SAH usually results from the rupture of a cerebral aneurysm at a vessel bifurcation (Suarez et al., 2006). Vasospasm of brain arteries is a common complication of SAH and can lead to a subsequent ischaemic brain injury (Fisher, 2008, Suarez et al., 2006).

1.1.2 | Treatments available for Ischaemic Stroke

Stroke caused by a blood clot blocking the artery can be treated by re-establishing blood flow in the affected area by dissolution of the blockage using thrombolytic drugs such as recombinant tissue-plasminogen activator (rt-PA). However, the use of rt-PA has also been shown to increase the risk of haemorrhagic transformation, limiting its acceptability (Wang et al., 2004). Earlier administration of rt-PA was restricted to within 3 hours of stroke-onset but now this window has been increased to about 4 hours (Ralea et al., 2009). This is a barrier to stroke therapy as many patients are presented more than 3 hours after symptom-onset (Alberts, 1993). Early recognition

of the signs of stroke is generally regarded as important and only detailed physical examination and medical imaging like CT and MRI techniques provide information on the presence, type, and extent of stroke (Ringleb et al., 2002). A patient with ischaemic stroke is given an antiplatelet like aspirin, clopidogrel or dipyradimole, or an anticoagulant (for embolitic therapy) like warfarin. The common side-effect caused by warfarin is haemorrhage and less commonly necrosis or purple toe syndrome. The risks of bleeding are increased when warfarin is combined with clopidogrel or aspirin (Delaney et al., 2007). Hemorrhagic stroke must be ruled out with medical imaging, since the above mentioned therapy would be harmful to patients with this type of stroke.

The other approach to reduce stroke damage has been the development of neuroprotective agents that interfere with the biochemical cascade of events that lead to cell death after stroke (Dirnagl et al., 1999). The assumption is that the core area of injury, where the ischaemia is most severe, will not be salvaged but that the area that surrounds the core (the penumbra), despite being compromised with low blood flow, can be saved under appropriate conditions. However, although over 37 potential neuroprotective agents have been studied in over 114 clinical trials, none is clinically efficacious or in use in the Western world (Kidwell et al., 2001).

In the absence of any other pharmacological intervention, the patient is reliant on medical care. Studies have shown that patients treated in hospitals with a dedicated stroke team or a stroke unit and a specialized care program for stroke patients have improved odds of recovery but this kind of treatment is difficult to achieve, especially in developing nations where issues of stroke infrastructure and costs obstruct efforts to set up efficient stroke care programs (Hussain and Shuaib, 2007). Stroke rehabilitation is another common treatment used for patients to help them return to normal life as much as possible by regaining and relearning the skills of everyday

living. It also aims to help the patient understand and adapt to difficulties, prevent secondary complications and educate family members to play a supporting role. Rehabilitation can last anywhere from a few days to months.

Typical research to develop therapies for stroke seek, (1) to interrupt the cascade of events that leads to cell death (Dirnagl et al., 1999) and (2) to harness the substantial intracerebral reorganization after stroke to promote functional recovery.

1.1.3 | Pathophysiology of ischaemic stroke

The characteristics of the brain injury depend on the severity and duration of the cerebral blood flow (CBF) reduction. In animal models, blood flow is most crucially reduced in the central region of the brain (infarct core) and is graded centrifugally from the core normally supplied by the occluded artery, due to residual perfusion from collateral blood vessels (ischaemic penumbra). The ischaemic penumbra is non-functional, however, retains structural integrity in contrast to the core which is structurally and functionally dead. Evidence indicates that, if the blood flow is not restored within hours, the penumbral region becomes part of the core region (Durukan and Tatlisumak, 2007, Richard Green et al., 2003). The process of cellular injury and death are remarkably different in these two regions. There appears to be two major modes of cell death that participate in ischaemic cell death: necrosis and apoptosis. While necrosis is more dominant in the core tissue, penumbral cells die by means of either mode, with apoptosis being more common for cells further away from the core. Within minutes of vascular occlusion and CBF reduction a complex sequence of pathophysiological events (ischaemic cascade) occurs (**Figure 1.2**) this is underpinned by the various events which are illustrated in **Figure 1.3**. Ischaemic brain injury may last hours or even days which leads to activation of the various components of the ischaemic cascade which include energy failure, elevation of intracellular

Ca^{2+} level, excitotoxicity, free radical formation, inflammation, apoptosis and BBB disruption (Smith, 2004).

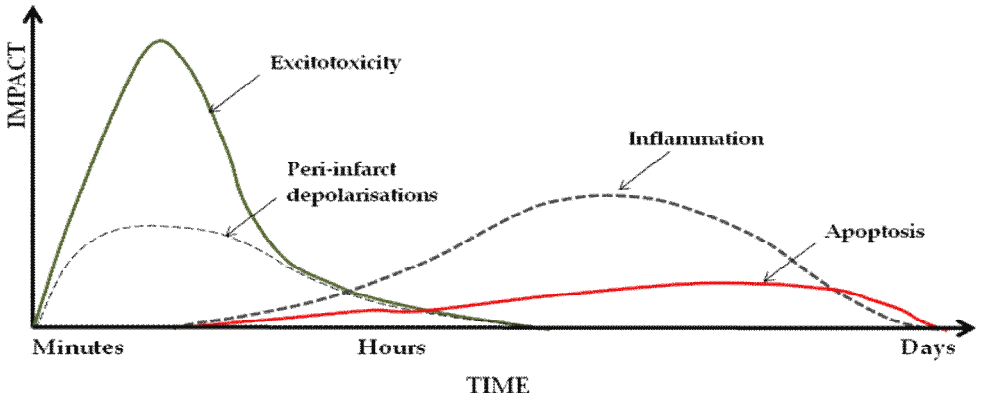

Figure 1.2: Putative cascade of damaging events after focal cerebral ischaemia.

Within minutes after the onset of the focal perfusion deficit, excitotoxic mechanisms can damage neurones and glia. In addition, excitotoxicity triggers a number of events that contribute to the demise of the tissue such as peri-infarct depolarisation and more-delayed mechanisms of inflammation and programmed cell death (modified Dirnagl et al., 1999).

1.1.3.1 | Energy failure

Brain is almost exclusively dependent on the continuous and steady flow of glucose and oxygen supplied through blood, which undergoes oxidative phosphorylation for energy production because it has no stores of energy and deprivation occurs in minutes only. The first consequence of CBF reduction is the depletion of oxygen and glucose that causes accumulation of lactic acid via anaerobic glycolysis. Acidosis may enhance free radical formation, interfering with intracellular protein synthesis that worsens ischaemic injury, yet the deleterious effects of acidosis are still unknown (Durukan and Tatlisumak, 2007, Mergenthaler et al., 2004) (**Figure 1.5**). Secondly, energy failure leads to disturbance of the Na^+/K^+-ATPase, in addition Na^+/Ca^{2+} transporter is reversed. Furthermore, the subsequent ion imbalance leads to elevation of

intracellular Na^+, Ca^{2+}, Cl^- and elevation of extracellular K^+ levels which causes cytotoxic oedema and leads to events triggered by excess of intracellular Ca^{2+} (**Figure 1.3**).

1.1.3.2 | Elevation of intracellular Ca^{2+} level

In neurons Ca^{2+} enters via voltage gated Ca^{2+} channels, N-methyl-D-aspartate (NMDA) and α-amino-3-hydroxy-5-methyl-4-isoxazole propionic acid (AMPA)-type glutamate receptor 2 operated channels, store-operated channels and the reverse operation of the Na^+/Ca^{2+} exchanger. Additional release from the organelles such as mitochondria, synaptic vesicles, endoplasmic reticulum and from Ca^{2+} binding proteins may further increase intracellular Ca^{2+} level (Dirnagl et al., 1999).

Calcium plays a unique role on the ischaemic pathophysiology (**Figure 1.3**) since it causes several damaging events by over activation of a variety of Ca^{2+} dependent enzymes, including kinases, phosphatases, cyclooxygenase, calcium dependent nitric oxide synthase and various proteases and endonucleases (**Figure 1.3**). As a result of formation of cytotoxic products such as free radicals, irreversible mitochondrial damage and inflammation, both necrotic and programmed cell death are triggered by excess of intracellular Ca^{2+} (Harris et al., 1981).

1.1.3.3 | Excitotoxicity

Energy depletion results in membrane potential loss and consequently neurons and glia are depolarized (Dirnagl et al., 1999). After depolarization, excitotoxic amino acids, especially glutamate, are released from the presynaptic neuron into the extracellular compartment in large amounts. Besides direct neurotoxicity of glutamate on neurons, the activation of glutamate receptors leads to a further increase of the intracellular Ca^{2+}, Na^+, and Cl^- levels; thus increasing the amount of the cytotoxic oedema and toxic events following elevation of intracellular Ca^{2+}.

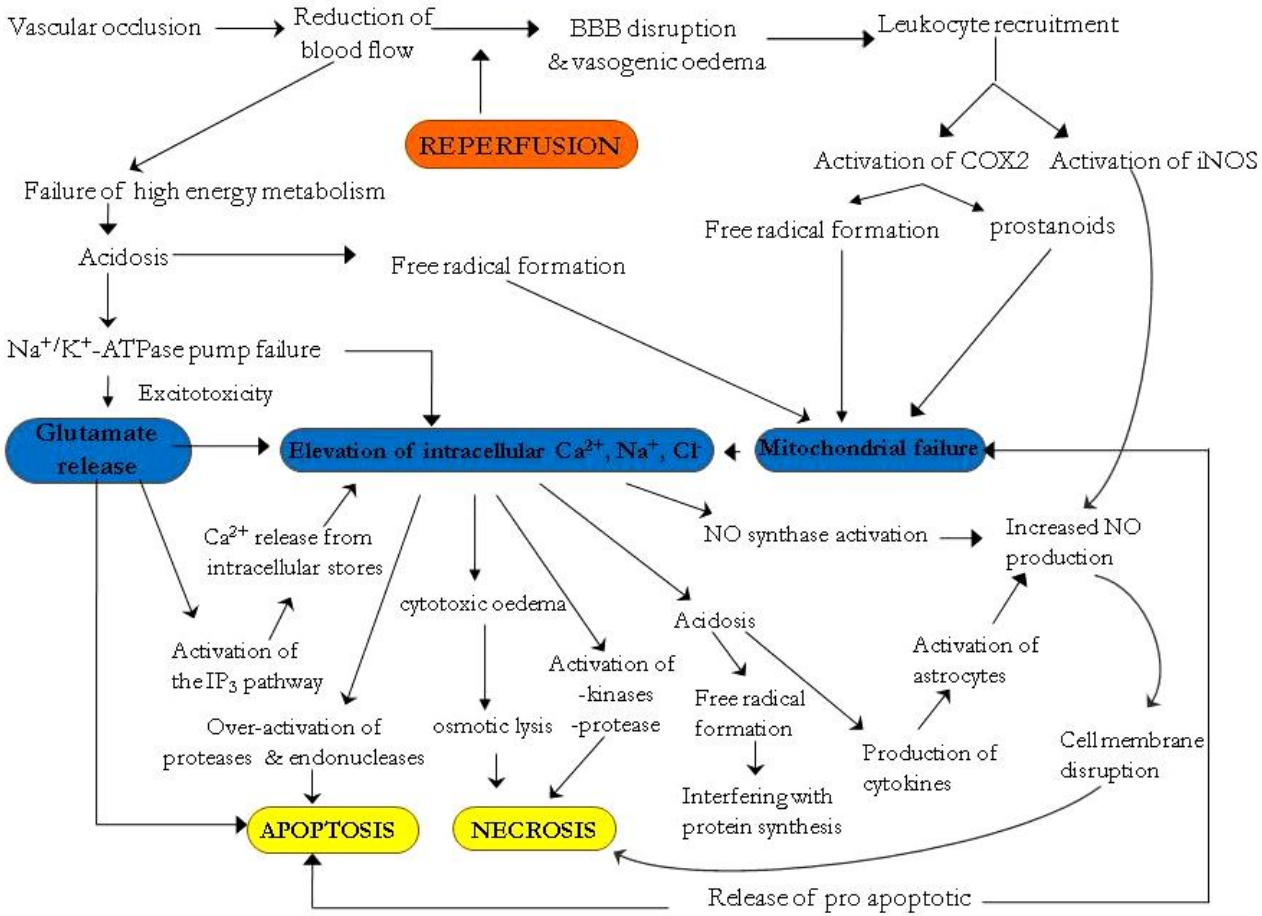

Figure 1.3: Schematic representation of major events that occur following cerebral ischaemia

ATP=Adenosine triphosphate, NO= Nitric Oxide, iNOS= induced nitric oxide synthase, COX2= Cyclooxygenase 2; adapted from Durukan et al., 2007.

These excitotoxic events can cause necrosis but can also initiate molecular events that lead to apoptosis (Dirnagl et al., 1999) (**Figure 1.3**).

The major excitatory transmitter, glutamate, is particularly toxic when levels are not controlled. Glutamate binds to metabotropic (Schoepp and Conn, 1993) or ionotropic receptors (Wisden and Seeburg, 1993). There are two types of ionotropic ligand binding glutamate receptors according to their sensitivity to agonists: NMDA and AMPA/kainic acid (KA) (Sved et al., 2002). Only NMDA binding to glutamate receptors and AMPA containing a glutamate receptor subunit 2 (GluR2) can mediate activation by increasing calcium permeability. However, activation of both receptors leads to an increase in sodium and potassium permeability and the resulting depolarisation can activate voltage-sensitive calcium channels (Morley et al., 1994) (refer to **section1.1.3.2**). Variations in NMDA receptor subunit composition also affect tissue outcome. Knockout mice deficient in the NMDA receptor 2A subunit show reduced cortical infarction after focal cerebral ischaemia compared to wildtype mice (Morikawa et al., 1998). Activation of metabotropic glutamate receptors may also contribute to the rise in intracellular calcium levels in ischaemia as a result of the mobilisation of calcium from intracellular stores (Morley et al., 1994).

1.1.3.4 | Formation of free radicals

As a consequence of reperfusion, oxygen radicals are produced during enzymatic conversions, such as the cyclooxygenase-dependent conversion of arachidonic acid to prostanoids. It is important to note that cytosolic phospholipase A_2 (PLA_2) is phosphorylated and liberates arachidonic acid in presence of Ca^{2+}/calmodulin dependent kinase (Muthalif et al., 2002). Free radicals are also generated during the inflammatory response after ischaemia. Furthermore, formation of mitochondrial permeability occurs under ischaemic conditions and leads to a burst

of free oxygen radicals and the release of proapoptotic molecules (Mergenthaler et al., 2004). Reactive oxygen species react irreversibly with several cellular constituents and can damage virtually any cellular component. Free radicals can cause lipid peroxidation, imbalance of ions, disruption of cell signalling, gene expression and membranes (Dirnagl et al., 1999). Free radicals thus serve as important signalling molecules that trigger inflammation and apoptosis.

1.1.3.5 | Inflammation

Within minutes of occlusion, there occurs upregulation of proinflammatory genes which produce mediators of inflammation such as tumour necrosis factor α and interleukin-1β. Neutrophils are the first inflammatory cells to arrive to the ischaemic tissue as early as within hours after reperfusion. After the expression of adhesion molecules at the vascular endothelium, neutrophils migrate into the brain tissue and release toxic substances such as reactive oxygen species and proteases. Thus, the presence of activated systemic neutrophils increases the potential for tissue injury during reperfusion after ischaemic stroke (Morrison et al., 2010). Neutrophils are followed by macrophages and monocytes that arrive within few days (Emerich et al., 2002). Chemokines (for example, interleukin-8 (Morganti-Kossman et al., 1997)) are produced in the injured brain and guide the migration of the inflammatory cells toward their target of damaged tissue (Barreiro et al., 2010). The resident macrophages of the CNS, microglia are also involved in the inflammatory response. Microglial response to injury suggests that these cells have the potential to act as diagnostic markers of disease onset or progression and could contribute to the outcome of neurodegenerative diseases (Yenari et al., 2010). Furthermore, the presence of activated microglia long after acute injury and in chronic disease suggests that these cells have an innate immune response to tissue injury and degeneration. This innate immune response includes release of reactive oxygen species, cytokines, and proteases (Perry et al., 2010).

However, the innate immune response can have beneficial as well deleterious effects on outcome after stoke, and a challenge will be to find ways to selectively suppress the deleterious effects of microglial activation after stroke without compromising neurovascular repair and remodelling (Perry et al., 2010).

1.1.3.6 | Apoptosis

Apoptosis is triggered by a number of processes, including excitotoxicity, free-radical formation, mitochondrial and DNA damage, cytochrome c release from mitochondria and inflammation. Apoptosis occurs after milder ischaemic injury, particularly within the ischaemic penumbra. It is an energy-consuming process, so reperfusion could potentiate apoptosis by restoring cellular energy (**Figure 1.3**). Following ischaemia, caspase activation occurs in response to proapoptotic signals such as upregulation of Bax and activation of death receptor family and downregulation of Bcl-2. Activated caspases are protein-cleaving enzymes that lead to characteristic DNA damage and cleavage of structural proteins which are essential for the integrity of the cell which leads to cell membrane damage (Mergenthaler et al., 2004). Apoptotic cells are rapidly removed by phagocytosis without eliciting an inflammatory reaction. Apoptotic cell morphology differs greatly from necrotic cell morphology. The former is characterized by a number of morphological features: shrinkage of the cytoplasm, condensation of chromatin and fragmentation of the cell. The necrotic cells become oedematous and lose their cellular architecture by cytoskeletal breakdown (Dirnagl et al., 1999, Love, 2003).

1.1.3.7 | BBB disruption

Damage of the vascular endothelium, toxic damage by inflammatory molecules and free radicals and especially destruction of the basal lamina by matrix metalloproteinases are potential causes

of BBB disruption which leads to vasogenic oedema and presumably haemorrhagic complications after stroke (Unterberg et al., 2004) (**Figure 1.3**). Brain oedema exacerbates the ischaemic process by its volumetric effect causing rise of intracranial pressure and dislocation of parts of the brain. BBB disruption continues for several days, even weeks without reaching its normal functioning and configuration. The degree of brain swelling is proportional to the size of the infarct. Transient ischaemia followed by reperfusion seems to exacerbate infarction (due to leukocyte recruitment (as discussed above)) mainly due to additional BBB damage which occurs earlier than in permanent ischaemia (no complete reperfusion) (Belayev et al., 1996).

In conclusion, as discussed earlier (**section 1.1.2**), due to their mechanism of action most cerebroprotective drug treatments must be given within a short time frame. Although rehabilitation treatment is prolonged, with residual disabilities not undergoing appreciable reduction after 3- 6 months, it is crucial to develop new alternative therapeutic strategies with less time constraints (Dirnagl et al., 1999). Moreover, the ability to model cerebral ischaemia in small animals serves as an indispensable tool in the stroke research field and is essential prior to launching any clinical trials.

1.1.4 | Models of experimental ischaemic stroke

Cerebral ischaemia comes in many forms, depending on the kind and severity of circulatory impairment as indicated in **section 1.1.1**. To cope with this variability many experimental models have been established in which blood flow is acutely or slowly, completely or incompletely, focally or globally, permanently or transiently interrupted. Successful translation of experimental findings can only be expected if the pathophysiology of the model replicates the essential criteria of the clinical situation (Perel et al., 2007). If not, injury and treatment concepts

are generated which are valid for the model but not for the disease, which perhaps explains why so many clinical trials have failed in the past (Hossmann, 2008).

To facilitate high throughput investigations of molecular injury pathways of brain ischaemia, *in vitro* models have found increasing application over the past years. In these models primary neuronal cultures, organotypic cultures are incubated in deoxygenated, glucose-free medium in order to mimic the interruption of the supply of oxygen and nutrients to brain parenchyma. All these models share several major disadvantages. First, these preparations are mostly derived from pups and not from adult brains; the results obtained have less in common with the *in vivo* condition of adult brain ischaemia and should be interpreted with caution (Hossmann, 2008). Secondly, *in vitro* preparations require incubation of culture media which differ substantially from the normal extracellular environment. Additionally, the preparation of the slice is associated not only with severe tissue trauma but also with a period of circulatory arrest before the slice is brought into the incubation medium. The control setting of such preparations signifies a post-traumatic, post-ischaemic recovery state which may be basically different from the intact brain (Widmann et al., 1991). Finally *in vitro* models, such as cells or whole tissue explants, can never show neurological deficits, nor do they have complete vasculature; an essential feature for studying the abnormal perfusion that characterises ischaemia (Hossmann, 2008). Hence, it is essential that *in vivo* animal models are also used to provide a living experimental system that contains neurones, glia, vasculature and cerebrospinal fluid (CSF).

1.1.4.1 | Animal selection

The use of small animals for stroke research studies presents clear advantages of lower cost and greater acceptability from ethical perspectives compared to larger animals. The rodent is the most commonly used animal in stroke studies because of many reasons, firstly, its resemblance

to humans in cerebrovascular anatomy (**Figure 1.4**) and physiology (Mhairi Macrae, 1992). Secondly, there is relative homogeneity within strains (Brinker et al., 1999) owing to inbreeding and most of all, the ease of conducting reproducible studies. Furthermore, the small brain size which is well-suited to fixation procedures and brain processing and the advantage over mice of larger body size for surgery (Takizawa et al., 1991) and to allow blood sampling during surgery. Apart from all these advantages, most new drugs that have recently shown potential neuroprotection in animal studies have failed in clinical trials. These failures have led to urgent need to improve current animal models and improve our understanding of the mechanisms underlying neuronal damage and consequent neuroprotection. Emphasis must be given to the use of transgenic mice (either over-expression or knockouts), which can provide a clear answer as to whether or not a specific protein of interest could be a potential therapeutic target (Chen et al., 2005, Shah et al., 2006).

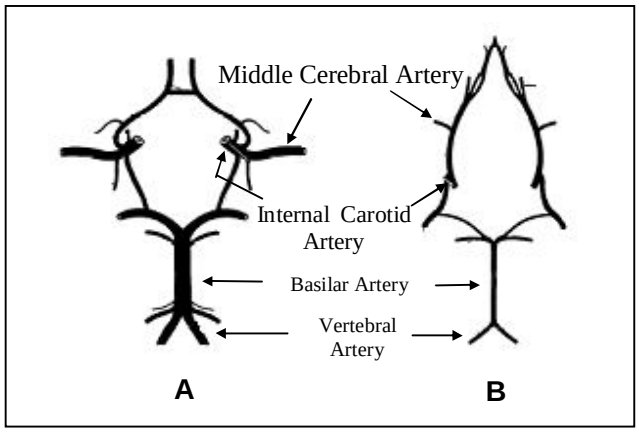

Figure 1.4: Brain vasculature at the circle of Willis

Organisation of the major cerebral arteries in humans (A) and rats (B) (adapted from Lee, 1995).

1.1.4.2 | Model selection

Most animal stroke models were developed to induce cerebral ischaemia within the middle cerebral artery (MCA) territory in order to be relevant to clinical situation. There are 2 major animal models of cerebral ischaemia: global and focal ischaemia. Global ischaemia occurs when cerebral blood flow is reduced throughout most or all of the brain, whereas focal ischaemia is represented by a reduction in blood flow to a very distinct, specific brain region. Complete global ischaemia can be achieved by decapitation in animal models. However, it is often preferable to reinstate blood supply to the ischaemic brain. This can be achieved after cardiac arrest but is technically demanding (Kofler et al., 2004). Therefore, common global ischaemia models involve blocking the major blood vessels that supply the forebrain and result in ischaemia over only a portion of the brain, for example, bilateral common carotid occlusion or four-vessel occlusion. Focal ischaemia occurs in humans when a single trunk artery, most frequently the middle cerebral artery (MCA), is occluded thus animal models of focal ischaemia usually involve occlusion of the MCA (Shah et al., 2006, von Kummer et al., 1993). Furthermore, experimental stroke may model either permanent or transient ischaemia. Permanent stroke models permit the study of cerebral ischaemia without the effect of reperfusion. In a model of transient cerebral ischaemia, an occluded artery is recanalized mimicking as it happens in most human stroke and allowing the consequences of reperfusion in the ischaemic territory (i.e. reperfusion injury) to be evaluated (Gursoy-Ozdemir et al., 2004).

Certainly there is not ‘one’ ideal ischaemic stroke model since human stroke itself is a diverse condition. Among different animal models available for focal cerebral ischaemia induction, those receiving following certain criteria may be ‘more’ ideal: (1) the ischaemic processes and pathophysiologic responses should be relevant to human stroke, (2) the technique used to

perform the modelling should be relatively easy and minimally invasive, (3) physiological variables can be monitored and maintained within normal range, (4) the ischaemic lesion size should be reproducible and (5) brain samples should be readily available for outcome measurements (Carmichael, 2005).

1.1.4.3 | Major rodent models of focal cerebral ischaemia

Permanent electrocoagulation models of middle cerebral artery occlusion (MCAO) have been extremely useful in identifying the contribution of the ischaemia component in the generation of tissue infarction. The intra-cranial approach of Tamura and colleagues (Tamura et al., 1981) and subsequent modifications has emerged as a standard method of permanent proximal MCAO using electrocoagulation and gives rise to infarction of both the cortex and the striatum. Variations in this method include more distal occlusion of the MCA, to restrict infarction to the cortex (Shigeno et al., 1985) and the use of alternative strains of rat to incorporate a recognised risk factor (for example, the use of spontaneously hypertensive stroke-prone rats). The Tamura model has offered one of the closest correlates to a focal cerebral infarct in human (Mhairi Macrae, 1992) and has the advantage of good reproducibility in infarct size and a lower mortality rate. But, while this model has provided a well controlled and reproducible environment to study the pathology and novel treatments applicable to focal ischaemia, like any model it does have constraints. One of these is surgical craniectomy; exposing the skull can cause dehydration of the muscle and other tissue and drilling the skull can lead to thermal damage from drilling and dehydration of the tissue around the craniectomy site. Craniectomy also introduces several variables not seen in the human disease situation; these include skull trauma, external blood vessel and muscle injury, changes in intracranial pressure and invasion of pathogens. Another major disadvantage of electrocoagulation of the vessel is the permanency of

the occlusion (Carmichael, 2005). As described below the intraluminal thread (ILT) model of focal ischaemia can be permanent or transient which incorporates reperfusion. Focal ischaemia incorporating reperfusion adds an extra layer of complexity to animal models but in addition, can also uncover possible injury associated with late reperfusion into ischaemic tissue and therefore reflect more closely the situation that occurs in the majority of human embolic strokes. Consequently, many investigators now use the intraluminal thread model as a method of transient or sometimes permanent focal ischaemia.

MCAO by the intraluminal thread was first introduced by Koizumi and colleagues (Koizumi *et al*., 1986) and subsequently the model was modified to reduce subarachnoid haemorrhage and premature reperfusion by Longa and colleagues (Longa et al., 1989). This technique can involve dissecting the external carotid artery, temporarily tying off the common carotid artery and using the external carotid artery as a path to pass a filament through the internal carotid artery to lodge in the junction of the anterior and middle cerebral arteries. The suture can be left in place for a variable duration of time and then removed to produce reperfusion. This technique does not require craniotomy and produces focal occlusion of a large cerebral artery as seen in human stroke. However, even with modifications such as coating the suture, MCAO is associated with an approximate 12% rate of subarachnoid haemorrhage in rats (Schmid-Elsaesser et al., 1998) and roughly 10% in the mouse (Tsuchiya et al., 2003). Also, dissection of the ECA renders the muscles of mastication ischaemic, producing difficulty in eating and weight loss. Although this does not alter overall infarct size, it is associated with poorer performance on post-stroke behavioural outcome measures. MCAO by the ILT produces primary ischaemic cell death in striatum and overlying frontal, parietal, temporal and portions of occipital cortex, but also variable damage in the thalamus, substantia nigra and hypothalamus (Garcia et al., 1995).

Damage to such a widespread and functionally diverse brain region is likely to produce complex motor, sensory and cognitive deficits.

In filament occlusion of 60 min duration or greater, hypothalamic damage is robust and occurs early (Garcia et al., 1995). Unlike rat MCAO, MCAO in the mouse leads to hypothermia (Barber et al., 2004) and is uniquely associated with substantial variations in the volume of damage within and between strains and generating large infarcts in brain structures (Carmichael, 2005). In several studies of global ischaemia C57BL/6 is more sensitive than BALBc and other strains (Yang et al., 1997). The mechanism for this interstrain difference in ischaemic cell death remains to be determined but may at least in part, be due to C57BL/6 having poorly developed posterior communicating arteries (McColl et al., 2004, Yang et al., 1997) which limits collateral flow to the territory distal to an occluded MCA thereby leading to significantly larger infarct volumes.

Correct placement without injury of the vessel wall is difficult to achieve and should be carried out under continuous blood flow control, e.g. by placing a laser Doppler flow probe on the thinned bone over the cortical surface of the MCA territory (Hossmann, 2008). Modifications of the original technique include ligation of the common carotid artery to hold the filament in place (Kawamura et al., 1991), adjustments of the tip size to the weight of the animal (Hata et al., 1998) and poly-L-lysine or silicone coating of the tip to prevent incomplete middle cerebral artery occlusion (Belayev et al., 1999).

The ILT model utilises a filament of pre-determined diameter, equivalent to the internal diameter of the internal carotid artery (ICA), at the point of origin of the MCA. At this point, the filament blocks the origin of the MCA and occludes all sources of blood flow from the ICA, anterior and

posterior cerebral artery. As this minimizes collateral blood supply from these territories, infarcts are very large and comprise up to two thirds of the total hemisphere. Restoration of blood flow is instituted by retracting the filament along the ICA towards the CCA to allow reperfusion through the Circle of Willis as shown in (**Figure 1.5**)

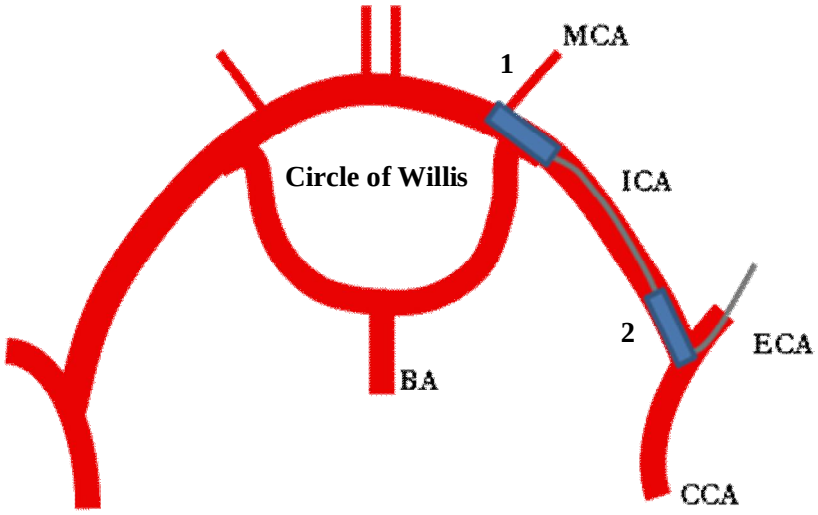

Figure 1.5: Illustration of the ventral view of arteries in the brain

Placement of the intraluminal filament occluding MCA (1) and either removal or retraction to (2) instigates reperfusion (adapted from (McAuley, 1995). CCA = Common Carotid Artery, ECA = External Carotid Artery, ICA = Internal Carotid Artery, BA = Basilar Artery and MCA = Middle Cerebral Artery.

The greatest advantage of the ILT model is the ease with which recirculation can be instigated. More importantly, reperfusion can be achieved when the animal is fully conscious since the filament can be exteriorised. One of the main disadvantages is unavoidable damage to the endothelial lining of the ICA (Nishigaya et al., 1991). This injury, exacerbated by reperfusion, can initiate pathological processes in the vessel wall, alter vascular reactivity and blood brain barrier permeability and may provide a source of emboli capable of occluding more distal vessels (Rabb, 1996).

Finally in an experimental stroke model, variables may be taken under strict control and researchers may address specific questions about how to develop novel stroke therapies. The most encouraging approach is directed towards cell replacement into ischaemic regions using stem cells. Interest in the field of stem cell biology is now widespread because of its potential application to the repair of tissues and organs that have been damaged by congenital defects, disease or trauma (Miller, 2006, Moody, 2005).

1.2 | Introduction to Stem cells

Stem cells are undifferentiated cells that are able to self-renew and give rise to at least one, but often many specialised cell types. Stem cells undergo both symmetric and asymmetric division and have a high degree of potency. The self-renewal capacity results in that at least one daughter cell will have the same potency as the mother cell (**Figure 1.6**). The high degree of potency results in the ability to form a large number of different mature cell types which will be discussed below (Anderson, 2001, Temple, 2001).

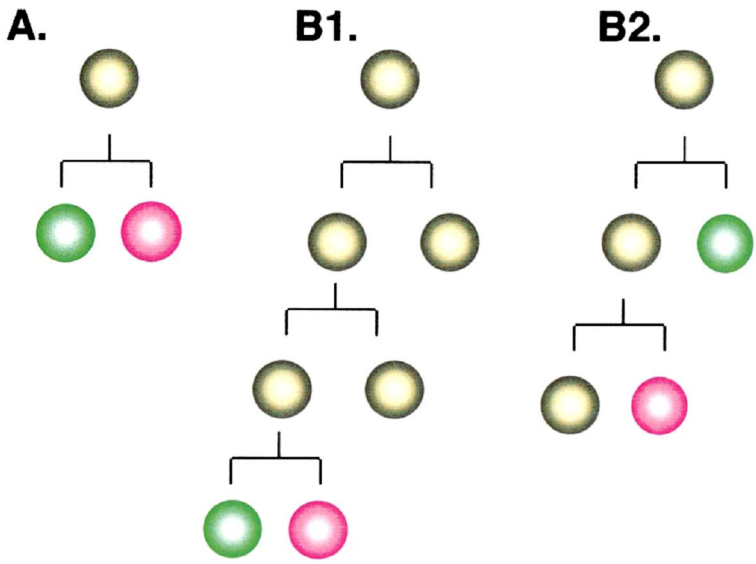

Figure 1.6: Non-Self-Renewing and Self-Renewing Multipotential Progenitors

(**A**) A non-self-renewing multipotential progenitor generates progeny that are immediately committed to different fates (green and pink spheres). (**B1**) A symmetrically dividing self-renewing stem cell divides to generate either two stem cells (gold spheres) or two committed progenitors (green and pink spheres). (**B2**) An asymmetrically dividing self-renewing stem cell divides to generate two committed progenitors(green and gold or pink and gold spheres) (modified from Anderson, 2001).

1.2.1 | Totipotent, Pluripotent and Multipotent stem cells

The ultimate stem cell is the fertilised egg. The fertilised egg is completely totipotent, that is it can form the entire embryo and the extra embryonic tissue such as the placenta. When the fertilised egg has undergone twelve divisions, it forms a blastocyst, one of the early developmental stages. The embryonic stem cells (ES cells) reside inside the inner mass of cells, the blastocyst (Smith, 2001). ES cells are pluripotent, which means they can give rise to all different cell types in the embryo, but not to the extraembryonic tissue. As the embryo develops, stem cells start to undergo asymmetric division and different cell lineages are formed. These stem cells, which can be isolated from the different parts of the developing embryo, are often referred to as somatic stem cells. In general somatic stem cells are multipotent, which means they can at least form two types of differentiated cell progenies (**Figure 1.7**).

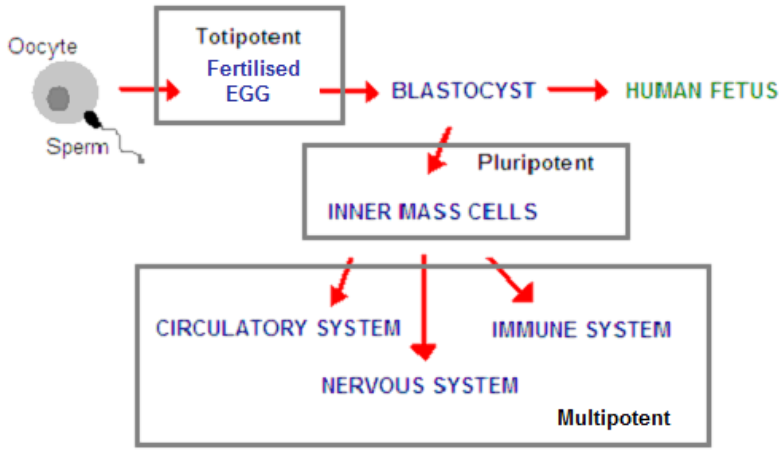

Figure 1.7: Different types of stem cell and their sources

The cells of the fertilised egg are totipotent, since they are able to differentiate into embryonic and extraembryonic tissues. Embryonic stem cells originate from an inner mass of cells within a blastocyst which are pluripotent. Multipotent cells can produce at least two types of differentiated cell progenies, e.g. nervous system can produce neuron and glia. Adapted from Smith, 2001).

Although it is part of the definition that stem cells should be able to divide without limits, they do not have to divide rapidly; in fact later in life many stem cells divide at a relatively low rate.

1.2.2 | Stem cell sources and outcome after transplantation

There are 5 main sources of stem cells:

- Foetal (embryonic) stem cells
- Neural progenitor cells
- Bone marrow stromal cells
- Multipotential cells
- Immortalised cell lines
- Induced Pluripotent stem cells

1.2.2.1 | Foetal (embryonic) stem cells

Embryonic stem cells (ESC), including the more recently described induced pluripotent stem cells (discussed later in this Chapter), comprise the most adaptable stem cells currently available, being able to differentiate into all adult cell types, including functional neurons (Benninger et al., 2003) and glia (Scheffler et al., 2003). Electrophysiological evidence of synaptic integration has also been acquired *in vivo* after transplantation of mouse (Wernig et al., 2004) and human (Roy et al., 2006) ES-derived cells.

Early transplantation experiments of foetal/embryonic stem cells established that grafted neurons survive and remain viable only if they are immature prior to having elaborate extensive axonal connections. Transplanted foetal neurons survive, integrate and ameliorate functional deficits in animal models of neurodegenerative diseases (Savitz et al., 2002). Very recently, Lee and colleagues used neural stem cells (NSCs) from foetal human brain and demonstrated early

intravenous NSCs injection caused anti-inflammatory functionality that promoted neuroprotection, mainly by interrupting splenic inflammatory responses after ICH (Lee et al., 2008). In order to avoid teratoma formation, most studies using ES-derived cells transplant pre-differentiated cells towards either neurons or neural precursors. Although for some disease models, ESCs have allowed the generation of cell types difficult to obtain from NSCs such as dopaminergic neurons (Bjorklund et al., 2002, Roy et al., 2006, Takagi et al., 2005) and motorneurons (Plachta et al., 2004), results after transplantation of ESC-derived cells for stroke (Buhnemann et al., 2006, Hayashi et al., 2006) have been similar to those obtained by using brain-derived NSCs, although perhaps yielding a higher percentage of neurons. Use of ES-derived cells is constricted by ethical concerns and limited availability (Wechsler, 2004).

1.2.2.2 | Neural progenitor cells

During the past few years, techniques have been developed that make it possible to isolate and expand, from developing and even adult central nervous system tissue, cells that have properties characteristic of early, multipotent, neural progenitor cells. Neural progenitor cells (NPCs) are isolated from the brain. They are found in the periventricular region and in the cerebral cortex during foetal development and have been shown to persist into adulthood (Savitz et al., 2002).

NSCs can differentiate into neurons (Kelly et al., 2004), astrocytes (Eriksson et al., 2003), oligodendrocytes (Pluchino et al., 2003) and possibly even endothelium (Wurmser et al., 2004) suggesting that NSCs have the capability of replacing most of the cell types affected by an ischaemic injury. Actual results in preclinical studies, however, have been quite varied (Burns et al., 2009).

After brain injury, including ischaemia, these cells react by migrating to the area of injury and can generate functional neurons that may form connections with host cells (Englund et al., 2002, Park et al., 2002). When transplanted into brains of rats subjected to ischaemia, these cells survive, differentiate and proliferate (Savitz et al., 2002). Majority of the studies have not observed significant changes in infarct size after NSC transplantation (Kelly et al., 2004, Pollock et al., 2006). However very recently, Harms and colleagues showed that intracerebral transplantation of murine NPCs attenuated neuronal apoptosis in response to focal ischaemia induced by transient MCAO and also prevented neuronal cell death of cortical neurons in response to oxygen-glucose deprivation (OGD) in culture. Moreover, this neuroprotection was blocked by the use of inhibitors of vascular endothelial growth factor (VEGF) suggesting that NPCs promote neuronal survival under ischaemic conditions via HIF-1a-VEGF signalling pathways (Harms et al., 2010). Furthermore, neuroprotective (Lee et al., 2007) and immunomodulatory (Pluchino et al., 2005) effects of NSCs to permit at least some cell replacement (Sinden et al., 1997) have collectively generated beneficial effects in multiple animal models of neurodegeneration and brain injury, including stroke.

As neural progenitor cells are derived from foetal brains, ethical issues similar to those with foetal stem cells limit availability (Wechsler, 2004). Another major obstacle for all types of neural progenitor stem cells is the expansion *in vitro* to the extent needed for transplantation. NPCs expanded *in vitro* lose the capacity to differentiate, which limit their ability to form functional grafts (Svendsen et al., 1996).

1.2.2.3 | Bone marrow stromal cells

Bone marrow stromal cells (BMSCs) can generate a variety of tissues, including bone, cartilage, adipose (Orlic et al., 2001), muscle, hepatocytes (Schwartz et al., 2002), glia and neurons (Sanchez-Ramos et al., 2000). When exposed to selective growth factors, human BMSCs differentiate into cells expressing markers of neural progenitors (Prockop, 1997, Sanchez-Ramos et al., 2000, Tropel et al., 2006). After brain injury, the mechanisms of recovery are likely due to the release of trophic factors (Chen et al., 2002), possibly promoting endogenous repair mechanisms, reducing cell death and stimulating neurogenesis and angiogenesis (Chen et al., 2003a, Chen et al., 2003b) rather than neuronal differentiation and implant integration to the injured ischaemic site. Unfortunately, the use of BMSCs is limited due to primarily two issues. Firstly, only a percentage of transplanted cells administered intravenously migrate to the ischaemic area. The rest spread to other areas of the brain and to other organs, where they could potentially change organ physiology and promote the formation of tumours (Wechsler, 2004). Secondly, both mouse (Miura et al., 2006, Tolar et al., 2007) and human (Rubio et al., 2005) MSCs may exhibit malignant transformations after extended culture *in vitro*, a concern that may be exacerbated by their immunosuppressive properties. Long-term follow-up studies are needed to address this issue (Wechsler, 2004). Very recently, Bakondi and colleagues demonstrated CD133 (glycoprotein; marker of hematopoietic stem/progenitor cells) derived from BMSC conditioned media significantly reduced cortical infarct volumes in mice when administered intra-cardiacally (arterial) when compared with the effects of CD133 derived from BMSC (cell) administration (Bakondi et al., 2009).

Clinically, in addition to transplanting BMSCs, endogenous BMC can be mobilized by G-CSF (Sprigg et al., 2006) and this too has led to significant improvement in functional outcomes

following stroke in animal models (Dunac et al., 2007). It should be noted, however, that G-CSF has neuroprotective actions on its own (Schabitz and Schneider, 2007) and promotes neurogenesis (Schneider et al., 2005). Thus, results may represent a combined effect. Clinical trials to assess G-CSF safety and efficacy after stroke are currently under way (Schabitz et al., 2008).

1.2.2.4 | Multipotential cells

Multipotent adult progenitor cells (MAPCs) have emerged as bone marrow-derived cells with greater potential than normal mesenchymal stem cells (MSCs) (Jiang et al., 2002). Specifically, MAPCs have been accounted to generate functional cell types from all three embryonic germ layers, including neural cells that exhibited mature electrophysiological properties *in vitro* (Schwartz et al., 2002, Serafini et al., 2007). Like MSCs, MAPCs have been shown to improve behavioural recovery in a rodent model of stroke (Zhao et al., 2002); however, *in vivo* neural differentiation of these cells after postnatal transplantation has not been demonstrated (Burns et al., 2006). A number of other multipotent stem cell populations from bone marrow with properties similar to MAPCs have also been described (Anjos-Afonso and Bonnet, 2007, Yoon et al., 2005). To our knowledge, however, none of these have demonstrated mature electrophysiological function after neural differentiation, nor have they been tested in models of ischemic brain injury.

The umbilical cord is another source of multipotent stem cells that, when exposed to selective growth factors, create progeny that stain for neuronal and glial cell markers (Wechsler, 2004). Even less is understood about the biology of human umbilical cord blood cells (HUCBCs). A study has already shown that intravenous infusion of these undifferentiated cells improved behavioural recovery. Approximately 1% of these cells survived and migrated to the ischaemic

hemisphere, where an estimated 2% expressed neuronal markers (Chen et al., 2001). Recently, Arien-Zakay and colleagues have used an HUCB mononuclear-enriched population of collagen-adherent cells, which can be differentiated *in vitro* into a neuronal phenotype (HUCBNP) and demonstrated neuroprotection which involved antioxidant(s) and neurotrophic factors *in vitro* (Arien-Zakay et al., 2009).

Intravenously administered HUCBCs also spread to various other organs, similar to BMSCs, limiting their use *in vivo*. Thus two major problems restrict the use of these above mentioned sources of stem cells 1) ethical issues and 2) the difficulty of obtaining enough stem cells with the desired characteristics to carry out potentially safe therapies. Isolating these cells from patients or embryos may not provide a sufficient number of cells to result in functional repair (Moody, 2005).

1.2.2.5 | Induced Pluripotent stem cells (iPS)

Beyond natural sources that are limited by stem cell availability, immune intolerance and lineage specification, the most recent platform that is developed uses bioengineered stem cells in regenerative medicine referred to as induced pluripotent stem cells (iPS) (Nelson et al., 2010). By utilising the ability to reprogram ordinary self-derived tissue sources, the novelty of bioengineered stem cells presents an unlimited supply of progenitor cells for practically all cell types and tissues of the adult body. Through control of the epigenetic environment within ordinary cell types, nuclear reprogramming reverses cell fate, converting mature cells back to the embryonic ground state (Jaenisch and Young, 2008). The transcription factors sets- Oct4, Sox2, c-Myc, and Klf4 or alternatively Oct4, Sox2, Nanog, and Lin28 (Yu et al., 2007) are sufficient to reprogram somatic cells into a pluripotent phenotype, during a sequential reversal. Multiple sources of tissue such as ordinary fibroblasts (Takahashi et al., 2007), keratinocytes (Aasen et

al., 2008) or adipose tissue (Sun et al., 2009) have been successfully reprogrammed. iPS bypasses the need for embryo extraction to generate genuine pluripotent stem cells. In the mouse, bioengineering strategies have yielded iPS cells sufficient for complete *de novo* embryogenesis as the highest evidence of pluripotent stringency (Boland et al., 2009). In humans, iPS cells have ensured comprehensive multi-lineage tissue differentiation by demonstrating the ability to give rise to all three germ layers in teratoma formation (Yu et al., 2007, Park et al., 2008). Optimization of iPS will likely produce specialised properties that improve stress tolerance, differentiation capacity and increase engraftment/ survival to improve regenerative potential.

The capacity of the therapeutic potential for iPS has been demonstrated in proof of principle studies for four diverse conditions to date (Table 1.1), namely sickle cell anaemia (Hanna et al., 2007), Parkinson's disease (Wernig et al., 2008), haemophilia A (Xu et al., 2009) and ischaemic heart disease (Nelson et al., 2009). The iPS clones in these studies were demonstrated to produce hematopoietic lineages, neural precursor cells giving rise to neuronal and glial cell types and functional cardiac tissue prior to therapeutic application, respectively. Furthermore, upon transplantation of iPS cells into target organs scaling from foetal brain to adult post-ischaemic heart tissue, progenitor cells migrated and differentiated *in situ* into target tissues. Together, these experimental models of diseases provide a proof-of-principle for therapeutic potential of iPS based strategies (Nelson et al., 2010).

The possibility for onco-genesis due to insertional mutagenesis that is inherent to stable genomic integration using retroviral or lentiviral vectors has been identified as a limitation (Yamashita et al.). However, it is important to recognize that the uniqueness of iPS cells has established a new

paradigm for personalized therapeutics across a diverse spectrum of chronic degenerative diseases (Table 1.1).

Disease condition	*Therapeutic outcome*
Sickle cell disease	Hematopoiesis, functional physiological improvement
Parkinson's disease	Dopamine production, symptomatic improvement
Hemophilia A	Decreased clotting time, survival benefit
Ischemic heart disease	Improved cardiac performance, in situ tissue repair

Table 1.1: Models of disease treated with iPS-based interventions.

Four diverse conditions studied till date using iPS cells in rodents and humans (Nelson et al., 2010).

Due to the above mentioned limitations and for reasons described below, the use of immortalised cell lines proves to be promising.

1.2.2.6 | Immortalised cells lines

Initially, cell lines were obtained only as tumour cells or as spontaneously immortalised variants of cells that grew readily in tissue culture. Furthermore, Borlongan and colleagues (Borlongan et al., 1998), using grafts of teratocarcinoma-derived Ntera2/D1 neuron-like cells (NT2N) showed improvements in passive avoidance and body swing tests after permanent middle cerebral artery occlusion in rats. Indeed, some functional recovery in stroke patients has been reported with NT2N grafts (Kondziolka et al., 2000). Hara and colleagues extended this research to further establish the post-mitotic status of NT2N cells by using "retroviral" strategy, transfecting these cells with the transcription factor Nurr1 (Nurr1 has been demonstrated to induce differentiation in CNS precursor cells *in vitro* (Kim et al., 2003)). This new cell line NT2N.Nurr1 displayed an

accelerated neuronal commitment and secreted a high level of the neurotrophic factor glial cell line-derived neurotrophic factor (GDNF) which, when transplanted into the rat stroke brain, expressed a neuronal phenotype and reduced behavioural impairments comparable to those produced by NT2N cells (Hara et al., 2008). The clinical utility of immortalised cells still remains unclear, some suggest that immortalised cell lines offer the best way to ensure use of well-characterized, stable cells and others believe that immortalisation renders an unacceptably increased risk for subsequent malignant transformation. To address this concern, some groups have generated "conditionally immortalised" cell lines that are immortal only in the presence of specific agents (Pollock et al., 2006).

Cell lines can be produced from primary cells by selection of spontaneously immortalised cells or with the help of recombinant cellular or viral immortalisation genes (May et al., 2005). Spontaneous immortalisation is generally more time-consuming and less efficient than procedures employing an immortalising gene. Recombinant cellular or viral immortalisation gene technologies require the growth of cells for extended periods of time in culture, under selective pressure, to obtain sufficient numbers of cells expressing the immortalising gene to allow experimentation (May et al., 2005). A frequently used immortalisation gene is the simian virus 40 (SV40) largeT antigen (TAg). It supports cell survival and growth by overcoming p53- and pRB-dependent cell cycle arrest (Ali and DeCaprio, 2001). However, the uncontrolled proliferation and additional effects of the immortalising gene can in addition influence the differentiation status and phenotype of a cell. A thermolabile mutant tsA58 has been isolated that allows to expand the cells under permissive conditions and then the examinations can be done while the influence of the TAg is reduced by a shift to higher temperatures (Tegtmeyer, 1975). Transgenic mice were generated that harbour SV40 strain tsA58 early region coding sequences

under the control of the mouse major histocompatibility complex H-2Kb class I promoter. This promoter is active at various levels in different tissues of the body but can be induced to higher levels of expression in almost all cells by exposure of the cells to interferon- gamma (IFNγ) (Jat et al., 1991).

The Maudsley hippocampal stem cell line clone 36 (MHP36) which is derived from the embryonic stage 14 (E14) hippocampal proliferative zone of the tsA58 transgenic mouse, which constitutively expresses the TAg under the control of IFNγ proves to be promising. MHP36 cells proliferate at low temperatures (33 °C) *in vitro* since the oncoprotein is active and give rise to various neuronal and glial precursor phenotypes at least in part by inductive signalling. When switched to the non-permissive temperature (37–39 °C), however, the oncoprotein is inactive, the cells cease division and demonstrate the capacity to differentiate, an important property of the cell lines which reduces the chance of producing tumours (Savitz et al., 2002, Sinden et al., 1997). They have been shown to improve outcomes in several models of impairment, including hippocampal ischaemia induced by 4-vessel occlusion, lesions to cholinergic forebrain projections and old age (Gray et al., 2000, Gray et al., 1999, Hodges et al., 2000a, Hodges et al., 2000b, Sinden et al., 1997).

With “on demand” tissue repair now possible, regenerative medicine is entering a new era of research and discovery focused on applying optimisation strategies to facilitate the acceleration of novel products and services to improve the value of patient care (Nelson et al., 2010, Hirai, 2002, Miller, 2006).

1.2.3 | Stem cell Therapy for Stroke

Acute ischaemic stroke caused by cerebral artery occlusion leads to infarction of brain tissue with acute loss of neurons, astroglia and oligodendroglia (Haas et al., 2005). Not long ago, the ability of the brain to restore function through regeneration of neural elements was thought to be non-existent. It is now known that not only does some regenerative capacity exist, but implanted cells can integrate into the host brain, survive, and reverse neurological deficits (Wechsler and Kondziolka, 2003). This section focuses on studies investigating the regenerative capacity of neural stem cells in stroke will be discussed. Stem cell therapy for stroke can be divided into two, an endogenous and exogenous approach (**Figure 1.8**).

The aim of the endogenous approach of stem cell therapy is to exploit the population of adult stem cells already physiologically present in the CNS, a process called neurogenesis. To be able to manipulate the endogenous adult progenitors, it is crucial to determine the extracellular signals that can stimulate cell division and regulate the fate of these neural stem and progenitor cells (Kuhn et al., 1997).

External stimulants such as enriched environment, physical activity or application of defined molecules such as fibroblast growth factor-2 (FGF-2), epidermal growth factor (EGF) (Kuhn et al., 1997) and VEGF (Jin et al., 2002) modulate neurogenesis. During development, growth factors provide important extracellular signals for regulating the proliferation and fate determination of stem and progenitor cells in the CNS (Calof, 1995) as well as ischaemic injury can trigger host stem cells to promote neurogenesis (Lindvall and Kokaia, 2005).

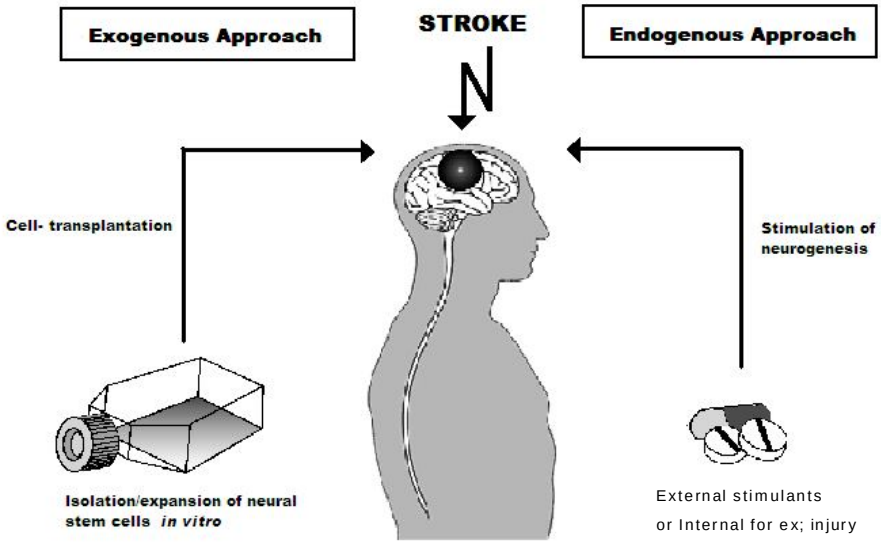

Figure 1.8: The endogenous and exogenous approaches of stem cell therapy in stroke (adapted from Haas et al., 2005).

Using the exogenous mode, CNS derived adult stem or precursor cells are administered locally or systemically after purification and propagation in culture. The main rationale to transplant neural stem cells is primarily to reconstruct the destroyed neuronal circuit (**Figure 1.8**) (Haas et al., 2005). These, implanted cells may induce host responses that both promote function of the graft and directly contribute to neurological recovery. Exogenous stem cells may act via multiple mechanisms to restore function following brain injury. Neuroprotective actions, which might include modulation of inflammation or secretion of neuroprotective compounds, may rescue dysfunctional neurons, thereby preserving existing neural circuitry. A summary of some of the potential mechanisms via which transplanted cells may yield functional benefits are illustrated in **Figure 1.9.**

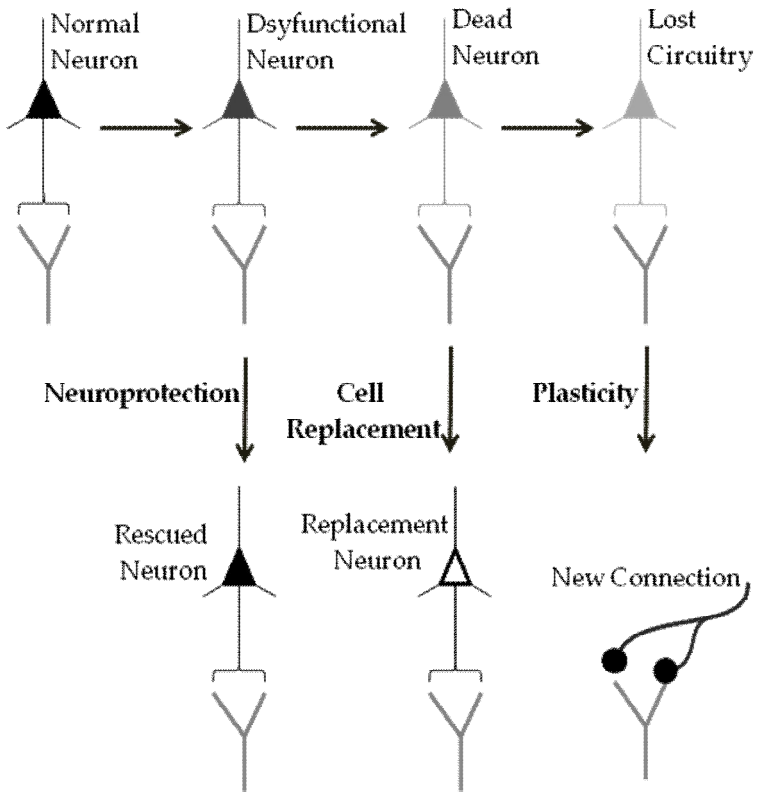

Figure 1.9: Mechanism of exogenous stem cells action.

Once a host neuron has died, stem cells may conceivably be used to replace the lost neuron; though, effective cell replacement might be dependent on maintenance of surrounding cytoarchitecture. Assuming original circuits cannot be preserved due to cavitation of the injury site, stem cells may still participate in the formation of new circuits. This may occur directly via synaptic incorporation into new circuitry or indirectly by supporting the formation or maintenance of new connections by host neurons. In either case, such formation of new synaptic connections is termed synaptic plasticity. An underlying relation between the functional benefit after cell transplantation following stroke and the synaptic integration of grafted cells has not yet been established (adatpted from Squire, 2003).

Despite the plethora of basic research providing evidence of functional recovery following stem cell transplants in models of stroke (Savitz et al., 2003) either endogenously or exogenously, to

date, the mechanisms underlying the observed improvements are still unclear and clinical evidence have been more variable (Lindvall and Kokaia, 2005).

The four major problems which restrict the success of stem cells are the survival, migration, differentiation and integration of the stem cells after transplantation. Future studies are needed to increase such survival and to correlate survival and functional outcome. The success of cell replacement therapy will depend much on the technological advances on the manipulation of stem cells through the elucidation of regulatory signals, trophic factors and their effects on proliferation, migration and differentiation (Yihua An, 2006).

During the past decade, it has been observed that oestrogen plays an important trophic as well as protective role in the adult brain. Oestrogen is essential not only for maintaining normal brain function but also thought to protect the brain against neurodegenerative diseases and injury (for reviews see (Behl, 2002, McEwen and Alves, 1999). Both *in vitro* and *in vivo* studies that utilize a variety of animal models show that the predominant form of oestrogen; oestradiol, prevents cell death, promotes neuronal survival, enhances neurite outgrowth, stimulates synaptogenesis, and regulates synthesis of neurotransmitters and their receptors under a wide range of experimental paradigms (Wise et al., 2001). The purpose of the present study was to investigate whether one can take advantage of the beneficial effects of oestrogen to improve the stem cell function in the ischaemic brain.

1.3 | Introduction to Oestrogen

1.3.1 | Oestrogen: brief overview of relevance to stroke and stem cells

Oestrogens are a group of steroidal compounds and are synthesised by the ovary and several other tissues including the brain. 17β-oestradiol is the predominant and most potent of the three endogenously synthesised oestrogens of all mammals including the adult premenopausal woman. The other two naturally occurring oestrogens are oestrone and oestriol. Like all steroidal hormones, oestrogen can readily diffuse across the cell membrane. Oestrogen acts by binding to three known types of oestrogen receptors (ERs), ERalpha (α), ERbeta (β) and GPR30 (Nilsson et al., 2001, Carmeci et al., 1997). Oestrogenic effects on brain cells can be classified as either genomic, which manifest over a time scale of hours and is mediated by soluble receptors which bind to target DNA and lead onto gene transcription, and non genomic, which is rapid, mediated by membrane bound receptors and does not affect gene transcription (McEwen and Alves, 1999, Nilsson et al., 2001).

Besides the effects of oestrogen on the reproductive system, studies that utilize a variety of animal models have shown that oestrogen modulates processes ranging from adhesion and migration to survival and proliferation for example of stem cells after injury, regulate cardiovascular function, organogenesis, angiogenesis and cancer (Prossnitz et al., 2008). Moreover, neurological processes such as stress responses, feeding patterns, sleep cycles and temperature regulation have also been shown to be modulated by oestrogen (Kelly and Levin, 2001). It has also been reported by McEwen and colleagues, that oestrogen influences synaptogenesis and contributes to synaptic plasticity (McEwen, 2001). Furthermore, oestrogen also exhibits neuroprotective effects by modulating protein levels of increased anti- and

decreased pro- apoptotic proteins (Sawada et al., 2000). Oestrogen also appears to influence neurogenesis in the hippocampus of rats (Suzuki et al., 2007). The sub ventricular zone (SVZ) lining the lateral ventricle is a major repository of neural stem cells in the adult brain. Under normal physiological conditions, the SVZ-derived neural precursor cells migrate to the olfactory bulb, where they differentiate into functional olfactory interneurons (Suzuki et al., 2007). However, various neurodegenerative conditions induced by cortical aspiration, traumatic brain injury, or cerebral ischaemia redirect the migration of neural precursor cells from their normal route toward the sites of injury, including the cortex and striatum, two brain regions that are most affected by MCAO (Suzuki et al., 2007). It was also observed that ERα and ERβ are essential mediators of oestrogen and the selective ablation of one form of ER completely prevents the ability of the hormone to modulate the number of immature neurons in the SVZ and that each receptor subtype exerts differential functional roles in modulating the number of newborn neurons (Suzuki et al., 2007).

1.3.2 | Oestrogen Biosynthesis, Dax-1 and Aromatase

Oestrogen synthesis is catalyzed by a microsomal (localised in the cytoplasm) member of the P450 superfamily, aromatase (P450arom, the product of the CYP19 gene). The expression of the aromatase gene is regulated in various human tissues via the use of tissue-specific promoters (Bulun et al., 1993). For example, P450arom expression in the gonads is regulated via the proximal promoter, promoter II (Sebastian and Bulun, 2001). Promoter II interacts with the transcription factors cAMP-responsive element-binding protein (CREB) and steroidogenic factor-1 (SF-1) (Carlone and Richards, 1997). SF-1 belongs to the nuclear receptor superfamily (NR5A1) and regulates gene transcription through its interactions with a number of co-regulators (e.g. CREB-binding protein, dosage sensitive sex reversal adrenal hypoplasia congenita critical

region on the X chromosome gene 1 (Dax-1), steroid receptor coactivator-1, early growth response-1 and Wilms' tumor suppressor gene (WT1)) (Ito et al., 1997, Gurates et al., 2003, Halvorson et al., 1998).

Dax-1 is an orphan member of the nuclear hormone receptor superfamily of transcription factors (Bardoni et al., 1994, Muscatelli et al., 1994, Swain and Lovell-Badge, 1997). In steroidogenic tissues, Dax-1 functions as a negative regulator of steroid production. In humans, mutations in the Dax-1 gene causes adrenal hypoplasia congenita (AHC) associated with hypogonadotropic hypogonadism (Muscatelli et al., 1994), whereas Dax-1 deficient mice display no major adrenal and pituitary phenotype (Guo et al., 1995). Dax-1 transcripts are expressed in the hypothalamus, pituitary, adrenal glands and gonads. This pattern of expression is markedly similar to that of SF-1 (Ikeda et al., 1996)). The co-localization of SF-1 and Dax-1 led to the suggestion of a functional interaction between these two orphan nuclear receptors (Ikeda et al., 1996). Consistent with this idea, Dax-1 interacts directly with SF-1 and inhibits SF-1-mediated transactivation (Zazopoulos et al., 1997) on the promoters of StAR (Lalli et al., 1997), CYP11A (Lalli et al., 1998) and CYP17 (Hanley et al., 2001) (**Figure 1.10**). Wang and colleagues showed significant increase in mRNA, protein, and enzymatic activity of aromatase, the enzyme accountable for the conversion of testosterone to oestradiol in Dax-1-deficient Leydig cells. Increased aromatase expression was supplemented by a 40-fold increase in intra-testicular oestradiol (Wang et al., 2001b). Dax-1 binds directly to the CYP19 promoter to down-regulate its transcription (Wang et al., 2001b) and also regulates oestrogen (Zhang et al., 2000) and androgen receptors (Holter et al., 2002) through protein-protein interactions (**Figure 1.10**).

In addition to steroidogenesis, recently it has been shown that Dax-1 is expressed at high levels in undifferentiated murine ES cells and that its expression is rapidly down-regulated during their

differentiation (Niakan et al., 2006). Furthermore, Dax-1 has been shown to be a direct target of, and interact with, Nanog and Oct4 (Loh et al., 2006). Recently, Khalfallah and group have demonstrated that Dax-1 knockdown in ES cells induced upregulation of multilineage differentiation markers and produced enhanced differentiation and defects in ES viability and proliferation (Khalfallah et al., 2009). These data taken together suggest that Dax-1 is an essential element in the molecular circuit existing in the ES cells to repress differentiation genes and to preserve their self-renewal and pluripotency.

In pre- and postmenopausal women, as in men, oestrogen is no longer regarded as only an endocrine factor, as it is produced in a number of extragonadal sites and acts locally at these sites in a paracrine and intracrine fashion (Roselli, 2007). These sites include breast, bone, vasculature, and brain. Within these sites, aromatase action can generate high levels of oestrogen locally without significantly affecting circulating levels. Circulating C19 steroid precursors are essential substrates for extragonadal oestrogen synthesis. The levels of these androgenic precursors drop markedly in women, probably from the mid to late reproductive years. This may be a fundamental reason why women are at increased risk of bone mineral loss and fracture and possibly decline of cognitive function, compared to men (Roselli, 2007).

Naftolin and colleagues demonstrated in mammals that the brain was an important site for oestrogen synthesis and that provided direct evidence that central neuroendocrine tissues were capable of converting androgens into oestrogens (Naftolin et al., 1971). These results formed the foundation for the classical (original) brain aromatase hypothesis, which has evolved to suggest that many, if not most, of the effects of gonadal androgens on neural cell function are mediated by local metabolism to oestrogen by cytochrome P450 aromatase (CYP 19).

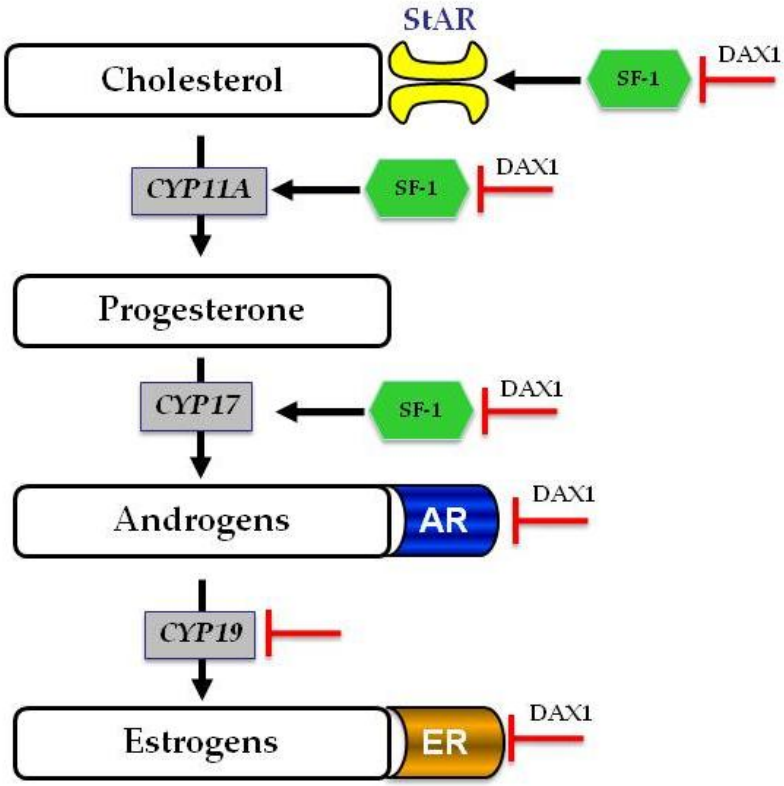

Figure 1.10: Schematic representation of pathway for the biosynthesis of steroids.

Dax-1 regulates key steps for steroid production by repressing the transcriptional activation of SF-1 on the promoters of StAR, CYP11A and CYP17. Dax-1 binds directly to the CYP19 promoter to down-regulate its transcription and also regulates oestrogen and androgen receptors through protein-protein interactions. CYP11A, CYP17 and CYP19 are, respectively, genes that encode for the P450 enzymes cholesterol side chain cleavage, 17-hydroxylase and aromatase. StAR is the mitochondrial cholesterol transporter protein. AR and ER are respectively androgen and oestrogen receptors (Martins et al., 2007).

More recently, it has been demonstrated that the brain can synthesize oestradiol *de novo* from cholesterol and that as such brain-derived oestrogen may play a novel role in neuronal and/or glial signalling (Hojo et al., 2004). Garcia-Segura and colleagues have shown that after a neurotoxic lesion induced by the systemic administration of kainic acid, expression of aromatase is increased by reactive glia in the hippocampus and in other brain areas that are affected (Garcia-Segura et al., 1999). McCullough and colleagues demonstrated a significant reduction in

the infarct size in aromatase knock-out (ArKO) mice when compared to female wild-type (WT) mice. Similarly in the same study they used the aromatase inhibitor, fadrozole and showed an increase in cortical and striatal damage in WT mice. Furthermore, restoration of plasma 17β-oestradiol to physiological levels completely reversed the ArKO female's susceptibility to injury (McCullough et al., 2003). Thus, suggesting aromatase was crucial to the observed endogenous neuroprotection in females and that enhancing local, non-gonadal oestrogen formation could have therapeutic implications in ischaemic neuropathology. In other words, aromatase can act to convert circulating androgens to active estrogenic metabolites in specific neural target tissues or may serve as part of endogenous neurosteroid machinery that supplies oestrogen directly to specific regions of the brain.

1.3.3 | Oestrogen Receptors structure and function

Two intranuclear ERs have been identified (see review(McEwen and Alves, 1999) of which ERα is localized on human chromosome 6 and in contrast ERβ sits on chromosome 14 (Enmark et al., 1997). ERα and ERβ thus represent two separate gene products and share a relationship to one another that is similar to those between, for instance, the glucocorticoid receptor and the progesterone receptor, which show a homology between their ligand-binding domains that corresponds to those of ERα and ERβ. Two of the most interesting sites on the ER molecule are its ligand binding domain (LBD), otherwise known as AF-2, and its growth factor binding domain, otherwise known as AF-1. In addition, the DNA-binding domain (DBD) is responsible for binding at oestrogen response elements (ERE) on the chromosome. This structural homology correlates with the findings that both receptors have similar DNA-binding properties (Pettersson et al., 1997), bind 17β-estradiol with similar affinity (Kuiper et al., 1997) and actually interacts with the co-activator SRC-1 (Tremblay et al., 1997). In contrast, the amino-terminal domain of

ERβ is shorter by about 80 amino acids and shows no sequence homology compared with that of ERα. Variability of the amino-terminal region between subtypes or isoforms of receptors for the same hormone is common within the nuclear receptor superfamily and generally results in functional differences (Delaunay et al., 2000). For instance, progesterone receptor isoforms A and B diverge exclusively in this domain and activate transcription from target genes differentially and in a cell-specific manner (Vegeto et al., 1993). The following diagram, adapted from (Gustafsson, 1999), compares the two receptors:

Figure 1.11: An illustration of the structure of the oestrogen receptors, ERα and ERβ.

The A/B domains form the NH_2 terminal, the C domain forms the DNA-binding domain (DBD) while domains D/E/F constitute the ligand-binding domain (LBD). The AF-1 and AF-2 activation units are part of the DNA-binding and ligand-binding domains, respectively. The two ER subtypes, ERα and ERβ, are almost identical in the DNA-binding domain (~95% homology) but differ in the ligand-binding domain (about ~60% homology). Differences in the ligand-binding domain are responsible in part for ligand-specificity, and the ratio of ERα and ERβ is a critical determinant of cellular response to endogenous oestrogen and other ER agonists and antagonists (Gustafsson, 1999).

Both ERα and ERβ are expressed in the brain, but they show a partly different distribution. Studies using in situ hybridisation indicate widespread distribution of ERβ mRNA throughout much of the brain, including olfactory bulbs, cerebellum and cerebral cortex (Kuiper and Gustafsson, 1997, Kuiper et al., 1998). ERα sites are associated with reproductive behaviour in

the hypothalamus (Toran-Allerand et al., 1992, Behl, 2002), while ERβ sites are predominantly expressed in the midbrain, dopaminergic and serotonergic neurons (Toran-Allerand et al., 1992, Behl, 2002). **Figure 1.12** shows the distribution of both types of ER in a coronal section of the rodent brain. ERα and ERβ can also form heterodimers when expressed in the same cells, forming additional possible variants for gene regulation (Pettersson et al., 1997). Production of knock-out mice deficient in ERβ (BERKOs) has enabled to differentiate the distant biological roles between the two ERs.

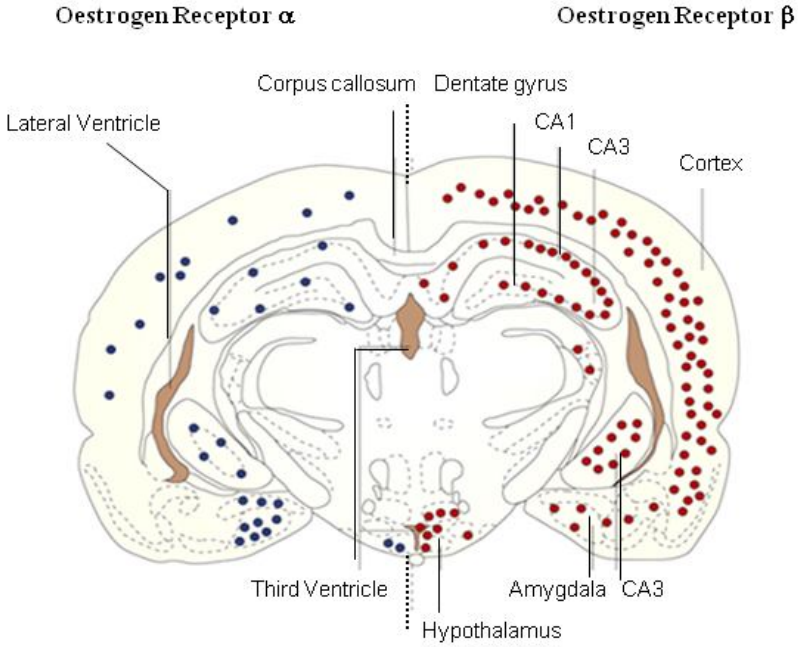

Figure 1.12: Expression of ERα and ERβ in the rodent brain

Coronal section of a rat brain at level of the dorsal hippocampus, dots indicate (blue) expression of ERα and (red) of ERβ (Shughrue et al., 2000).

Furthermore, examples are accumulating of different respective modes of regulation of ERα and ERβ. For instance, in vascular tissue, where both ERα and ERβ appear to be expressed,

experimental denudation involving removal of the endothelial cell layer leading to smooth muscle cell proliferation is accompanied by a huge increase (up to 80-fold) of ERβ expression in smooth muscle cells and endothelial cells, whereas the expression of ERα in these cells is unaffected (Lindner et al., 1998). In this particular case, it may be speculated that ERβ mediates the protective effect of estrogens on vascular lesions involving inhibition of smooth muscle cell proliferation. These results are in good agreement with previous experiments performed in knock-out mice, deficient in ERα, showing that the vascular protective effect of estrogens in experimental vascular lesions is unchanged despite the absence of ERα (Iafrati et al., 1997). Recent studies reveal the existence of a novel G protein-mediated signalling by oestrogen (Wyckoff et al., 2001) and localization of oestrogen binding sites to membranes (Kelly and Levin, 2001) suggesting the possibility of a 7-transmembrane G protein-coupled receptor family member being involved in certain aspects of oestrogen function. The cloning of an orphan GPCR from oestrogen responsive MCF7 cells provided the impetus to test whether this receptor could mediate any of the effects of oestrogen in cells lacking classical oestrogen receptors (Carmeci et al., 1997, O'Dowd et al., 1998, Prossnitz et al., 2008). In 2000, Filardo et al. demonstrated MAP kinase (Erk1/2) activation by oestrogen in breast cancer cell lines expressing GPR30 but not in cell lines lacking the receptor (Filardo et al., 2000). Subsequent studies by other groups reported that GPR30 promotes oestrogen-mediated inhibition of oxidative stress-induced apoptosis by promoting Bcl-2 expression in keratinocytes (Kanda and Watanabe, 2003) and furthermore, it promotes cell growth by upregulation of cyclin D expression (Kanda and Watanabe, 2004). All in all, these reports suggest that GPR30 may mediate, in part, the regulation of cellular functions, including growth, proliferation and apoptosis (Prossnitz et al., 2008).

1.3.4 | Actions of Oestrogen Receptors

1.3.4.1 | Genomic intra-nuclear receptor-dependent actions

The direct genomic mode of action of ERs involves binding of the ligand to the cytoplasmic receptor, translocation to the nucleus and binding to EREs in gene promoters, ultimately leading to the induction of gene transcription. Direct transcriptional modulation via ERα or ERβ requires at least 45 minutes (Kuiper et al., 1997) (**Figure 1.13**).

1.3.4.2 | Indirect genomic membrane receptor-dependent actions

Oestrogen potentiates kainate induced currents in the hippocampus via cAMP-dependent phosphorylation (Gu and Moss, 1996, Wong and Moss, 1992), increases cAMP accumulation in breast cancer cells (Aronica et al., 1994), and rapidly activates mitogen activated protein kinase (MAPK) in neuroblastoma (Watters et al., 1997) and non-neuronal cells (Migliaccio et al., 1996). These rapid effects of oestrogen could be explained by the presence of plasma membrane-associated ERs, coupled to signal transduction pathways more typically associated with growth factors such as, leading the neurotrophins to gene regulation (Hefti, 1986, Singer et al., 1999) (**Figure 1.13**).

In culture, activation of MAPK has been shown to occur in minutes after oestrogen treatment and can be blocked using an ER antagonist (ICI 182, 780) (McEwen, 1981). Oestrogen has also been reported to directly regulates c-myc and cyclinD1 levels, which affects the cell cycle (Brannvall, 2004). In addition, a central downstream target of MAPK and Akt signalling is the enzyme glycogen synthase kinase-3β (GSK-3β) - an important modulator of nerve-cell survival (Behl, 2002, Singer et al., 1999).

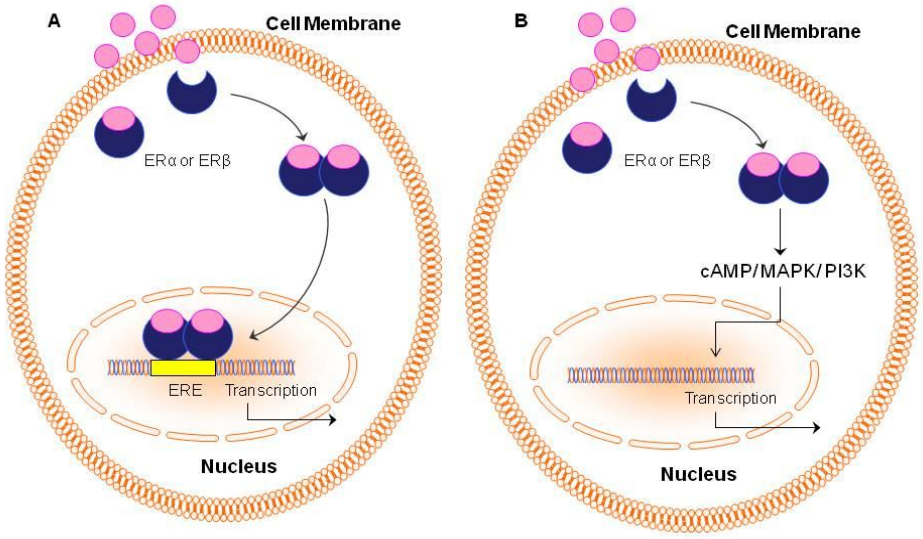

Figure 1.13: Direct and In-direct mode of action of oestrogen

(A) The classical mode of action of oestrogen receptors (ERs) involves binding of the oestrogen to the cytoplasmic receptor, translocation of the bound receptor to the nucleus and binding to the oestrogen response elements (EREs) in the gene promoters, ultimately leading to the induction of gene transcription. (B) In addition to this genomic mode of action, ERs might interact directly with various intracellular signalling pathways, which include the cyclic AMP, mitogen-activated protein kinase (MAPK) and phosphatidylinositol 3-kinase (PI3K) pathways, thereby affecting the transcription of several other target genes (Behl, 2002).

1.3.4.3 | Non-Genomic, Membrane Receptor-Dependent Actions

Besides this genomic action, there is a growing body of evidence that oestrogen may also cause rapid activation of signal transduction pathways. These effects are characterised by their rapid onset (seconds to minutes) and do not require changes in gene transcription. Instead, it is proposed that oestrogen, bound to a membrane receptor, acts directly at ion channels. This results in altered neuronal current conductance or transcellular ion flux. Many oestrogen-dependent neurological events are mediated by membrane-based ion fluxes, often involving calcium (Morley et al., 1994) or calcium-dependent potassium channels (reviewed in (Kelly and Levin, 2001). These actions are extremely rapid and appear to involve membrane-associated

signalling complexes that are capable of responding to very low concentrations of oestrogens. Kinetics of such responses are incoherent with a mechanism requiring gene transcription. One such pathway is a direct effect of oestrogen on ion channels (within 5 minutes), but the components of this pathway have yet to be elucidated. A direct link between ERs (proposed to be membrane-bound) and the MAPK signalling cascade has been demonstrated in several cell types, including neurones (Singer et al., 1999). The MAPK cascade is an incompletely understood chain of molecular events but it is proposed to be mediated in neurones by the Ras/Raf pathway, as shown in **Figure 1.14**. Activation of Ras, a proto-oncogene product, is followed by the activation of B-Raf and Mek1/2. Oestrogen rapidly induces the phosphorylation of extracellular-signal-regulated kinase 1/2 (Erk1/2). Likewise, ERs interact with the phosphatidylinositol 3-kinase (PI3K) signalling pathway, leading to the activation of its downstream effector Akt.

1.3.4.4 | Non-Genomic, Receptor-Independent Actions

Oestrogen can also act directly, with no need for receptors, second messengers or protein synthesis. The direct free-radical scavenging activity of 17β-oestradiol is fully independent of the activation of ERs or of any other signalling pathways; the only prerequisite is the phenolic structure in the A ring of the steroid (Behl et al., 1997, Green et al., 1997).

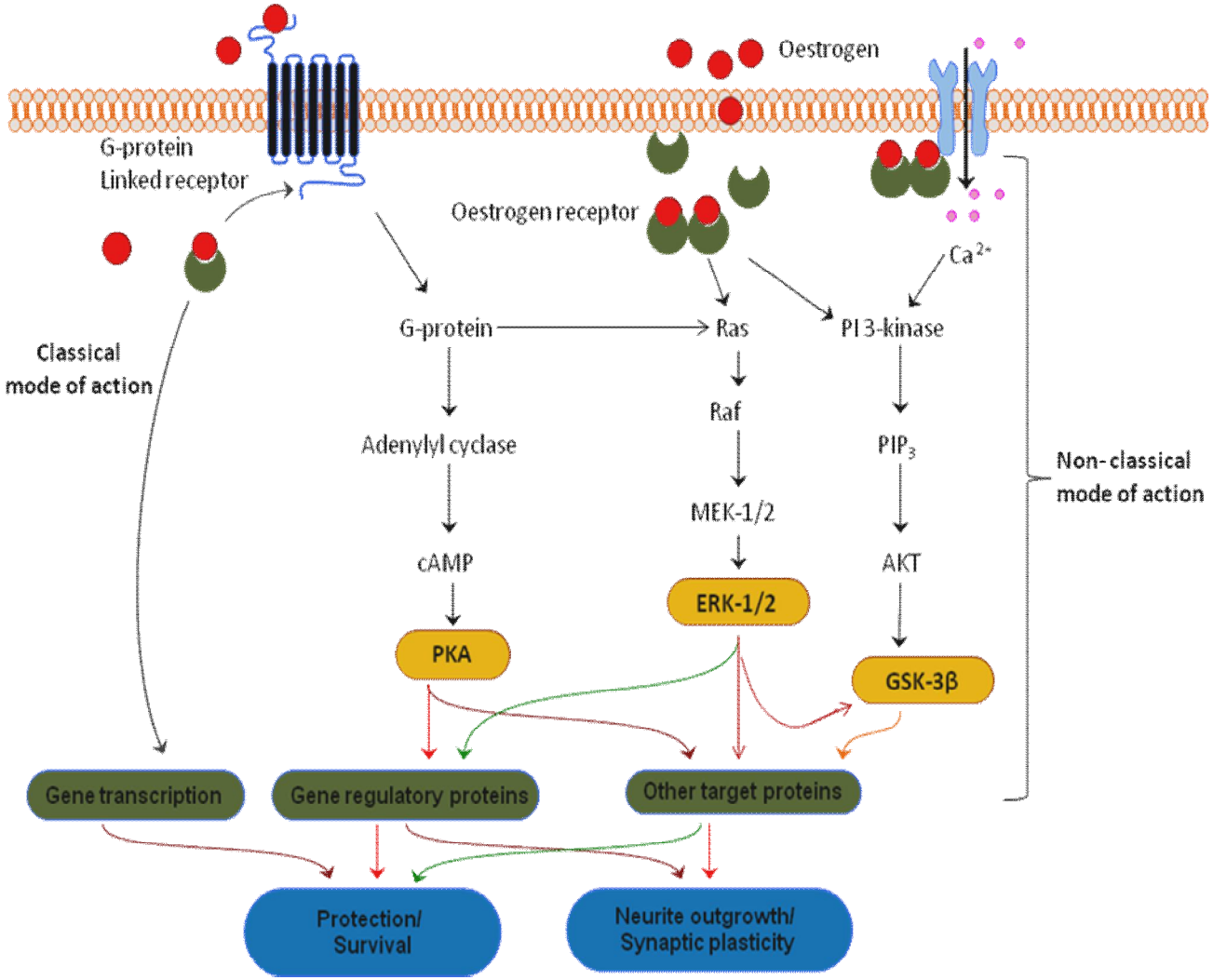

Figure 1.14: Intracellular signalling of oestrogen

ERs can interact directly with the MAPK signalling pathway through the activation of Ras, Raf and induce the phosphorylation of Erk1/2. Likewise, ERs interact with the PI3K signalling pathway, leading to the activation of its downstream effector Akt. Interestingly, a central downstream target of MAPK and Akt signalling is the enzyme glycogen synthase kinase-3β (GSK-3β) an important modulator of nerve-cell survival. Moreover, oestrogen rapidly induces the phosphorylation of cAMP through adenylyl cyclase and PKA (Behl, 2002).

1.3.5 | Oestrogen and Stroke: Experimental Studies of neuroprotection

Oestrogen has traditionally been viewed as a neuroprotective agent against experimental stroke (Hurn and Macrae, 2000). The actions, receptors, precursors and metabolites of oestrogen have been closely examined through *in vivo*, *in vitro* and transgenic studies. Neuroprotection offered by oestrogen has been confirmed from studies that include endogenous oestrogen in females or ovariectomized females and exogenously administering oestrogen over males. The latter allows comparison between animals with very specific (physiological or pharmacological) levels of oestrogen and those with no oestrogen.

1.3.5.1 | Pre-clinical *in vivo* studies utilising endogenous oestrogen

Various studies comparing intact male and female animals have demonstrated decreased volumes of ischaemic brain damage in females possibly due to the higher endogenous oestrogen levels in female compared to male. Female rats have been reported to exhibit reduced infarct sizes after transient focal ischaemia compared to age-matched male rats (Liao et al., 2002, Wang et al., 1999, Zhang et al., 1998). Jia and colleagues have also demonstrated that ischaemia upregulated Fas and FADD expression and increased caspase-8 and caspase-3 activation in ovariectomised (OVX) female mouse cortex, which were significantly attenuated by oestradiol treatment. This attenuation of Fas expression resulted in smaller infarct in the oestrogen treated OVX compared to untreated OVX mice suggesting that inhibition of ischaemia-induced Fas-mediated apoptosis is an important mechanism of neuroprotection by oestrogen in cerebral ischaemia (Jia et al., 2009). A study carried out by He and colleagues found that no protection was offered to hippocampal CA1 neurones after transient global ischaemia in intact compared to ovariectomized female rats (He et al., 2002). However, neuroprotective effects of circulating

oestrogen in females are not yet clear in all reports. While, higher levels of endogenous oestrogen (pro-oestrus) reduced infarct size after permanent focal ischaemia compared to lower endogenous levels (metoestrus) in stroke-prone spontaneously hypertensive (SHRSP) rats, this protection was absent in normotensive rats (Carswell et al., 2000). A possible explanation given for this strain difference is the increased severity of the stroke model in the SHRSP group, which may mean that these animals derived greater benefit from oestrogen's neuroprotective mechanisms. Taken together these studies indicate that the effects of endogenous oestrogen in ischaemic brain are complex.

1.3.5.2 | Pre-clinical *in vivo* studies utilising exogenous oestrogen

Pre-treatment with 17β-oestradiol has been shown to protect the brain from both permanent (Dubal et al., 1998) and transient focal ischaemia (Simpkins et al., 1997); transient forebrain ischaemia (Wang et al., 1999) and global ischaemia in ovariectomized females (He et al., 2002). A range of doses of 17β-oestradiol have been reported to significantly decrease the volume of damage seen after various models of MCAO and global ischaemia for example; physiological plasma levels of 17β-oestradiol from 20pg/ml to 87pg/ml (Dubal et al., 1998, He et al., 2002, Wang et al., 1999) and pharmacological levels up to 160pg/ml (Zhang et al., 1998). Neuroprotection is not limited to females; oestrogen also appears to act as a neuroprotectant in males. Toung and colleagues demonstrated that pre-treatment of male rats with either a single injection or a continuous regime of 17β-oestradiol treatment decreased infarct volume after transient MCAO (Toung et al., 1998).

However, within these many studies demonstrating neuroprotection, some anomalies are evident. The detrimental effects of oestradiol treatment have been reported by various studies depending on the model of cerebral ischaemia (Bingham et al., 2005, Carswell et al., 2004,

Gordon et al., 2005); dose of oestradiol administered (Rusa et al., 1999) for example, He and colleagues showed an amelioration of ischaemic damage in the hippocampal CA1 region in OVX female rats pre-treated with 17β-oestradiol. The authors observed that the 17β-oestradiol serum levels of intact and OVX rats were very similar and low (9 and 3pg/ml, respectively) compared to the rats exogenously administered with 17β-oestradiol (87pg/ml); time of administration (Simpkins et al., 1997, Zhang et al., 1998) and the severity of insult (Vergouwen et al., 2000). More recent findings from the Women' Health Initiative have reported that oestrogen might under some circumstances actually increase the risk of neurodegeneration (Suzuki et al., 2007). Therefore, it becomes even more critical to investigate when oestrogen is beneficial and more importantly, its mechanism of action.

Against this background, importance has been placed on investigating more selective oestrogenic compounds, particularly, a unique class of drugs called selective oestrogen receptor modulators (SERMs) (Littleton-Kearney et al., 2000, Murphy et al., 2003). SERMs can act as either oestrogen agonists or antagonists in different tissue types (Katzenellenbogen and Katzenellenbogen, 2002). This tissue selectivity appears to be due to the ability of SERMs to induce different conformational changes to that of oestrogen following ligand binding to both ER subtypes (α or β), as well as the subsequent recruitment of co-activator and /or co-repressor proteins (Lewis and Jordan, 2005). Beneficial effects of these drugs are apparent in pre-clinical research. The classical synthetic SERM, raloxifene provides neuroprotection from kainate injury (Ciriza et al., 2004) and striatal dopamine depletion (Callier et al., 2001) Furthermore, tamoxifen has been shown to reduce infarct volume following permanent MCAO (Kimelberg et al., 2003) and transient MCAO (Kimelberg et al., 2000) in rats. LY353381, a raloxifene analogue with better bioavailability, was able to reduce infarct volume in the striatum of ovariectomised female

rats with transient MCAO (Rossberg et al., 2000). On the other hand, another novel SERM, LY362321, was unable to provide protection from transient MCAO in ovariectomized female rats (Farr et al., 2008).

1.3.5.3 | Clinical studies utilising oestrogen

There are now approximately ten randomized placebo-controlled clinical trials that have examined the effects of HRT (hormone-replacement therapy), oestrogen alone or the SERMs tamoxifen and raloxifene on coronary heart diseases, vascular disease or stroke (reviewed in (Billeci et al., 2008)).

Evidence exists for the potential protective effects of circulating ovarian hormones in stroke (Haberman et al., 1981). Some evidence from observational studies has indicated that HRT reduces the risk of stroke in postmenopausal women (Pedersen et al., 1997). However, these observational studies are open to bias: women who chose to take HRT may also have had healthier lifestyles. The WHI (Women's Health Initiative) trial was the largest, designed to examine the effects of oestrogen and progestin or oestrogen alone, on breast cancer and the incidence of cardiovascular disease in post-menopausal women. The trial which included oestrogen and progestin was concluded prematurely in 2002 due to a significantly higher incidence of stroke (Wassertheil-Smoller et al., 2003), cardiovascular disease, venous thromboembolic disease and breast cancer in the treated group (Rossouw et al., 2002). The oestrogen alone trial was successively terminated in 2004 after the results indicated an increased risk of stroke (Hendrix et al., 2006) and venous thrombosis (Anderson et al., 2004) in the treated group. Before the WHI trial with view to stroke, The WEST (Women's Estrogen for Stroke Trial) assessed whether oestrogen alone reduced the risk of secondary occurrence (Kernan et al., 1998). Three years later, the incidence of stroke recurrence was equal between the oestrogen and

placebo groups, but mortality and severity symptoms were slightly worse in the oestrogen group (Viscoli et al., 2001).

There are only a few SERMs currently approved for use in humans, with the most common being raloxifene and tamoxifen. Raloxifene is currently prescribed to reduce bone loss and has been shown to reduce the risk of breast cancer in post-menopausal women (Cummings et al., 1999) whereas; tamoxifen is prescribed to treat breast cancer (Fisher et al., 1998). To date, there are few clinical trials that have examined the effect of SERMs on the same outcome measures used in the WHI trial. The MORE (Multiple Outcomes of Raloxifene Evaluation) trial was devised to observe the effects of raloxifene treatment on the occurrence of fracture. The study concluded, three year later, that raloxifene significantly reduced the incidence of fracture, increased bone density and reduced ER-positive breast cancer (Cauley et al., 2001).

In general, the pre-clinical literature reports the capacity of oestrogen to protect against stroke-induced brain damage, which is contradictory to the clinical results of the WHI trial and clinical meta-analyses. Several explanations can be offered which are reviewed by Carswell and colleagues (Carswell et al., 2010). One of the major explanations for this discrepancy that should be pointed out is the STAIR (Stroke Therapy Academic Industry Roundtable) criteria (Fisher et al., 2009). The STAIR scoring system allocates one point for each of the following eight criteria: (i) a dose-response relationship investigation; (ii) inclusion of randomization in the study design; (iii) determination of the optimal time window of the treatment investigated (iv) monitoring of physiological parameters; (v) blinded outcome assessment; (vi) assessment of at least two measures of outcome (e.g. infarct size and sensorimotor function); (vii) outcome assessment in the acute phase (1–3 days) and (viii) outcome assessment in the chronic phase (7–30 days). Most of the pre-clinical studies that were detailed and scored for quality scored only 1-4 points out of

a possible 8. However, even when the STAIR criteria have been fulfilled, it is no guarantee that a drug will show efficacy in humans. For example, the free radical scavenger NXY059, which passed the STAIR criteria, failed in subsequent clinical trials (Diener et al., 2008), although it later appeared that NXY059 had poor blood-brain barrier penetrability.

Clearly, more research is required to fully elucidate the mechanisms which promote the beneficial and detrimental effects of oestrogen. However, for the future different strategies utilising the beneficial oestrogenic effects and excluding the detrimental effects will be of importance.

1.3.6 | Mechanisms of Action of Oestrogen in Stroke

Oestrogens exert their actions through many mechanisms that may act alone or interact with each other under various circumstances. The classification of mechanisms of action can be divided into several major categories and are summarised below.

1.3.6.1 | Role of ER subtype in neuroprotection in stroke

ER knockout mice have provided a very helpful tool to investigate the role of ERα and β in the whole animal and during the complete life span of that animal. Using ERα and ERβ knockout mice, a study by Sampei and colleagues also dismissed a link between ERα and reduced infarction after MCAO. This study found no increase in infarct volumes after transient MCAO in ERα knock-out compared to wildtype mice (Sampei et al., 2000). However, oestradiol synthesis and secretion increase exponentially in these mice leading to hugely increased oestradiol levels and these increased levels may be decreasing infarct volume through receptor-independent mediated mechanisms such as antioxidant actions (Sampei et al., 2000). Dubal and colleagues demonstrated no protection with pre-treatment of 17β-oestradiol (physiological

levels) compared to vehicle in ERα knock-out mice after permanent MCAO. Although protection was observed with pre-treatment of 17β-oestradiol versus vehicle in both, wildtype and ERβ knockout mice implying a role for ERα, rather than ERβ in neuroprotection (Dubal et al., 2001).

1.3.6.2 | Genomic intra-nuclear receptor-dependent actions

These genomic effects are delayed in onset and prolonged in duration. Oestrogen couples with ERs (ERα or ERβ) to increase the transcription of specific genes described in **section 1.3.4**. There are many possible genes that may have the necessary ERE present to participate in this mode of action, including genes that influence apoptosis and those that affect neurogenesis.

1.3.6.2.1 Apoptotic and Anti-apoptotic Genes

Several of the known anti-apoptotic genes (for example, Bcl-2 and Bcl-xL) are transcriptionally activated by oestrogen, whereas pro-apoptotic genes (for example, *bnip2*) are down-regulated. This indicates that oestrogen may protect neural cells from apoptotic death by affecting the balance between apoptotic and anti-apoptotic genes (Belcredito et al., 2001, Meda et al., 2000, Patrone et al., 1999). Dubal and colleagues demonstrated that pre-treatment of ovariectomised rats with 17β-oestradiol increased the expression of Bcl-2 in the ischaemic penumbra after focal cerebral ischaemia compared to ovariectomised rats pre-treated with vehicle (Dubal and Wise, 2001). The role of Bcl-2 in protection of the brain against ischaemic stroke damage has also been demonstrated by a reduction of infarct volume after MCAO in ovariectomised transgenic mice which over-express the Bcl-2 gene compared to wildtype ovariectomised mice (Alkayed et al., 2001). These results have also been shown *in vitro;* 17β-oestradiol has been demonstrated to increase Bcl-2 levels in human NT2 neurones (Singer et al., 1998). Induction of genes such as

Bcl-2 and Bcl-xL, through these ER-dependent actions, may have multiple downstream effects that together suppress apoptosis and favour cell survival (Bratton et al., 2010, Hill et al., 2009).

1.3.6.2.2 Neurogenesis and Structural Genes

Mature neurons can compensate for injury by re-establishing functional connections through neurite regrowth in dendrites and axons (Li et al., 1998). Oestrogen may modify the expression of microtubule-associated proteins (MAPs) via genomic mechanisms, which promote tubulin polymerisation or microtubule stability during process extension. These effects may lead to changes in neuronal circuitry that enhance the protective actions of oestrogen (Reyna-Neyra et al., 2002). Oestrogen has also been shown to induce tau proteins, such as MAP-1a and MAP-2, which are markers of dendritic growth (Ferreira and Caceres, 1991). Oestrogen, bound with ERs, has also been shown to increase the expression of Gap-43 mRNA (Shughrue and Dorsa, 1993). Gap-43 is a phosphoprotein that has been implicated in axonal elongation and synaptogenesis (Chakravarthy et al., 2008). Furthermore, 17β-oestradiol has been shown to stimulate neurogenesis in the SVZ of adult ischaemic brain after injury (Brown et al., 2009).

1.3.6.2.3 Astrocytes, Oligodendrocytes, Microglia and Cell Processes

ERα immunoreactivity has been demonstrated on an ultrastructural level in the hippocampus, namely in unmyelinated axons, axon terminals containing small synaptic vesicles. ERα in synaptic vesicles of axon terminals is of potential functional relevance, given that oestrogen can influence neurotransmitter release (see review (McEwen, 2001)). However, any other possible roles of axonal ERs in healthy or injured cells are unclear. ERα immunoreactivity was demonstrated in asymmetric and symmetric synapses in dendritic spines and glial processes, suggesting that both excitatory and inhibitory transmitter systems are associated with

ERα (Milner et al., 2001). McEwen in 2002 reported the presence of the ER in dendrites and axon terminals in the hypothalamus (McEwen, 2002). Bingham and colleagues demonstrated they do not protect axons from ischaemic injury (Bingham et al., 2005). ERβ has been also detected in oligodendrocytes (Platania et al., 2003) and ERs has been found in bovine myelin sheaths, indicting a potential role for oestrogen in myelin maintenance or functions (Arvanitis et al., 2004). These ERs had similarities to ERβ but were believed to be a non-classical membrane-associated ER.

Neurons, oligodendrocytes and astrocytes are all capable of steroidogenesis (Zwain and Yen, 1999). Furthermore, for more than two decades it has been known that astrocytes are one of the cellular targets of oestradiol in the brain (Tranque et al., 1987). ERα has been documented to be expressed in astrocytes after injury (stab wound) (Garcia-Ovejero et al., 2002). Sato and colleagues also demonstrated the presence of ERα in cultured astrocytes. In this study, ERα was co-localised with the glutamate-aspartate transporter (GLAST) on the plasma membrane of astrocytes. Activation of ERα was found to down-regulate GLAST, thereby decreasing the glutamate uptake activity of astrocytes. This is a potentially harmful action of oestrogen as this decrease in glutamate uptake could lead to toxic levels of extracellular glutamate and subsequent cell death by excitotoxic pathway (Sato et al., 2003). ICI 182, 780, a nuclear oestrogen antagonist, completely blocked these effects of oestrogen, demonstrating the actions to be mediated by nuclear ERs (Sato et al., 2003). Another important mechanism that may be associated to the neuroprotective actions of oestradiol relevant to stroke is the control of brain oedema by the enhancement of aquaporin-4 expression in reactive astrocytes and peri-vascular glial processes (Tomas-Camardiel et al., 2005).

Furthermore, oestradiol delays the exit of oligodendrocyte progenitor cells from the cell cycle, enhances myelin membrane sheet formation (Arevalo et al., 2010, Marin-Husstege et al., 2004) and the synthesis of myelin basic protein (Jung-Testas et al., 1992) by oligodendrocytes. The actions of oestradiol on the glial cells involved in myelin formation may be highly relevant under pathological conditions. Oestrogen protects against white matter damage and promotes remyelination in experimental models of CNS demyelination (Kipp and Beyer, 2009) and neurodegeneration (Gerstner et al., 2009, Gerstner et al., 2007).

In addition, significant experimental evidence is present that shows 17β-oestradiol may directly or indirectly regulate three distinct components of the inflammatory response: 1) microglial activation (Vegeto et al., 2008), 2) activation of transcription of inducible nitric oxide synthase (iNOS) (Vegeto et al., 2001) and 3) the activation of cytokines/chemokines. Each component represents a distinct feature of inflammation that is not necessarily mutually exclusive. *In vivo* and *in vitro* studies also pinpoint role(s) for both ERα (Tiwari-Woodruff et al., 2007, Vegeto et al., 2003) and ERβ (Baker et al., 2004, Tiwari-Woodruff et al., 2007) as regulators of the brain's inflammatory response.

1.3.6.2.4 Vascular system

The vasculature is recognised as an important target for oestrogen action. Normal blood cells are complex structures; with walls comprised principally of smooth muscle cells and an endothelial cell lining. ERα and ERβ have been identified in vascular smooth muscle (Karas et al., 1994) and endothelial cells (Venkov et al., 1996, Klinge et al., 2005). In normal blood vessels, the endothelium releases NO in response to a variety of stimuli, leading to vasodilation (Irribarra et al., 2000). But, in diseased blood vessels with dysfunctional endothelium, release of NO is attenuated (Irribarra et al., 2000, Moncada and Higgs, 1993). Oestrogen increases the

expression of many genes in the cardiovascular system (reviewed in (Mendelsohn and Karas, 1994)), including NOS (**Figure 1.15**). Thus, eNOS is both rapidly activated by oestrogen, as described above, and the eNOS gene expression is also upregulated by oestrogen. Oestradiol has been shown to induce iNOS in rat aorta, which attenuates vasoconstriction (Binko and Majewski, 1998), suggesting that oestrogen may also enhance vascular bioavailability of NO by beneficial effects on this inducible form of NOS.

1.3.6.3 | In-direct genomic membrane receptor-dependent actions

Oestrogen has been proposed to bind to receptors located out with the cell nucleus, at the plasma membrane of the cell (see **section 1.3.4**). This could lead indirectly to gene transcription, by modulating intracellular signalling processes, such as the MAPK cascade. This pathway is very fast, in contrast to genomic, nuclear-receptor-dependent actions. The MAPK cascade is involved in cell proliferation, neuronal differentiation (Kyosseva, 2004) and neuronal survival (Toran-Allerand, 2004).

Rapid effect of oestrogen on neuronal excitability has been known for a number of years and has been reviewed by Rønnekleiv and colleagues (Ronnekleiv et al., 2007). Oestradiol treatment has also been well documented to increase hippocampal NMDA receptors expression (Foy et al., 2008, Zamani et al., 2004, Woolley et al., 1997). The promoters of the rat NMDA receptor subunit 1 (Bai and Kusiak, 1997) and 2B (Klein et al., 1998) has been cloned and no ERE has been reported, indicating that non-genomic or indirect genomic actions are responsible for this increase. There is evidence for interactions of ERs with second messenger systems (Kelly and Levin, 2001, Brinton, 2001) indicating indirect genomic actions to be responsible for the actions of oestrogen on NMDA. It has been reported that 17β-oestradiol mediated activation of the MAPK pathway in the rodent hippocampus was involved in the rapid effect of oestrogen on

NMDA receptors (Bi et al., 2000). Other groups added to this theory by showing that inhibitors of MAPKs can block the neuroprotective effect of oestrogen against glutamate toxicity (Singer et al., 1999, Bi et al., 2000). The actions of oestrogen to increase NMDA receptors may be important in synaptogenesis and plasticity. Antagonists of NMDA receptors were found to block oestrogen-induced synaptogenesis on dendritic spines in ovariectomised female rats (Woolley et al., 1997). Another study by Brann and colleagues also reported an increase in mRNA levels for NMDA receptors in the cerebral cortex of rats following oestradiol replacement (Brann et al., 1993). However, as described in **section 1.1.3.2**, NMDA receptor is an ionotropic subtype of glutamate receptor. Upregulation of NMDA receptors could increase levels of glutamate to excitotoxic levels. Therefore, an upregulation of NMDA receptors could lead to excitotoxic cell death, thereby providing a possible detrimental action of oestrogen.

However, in contrast to this theory and the above reports, oestrogen has also been reported to inhibit NMDA-induced toxicity in primary cultures of rat cortical neurones (Kajta et al., 2001, Kajta et al., 2002). Furthermore, Singer and colleagues also showed oestrogen to protect against glutamate toxicity of primary cortical neurones and reported the pathway to this protection to be through activation of the MAPK cascade (Singer et al., 1999). There may be an imbalance between excitation and inhibition of NMDA receptors by oestrogen that ultimately determines neuronal injury and death after insults such as cerebral ischaemia.

1.3.6.4 | Non-Genomic, Membrane Receptor-Dependent Actions

The effect of oestrogen on calcium channels and calcium release from intracellular stores has emerged as a possible cellular mechanism of oestrogen action that is relevant to excitability and neuronal vulnerability to damage. In the proposed non-genomic pathway for oestrogen action on calcium homeostasis, 17β-oestradiol activates a G-protein-coupled receptor in rat neostriatal

neurones and, within seconds, suppresses currents mediated by L-type calcium channels (Mermelstein et al., 1996). This action could prevent massive influxes of calcium to a cell, thereby protecting it from injury. The oestrogen antagonist, tamoxifen, was found to mimic rather than block this action (Mermelstein et al., 1996), thus further supporting the presence and use of a unique ER on the cell surface.

In addition, native oestrogen or exogenous 17β-oestradiol can act as direct vasodilators or through vasodilatory mediators during ischaemic stress. Numerous studies document vasomotor effects of oestrogen under non-ischaemic conditions and 17β-oestradiol is a dilator of most vascular beds (reviewed in (Mendelsohn and Karas, 1994, White et al., 1995a, White et al., 1995b) (**Figure 1.15**). The flow enhancement effects of oestradiol have been demonstrated convincingly in global and forebrain ischaemia (Hurn and Macrae, 2000, Pelligrino et al., 1998) and limited evidence is available in focal cerebral ischaemia (Alkayed et al., 2001, Shi et al., 1998). This may result from limitations of the methodologies to measure cerebral blood flow or may suggest that for focal cerebral ischaemia, the protective effects are nonvascular. Under basal conditions, the rapid vasodilatory effects of oestradiol do not require changes in gene expression and are produced in part by oestrogen-stimulated increases in endothelial NOS activity (Mendelsohn and Karas, 1994). These non-genomic, receptor-dependent effects are applicable to 17β-oestradiol, mediated through membrane-bound ERα and are executed through signal transduction pathways such as the Akt/PKB cascade (Bucci et al., 2002).

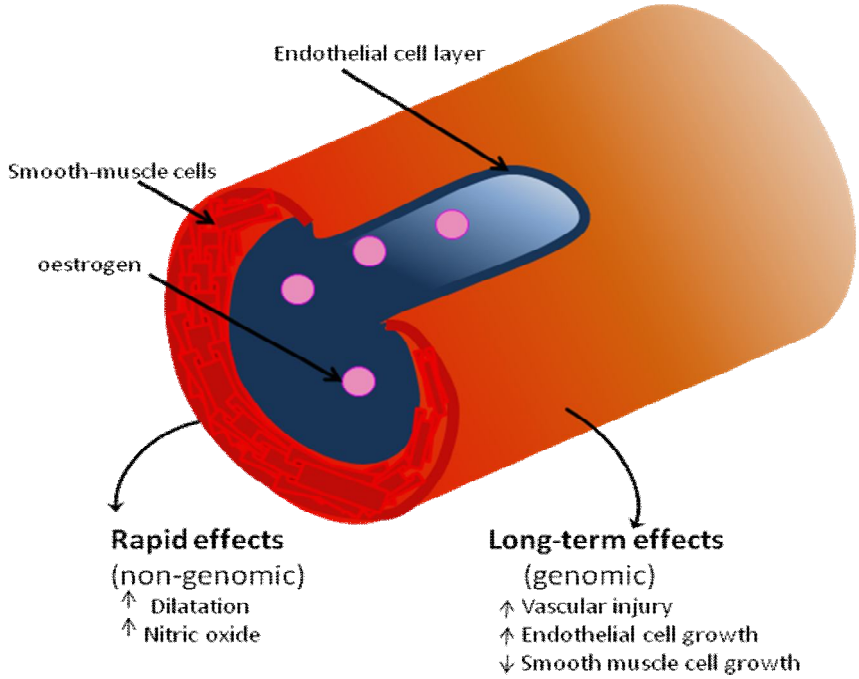

Figure 1.15: Direct effects of oestrogens on blood vessels.

Vascular endothelial and smooth-muscle cells express the three known ERs. Oestrogen has both vasodilatory effects and longer-term actions that inhibit the response to vascular injury. These effects are mediated by direct actions on vascular endothelial cells and smooth-muscle cells. The rapid effects of oestrogen are believed to be non-genomic, whereas longer-term effects involve changes in gene expression (Mendelsohn and Karas, 1994).

1.3.6.5 | Non-Genomic, Receptor-Independent Actions

As described in **section 1.3.4.4** the hydroxyl group at the A ring of oestrogen can donate a hydrogen, thereby detoxifying accumulating free oxygen radicals. A chemical study carried out in the absence of living cells or cellular abstracts showed a very high dose of 3 of the oestrogens, 17β-, 17α-oestradiol or oestriol, to reduce the generation of free radicals, whereas other steroids were ineffective (Mooradian, 1993). This suggests that it is features of the oestrogen A ring, present in these 3 oestrogens, involving the 3 hydroxyl group, that has the ability to interfere with free radical production in the absence of proteins or other cellular materials. However, the

concentration of oestrogen needed to permit antioxidant actions has been shown in this study and others (Behl et al., 1997, Green et al., 1997) to be above the physiological range. But, accumulation of oestrogen in cellular membranes over time could reach this level and the effective concentration could be reduced to physiological levels in the presence of supporting antioxidants such as glutathione (Green et al., 1998). Disruption of mitochondria, generation of free radical and subsequent oxidative damage is an important cellular destruction process after cerebral ischaemia and it has been shown that 17β-oestradiol can act as an antioxidant to minimise the damage caused by this process (Wang et al., 2001a).

1.3.6.6| Oestrogen and Neurotrophins

Neurons in male and female animals have been shown to co-express oestrogen and neurotrophin receptors (Miranda et al., 1993b, Miranda et al., 1993a, Toran-Allerand et al., 1992). Oestrogen and the neurotrophins may influence each other's actions by regulating receptor and/or ligand availability through reciprocal regulation at the level of gene transcription. Toran-Allerand and colleagues showed that oestradiol receptors co-localise with the receptors for these neurotrophins, $p75^{NTR}$ (Toran-Allerand et al., 1992), trk A and trk B (Miranda et al., 1993a) in the basal forebrain. It has been hypothesised that oestradiol may protect against injury by increasing neurotrophin or neurotrophin receptor expression. Whether trophic effects mediate the protective actions of oestradiol on the adult brain in the face of injury is less clear. The co-localisation of ERs, neurotrophins and their cognate receptors suggests potential complex autocrine, paracrine and neuroendocrine interactions between oestrogen and neurotrophins can occur.

Oestradiol influences several growth factors that may mediate its protective actions in the brain. Few of the best studied are the insulin-like growth factor 1 (IGF-1) (Garcia-Segura et al., 2001)

and brain derived neurotrophic factor (BDNF) (Sohrabji and Lewis, 2006). The first evidence for IGF-1 and oestrogen interactive effects on neurons was provided by (Toran-Allerand et al., 1988), showing that in explant cultures of foetal rat hypothalamus, oestrogen and insulin have a synergistic action on neuron growth, an effect perhaps mediated by IGF-1 receptors. Furthermore, oestradiol modulates IGF-1 levels and cooperates with IGF-1 in inducing dendritic growth and synaptic plasticity (Duenas et al., 1996, Mendez et al., 2003). Several points of convergence of IGF-1 and oestrogen signalling may be involved in neuroprotection. For instance, both oestradiol and IGF-1 activate MAPK. MAPK interferes with c-Jun N-terminal protein kinase activation (JNK), protecting cells from apoptosis (Cheng and Feldman, 1998). Jezierski and colleagues showed injections of a neutralizing antibody to the BDNF receptor trkB reduced CREB-phosphorylation in a forebrain circuit and combined injections of anti-trkB and the receptor for nerve growth factor, anti-trkA reduced oestrogen-mediated increases in ChAT expression (Jezierski and Sohrabji, 2003), indicating that oestrogen may exert its actions via a neurotrophin receptor complex.

1.3.7 | Functional Recovery and Oestrogen

Stroke is not only a leading cause of death, but also of disability in humans (Youman et al., 2003). Improving functional outcome after stroke is the ultimate goal of stroke treatment. Behavioural studies have demonstrated that ovariectomised adult rats display impaired learning and memory, which was reversed with oestradiol replacement (Barha et al., 2010). Treatment with oestrogen in the undamaged brain has been reported to increase anxiety, fear learning and running wheel activity, suggesting an overall arousing effect of the hormone (Bowman et al., 2002, Das et al., 2002).

The MCAO model of focal ischaemia typically results in extensive neuronal death in the cortex and caudate putamen regions of the brain (Tamura *et al*., 1981). However, it can be difficult to distinguish the extent to which neuronal damage in each of these regions contributes to altered sensorimotor performance because the caudate putamen receives extensive input from the sensorimotor regions of the cortex (DeVries et al., 2001). Numerous studies have reported functional deficits in rodents after focal cerebral ischaemia (see review (DeVries et al., 2001). However, there are fewer studies examining the effects of oestrogen treatment on functional recovery after focal ischaemia.

Li and colleagues investigated the effects of gender on behavioural testing after stroke in mice (Li et al., 2004). They found that oestrogen treatment increased the speed of recovery in the cylinder test, a measure of forelimb use, after transient MCAO (Li et al., 2004). In contrast, Farr and colleagues investigated the mechanisms by which oestrogen promotes repair and recovery in the peri-infarct zone. They found that 17β-estradiol treatment post- permanent MCAO did not influence recovery of function using the cylinder and the vibrissae-evoked forelimb placing test or synaptogenesis (Farr et al., 2006). Alongside they also investigated the contribution of ERβ in the permanent MCAO model using selective ERβ agonists, diarylpropiolnitrile (DPN) and did not observe a difference in infarct size or sensorimotor function in rats (Farr et al., 2007).

There are many reports of oestrogen treatment providing neurorestoration and re-modelling after focal ischaemia with one of the many proposed mechanisms being enhanced plasticity and neurogenesis (see **sections 1.3.6.1**). Therefore, it may be expected that oestrogen could enhance functional recovery after stroke.

1.3.8 | Oestrogen and Stem cells

Brannvall and colleagues showed that embryonic and adult NSC expresses both ERα and ERβ (Brannvall et al., 2002). Furthermore they showed that 17β-estradiol can influence proliferation and differentiation of embryonic NSC and that the effect of 17β-estradiol on cell proliferation was dependent on the presence of other growth factors such as epidermal growth factor (EGF), and that the steroid hormone can promote neurogenesis of embryonic NSC (Brannvall et al., 2002). Fried and colleagues also reported the presence and sub-cellular localization of ER in human embryonic NSCs and that the expression of the receptor was regulated by oestrogen (Fried et al., 2004). Alongside, Kishi and colleagues showed that oestrogen promotes differentiation and survival of dopaminergic neurons derived from human embryonic NSCs *in vitro* and *in vivo* (Kishi et al., 2005).

Experiments in several animal models revealed that oestrogen accelerates re-endothelialisation processes after injury. Strehlow and colleagues showed that lack of oestrogen increased neointima formation and that this effect was inhibited by oestrogen replacement therapy, after carotid artery injury in mice (Strehlow et al., 2003). Recently, Sun and co-workers have reported that oestrogen affects the healing of ischaemic myocardium partially through paracrine growth hormone production by the BMSCs and facilitates recruitment of EPCs to the ischaemic myocardium (Sun et al., 2010). Oestrogen can also reduce the proliferation of the cardiac fibroblasts thus effectively enhancing the neo-vascularisation at the ischaemic border zone and limiting pathological myocardial remodelling. Very recently, Lemieux and group identified key factors involving adhesion, migration, and proteolysis were regulated by 17β-estradiol which influences the functional organization of the bone marrow derived stem cell niche (Lemieux et al., 2008).

1.4 | Aims of the study

The aim of the present study was,

- To determine whether an immortalised temperature sensitive murine neural stem cell line, the Maudsley hippocampal stem cell line clone 36 (MHP36) could improve behavioural outcome in mice,
- To characterise the MHP36 cells for oestrogen,
- To determine whether MHP36, genetically modified to over-express oestrogen (Dax-1KD-MHP36), completely restore sensorimotor function after transient MCAO in mice and
- To determine the mechanism by which oestrogen promotes the enhanced functional outcome.

CHAPTER 2

GENERAL MATERIALS AND METHODS

2.1 | Materials

2.1.1 | Animals

C57BL/6 mice were purchased from Charles River Labs (UK) for studies performed in Chapters 5 and 6 and from in-house stocks for Chapter 4. They were housed in a temperature and light-controlled animal care facility and given food and water ad libitum.

2.1.2 | Sutures

- A non-sterile silk thread for ligations (18020-60 FST, Germany).
- A 5-0 nylon monofilament resin coated for occlusion of MCA (Ethicon, UK).
- A 7-0 silicone coated filament for occlusion of MCA (7-0CL9TD023RE Doccol, USA).
- A 5-0 mersilk suture for closing the skin incision (Ethicon, UK).

2.1.3 |Special equipment and surgical instruments

- A tabletop anaesthesia machine with scavenger (Supernova, UK).
- An operating microscope (Carl-Zeiss, Germany).
- A hot-bead dry steriliser- Germinator 500 (Southpointe Surgical, USA).
- A lubricated homeothermic blanket and temperature probe (Harvard Apparatus, UK).
- A diathermy probe and unit (Bipolar Coagulation Unit).
- Laser Doppler (Moor Instruments- dual channel, UK).
- Triangular swabs (Royem Scientific, USA).
- Microvascular clip (FST, Germany).
- Forceps - Dumont 90° angled (11253-29 FST, Germany).
- Dual manipulator stereotaxic frame for small species (Harvard Apparatus, UK)
- Mouse stereotaxic adaptor and ear bars (Harvard Apparatus, UK)

2.1.4 | Antibodies

- Anti-aromatase (raised in rabbit) gift from J. Hutchison, L. Garcia-Segura (Madrid, Spain).
- Anti-ERα (raised in mouse, Novachem, Australia).
- Anti-ERβ (raised in mouse, CO1531) gift from G. Greene (Chicago, USA).
- Anti-GPR30 (raised in rabbit, Abcam, UK).
- Anti-Dax-1 (raised in rabbit, Abcam, UK).
- Anti-GAPDH (raised in mouse, Abcam, UK).
- Anti-p38 (raised in rabbit, Santa Cruz, UK).

2.1.5 | Chemicals and reagents

All reagents were purchased from Sigma (Poole, UK) unless otherwise stated in the text.

2.2 | Methods

2.2.1 | Cell culture

The derivation and culture of the MHP36 cell line was as previously described (Sinden et al., 1997). Briefly, this immortalised cell line was originally derived by dissecting embryonic day 14 hippocampal proliferative zone of heterozygotic H-2K^b-tsA58 transgenic mice, in which a temperature-sensitive mutant of the SV40 large T antigen is brought under the control of the interferon-inducible H-2K^b promoter.

In culture, MHP36 cells were grown in serum-free medium at their permissive temperature of 33 °C, interferon-gamma (IFN-γ)$^+$ in an atmosphere of 5 % CO_2 and humidified air. They were cultured in DMEM/F12 (Gibco, UK) with the following additives, 0.03 % bovine serum albumin (BSA) Path-o-cyte (ICN), 54 ng/ml progesterone, 15 µg/ml putrescine, 5 µg/ml bovine pancreatic insulin, 38 ng/ ml selenium, 94 µg/ml human apo-transferrin, 2 mM L-glutamine (Gibco, UK), 9.4 U/ml heparin, 317 ng/ml tri-iodo-thyronine, 380 ng/ml L-thyroxine, 10 ng/ml basic fibroblast growth factor (bFGF) (Peprotech, USA), 1.2 ng/ml IFN-γ (Peprotech, USA). Cells were fed by replacing media every second day, and passaged by discarding the medium and washing with Hanks Balanced Salt Solution (HBSS) (Gibco, UK) without Ca^{2+} and Mg^{2+} to aid detachment. After a brief wash, cells were incubated at 33 °C with 5 ml versene (Gibco, UK) until dislodged. Following this, solution was inactivated by adding an equal amount of HBSS with Ca^{2+} and Mg^{2+}. Cells were spun-down and re-suspended in the media before being re-plated onto flasks or plates which were pre-coated with 1 µg/ml fibronectin.

2.2.2 | Immunocytochemistry

Immunocytochemistry involves the detection of antigens in cells. An antigen on a cell can be labelled using a primary antibody with one (monoclonal) or more than one (polyclonal) site for binding to the antigen. A biotinylated secondary antibody can then be applied to bind to the primary antibody. The signal identifying the antigen is amplified with the addition of a horseradish peroxidase (HRP)-streptavidin buffer, which couples to the biotinylated secondary antibody. A visualisation chromogen, such as 3,3'-diaminobenzidine (DAB), reacts with this complex to produce a visible brown deposit representing antigenic cells where the antigen is present (**Figure 2.1A**).

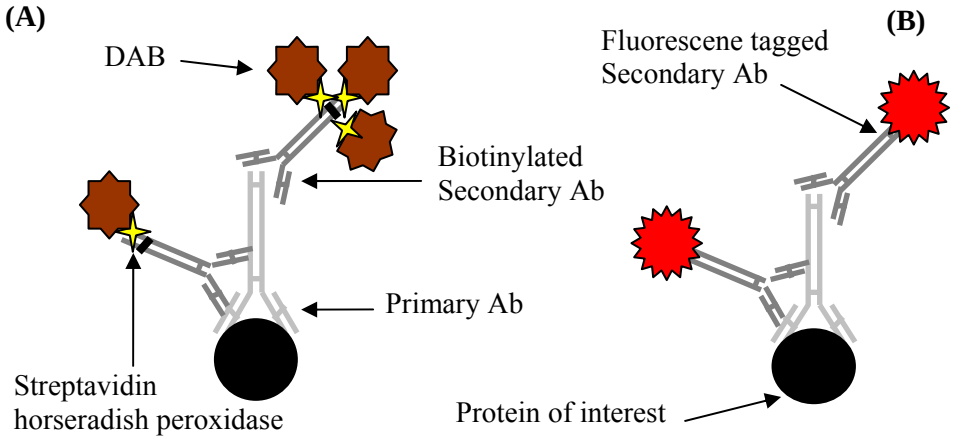

Figure 2.1: Schematic representation of Immunostaining using primary and secondary antibody.

(**A**) Immunocytochemistry using DAB as a chromogen. (**B**) Immunofluorescene using fluorescent dye tagged to the secondary antibody. Ab= Antibody

MHP36 cells were grown on fibronectin-coated cover slips and fixed by aspirating the culture medium and applying 4 % paraformaldehyde in phosphate buffered saline (PBS) for 10 min.

Cells were then treated with 3 % H_2O_2 in distilled water for 30 min to block endogenous peroxidase. Non-specific binding was blocked using 1 % BSA in PBS (blocker solution) for 1 h at room temperature and then primary antibody specific for the protein of interest added without washing. The primary antibody was prepared in blocker solution, cover slips were incubated overnight at 4 °C. The primary antibodies were reacted using biotinylated IgG followed by incubation with a HRP-streptavidin buffer for 20 min, using DAB as a chromogen. After washing, cover slips were mounted on slides using Mowiol and stored in the cold room until they were viewed and photographed. HeLa (cervical cancerous cell line) cells were used as positive control. A negative control was included in every immunohistochemistry run. These cover slips followed the same protocol as the others except that the primary antibody was omitted. Cover slips were instead incubated with blocker alone.

2.2.3 | Immunofluorescence of tissue and cells

Tissue or cells were fixed, blocked and incubated in primary antibody overnight at 4 °C in a wet box. The secondary antibody IgG bound to Texas red (Vector labs, UK), Alexafluor 555 (Chemicon, UK) or fluorescein isothiocyanate (FITC) made in PBS was applied for 1 h at room temperature. After washing in PBS, cover slips were mounted (Vectashield hard set with DAPI, Vector Labs, UK) (**Figure 2.1B**) and stored in the dark at 4°C until they were viewed and photographed using a Nikon Eclipse™ E600 Oil Immersion microscope connected to a photometrics (CoolSnap™ Fx) digital camera managed by MetaMorph™ software (Universal Imaging Corporation, USA). HeLa and MCF7 cells were used as positive control.

2.2.3.1 | Immunofluorescence Image Analysis

The resulting images acquired were entered into Image-J system (Universal Imaging, USA) software program where they were analysed to derive the intensity of fluorescence across a set area for each region of interest (ROI). The analysis setup consisted of standard procedures, including spatial calibration, image acquisition and thresholding.

For purpose of main study (described in Chapter 5 & 6) - Three animal brains were randomly (confirmed with behavioural data to avoid bias selection) stained for the different markers. During image acquisition, the threshold and gain on the confocal laser microscope were set using the control for each run of staining. This helped to subtract the background fluorescence. The obtained values used for graphical representation are a ratio of intensity and area. ROI for differentiation consisted of the ipsilateral striatum and somatosensory cortex within each brain. ROI for synaptic plasticity consisted of the ipsilateral striatum and somatosensory cortex and contralateral striatum and somatosensory cortex within each brain. Two images were taken in each ROI; the cortex and the striatum for quantification. No comparisons were made between the cortex and striatum.

2.2.4 | Western Blotting of tissue and cells

Whole cell extracts were prepared by harvesting cells from 100 % confluent 6 well plates in 1X loading buffer (2 % w/v sodium dodecyl sulphate (SDS), 50 mM dithiothreitol (DTT), 10 % glycerol, 63 mM Tris–HCl (pH 6.8), 5 mM ethylene-diamine-tetra-acetic acid (EDTA) , 2 mM sodium pyrophosphate anhydrous ($Na_2P_2O_7$), 0.007% w/v bromophenol blue). Tissue extracts were prepared by homogenising weighed tissue in five volumes of homogenisation buffer (20mM Tris-base buffer, (pH 7.4), 10 µl/ml protease inhibitor cocktail, 1mM DTT) using an

ultraturrax (Labortechnik, UK). The tissue samples were stored at -80 °C until use. Proteins were separated on a 10 % medium polyacrylamide denaturing gel using running buffer for 90 min at constant voltage (120 V) and were electrophoretically transferred using transfer buffer to a nitrocellulose membrane (Amersham Pharmacia Biotech) for 90 min at constant current (300 mA). The membrane was blocked for 90 min at room temperature with 2 % BSA made in 150 mM NaCl, 50 mM Tris-HCl, 0.2 % (v:v) Tween-20 (NATT) buffer and then probed with a primary antibody in 0.2 % BSA in NATT, overnight. After being washed in NATT for 90 min (15 min each), the membrane was incubated for 90 min with a specific secondary antibody in 0.2 % BSA in NATT. The signal was developed by enhanced chemiluminescence (ECL; GE Healthcare, UK Amersham Pharmacia Biotech) and visualised on a Kodak BioMax film (**Figure 2.2**). Blots were stripped and re-probed with housekeeping proteins for internal control for loading. The protein mass was determined by evaluating the intensity of the bands by scanning video densitometry and expressed (Prot. Expression) as arbitrary units (A.U.) normalised to housekeeping protein expression.

2.2.5 | Bradford's Assay

To determine the concentration of protein in the MHP36 cells sample analysed for aromatase in Western blotting, Bradford's assay was used. The method is based upon the formation of a complex between the dye, Brilliant Blue G, and proteins in solution. The protein-dye complex causes a shift in the absorption maximum of the dye from 465 to 595 nm. The amount of absorption is proportional to the protein present. The Bradford's assay was as previously described (Bradford, 1976). Briefly, whole cell lysates were analysed in duplicates using a commercially available Bradford Reagent (range: 1–1000 µg protein/ml). To determine the

protein concentration of a sample from its absorbance, a standard curve of BSA was plotted (1 µg/µl) which was used to extrapolate the concentration of the sample.

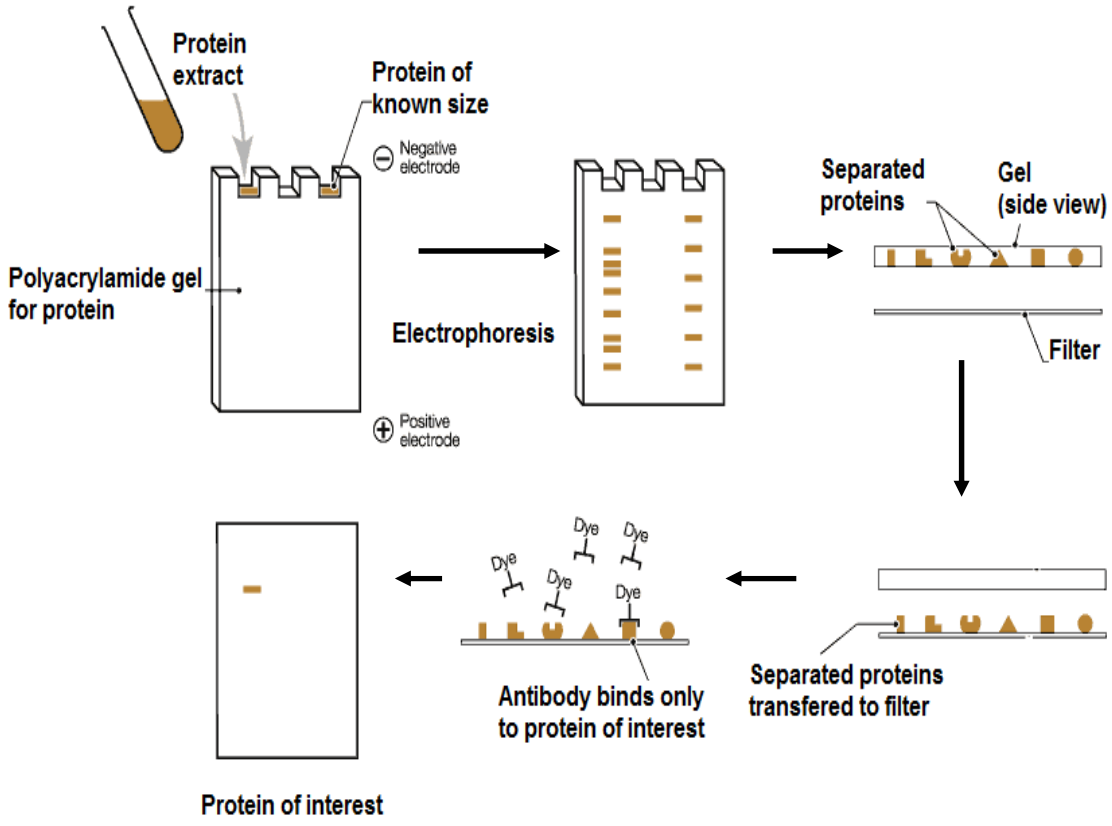

Figure 2.2: Schematic representation of western blotting

2.2.6 | Reverse transcription (RT)-PCR

2.2.6.1| RNA isolation and cDNA synthesis

Total RNA was extracted from suspensions of MHP36 cells by using an RNeasy Mini kit (Qiagen, UK) according to manufacturer's instructions. The quantity of RNA extracted was

determined by spectrophotometric determination and calculating the A260/A280 ratio. The purity of the sample obtained was ≥ 1.7. Aliquots of 3 µg of total RNA were incubated with 0.5 µl oligo(dT), 1 µl of dNTP mix (10 mM each dATP, dCTP, dGTP, dTTP) and diethyl pyrocarbonate (DEPC)-treated H_2O for 5 min at 65 °C and further incubated on ice for at least 1 min to avoid reannealing. The RT reactions were performed with 13 µl of the RNA solution treated as above with 4 µl of first strand buffer (5X), 1 µl of 0.1 M DTT, 1 µl of DEPC-H_2O and 1 µl of SuperScript III reverse transcriptase (200 units/µl) (Invitrogen, UK) for 60 min at 42 °C.

The primers used for aromatase were:

Sense (first round): 5'-AGCATGCGGTACCAGCCTGT-3' (1128-1147)

Antisense (first round): 5'-TCATCATCACCATGGCGATGT-3' (1363-1383) (Liu et al., 2007).

Product size: 256bps

Sense (second round): 5'-GGATGTGTTGACCCTCATGAGAC-3' (596-618)

Antisense (second round): 5'-GATGTTTGGTTTGATGAGGAGAGC-3' (714-740)

Product size: 145bps

The primers used for ERα were (designed in-house):

Sense: 5'-AATTCTGACAATCGACGCCAG-3'

Antisense: 5'-GTGCTTCAACATTCTCCCTCCTC-3'

Product size: 345bps

The primers used for ERβ were (designed in-house):

Sense: 5'-CTTGGTCACGTACCCCTTAC-3'

Antisense: 5'-GTATCGCGTCACTTTCCTTT-3'

Product size ERβ 1: 250bps and ERβ 2: 304bps

The primers used for GPR30 were (designed in-house):

Sense: 5'-CCTTAAGCTGCTGGAATTGTGG-3' (340-359) (5UTR)/

5'-CGACTACTCCAGCCCAAACTGTTG-3' (618-637) (ORF)

Antisense: 5'-GCCGCCAGGTTGATGAAGTAC-3' (899-918)

Product size using 5UTR forward primer: 250bps

Product size using ORF forward primer: 301bps

The GPR30 has its coding sequence in exon 3 only to exclude the interference of genomic DNA; one forward primer was located in exon 2 (5UTR forward) and another set was designed in the open reading frame (ORF) (**Figure 2.3**).

2.2.7 | PCR reaction

PCR reactions were performed using 1 µl of cDNA in 49 µl of reaction mixture containing: 5 µl forward primer and reverse primer each, 25 µl of HotStar DNA polymerase buffer (2X) (Invitrogen, UK) and 14 µl of DEPC-H_2O. Reactions were placed in a thermal cycler programmed thus: PCR amplification, 35 cycles of 94 °C for 1 min, 55 °C for 30 s and 68 °C for 1 min with a final extension of 68 °C for 5 min. Products (15 µl PCR product + 2 µl gel loading solution) were resolved on a 2 % agarose gel. Reactions lacking RT were included as negative controls and blanked using water.

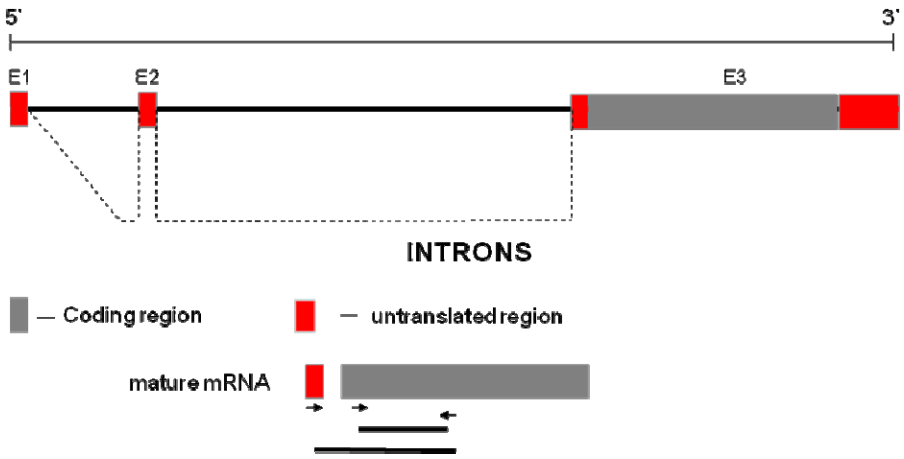

Figure 2.3: Representative for GPR30 sequence and primer locations

2.2.7.1 | Semi-nested PCR reaction

Semi-nested PCR was performed for aromatase only since the amplicon was negligible using standard PCR. Reaction 1 (forward of second round and reverse primer of first round) was placed in a thermal cycler programmed thus: PCR amplification, 25 cycles of 94 °C for 1 min, 55 °C for 30 s and 68 °C for 1 min 30 s with a final extension of 68 °C for 5 min. Reaction 2 was set up using the product obtained from Reaction 1 (1 µl of product and 49 µl of master mix (first round of primers), as described above). **Figure 2.4** explains the concept of semi-nested PCR. Products (15 µl PCR product + 2 µl gel loading solution) were resolved on a 2 % agarose gel. Reactions lacking RT were included as negative controls and blank using water.

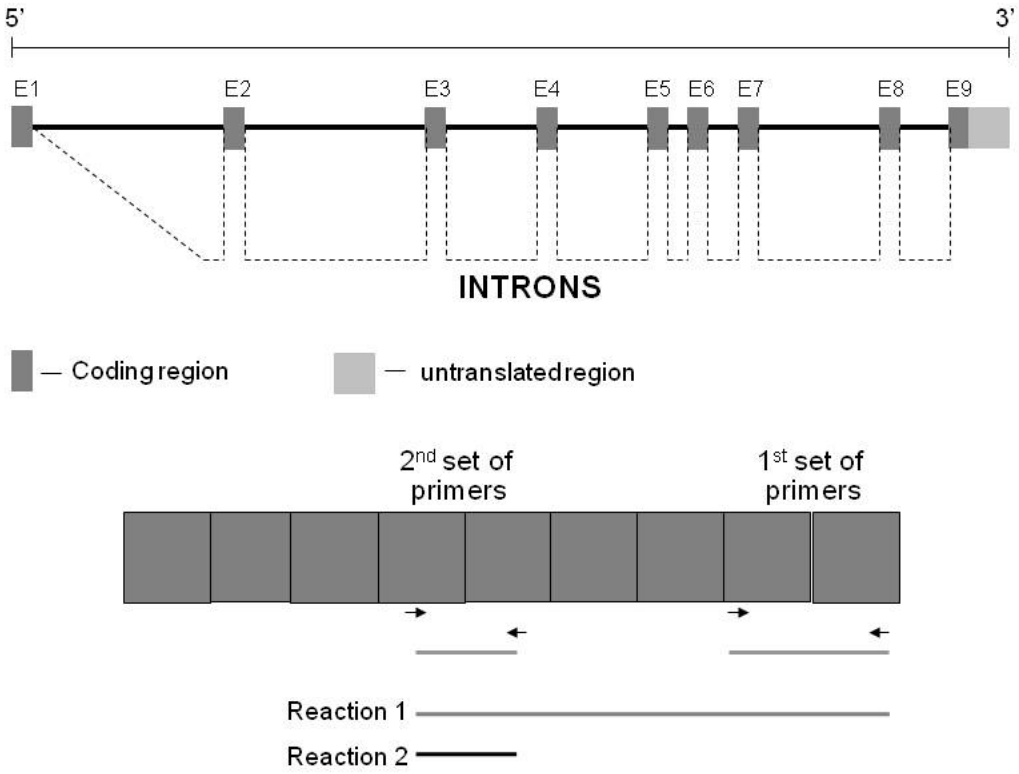

Figure 2.4: Semi-nested PCR for aromatase displaying sequence and primer locations

2.2.7.2 | Sequencing the amplicon

The PCR products were gel isolated using the QIAquick Gel Extraction kit (Qiagen, UK), and the sequences were purified and then sequenced at the University of Strathclyde Molecular Biology Facility using Big Dye Terminator v3.1 Chemistry (Applied Biosystems, UK) and a 3100-Avant Genetic Analyzer (Applied Biosystems, UK). At the end of the sequencing a chromatogram was obtained which included the sequence of the amplicon and could be viewed using software Chromas (Technelysium, Australia). Each forward and reverse template was sequenced and stitched to obtain the amplicon sequence of the desired size. This stitched sequence was then searched as a query against the murine database for 100 % hits to each

protein of interest to confirm the purity of the sample. This was carried out for each protein of interest for confirmation.

2.2.7.3 | Design of primers

Mouse aromatase, ERα, ERβ and GPR30 primers were chosen from inspection of the cDNA sequence of the aromatase, ERα, ERβ and GPR30 genes from the Nucleotide sequence database in GenBank. A search was then performed using Basic Local Alignment Search Tool (BLAST) to determine the location of exon–exon junctions and primers were designed by specifying a target region corresponding to the junctions. The specificity of the primer pair enclosed sequences was confirmed by BLAST search and the absence of polymorphisms in these regions was verified. To avoid detection of contaminating genomic DNA, the primers were located in exons and not in introns (Liu et al., 2007). The sequence for mouse aromatase, ERα, ERβ and GPR30 mRNA was obtained from GenBank (Gene ID: 13075, 13982, 13983 and 76584 respectively). The second set of primers was designed after personal communication with L. Garcia-Segura (Madrid, Spain) (provided with the aromatase antibody). The primers were ordered from Eurofins Ltd.

2.2.8 | Genetic modification of MHP36 cells to over-express oestrogen

The genetic modification of the MHP36 cells was carried out in King's College, London by Dr. Dafe Uwanogho who then supplied the genetically modified stem cells for characterisation and transplantation. Briefly, two approaches were carried out 1) Dax-1 knock-down and 2) aromatase over-expression to achieve subsequent enhanced oestrogen synthesis.

2.2.8.1 | Dax-1 Knockdown

The insert was a short hairpin RNA (shRNA) targeted to Dax-1 (Mission RNAs from Sigma) which resulted in the degradation of Dax-1 RNA and so the attenuation of Dax-1 protein expression. Lentiviral particles, made using standard protocols, were used to transduce stem cells at various multiplicity of infections (MOIs) and then stably expressing stem cells were selected using puromycin. The biological consequence of the insert was the same as removing Dax-1. However, the knockdown process will never be 100 % so there will always be some Dax-1 presence. The level of expression of aromatase and oestrogen production have been characterised following this procedure (discussed in **Chapter 3**).

2.2.8.2 | Aromatase over-expression

Briefly, a cassette containing genes encoding the full length human aromatase and a blasticidin resistance gene was isolated by cutting the parental expression plasmid with BglII and XmnI. The resulting fragment was gel purified and used to stably transfect the stem cells which were selected using blasticidin.

2.2.9 | Measurement of 17β-Oestradiol

2.2.9.1 | Extraction of 17β-Oestradiol

The assay used to measure 17β-oestradiol levels was designed to analyse human plasma. The steroid releasing agent was not designed to remove rodent binding proteins. Therefore, the 17β-oestradiol was first extracted from the neural stem cells or supernatant (media) and reconstituted in steroid-free human serum (DRG International Inc., USA) before being measured using the 17β-oestradiol Immunoassay (ELISA, DRG International Inc., USA). Briefly, to 200 µl of sample, 800 µl of methanol was added to an Eppendorf and subsequently vortexed for 1 min. The samples were then centrifuged at 10,000 rpm for 5 min. The supernatant was vacuum-dried (Savant Instruments Inc., USA) until only a white residue (the 17β-oestradiol) remained (~ 5 hrs). This was reconstituted with 100 µl of steroid-free human serum and vortexed thoroughly. The sample was now 2.0 times more concentrated and was ready to be measured using the ELISA kit.

2.2.9.2 | ELISA

The DRG oestradiol ELISA kit a solid phase enzyme-linked immunosorbent assay (ELISA) based on a competitive binding. The micro-titre wells are coated with a polyclonal antibody directed towards an antigenic site on the oestradiol molecule. Endogenous oestradiol from the sample competes with the oestradiol-horseradish peroxidase conjugate for binding to the coated antibody. After incubation, the unbound conjugate is washed off. The amount of bound peroxidase conjugate is inversely proportional to the concentration of oestradiol in the sample. After addition of the substrate solution, the intensity of colour developed is inversely proportional to the concentration of oestradiol in the sample. See **Figure 2.5** for a detailed

flowchart of the methodology. The intra and inter assay variability is shown below for plasma used as positive control from female mice:

Sample	Mean (pg/ml)	CV%	n
Plasma	22.50	6.3	3
Plasma	26.09	11.3	3
Plasma	18.9	8.8	3

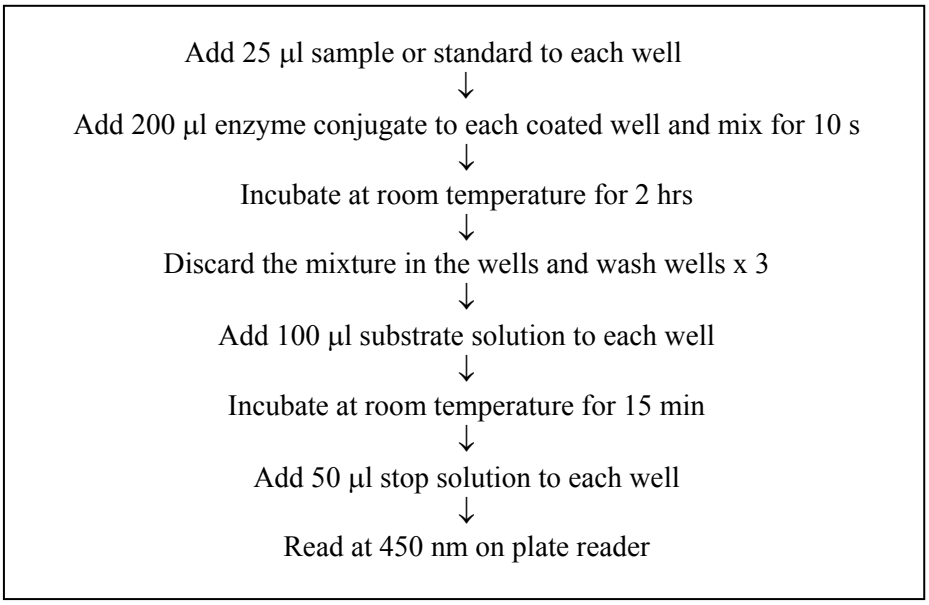

Figure 2.5: Protocol for measuring 17β-oestradiol levels using ELISA

Schematic representation of the procedure involved in measuring 17β-oestradiol levels from sample or standards.

2.2.10 | Surgical Techniques

2.2.10.1 | Preparation of Animals for Surgery

All experiments were carried out under licence from the British Home Office and were subject to the Animals (Scientific Procedures) Act, 1986. C57BL/6 mice were bred in-house or purchased from Charles River, UK.

Housing: Animals were housed in groups with conditions of a 12-hour light-dark cycle with food and water *ad libitum* unless otherwise stated.

Anaesthetic: C57BL/6 mice were anaesthetised in a Perspex chamber with 3 % isoflurane (Supernova, UK) in the presence of oxygen supplied at 1 L/min. After 2 to 3 min, the anaesthesia was switched to the mask and the animal was placed on the face-mask and the isoflurane level was lowered from 1.5 to 1.75%.

Temperature Monitoring: Throughout all procedures, the animal's body temperature was monitored using a rectal probe (Harvard Apparatus, UK) and kept within physiological limits (37.0 °C ± 0.5 °C) using a homeothermic blanket (Harvard Apparatus, UK) or heat lamp.

2.2.10.2 | Middle Cerebral Artery Occlusion (MCAO)

Permanent MCAO: The mice were anaesthetised as described above. The method of occlusion used was a modified version of Longa and colleagues (Longa *et al*., 1989) and is illustrated in **Figure 2.6**. A midline neck incision was made and the salivary glands were revealed, the glands were retracted on to saline-moistened gauze (glands were kept hydrated throughout the procedure with saline). With the help of blunt dissections, the left common carotid artery (CCA), external carotid artery (ECA), internal carotid artery (ICA) and vagus nerve were exposed. The

occipital artery and the sub-thyroid artery branching from the ECA were diathermised. The following series of ligatures were made in order (refer to **Figure 2.6C**).

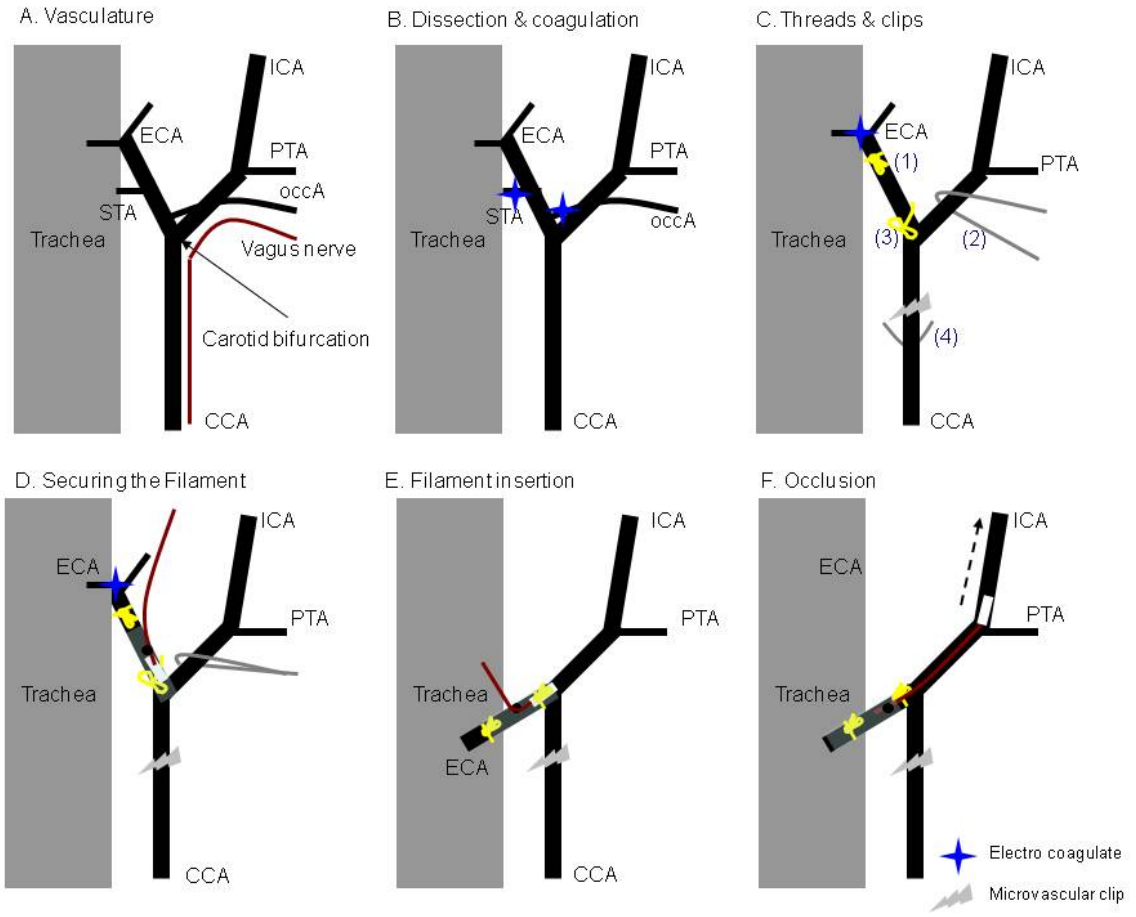

Figure 2.6: Schematic representation of the intraluminal filament middle cerebral artery occlusion (MCAO) surgery.

(1) A permanent ligature (non-sterile 6-0 silk suture thread, FST, Germany) was placed around the ECA ensuring maximum distance from the bifurcation. (2) A thread was looped around the ICA (ensuring no tension applied). (3) A loose ligature around the ECA, proximal to the ligature,

was tied to secure the filament later in the procedure. (4) A thread around the CCA was placed to lift the CCA to temporarily occlude using microvascular clip. Once the threads were tied, the CCA and ICA were temporarily occluded using microvascular clip and applying tension to the thread, respectively. The ECA was diathermised above ligature (1). A small incision was made in the ECA trunk. The occluding filament was inserted through the ECA into the ICA and advanced approximately ~8 mm to the origin of the MCA (**Figure 2.6D**). The filament was held in place using ligature (3). The microvascular clip and the ligature (2) were removed from the CCA and the ICA after the end of occlusion, respectively, the neck wound was sutured. The animal was administered 0.5 ml saline to prevent dehydration. When fully conscious, the animal was moved to a recovery room where it was kept homeothermic and monitored regularly over the next 24 hrs.

Transient MCAO: The same procedure for permanent MCAO was followed except, the filament was left in the animal for the time of occlusion under anaesthesia and the filament was withdrawn from the artery to allow reperfusion. The ECA was electro-coagulated to prevent bleeding and the neck wound was sutured. The anaesthetic was withdrawn and the animal was given 0.5 ml saline. When fully conscious, the animal was moved to a recovery room where it was kept homeothermic and monitored regularly over the next 24 hrs. Animals were housed in the animal unit for the rest of the experiment and monitored regularly.

Sham surgery: During the establishment of the MCAO model in Chapter 4, sham operated mice were used as controls. The most typical sham surgery described in the literature uses the same procedure as MCAO where the filament is inserted and advanced until the MCA origin and immediately removed (McColl et al., 2004, Tureyen et al., 2004). This procedure damages the endothelium and causes the beginning of the ischaemic cascade which is a part of the MCAO

(Tureyen et al., 2004). Thus the present study used two procedures to establish the sham surgery. Procedure 1 involved, a slight variation from the procedure used by De Simoni and group, in which all the arteries were permanently ligated, threads were tied (as described in **section 2.2.10.2**) and the common carotid artery (CCA) was clipped for the time of occlusion (CCAO) (De Simoni et al., 2003). In addition, a second procedure was performed in which all the arteries were exposed and permanent ligatures as described above were performed but refrained from clipping the CCA (no CCAO) or inserting the filament.

2.2.10.3 | Laser Doppler Flowmetry

Just prior to the MCAO procedure, using a dorsal approach, a small incision was made on the left side in the skin between the eye and ear. The muscle was blunt dissected until the skull was reached and the MCA, which runs vertically closer to the eye, was visualised. The laser Doppler probe (diameter of 0.8 mm, Moore Instruments Ltd, UK) was calibrated using a perfusion flux standard (Moore Instruments Ltd, UK), then placed on the bone near the MCA and the local cortical blood flow measured before, during and after MCAO. This gave an indication of when the blood flow through the MCA and surrounding vessels had been reduced, indicating that the MCA had been successfully occluded.

2.2.11 | Stereotaxic surgery in mice

2.2.11.1 | Preparation of MHP36 cells for transplantation stereotaxically

MHP36 cells were cultured from stocks and maintained in an undifferentiated state at 33 ^{o}C (Passage number 52 – 70). Before grafting, cells were labelled with the membrane bound fluorescent marker PKH26. Briefly cells were incubated for 2 min as described by Mellowdew

et al. (Mellodew et al., 2004). Cells were then suspended in 1 mM N-acetyl-l-cysteine (NAC) in HBSS without Ca^{2+} or Mg^{2+} at a concentration of 25,000 cells/ µl.

2.2.11.2 | In vivo stereotaxic injections using dye or MHP36 neural stem cells

Mice were anaesthetised as described in **section 2.2.10.1** and mounted on a stereotaxic frame. Using bregma as a reference point, a 2-µl Hamilton syringe (Hamilton, UK) was moved to the following coordinates: (pilot study): Medial/Lateral + 2 mm, Anterior/Posterior - 0.50 mm), (main study): (Medial/Lateral + 2 mm, Anterior/Posterior - 0.26 mm). A burr hole was made, the dura was removed and the syringe was descended to a depth of (Ventral: (pilot study: -3 mm) (main study: -1.5 and -3 mm) from the surface of the brain. The co-ordinates used for the pilot study were used from previous study carried out in mice in a global ischaemic model (Wong et al., 2005). The co-ordinates used in the main study are reproducible from Wong et al., 2005 but instead of having one site deposit of cells as used by them; we chose two sites, to allow maximum area of access to the cells (cortical as well as striatal). Cell suspension or vehicle (0.5 µl) was injected over 2 min, and the syringe was left in place for another 2 min after injection to allow diffusion away from the tip. Animals were sutured and recovered till the end of the experiment. Treatment for immunosupression was not carried out in the present study because Modo and colleagues showed that survival of MHP36 grafts was not affected by immunosupression (Modo et al., 2002) and because mice were used in this study. Viability was assessed using trypan blue exclusion in a haemocytometer before and after transplantation. Pre-graft viability averaged ~ >80 % were used in each experiment and post-graft viability was observed to be ~>70 %.

2.2.12 | Termination of Experiment and Processing of Tissue

After the assigned recovery period each animal was terminated using CO_2. Unless it was to undergo perfusion fixation (described below) the animal was decapitated and the brain removed immediately to be processed appropriately (fresh frozen).

2.2.12.1 | Fresh Freezing

Fresh freezing is a very rapid way to handle tissue, as there is no post-fixation or processing period. However, the tissue has less definition at a cellular level. Tissue was treated in this way for pilot studies.

The brain was immersed in -42 °C isopentane (VWR, International) for 2 to 3 min, then mounted and covered onto a chuck with embedding matrix (Thermo-Shandon, UK). The brain was stored at -20 °C until it was sectioned (20 μm coronal sections) using a cryostat (Bright Instrument Co. Ltd., UK).

2.2.12.2 | Perfusion-Fixation

Chemical fixation is the common method used to preserve tissue and results in less distortion of the tissue than methods such as fresh freezing or heat based techniques. Fixation with paraformaldehyde results in good cellular definition of the tissue and, if carried out carefully, will produce few artefacts.

Mice were placed in a supine position; an incision was made below the sternum to expose the rib cage. The diaphragm was cut away from the rib cage and the rib cage cut at either side to expose the heart. A 21-guage needle (Emoven, UK) attached to the perfusion apparatus was inserted into the heart and clamped in place. The right atrium was incised and a constant pressure applied

using an infusion/withdrawal pump (Harvard Apparatus, UK) to allow the perfusion of about 20 ml heparinised saline. When the saline outflow from the atrium was bloodless, 30 ml fixative and 4 % PFA at a rate of 5 ml per minute was perfused.

2.2.12.3 | Post-Perfusion Fixation

Following perfusion fixation, the brain was dissected out and immersed in 4 % PFA for 24 hrs. The brain was then cryo-protected in 30 % sucrose solution for 24 hrs until the brain sinks. The brain was then placed in a 2800 Frigocut E cryostat (Reichert–Jung Leica, Germany) and sectioned in 20 μm thick sections processed as described below.

2.2.13 | Measurement of Brain Damage

2.2.13.1 | Sectioning of Tissue

Serial sections were cut at 20 μm at 8 pre-determined coronal levels (see **Figure 2.7**) and collected onto super-coated slides (VWR, UK) (fresh frozen brains) or gelatine coated slides (perfusion fixed brains). Three sections were collected onto each slide and one slide from each coronal level was stained with Haematoxylin (Surgipath Ltd., Europe) and Eosin (Surgipath Ltd., Europe) to demonstrate areas of lesion described below.

Gelatin coating of slides: 0.5 % gelatine solution is prepared by heating to 60 °C till dissolved completely and 0.05 % chromium potassium sulphate is added. Glass slides are immersed in 96 % ethanol containing 3 % 1N HCl for 20 min followed by 2 quick immersions in distilled H_2O. This is followed by 3 quick immersions in the freshly prepared 0.5 % gelatine solution and slides are dried overnight and stored in the dark for future use.

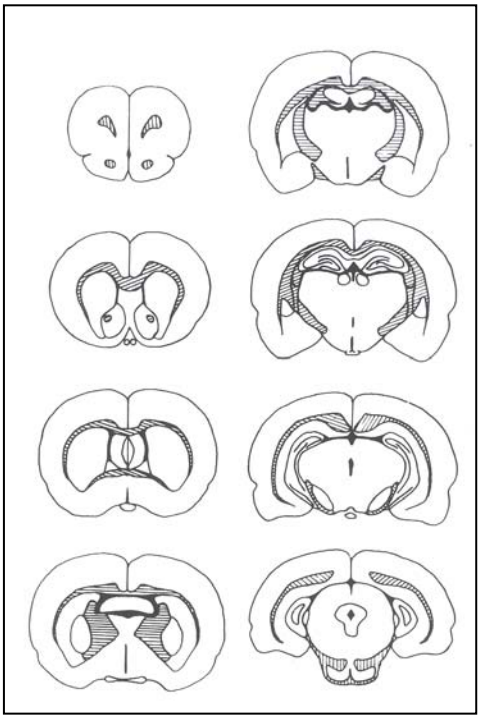

Levels	Interaural distance (mm)
1	6.02
2	4.66
3	3.94
4	3.34
5	2.86
6	1.98
7	1.00
8	0.16

Figure 2.7: Line diagrams of 8 pre-determined coronal levels used for measurement of lesion volume.

Brains sections are collected at these levels and volume of lesion is calculated using the interaural distances (Osborne et al., 1987).

2.2.13.2 | Haematoxylin and Eosin Staining

Haematoxylin and eosin staining is commonly used to demonstrate areas of ischaemic damage. Haematoxylin stains cell nuclei dark blue and eosin stains the cell cytoplasm and surrounding neuropil pink. Cryostat cut sections were fixed in 10% formal saline (0.9% w/v NaCl to 10% formaldehyde) for 10 min then dehydrated and rehydrated to remove fat. Rehydration through graded alcohol (100 % and 70 %) and water, sections were placed in haematoxylin for 3 min and then washed in running water. The sections were differentiated in acid alcohol (500 ml of 100 % ethanol, 5 ml of conc. HCl) and washed again. The sections were placed in Scots Tap Water

Substitute for 2 min, washed again in running water and placed in eosin for 3 min. The tissue was then dehydrated, cleared in Histoclear for 2 min each and mounted using DPX mounting medium (Raymond A Lamb Laboratory Supplies, UK). The haematoxylin and eosin stained sections were viewed under a light microscope at a range of magnifications to accurately determine the boundary of lesion and specific characteristics of irreversible cell death were identified (**Figure 2.8**). Ischaemic neurons were pyknotic (shrunken and triangular in shape) with cellular incrustations. The neurons also showed an eosinophilic cytoplasm and the surrounding neuropil was disrupted and displayed pallor. **Figure 2.9** shows examples of boundary of infarct and peri-infarct compared to healthy tissue after 24 hrs recovery.

2.2.13.3 | Areas of Damaged Tissue

MCAO lesion: In Chapter 4, areas of infarct in fresh-frozen tissue sections were identified by the pallor of the neuropil. Areas of infarct were measured directly from each section using image analysis (MCID, Imaging Research Inc., Canada). However, to delineate areas of lesion obtained in Chapter 5 & 6 after perfusing the tissue, the characteristics of ischaemic neurons and surrounding tissue were identified and delineated onto the appropriate coronal line diagram and measured using MCID. Using the MCID software, areas were calculated for each level namely; hemisphere area contralateral (HA_{contra}), hemisphere area ipsilateral (HA_{ipsi}) and lesion area uncorrected (LA_{un}).

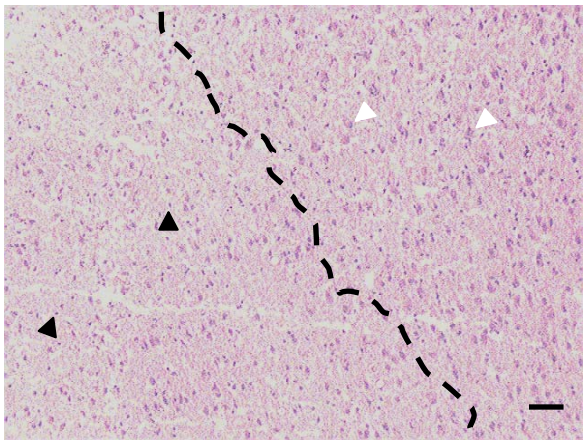

Figure 2.8: Haematoxylin and eosin staining at the boundary of infarct in fresh frozen cryostat sections

Animals with 60 min occlusion and 24 hrs recovery after transient MCAO (black arrow: dead neuron, white arrow: alive neuron) (Bar = 50 µm).

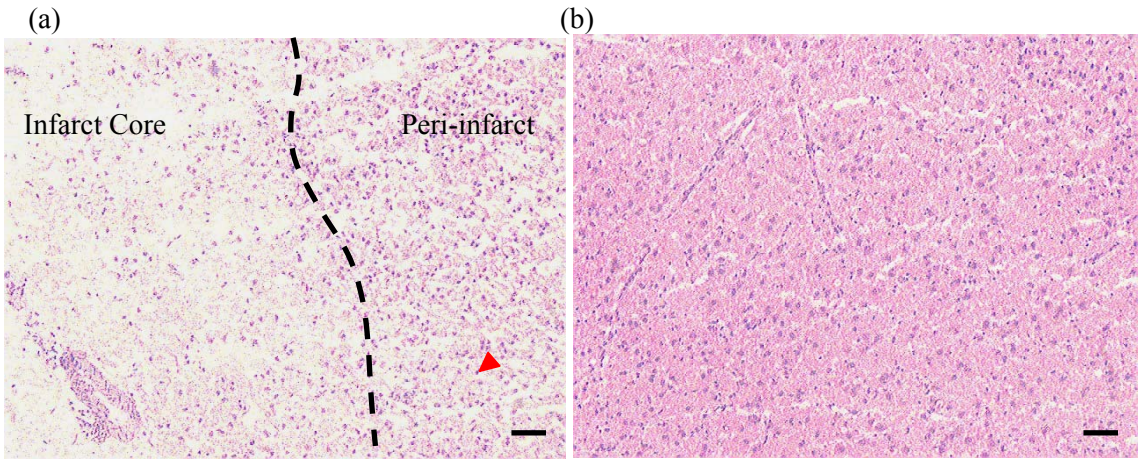

Figure 2.9: Haematoxylin and eosin staining comparing infarct and normal tissue in fresh frozen cryostat sections

(a) Damaged infarct core and peri-infarct tissue, (b) undamaged healthy area in brain tissue 24 hrs after tMCAO (red arrow points to a typical ischaemic) (Bar = 50 µm).

2.2.13.4 | Measuring Volume of Damage

After analysing the damaged area under the microscope, volume of tissue and damage for each brain were calculated from the integration of these areas using the known distance between the stereotaxic coordinates of the coronal levels. An example of a hemispheric tissue volume calculation is shown below.

$$HV_{contra} = HA_{contra} * (\text{distance between stereotaxic coordinates + thickness of section})$$

2.2.13.5 | Correction for oedema

The following formula was used to calculate the volume of infarct corrected and uncorrected for oedema (Gerriets et al., 2004, Bouley et al., 2007).

$$LV_{correc} = (HV_{contra} - (HV_{ipsi} - LV_{un})$$

$$\%LV_{correc} = \left[\frac{(HV_{contra} - (HV_{ipsi} - LV_{un})}{HV_{contra}} \right] * 100$$

$$\%LV_{un} = (LV_{un}/HV_{contra}) * 100$$

Where,

LV_{correc} is lesion volume corrected

LV_{un} is lesion volume uncorrected

2.2.14 | Behavioural Testing

Each animal underwent neurological testing at three occasions during the experimental plan to ascertain a "normal" and/or "deficit" score. Furthermore, for a detailed motor deficit testing caused after experimental stroke, the ladder rung as well as the cylinder test were used. The animals were tested at various time points after MCAO to monitor any neurological deficit and functional recovery.

2.2.14.1 | Clark's Deficit Score (CDS)

Each mouse was rated on two neurologic function scales, 24, 72 and 96 hrs after the induction of ischemia, unique to the mouse (Clark et al., 1997) to establish severity of deficit in each mouse. Scores for both scales range from 0 (healthy) to 28 (severe deficit, animal needs to be put down) and represent the sum of the results of all categories for each scale. The general deficit scale evaluates hair (0–2), ears (0–2), eyes (0–4), posture (0–4), spontaneous activity (0–4), and epileptic behaviour (0–12), whereas the focal deficit scale evaluates body symmetry (0–4), gait (0–4), climbing on a surface held at 45° (0–4), circling behaviour (0–4), front limb symmetry (0–4), compulsory circling (0–4) and whisker response to a light touch (0–4) (De Simoni et al., 2003). Animals that received a score >21 on the focal deficit scale were excluded from the study.

General deficits evaluate using the following scale.

Fur (score 0-2)

The animal is observed on the working desk without interferences or stimulations.
0 - Fluffy, clean, tidy.
1 - Localized pilo-erection and/or dirty fur limited to one or two areas of the body (usually nose and eyes).
2 – Pilo-erection or dirty fur in more than two areas of the body.

Ears (score 0-2)

The animal is observed on the working desk without interferences or stimulations.
0 - The ears are normally stretched latero-posteriorly and respond to the noises.
1 - One or both ears are lateral without being stretched behind.
2 - As score 1, but unable to respond to the noises.

Eyes (score 0-4)

The animal is observed on the working desk without interferences or stimulations.
0 - Open, clean, following quickly any movements around the animal.
1 - Open and with a mucosal and watery dirt, following slowly any movements.
2 - Open with mucosal dark dirt.
3 - Oval opening of the eyes, with mucosal dirt.
4 - Shut.

Posture (score 0-4)

The animal was observed on the working desk and subsequently held on the palm and swung to test its balance.
0 - The animal is upright on its 4 legs, with its back parallel to the desk and keeping balance using the 4 legs.
1 - The animal is stooped when walks and lowers itself to gain balance.
2 - The head or a part of the trunk resting on the desk.
3 - The animal lies on a side, but it can still straighten up with a big effort.
4 - The animal lies on the desk unable to straighten up.

Spontaneous activity (score 0- 4)

Animal is allowed to freely move in an open area.
0 - The animal is alert and explores continuously.
1 - The animal looks like alert, but is calm and listless.
2 - The animal starts and stops to explore slowly and iteratively.
3 - The animal is lethargic, numb and moves on-site.
4 - The animal is still, moving occasionally on handling.

Epileptic seizures (score 0-12)

Any seizures during the test are taken into consideration. Seizures could hide other deficits, thus the score for this parameter is higher than the previous ones.
0 - Absence of epileptic seizures.
3 - The animal is hardly handled. It could show hyper-activity and tend to climb the cage walls.
6 - The animal is aggressive and nervous, staring somewhere.
9 - Extremely excitable, frenzy, seizures after stimulation.
12 - Epileptic seizures, breathing variations and loss of consciousness.

Focal deficits evaluate on the following scale-

Body symmetry (score 0-4)

The animal is observed while resting on the working desk.

0 - Both sides are raised from the desk, the 4 legs are symmetrical under the body and the tail is straight.

1 - Mild asymmetry: body lies on ipsi-lateral side, the tail is bent in comparison to the median line.

2 - Moderate asymmetry: body lies on ipsi-lateral side, legs at the ischemic side are extended laterally, the tail is bent.

3 - Clear asymmetry: body is bent and the ischemic side lies on the desk.

4 - Extreme asymmetry: body and tail are clearly bent and ischemic side lies constantly on the desk

Walking (score 0-4)

The animal is observed while walking on the working desk.

0 - Normal walking, flexible, symmetric and quick.

1 - Still, mechanic walking. The animal is stooped, reduced speed.

2 - Slight limp, asymmetric movements.

3 - Severe limp, the animal often falls, clear walking deficits.

4 - Not moving. Movement after simulation is limited to three steps.

Sloping desk climbing (score 0-4)

The animal is positioned on a coarse desk, 45° sloping.

0 - The animal climbs quickly.

1 - The animal climbs slowly with a lot of effort.

2 - The animal can only keep the position on the sloping desk.

3 - The animal slowly falls towards the bottom.

4 - The animal falls immediately, unable to avoid it.

Circling behaviour (score 0-4)

The animal is observed while walking.

0 - The animal turns equally to left and right.

1 - The animal turns preferentially to one side.

2 - The animal turns towards one side, although inconstantly.

3 - The animal turns constantly towards one side.

4 - The animal swings slowly on-site or remains still.

Forelimbs symmetry (score 0-4)

The animal is hang from its tail and the forelimbs are observed.

0 - Both forelimbs are extended towards the desk, vigorously moving

1 - Mild asymmetry with ipsi-lateral forelimb not completely extended.
2 - Moderate asymmetry; ipsi-lateral forelimb is kept on the trunk. Observe mild contortion of the body towards the ipsi-lateral side.
3 - Extreme asymmetry with ipsi-lateral forelimb clearly adhering to the trunk.
4 - Slow or no movements of the forelimbs (due to mild asymmetry)

Mandatory circling behaviour (score 0-4)

The animal is hang from its tail keeping the forelimbs in touch with the desk. This position allows detecting hemi-paralysis through the appearance of a circling movement of the animal.
0 - The animal extends equally both forelimbs.
1 - The animal extends both forelimbs, but starts to circle from one side preferentially.
2 - The animal turns slowly towards one side.
3 - The animal turns slowly towards one side without completing an entire circle.
4 - The animal is still and the anterior part of the trunk lies on the working desk. Few and slow movements.

Whisker response (score 0-4)

The animal is stimulated on the whiskers and on the ears.
0 - Symmetric response: the animal looks towards the stimulated side and goes away from the source of stimulation
1 - Delayed response on the ipsi-lateral side, normal on the contra-lateral.
2 - No response on the ipsi-lateral side, normal on the contra-lateral.
3 - No response on the ipsi-lateral side, delayed on the contra-lateral.
4 - No response on both sides.

2.2.14.2 | Ladder rung task apparatus and analysis

The ladder rung task was adapted from the ladder rung walking task used previously in rats (Metz and Whishaw, 2009, Metz and Whishaw, 2002). The ladder rung apparatus was composed of two Plexiglas walls (69.5 cm×15 cm). Each wall contained 121 holes of 0.20 cm diameter, spaced 0.5 cm apart, and located 1 cm apart from the bottom edge of the wall (Farr et al., 2006). The holes could be filled with 8 cm long metal bars, diameter 0.10 cm, in any pattern. The walls were spaced 5 cm apart to allow for passage of a mouse but prevent it from turning around. The entire apparatus was placed atop two standard mouse housing cages, 17 cm above the ground.

Animals were tested in an irregular pattern in which the distance of the rungs varied, ranging from 0.5 to 2.5 cm. The animals' performance was video-recorded from the side, at pre-, post-MCAO and 1, 2 and 4 weeks after stem cell transplantation. All video recordings were analysed frame-by-frame. Each of the four limbs was scored for placement errors with each step being scored, however, the first two initiation steps and last two final steps were omitted when an animal paused. Each step was scored according to the quality of limb placement based on the scale adapted from (Metz and Whishaw, 2002, Farr et al., 2006). The rate at which the animal crossed the ladder was not measured. The following scale was used -

0 Points: *Total miss*. The stepping limb did not make contact with the rung, which induced a fall. This fall disturbed the body weight support and the stepping cycle was interrupted.

1.0 Point: *Deep slip*. The stepping limb contacted the rung and slipped, causing the animal to still fall. This fall disturbed body weight support and the stepping cycle was interrupted.

2.0 Points: *Slight slip*. The stepping limb contacted the rung and slipped, but no fall was observed and the animal continued walking.

3.0 Points: *Replacement*. The stepping limb made contact with the rung but was subsequently moved and placed on another rung. In addition the mouse did not bear weight on the stepping limb during the initial rung contact.

4.0 Points: *Correction*. The stepping limb aimed for one rung but prior to contact was placed on another rung or the limb was placed on one rung and slightly repositioned its placement.

5.0 Points: *Partial placement*. The stepping limb contacted the rung with either digit tips of the forelimb or the toes or heel of the hind limb. The limb was fully weight bearing.

6.0 Points: *Correct placement*. The stepping limb contacted the rung with the palm and digits closed around the rung. The limb was fully weight bearing.

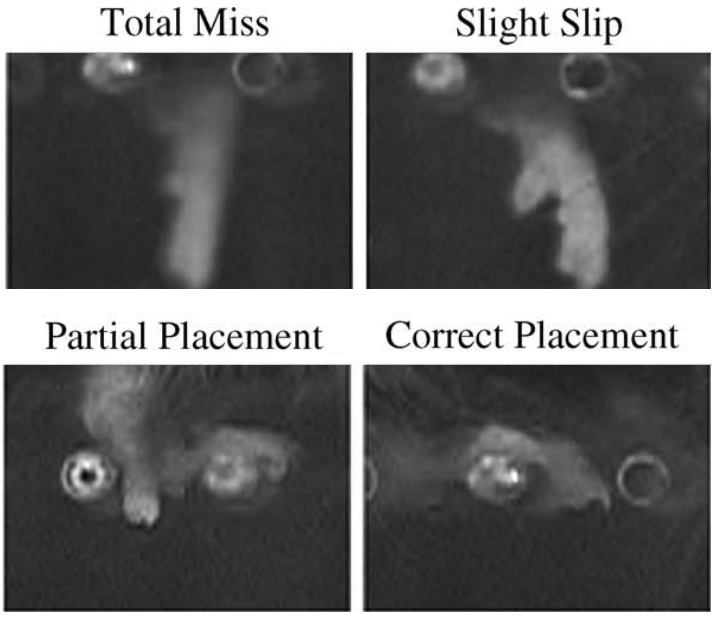

Figure 2.10: Photographs illustrating fore-limb placement categories in the ladder rung test. A total miss was scored as 0, slight slip was scored as 2 (Top panel), partial placement was scored as 5 and correct placement was scored as 6 (Bottom panel) (illustration adapted from Farr et al., 2006).

2.2.14.3 | Cylinder task apparatus and analysis

The cylinder or spontaneous forelimb test (Schallert et al., 2000) modified for mouse (Baskin et al., 2003), involves the use of a 10 cm diameter transparent cylinder. Each animal was placed in the cylinder and its spontaneous activity to rear up on its hind limbs and explore the vertical surface with its forelimbs was observed. Mice were removed from the cylinder after completing 10 rears (approximately 2 mins). Videotapes were analyzed in slow motion and the number of times each paw was used to contact the cylinder wall and push off from or land on the floor were recorded. Animals used either a single forelimb or both forelimbs for an exploration. The number of both, right only, or left only explorations was counted in a two min recording interval. One pre-injury measurement was taken to control for limb preference.

The laterality score (Schallert et al., 2000) was computed as follows:

(# of right only − # of left only) / (# of right only + # of left only + # of both)

For normal uninjured performance where an animal has no preference for right or left forelimb, the score is at or near zero. Post-MCAO measurements were taken at 48 hrs and at 1, 2 and 4 weeks time points. Animals showed a tendency, in the measurements at 48 hrs injury, to explore the cylinder less frequently and to spend a larger proportion of time engaged in grooming activities. Additional two min trials were performed until at least 10 rearing observations were made (Onyszchuk et al., 2007).

2.2.14.4 | Video recording and analysis equipment

The mice were filmed with a high speed Panasonic digital camcorder (30 frames/s; shutter speed of 1/1000). The digital videotapes were analysed using a HP Pavilion DV2000 laptop. Single frames were imported from the digital video records using Windows media player on a Windows operating system.

2.2.15 | Statistics

All results are expressed as the mean ± standard error (SEM); n = number of experiments or animals used. All graphs generated and statistical analysis carried out using Prism 5.0 unless otherwise specified. Values of $p<0.05$ were considered to be statistically significant. The specific statistical tests employed are detailed in each Chapter separately.

CHAPTER 3

CHARACTERISATION OF MHP36 NSC FOR OESTROGEN *IN VITRO*

3.1 | Introduction

MHP36 is a clonal line whose differentiation can be accurately controlled *in vitro*, thus providing a robust and manipulable model for stem cell differentiation (Sinden et al., 1997). It has been shown to improve outcome in several models of impairment, including hippocampal ischaemia induced by global ischaemia and old age (Hodges et al., 2000a, Hodges et al., 2000b, Sinden et al., 1997, Wong et al., 2005). In the rat global ischaemia model when MHP36 cells are grafted dorsally to the damaged area they migrate to and selectively repopulate the hippocampic CA1 layer differentiating into both neurons and glia. When grafted animals were tested in the Morris water maze, they showed recovery of the lesion-induced spatial learning (Sinden et al., 1997). Furthermore, Modo and colleagues showed that although ischaemic brain damage produced a localised immune response, there was no significant acute immune response directed towards grafted MHP36 cells in the MCAO model of stroke (Modo et al., 2002) suggesting that the MHP36 cells are a potential candidate for transplantation. It is evident that further work that clarifies the involvement of species related effects (use of mice) in transient MCAO model, improvement of integration and differentiation of MHP36 cells *in vivo* will be of exceptional value to refine our knowledge of stem cells therapy after stroke.

McEwen and colleagues have shown that oestrogen influences synaptogenesis and contributes to synaptic plasticity (McEwen, 2001). Oestrogen also appears to influence neurogenesis in the hippocampus of rats (Suzuki et al., 2007) and modulates processes

ranging from survival and proliferation *in vitro* (Brannvall et al., 2002) to adhesion and migration, to angiogenesis and cancer (Prossnitz et al., 2008a). The sub ventricular zone (SVZ) lining the lateral ventricle is a major repository of neural stem cells in the adult brain. Under normal physiological conditions, the SVZ-derived neural precursor cells migrate to the olfactory bulb, where they differentiate into functional olfactory interneuron (Suzuki et al., 2007). However, various neurodegenerative conditions induced by cortical aspiration, traumatic brain injury, or cerebral ischaemia redirect the migration of neural precursor cells from their normal route toward the sites of injury, including the cortex and striatum, two brain regions that are most affected by MCAO and it was also observed that ERα and ERβ are essential mediators (Suzuki et al., 2007). Moreover, the selective ablation of one form of ER completely prevents oestrogen's ability to modulate the number of immature neurons in the SVZ and that each receptor subtype exerts differential functional roles in modulating the number of newborn neurons (Suzuki et al., 2007). Oestrogen acts by binding to two known types of oestrogen receptors (ERs), ERα and ERβ (Brannvall et al., 2002, Nilsson et al., 2001) but GPR30 is the newer identified G-protein coupled receptor which is also activated by oestrogen (as described in **section 1.3.2**). The physiological functions of oestrogen in brain tissue have usually been attributed to its effect on neurons, which express ERs. In view of the fact that oestrogen can affect neuronal development and survival, one would hypothesize whether the hormone also influences NSCs, which are precursors for mature neurons. Thus, we have characterised the MHP36 cells for the enzyme that synthesis oestrogen; aromatase and the known nuclear ERs; ERα and ERβ and plasma membrane receptor, GPR30.

Furthermore, to investigate our hypothesis, if increased oestrogen synthesis by the MHP36 stem cells improves the success of stem cell based therapy for stroke MHP36 cells were genetically modified to alter their expression of oestrogen by over-expressing aromatase or

by knocking down Dax-1 (dosage-sensitive sex reversal adrenal hypoplasia congenita region on X-chromosome, gene-1). Aromatase enzyme activity catalyzes the conversion of androgens to oestrogens in specific brains regions (Lephart, 1996). On the other hand, Dax-1 represses the trans-activation of the aromatase gene (Wang et al., 2001). Therefore knock down of Dax-1 causes these cells to have raised aromatase expression and thereby increased oestrogen production. We initially characterised both the genetically modified clones using Western blots, however only one of the Dax-1 knock-down clones was successfully over-expressing oestrogen and thus thoroughly characterised for oestrogen in this Chapter.

3.2 | Methods

3.2.1 | Cell maintenance

In culture, MHP36 cells were grown and maintained at their permissive temperature of 33°C. In addition, Dax-1 knock-down MHP36 (Dax-1KD-MHP36) and aromatase over-expressing cells were cultured similarly except that the media was additionally supplemented with 8 μg/ml puromycin and 7 μg/ml blasticidin, respectively (as described in **section 2.2.1**).

3.2.2 | Genetic modification of MHP36 cells to over-express oestrogen

Briefly, two approaches were carried out to over-express oestrogen, 1) Dax-1 knockdown and 2) Aromatase over-expression. The genetic modification of the MHP36 cells was carried out in King's College, London by Dr. Dafe Uwanogho who then supplied the genetically modified stem cells clones (Dax-1= five; Aromatase= two clones) for characterisation and transplantation (as described in **section 2.2.8**).

3.2.3 | Immunocytochemistry and Immunofluorescene

3.2.3.1 | Characterising the MHP36 for aromatase

MHP36 cells were grown on fibronectin-coated cover slips (as described in s**ection 2.2.1**). These cells grown on cover slips were used for immunocytochemistry (as described in s**ection 2.2.2**). HeLa cells were used as a positive control. A negative control was included in every immunocytochemistry run.

3.2.3.2 | Characterising the MHP36 for aromatase, ERs and GPR30

MHP36 cells were grown on fibronectin-coated cover slips (as described in **section 2.2.1**). The primary antibodies used were as follow: anti-aromatase (raised in rabbit); dilution: 1:

100, anti-ERα (raised in mouse); dilution: 1: 100, anti-ERβ (raised in mouse); dilution: 1: 50 and anti-GPR30 (raised in rabbit) dilution: 1: 100 (see **section 2.2.3**). HeLa and MCF-7 cells were used as positive control. A negative control was included in every immunostaining run.

3.2.3.3 | Characterising the Dax-1KD-MHP36 for Dax-1 and aromatase

Dax-1KD-MHP36 cells were grown on fibronectin-coated cover slips (as described in **section 2.2.1**. The primary antibodies used were as follow: anti-Dax-1 (raised in rabbit); dilution: 1: 100 and anti-aromatase (raised in rabbit) (see **section 2.2.3**). MHP36 cells were used as a control for quantification. A negative control was included in every immunostaining run.

3.2.4 | Western blotting

3.2.4.1 | Characterising the MHP36 for aromatase, ER alpha and GPR30

Whole cell extracts or tissue samples were prepared, separated electrophoretically and then probed with the same primary antibody used in immunofluorescence for aromatase at 1:10000, ERα at 1:5000 and GPR30 at 1:10000 in 0.2% BSA in NATT, overnight (as described in **section 2.2.4**). Specific secondary antibodies were used at 1:10000 dilutions in 0.2% BSA in NATT. The signal was developed by enhanced chemi-luminescence and visualized on a Kodak BioMax film. Blots were stripped and re-probed with anti-GAPDH antibody or total p38 (Santacruz, UK) (normalised to house-keeping protein) (as described in **section 2.2.4**).

3.2.4.2 | Characterising the Dax-1KD-MHP36 for Dax-1 and aromatase

Dax-1KD-MHP36 samples were prepared and separated as described in **section 2.2.4**. The same primary antibodies were used in immunofluorescence. MHP36 cells were used as a control for quantification.

3.2.4.3 | Effects of oestrogen on the expression of aromatase in MHP36 cells

Cells were stimulated for different time points starting at 0 hrs until 48 hrs with either vehicle (EtOH) or 17β-oestradiol (100 nm). Cell were harvested in 1X sample buffer and subjected to Western blotting as described in **section 2.2.4**.

3.2.5 | RT-PCR

Reverse transcriptase (RT-PCR) was performed as described in **section 2.2.6**. Aromatase: semi-nested PCR; ERα: standard PCR; ERβ: standard PCR; GPR30: standard PCR.

3.2.6 | ELISA

17β-oestradiol levels in the Dax-1KD-MHP36 cells were measured using an ELISA after extraction of oestradiol from the cells as well as supernatant (media) (as described in **section 2.2.9)**. Plasma from female mouse was used as a positive control.

3.2.7 | Statistics

All results are expressed as the mean ± SEM, n=3 in all experiments unless otherwise stated. Statistical evaluations between MHP36 and Dax-1KD-MHP36 cells were carried out using unpaired, 2-tailed Student's *t*-tests, unless otherwise stated. Values of p□0.05 were considered to be statistically significant.

3.3 | Results

3.3.1 | MHP36 and Dax-1KD-MHP36 cell culture maintenance

The MHP36 cells proliferated as a monolayer (**Figure 3.1A**) at a permissive temperature of 33 °C. The rounded off cells could be dividing and floating cells were dead and cleared off the flask while feeding. The Dax-1KD-MHP36 (five clones) and aromatase (two clones) cells once genetically modified by Dr. Dafe Uwanogho were transported, to be grown from frozen stocks which also proliferated as a monolayer (**Figure 3.1B & C**) at a permissive temperature of 33 °C plus puromycin (Dax-1KD-MHP36) or blasticidin (Aromatase). Both these genetically modified cells were similar in appearance and cell proliferation rates, although this parameter was not directly assessed. Out of the two types of approaches, only the Dax-1 knock-down genetic modification was successful in over-expressing oestrogen and was characterised thoroughly and used in future experiments. These cells were referred to as Dax-1KD-MHP36 cells throughout the thesis.

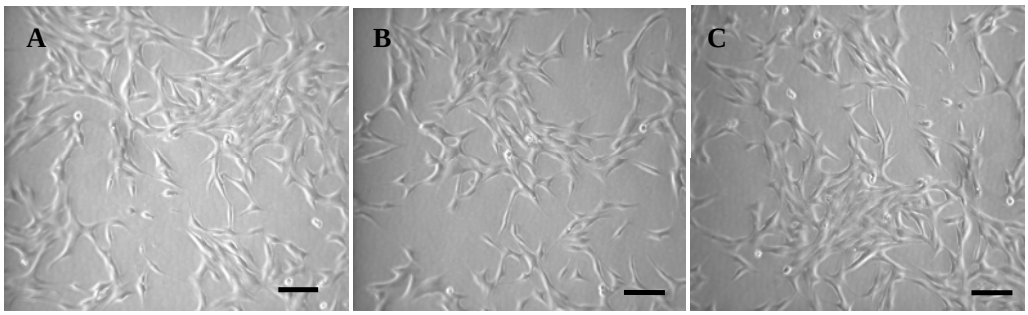

Figure 3.1: Different neural stem cells used in maintenance *in vitro*

(**A**) MHP36 cells in maintenance in the permissive condition (33 °C in an atmosphere of 5% CO_2 and humidified air). (**B**) Dax-1KD-MHP36 cells in maintenance in the permissive condition. (**C**) Aromatase over-expressing cells in the permissive condition (Bar = 100 μm).

3.3.2 | Immunocytochemistry

3.3.2.1 | Characterising the MHP36 for aromatase

Immunocytochemistry evidence of the presence of aromatase protein can be visualised in the light microscopy images in **Figure 3.2A**, which shows positive staining of MHP36 cells bound by an antibody directed towards aromatase and reported with a DAB reaction. Expression of aromatase was observed within the cytoplasm and not in the nucleus. The specificity of the antibody was confirmed by staining the human cervical cancerous cell line, HeLa (**Figure 3.2B**).

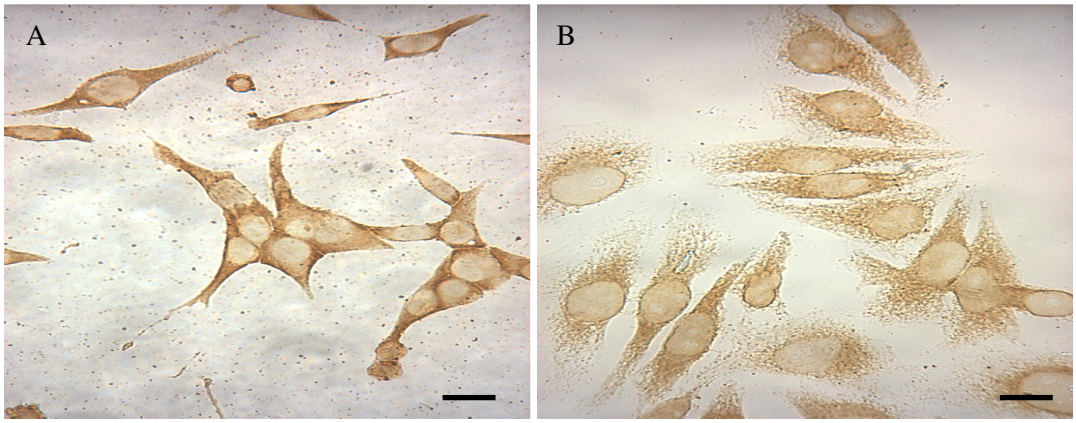

Figure 3.2: Immunocytochemistry to examine the expression of aromatase.

(**A**) Positive staining for aromatase shown in MHP36 cells using 1:50 dilution of primary antibody reported with DAB reaction. (**B**) Positive control staining of the HeLa cells for aromatase as described in **section 2.2.2**. Negative controls were included but are not shown (Bars: A-B 50μm).

3.3.3 | Immunofluorescence

3.3.3.1 | Characterising the MHP36 for aromatase

Immunocytochemistry results were confirmed with immunofluorescence staining. Cells seeded on the cover slips stained positive for aromatase. Again immunofluorescene staining was restricted to the cytosol (**Figure 3.3A**) and was comparable to the positive control cell line (**Figure 3.3B**).

3.3.3.2 | Characterising the MHP36 for ER alpha and beta

The MHP36 cells were characterised for ERα and ER β. Cells were grown at the permissive temperature of 33 °C for 24 hrs. They were then fixed and stained with the mouse anti-ERα antibody and counterstained for DAPI (nuclear staining). Consistently, none of the MHP36 cells stained for ERα when compared to the positive control, breast cancer cells MCF-7, which stained the nucleus for ERα (**Figure 3.4 A-B**). On the other hand, when MHP36 cells were stained with the mouse anti-ERβ antibody, all cells stained with a high intensity fluorescence pool in the cytoplasm, comparable with the MCF-7 cells (positive for ERα and β) (**Figure 3.5**).

3.3.3.3 | Characterising the MHP36 for GPR30

Cells were grown on cover slips for 24 hours until 70% confluency. They were then fixed and stained with the rabbit anti-GPR30 antibody. All the cells were counterstained for DAPI (nuclear staining). MCF-7 cell stained intracellular sites for GPR30 (**Figure 3.6**) confirming localisation as observed by Revankar and colleagues (Revankar et al., 2005).

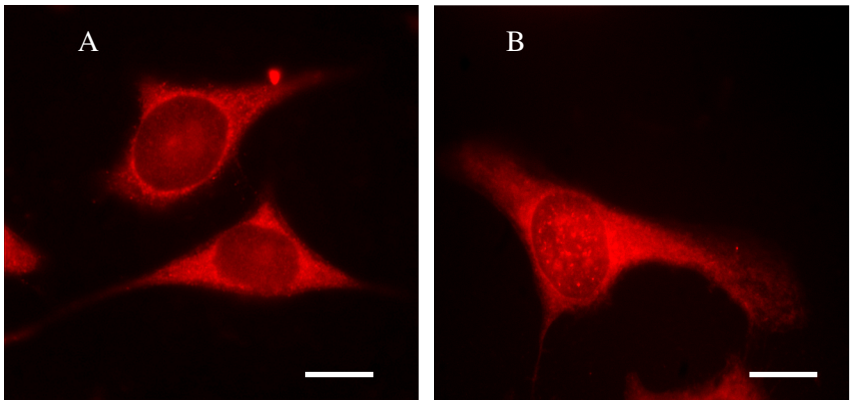

Figure 3.3: Immunofluorescence staining to examine the expression of aromatase.

(**A**) Staining for aromatase observed in MHP36 cells, using 1:50 dilution of primary antibody reported by Texas Red. (**B**) Positive control staining of the HeLa cells for aromatase as described in **section 2.2.3**. Negative controls were included but are not shown. One representative of four individual experiments is shown (Bars: A-B 20μm).

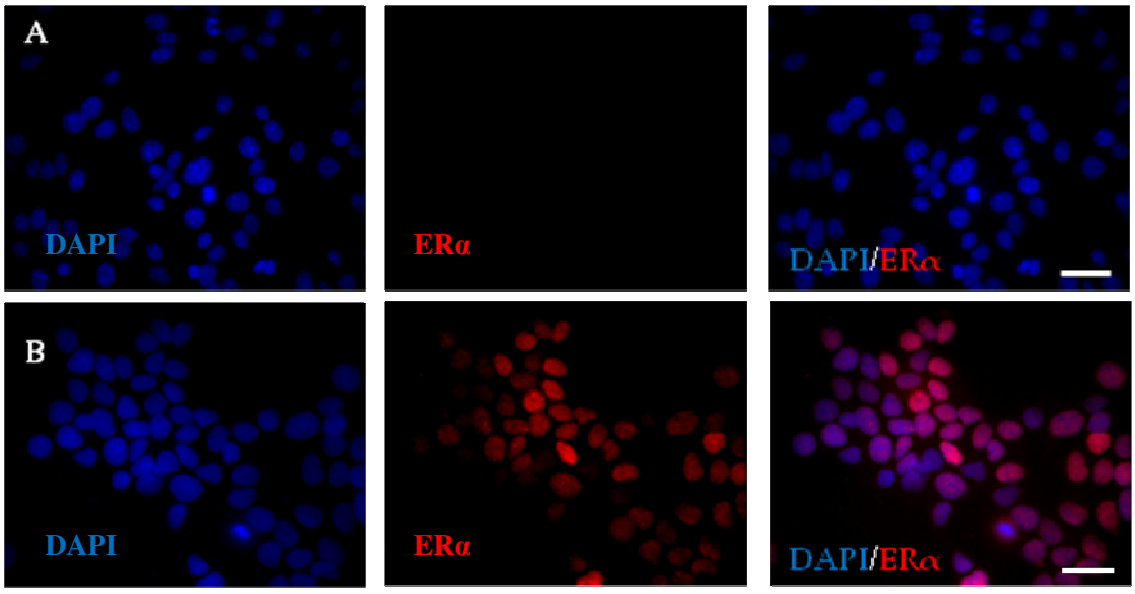

Figure 3.4: Immunofluorescence staining examining the expression of ER alpha.

(**A**) Staining for ERα in MHP36 cells using 1:250 dilution of primary antibody reported by Alexafluor-555, counterstained with DAPI (nuclear). (**B**) Staining of the MCF-7 cells for ERα as described in **section 2.2.3**. Negative controls were included but are not shown. One representative of four individual experiments is shown (Bars: A-B 50 μm).

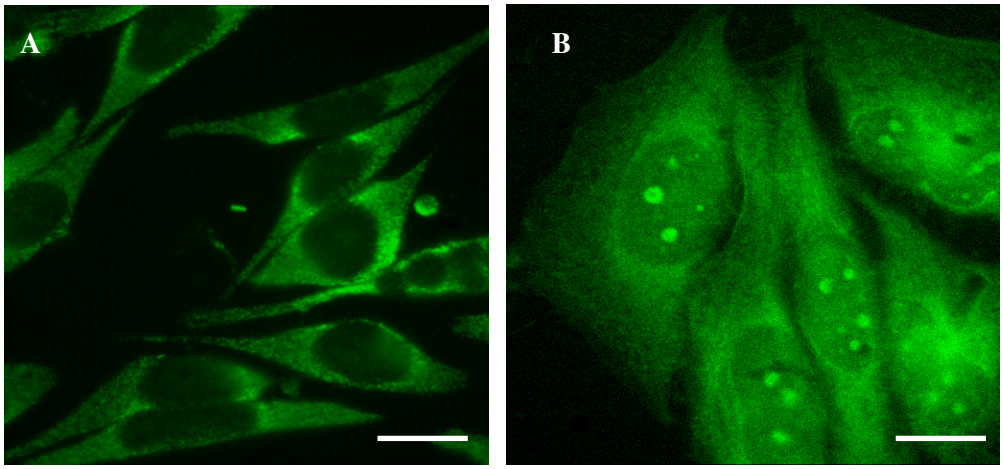

Figure 3.5: Immunofluorescence staining to examine the expression of ER beta.

(**A**) Cytoplasmic staining for ERβ observed in MHP36 cells using 1:50 dilution of primary antibody reported by FITC. (**B**) Staining of the positive control, MCF-7 cells (are larger in appearance) for ERβ as described in **section 2.2.3**. Negative controls were included but are not shown. One representative of four individual experiments is shown (Bars: A-B 50μm).

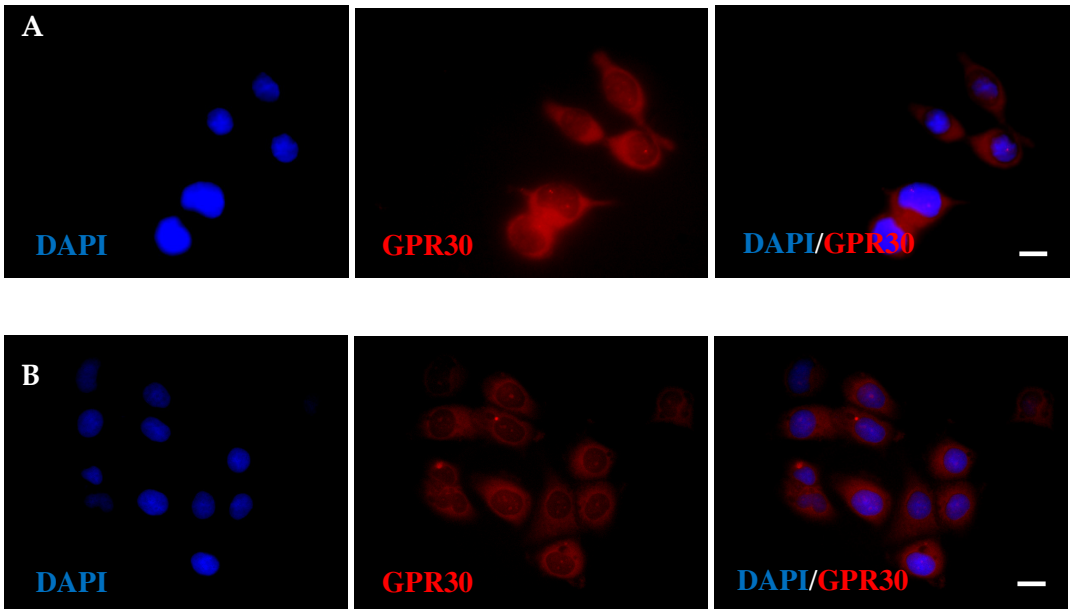

Figure 3.6: Immunofluorescence staining to examine expression of GPR30.

(**A**) MHP36 and (**B**) MCF-7 cells (positive for GPR30 receptors) counterstained with DAPI (nuclear staining) as described in **section 2.2.3**. Negative controls were included but are not shown. One representative of four individual experiments is shown (Bars: 50 μm).

3.3.4 | Western Blotting

3.3.4.1 | Characterising the MHP36 for aromatase

In order to confirm results obtained by immunostaining for aromatase in the MHP36 cells, western blot analysis was carried out. A band was observed with a molecular size of approximately 52kDa in both the MHP36 cells as well as the positive control cancerous cell line HeLa (**Figure 3.7**).

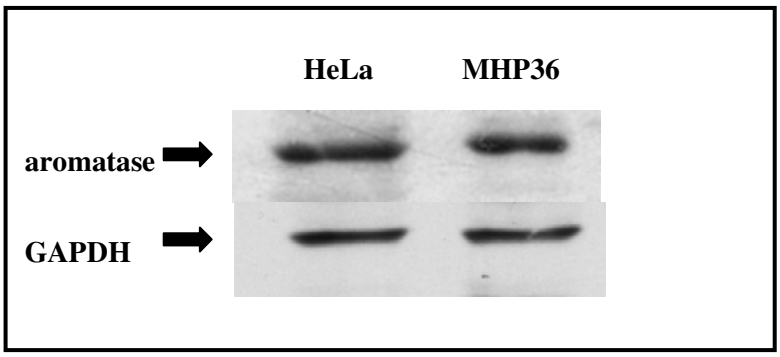

Figure 3.7: Western blot demonstrating expression of aromatase.

Whole cell lysate of MHP36 cells was blotted for aromatase protein, which appeared as a single band at approximately 52 kDa comparable to the positive control HeLa cell line. The blots were re-probed for anti-GAPDH for normalisation as described in **section 2.2.4**. One representative experiment of 3 is shown.

3.3.4.2 | Effects of oestrogen on the expression of aromatase in MHP36 cells

The effect of 17β-oestradiol (100 nM) on the expression of aromatase in the MHP36 cells was determined by Western blotting. The protein mass was determined by evaluating the intensity of the bands by scanning video densitometry and expressed (Prot. Expression) as arbitrary units (A.U.) normalized to GAPDH expression (housekeeping protein). The protein expression of aromatase was not significant but had a trend to increase after 2 hours of stimulation with 17β-oestradiol when compared to ethanol (**Figure 3.8**).

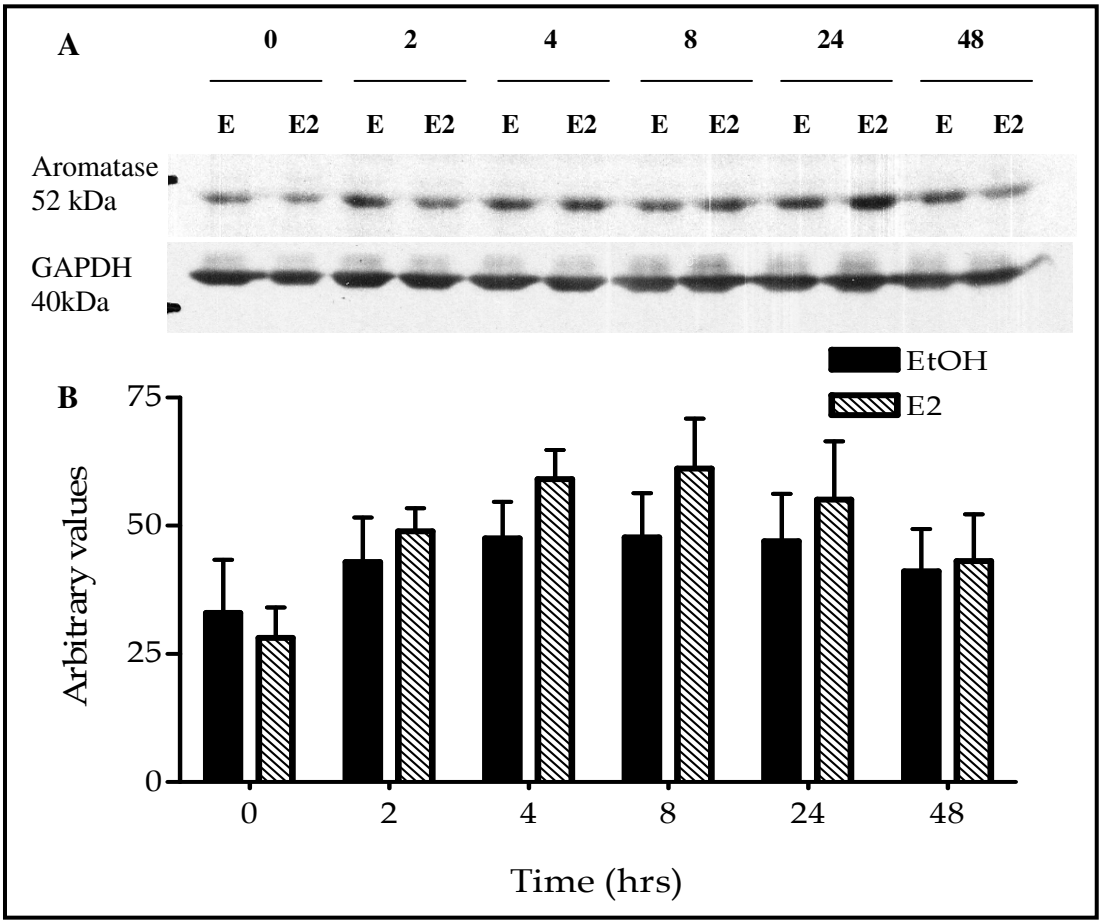

Figure 3.8: Effects of 17β-oestradiol on aromatase expression at different time-points.

(**A**) Top panel showing aromatase protein expression and bottom panel showing GAPDH expression as a housekeeping protein. (**B**) Graph plotted as ratio of Aromatase expression over GAPDH expression on the Y-axis and different time points on X-axis in hrs. Data presented as mean ± SEM, n=4 independent experiments. One representative experiment of 4 is shown. E2 versus EtOH was not significant. E2= 17β-oestradiol (100 nM); E= ethanol.

3.3.4.3 | Characterising the MHP36 for ER alpha and GPR30

In order to confirm results obtained by immunostaining, Western blot analysis was carried out to detect the absence or presence of ERα and GPR30 proteins, respectively in MHP36 cells. No band was observed in the MHP36 cells when compared with the positive control cells (positive for ERα and β) which gave a band of a molecular size approximately 60kDa (**Figure 3.9**) consistent with that known for ERα. Despite increasing levels of protein

loading, as demonstrated by GAPDH expression, no expression was observed in the MHP36 and MB-MDA cells. The graph represents the percent increase in protein expression in MCF-7 cells as opposed to the lack of expression in MHP36 and MB-MDA cells.

Western blotting for ERβ was also performed but no conclusive result was obtained due to the antibody used.

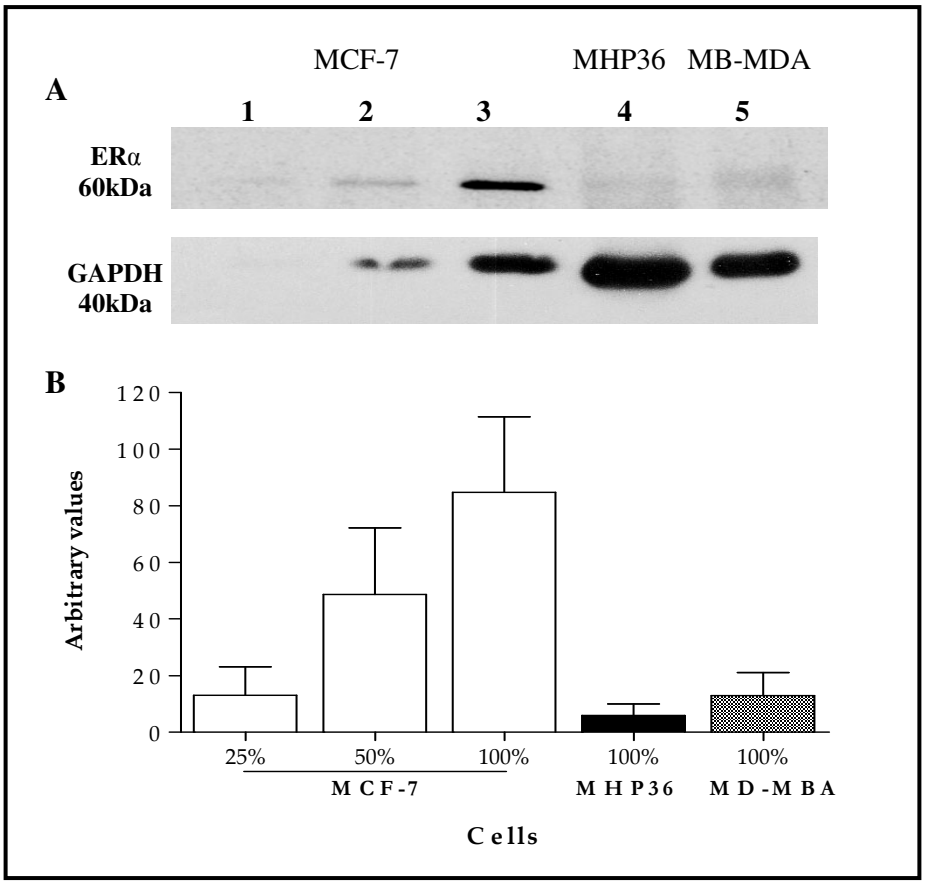

Figure 3.9: Western blot to detect the oestrogen receptor alpha protein in MHP36 cells.

(**A**) (Top) Lane 1: 25% of the total protein of MCF-7 cells, Lane 2: 50% of the total protein of MCF-7 cells, Lane 3: total protein of MCF-7 cells, Lane 4: total protein of MHP36 cells, Lane 5: total protein of MB-MDA cells (negative for oestrogen receptors). Bottom panel showing GAPDH expression used as a housekeeping protein. (**B**) Graph plotted as protein mass determined by evaluating the intensity of the bands by scanning video densitometry and expressed as arbitrary units (A.U.) on the Y-axis and different cells on X-axis. One representative experiment of 3 is shown.

Furthermore, a band of molecular size of approximately 50kDa was observed in the MHP36 cells when compared to positive control cells consistent with that known for GPR30 (**Figure 3.10**).

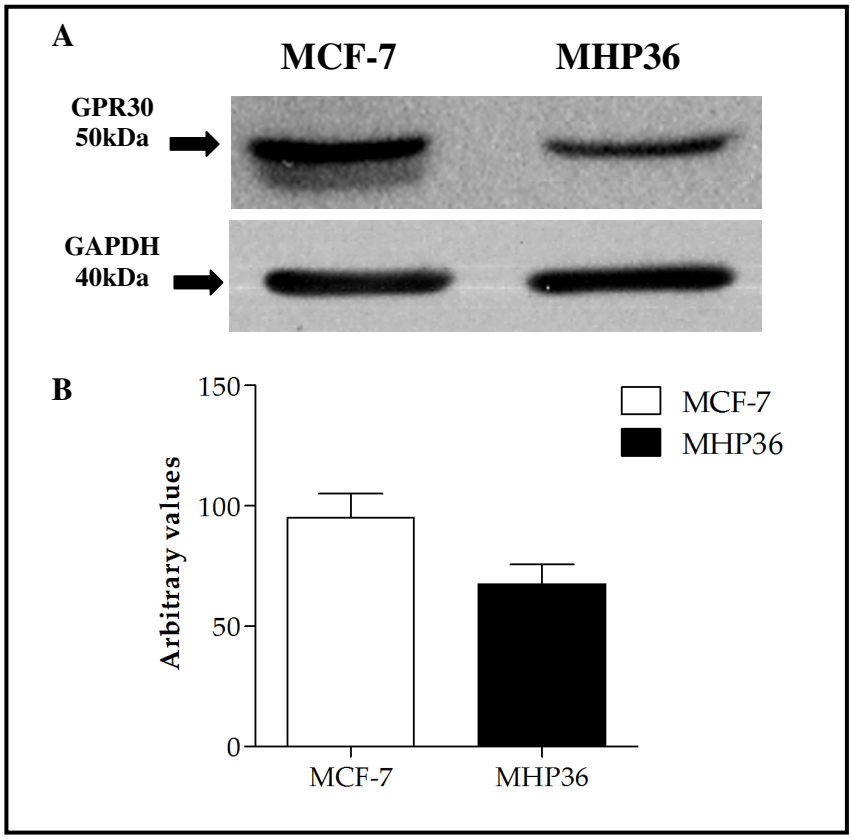

Figure 3.10: Western blot to detect the GPR30 protein in MHP36 cells.

(**A**) (Top) Western blot of MHP36 cells to detect GPR30 protein which appeared as a single band at approximately 50 kDa when compared to the positive control cell line MCF-7. Bottom panel showing GAPDH expression used as a housekeeping protein. (**B**) Graph plotted as protein mass determined by evaluating the intensity of the bands by scanning video densitometry and expressed as arbitrary units (A.U.) on the Y-axis and different cells on X-axis. One representative experiment of 3 is shown.

3.3.5 | Reverse transcriptase (RT)-PCR

To confirm the results obtained at the protein level, RT-PCR was carried out to detect the expression of mRNA aromatase in the MHP36 cell line; using specific primers chosen from the mouse DNA sequence and amplified with the thermal cycler (see **section 2.2.6** for detailed method). The expression of aromatase mRNA was not observed with the first batch of primers that were used on MHP36 isolated RNA (**Figure 3.11**). One representative experiment of 3 is shown. β2-microglobulin was used as a housekeeping protein. A second set of primers were designed and tested for aromatase mRNA expression which also failed (**Figure 3.11**) as compared to the positive tissue sample; testis. Further to that a semi nested PCR was carried out (see **section 2.2.7.1** for detailed method).

Figure 3.12 shows a semi-nested PCR in which, the first round of PCR reaction gave an amplicon of ~800bps. This amplicon was then used as a template and each set of primers was tested. This gave a single band of the respective size and was verified by sequencing. The signal in the testis was stronger when compared to the standard PCR reaction confirming that the semi-nested PCR worked based on results observed from standard RT-PCR.

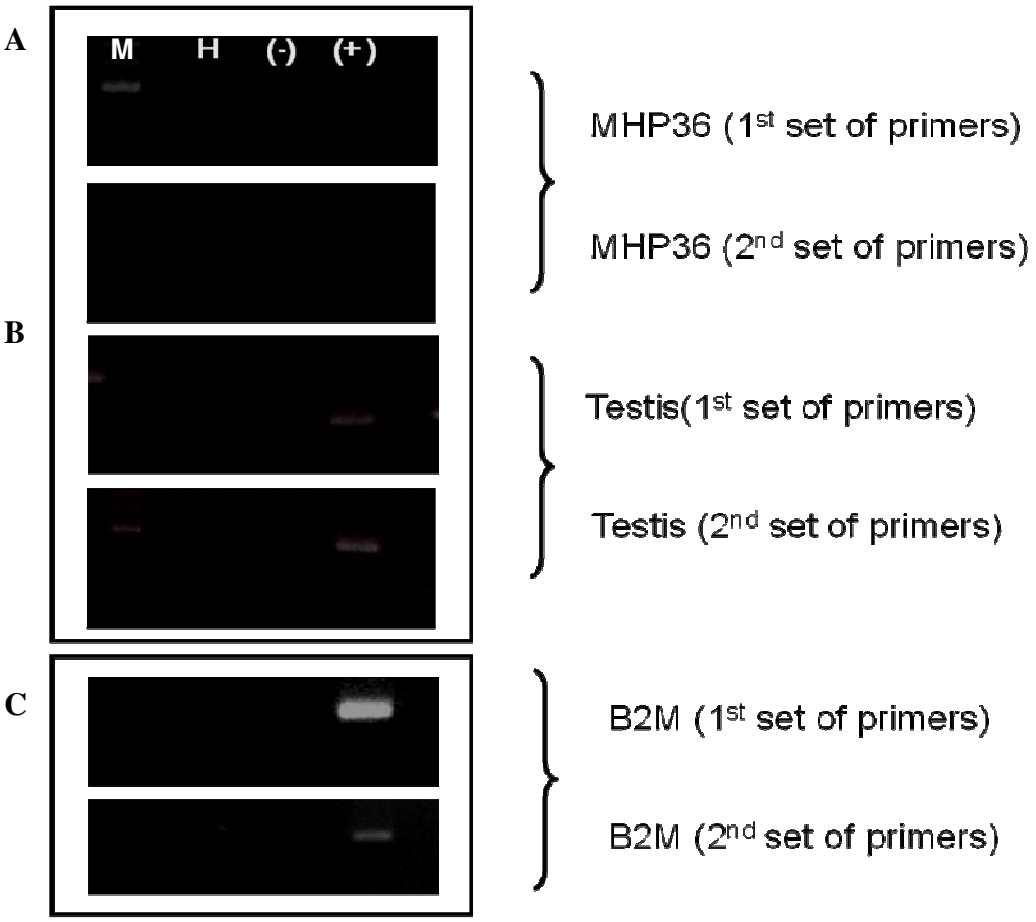

Figure 3.11: Reverse transcriptase-Polymerase Chain Reaction (RT-PCR) for aromatase.

(**A**) (Top) First set of primers in MHP36 cells (Bottom) second set of primers in MHP36 cells. (**B**) (Top) first set of primers in testis results in results in a 256bps amplicon (Bottom) second set of primers in testis resulted in a 145bps amplicon. (**C**) β2-microglobulin (B2M) used as a housekeeping protein for internal loading control. Three reactions were setup comprising of RT (-), RT (+), H = H_20 and M = molecular weight marker. One representative of three experiments is shown.

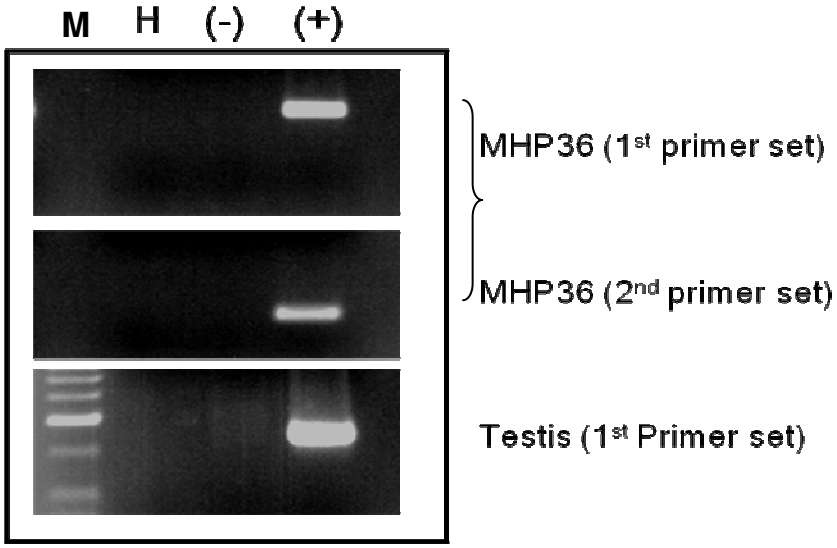

Figure 3.12: Semi nested RT-PCR for aromatase.

Semi nested PCR for aromatase showing a single band (1st set of primers: 256bps) (2nd set of primers: 145bps) in MHP36 cells as compared to positive mouse tissue; testis. Three reactions were setup comprising of RT (-), RT (+), H = H_20 and M = molecular weight marker. One representative of three experiments is shown.

Figure 3.13 shows a PCR reaction for the three receptors of oestrogen namely; ERα, ERβ and GPR30. ERα did not show any amplicon as compared to the positive mouse tissue; ovary. Similarly, ERβ (both iso-forms, 2 bands) is expressed at a low level in the cells. GPR30 also showed a band of an expected size. Furthermore, these amplicons were verified using sequencing. All the RT-PCR results confirmed the results obtained using immunofluorescence and western blotting which concludes presence of aromatase, ERβ and GPR30 and absence of ERα in the MHP36 cells.

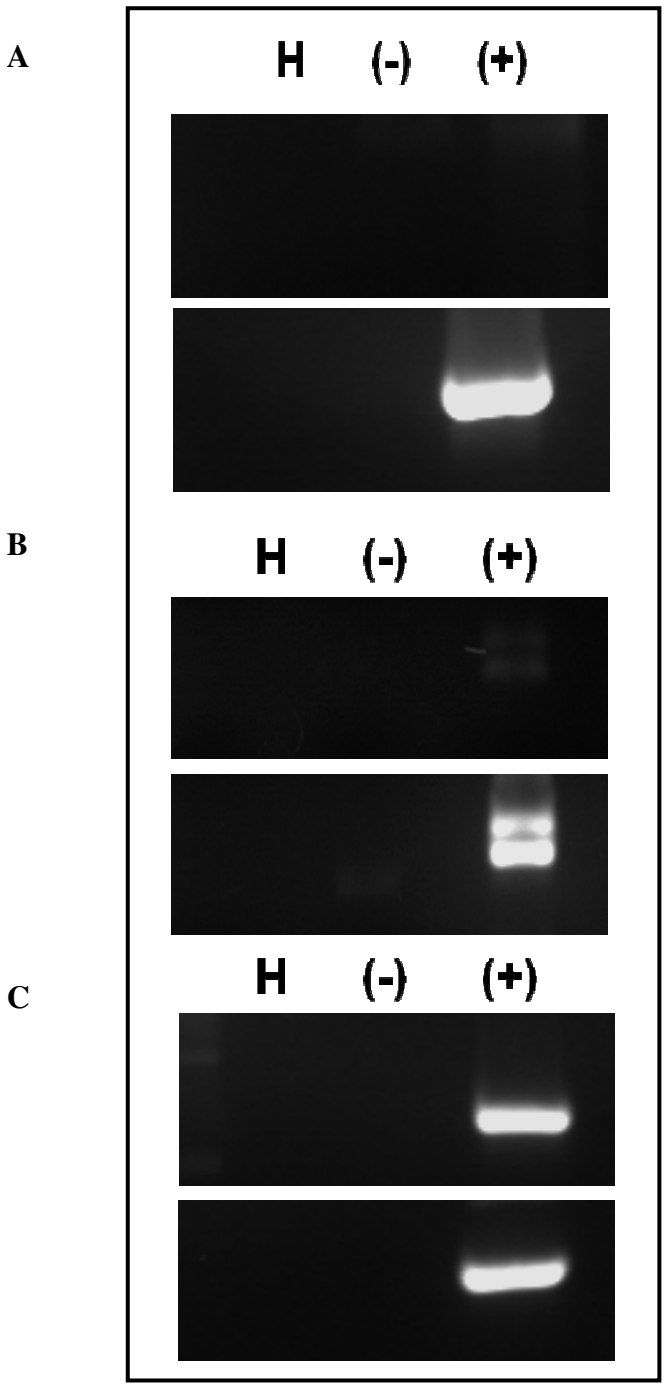

Figure 3.13: RT-PCR for oestrogen receptors and GPR30.

(**A**) (Top) RT-PCR for ERα in MHP36 cells and (Bottom) positive mouse tissue; ovary. (**B**) (Top) RT-PCR for ERβ and (Bottom) positive mouse tissue; testis (**C**) (Top) GPR30 in MHP36 cells and (Bottom) positive mouse tissue; testis. Three reactions were set-up RT (-), RT (+) and H_20. One representative of three experiments is shown.

3.3.6 | Characterisation of the Dax-1KD-MHP36 cells for oestrogen

3.3.6.1 | Characterisation of Dax-1 using immunofluorescence staining

Once the Dax-1KD-MHP36 cells were successfully maintained *in vitro* (**section 3.3.1**) they were characterised for Dax-1 protein knockdown to confirm genetic modification. Dax-1 protein was significantly knocked down in the Dax-1KD-MHP36 cells (**Figure 3.14A & B**) which led to a significant decrease in average density per pixel as opposed to the MHP36 cells as shown in the graph.

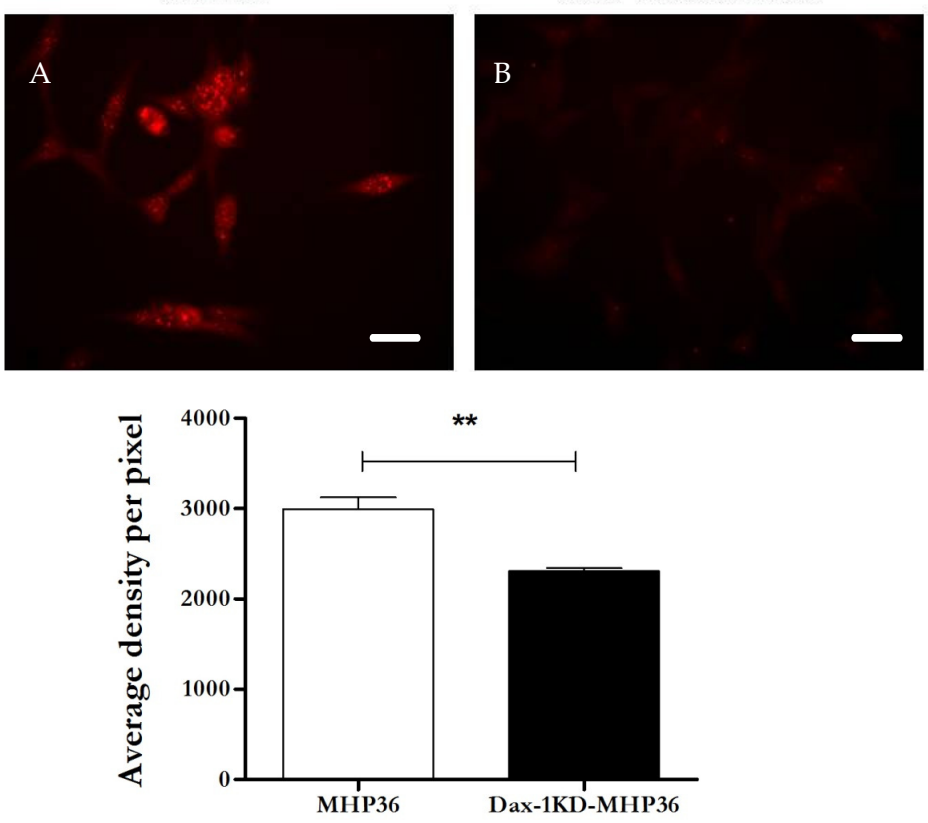

Figure 3.14: Immunofluorescence for Dax-1 in MHP36 and Dax-1KD-MHP36 cells.

(**A**) Dax-1 protein expression localised in the nucleus in MHP36 cells. (**B**) Reduced Dax-1 protein expression in the nucleus due to knockdown of Dax-1 protein in Dax-1KD-MHP36 cells. Graphical representation of Dax-1 expression obtained after image analysis using Image J Software. The Y-axis represents average density per pixel (at least 10 cells per field). Statistical analysis was performed using un-paired t-test (** $p<0.01$). One representative experiment of 3 is shown (Bar = 40μm).

3.3.6.2 | Characterisation of aromatase using immunofluorescence staining

Furthermore, Dax-1KD-MHP36 cells were analysed for expression of aromatase. A similar staining pattern was observed, of cytosolic and not nuclear staining in the Dax-1KD-MHP36 cells which was significantly increased when compared to MHP36 cells (**Figure 3.15A & B**). This led to a significant increase in average density as shown in the graph.

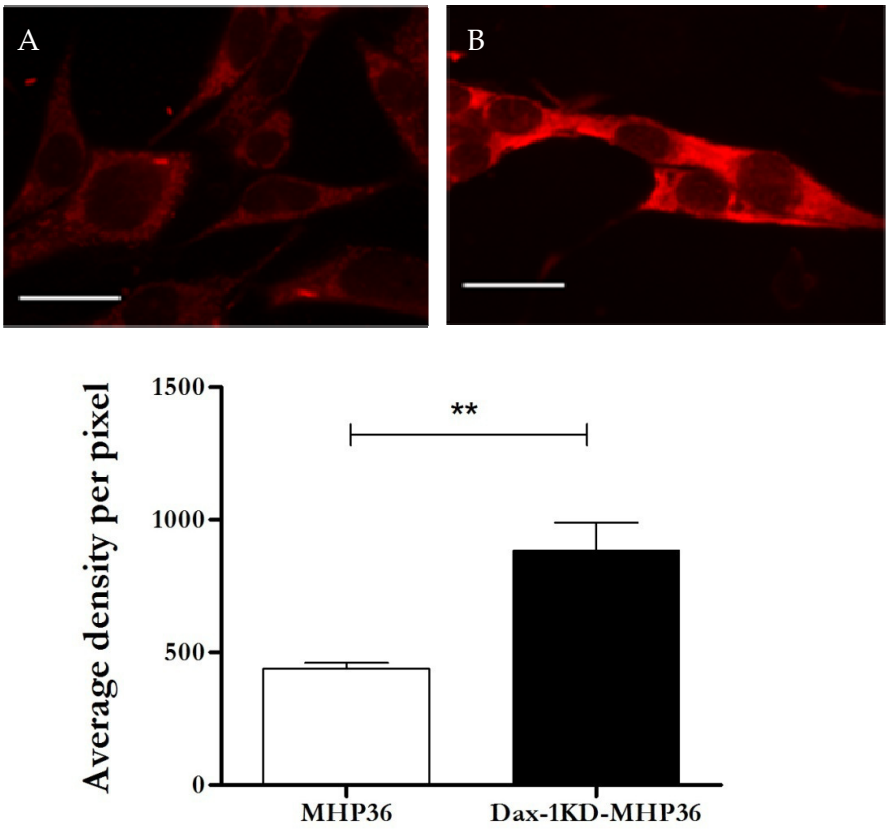

Figure 3.15: Immunofluorescence for aromatase in MHP36 and Dax-1KD-MHP36 cells.

(**A**) Aromatase protein expression localised in the cytoplasm in MHP36 cells. (**B**) Over-expression of aromatase due to successful knockdown of Dax-1 in Dax-1KD-MHP36 cells. One representative experiment of 3 is shown. (Bar = 80µm). Immunofluorescence for aromatase represented as a graph using Image J Software. The Y-axis represents average density per pixel (at least 10 cells per field). Statistical analysis was performed using unpaired t-test (**$p<0.01$).

3.3.6.3 | Characterisation of Dax-1 and aromatase using Western blotting

In order to confirm results obtained by immunostaining in Dax-1KD-MHP36 cells for Dax-1 (**Figure 3.16A & B**) and aromatase (**Figure 3.17A & B**), Western blot analysis was carried out. A band with a molecular size of approximately 50kDa (Dax-1) and 52kDa (aromatase) in all the samples namely; MHP36 (first lane), Dax-1KD-MHP36 (second lane) and MCF-7 (third lane) cells was observed. The expression of Dax-1 was significantly decreased and expression of aromatase was significantly increased in the Dax-1KD-MHP36 cell when compared to MHP36 cell.

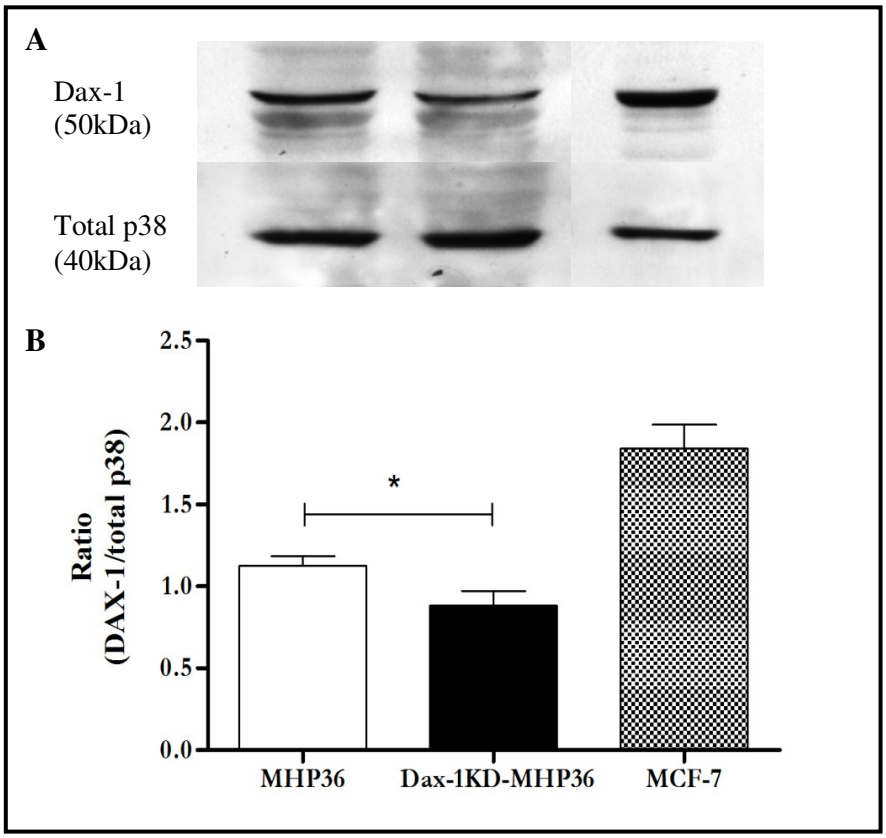

Figure 3.16: Western blotting for Dax-1 protein in whole cell lysate.

(**A**) (Top) Decreased expression of Dax-1 protein in Dax-1KD-MHP36 when compared to MHP36. (Bottom) Total p38 (MAPK) protein expression which was used as an internal loading control. One representative experiment of 3 is shown. (**B**) Graph plotted as ratio of Dax-1 expression over total p38 expression on the Y-axis and different cell lines on X-axis. MCF-7 breast cancer cell line was used as a positive control. Data represented as mean ± SEM, n=3. Statistical analysis was performed using unpaired t-test (*$p<0.05$).

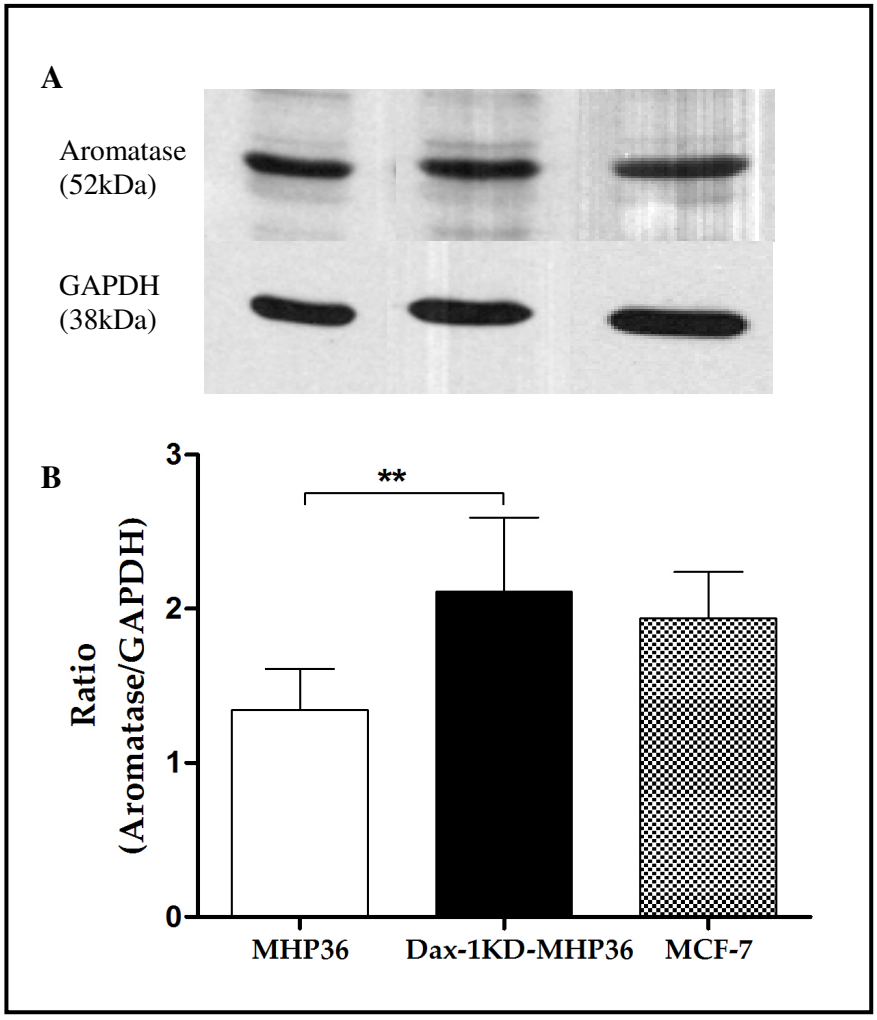

Figure 3.17: Western blotting for aromatase protein in whole cell lysate.

(**A**) (Top) Increased expression of aromatase protein in Dax-1KD-MHP36 when compared to MHP36 cell. (Bottom) Expression of GAPDH used as internal loading control. (**B**) Graph plotted as ratio of aromatase expression over GAPDH expression on the Y-axis and different cell lines on X-axis. MCF-7 breast cancer cell line was used as a positive control. Statistical analysis was performed using un-paired t-test (**p<0.01). One representative experiment of 3 is shown.

3.3.6.4 | Characterisation of oestrogen using ELISA

The data indicates that Dax-1KD-MHP36 cells had a significant increase in levels of 17β-oestradiol in their supernatant (media) (51.36±0.87 pg/ml, mean ± S.E.M., n=3) when compared to MHP36 cells (20.9±1.77 pg/ml, mean ± S.E.M., n=3) as well as a higher level of 17β-oestradiol was observed in the cells (Dax-1KD-MHP36= 27.88±3.8 pg/ml; MHP36= 7.4±0.05 pg/ml). The levels of 17β-oestradiol in plasma obtained from female Dax-1 (heterozygous) is in unison with the literature suggesting high sensitivity of the assay. (**Figure 3.18**).

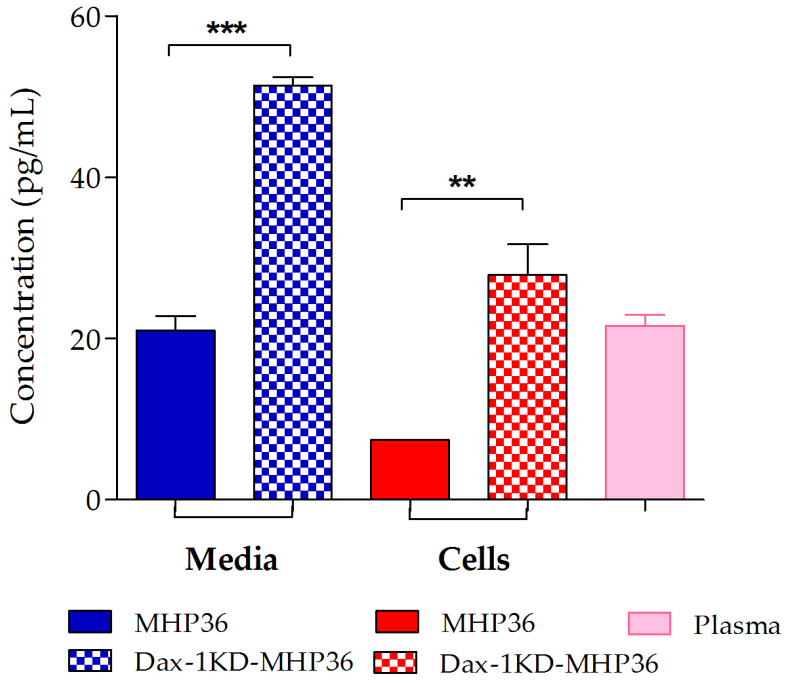

Figure 3.18: Concentration of oestrogen (17β-oestradiol) assessed using ELISA.

Significant increase in concentration of 17β-oestradiol in supernatant media (blue) and cell (red) in the Dax-1KD-MHP36 when compared to MHP36 cells. Consistent concentration of 17β-oestradiol observed in plasma from female Dax-1 (heterozygous) animal using ELISA as described in section 2.2.9 which was used as a positive control. All samples were analysed in triplicates. Statistical analysis was performed using one-way analysis of variance with post-hoc Bonferroni's test. Data represented as mean ± S.E.M., n=3, **p < 0.01; ***p < 0.001 versus MHP36.

3.4 | Discussion

The key findings of this chapter are 1) MHP36 cells express ERβ and GPR30 and have the capacity to synthesise and release oestrogen and 2) genetically modified Dax-1KD-MHP36 cells successfully achieved significantly increased synthesis and release of oestrogen demonstrated using Western blotting, immunofluorescence and ELISA.

Initially the MHP36 cells were characterised alone and a baseline aromatase expression was observed using immunostaining and Western blotting. Moreover, oestrogen administered to MHP36 cells showed a trend to elevate expression of aromatase. This was not significant since the baseline endogenous expression of aromatase was high which was probably due to the IFN-γ in the media stimulating the expression of aromatase. And MHP36 cells could not be starved since they were grown in serum free medium. A closer analysis using RT-PCR confirmed the results of the immunostaining after standardising the PCR reaction and carrying out a more sensitive approach of semi-nested PCR. The use of β2- microglobulin (house keeping protein) in the RT PCR confirms the validity of mouse RNA and cDNA synthesis but not that of the primers for aromatase. To analyse the validity of the primers, mouse testis tissue positive for aromatase was used. In addition to endocrine-derived hormones, recent experiments have demonstrated that hippocampal neurons may also be exposed to locally synthesized brain neurosteroids, such as pregnenolone (PREG) (Baulieu, 1997, Hojo et al., 2004, Kawato et al., 2002, Kawato et al., 2003, Kimoto et al., 2001) and its sulphated ester (Hojo et al., 2004) that in presence of aromatase synthesise 17β-oestradiol locally.

Neurosteroids such as 17β-oestradiol are synthesized in the brain, and the cerebellum is a major site for neurosteroid formation (Sakamoto et al., 2003). In the adult mammalian rat brain significant localization was demonstrated for cytochrome P450 aromatase, in pyramidal neurons in the CA1–CA3 regions, as well as in the granule cells in the dentate

gyrus, by means of immunohistochemical staining of slices (Hojo et al., 2004). Our findings of aromatase protein in the MHP36 neural stem cells are in agreement with these findings, since the MHP36 cells are isolated from the proliferative zone of the mouse hippocampus. These results indicate the need to reconsider the belief that these sex steroids are produced only in the gonads and reach the target brain via blood circulation. Rather, such steroid hormones may be produced endogenously in the adult brain, where they play an essential role in the plasticity and protection of neurons. With this background, the approach of genetic modification was used to either over-express aromatase or knockdown Dax-1 in these MHP36 cells to eventually have a cell line that would be over-expressing oestrogen to test the hypothesis (see below).

Western blotting and immunostaining demonstrated that the MHP36 cells do not express the ERα which was confirmed by RT-PCR. The MHP36 cells expressed low levels of ERβ observed by RT-PCR. Furthermore, little success was achieved in showing the expression of ERβ in the MHP36 cells using Western blotting. This could be due to the antibody, since ERβ are nuclear receptors and stain the nucleus, (personal communication with Dr. G. Greene, gift of ERβ antibody) in the present study ERβ was observed densely populated at the nuclear membrane using immunostaining and could not show a nuclear translocation after stimulating the MHP36 cells with 17β-oestradiol. The presence of ERs are well documented in the adult mammalian brain (see review (Toran-Allerand, 2004b, Toran-Allerand, 2004a) and **section 1.3.3**). Studies using in situ hybridisation indicate widespread distribution of ERβ mRNA throughout much of the brain, including olfactory bulbs, cerebellum, hippocampus and cerebral cortex (Kuiper and Gustafsson, 1997, Kuiper et al., 1998) while ERα sites are associated with only reproductive behaviour in the hypothalamus (Brannvall et al., 2002, Behl, 2002). As mentioned earlier the MHP36 neural stem cells are

isolated from the proliferative zone of the mouse hippocampus and our findings of presence of ERβ and not ERα in these cells are plausible, justified by previous discussed evidence.

The existence of G protein-mediated signalling by oestrogen (Wyckoff et al., 2001) and localization of oestrogen binding sites to membranes (Kelly and Levin, 2001) suggested the possibility of a 7-transmembrane G protein-coupled receptor family member being involved in certain aspects of oestrogen function. Although, the majority of GPCRs are expressed in the plasma membrane surprisingly, we observed intracellular localisation of GPR30 in the MHP36 cell as well as the positive MCF-7 cells and this has been confirmed with subsequent studies (Gobeil et al., 2006, Prossnitz et al., 2008b, Revankar et al., 2005). Using sub cellular markers, Revankar and colleagues identified this compartment as the endoplasmic reticulum. In addition, they were unable to detect GPR30 on the plasma membrane, as defined by staining of the actin cytoskeleton to delineate the plasma membrane from the cell interior. This has been confirmed for endogenously expressed GPR30 as well (Revankar et al., 2005). Such localization is at odds with the conventional paradigms of GPCR function, which place functional GPCRs in the plasma membrane. In fact Filardo and colleagues originally described GPR30 as a plasma membrane receptor, a logical assumption, despite the lack of experiments to examine receptor localization. To complicate this issue further, Thomas and colleagues published an article providing evidence that GPR30 was in fact found in the plasma membrane though no staining of sub cellular markers was provided (Thomas et al., 2005). Their argument was based on two observations: (1) an annular staining pattern of endogenously expressed GPR30 in SKBr3 breast cancer cells and (2) the presence of tritiated oestrogen-binding sites in isolated cell membranes. More recently, Funakoshi and colleagues also reported expression of GPR30 in the plasma membrane (Funakoshi et al., 2006). In conclusion, there remains some controversy against the site of GPR30 expression. Interestingly, it has been shown that the G

protein βγ subunits are initially targeted to the endoplasmic reticulum, where they subsequently associate with G protein α subunits, providing the requisite machinery for GPR30 to initiate signalling (Prossnitz et al., 2008a). From that point, it is certainly possible that under the appropriate conditions, intracellular GPR30 could exist or translocate to the cell surface or vice versa. However, given the fact that GPR30's ligand oestrogen is membrane permeable, an intracellular localization of the receptor is certainly consistent with its function. Using immunostaining, Western blotting and RT-PCR the expression of GPR30 was confirmed in MHP36 cells.

The clones over-expressing aromatase were not observed to over-express oestrogen successfully and thus were not used further in the study (data not shown). This could be partly explained by two reasons- firstly, it could be the unstable-transfection method employed using expression plasmid. Secondly, since the rate limiting step in the steroid biosynthesis pathway is up-stream to aromatase, the turn-over to be significantly visualised is less. The Dax-1KD-MHP36 cells showed a significant increase in expression of aromatase and eventually an increase in levels of oestrogen production and release when compared to the MHP36 cells.

In conclusion, the characterization of the MHP36 cells as well as Dax-1KD-MHP36 cells for oestrogen raises interesting aspects of its oestrogen-related properties after experimental stroke and helps explore the clinical application of cell replacement therapy, as well as gene therapy. Our results suggest that this conditionally immortalised cell line could serve as a potential model for studying the contributions of oestrogen on the improvement of survival and differentiation of neural stem cells after transplantation into experimental stroke. Whether the increased local endogenous production of oestrogen via aromatase by the Dax-1KD-MHP36 cells helps improve the integration and differentiation of cells *in vivo* after experimental stroke is elucidated in **Chapter 6**.

CHAPTER 4

ESTABLISHMENT OF THE TRANSIENT STROKE MODEL IN MICE

4.1 | Introduction

MCAO by the intraluminal thread (ILT) was first introduced by Koizumi and colleagues (Koizumi et al., 1986) and subsequently the model was modified to reduce subarachnoid haemorrhage and premature reperfusion by Longa and colleagues who used a slight modification of the method and demonstrated that an area of infarction corresponding to the MCAO perfusion territory was produced by this procedure (Longa et al., 1989) (see **section 1.1.4.3** for details). The greatest advantage of the ILT model is the ease with which recirculation can be instigated. More importantly, reperfusion can be achieved when the animal is fully conscious since the filament can be exteriorised. With every animal model there are disadvantages and the most common are the source of variability and high mortality rate which may be contributed by various factors of which few are described below.

Filament type- One of the major sources of variability among animal experiments may be due to the filament used to block the origin of the MCA. Three filament types have been produced endeavouring to reduce variability 1) silicon or poly-L-lysine coated 2) bulb and 3) resin coated. Many studies have reported that uncoated filaments cause high mortality rates, for example, 80% after 60 minutes of MCAO (Kitagawa et al., 1998) and >85% after 180 minutes of MCAO (Connolly et al., 1996). SAH resulting from excessive insertion pressure of the intraluminal filament also has been documented. Schmid-Elsaesser and colleagues chose to coat their

filament and demonstrated that this was associated with a higher rate of successful occlusions and a lower rate of SAH (Schmid-Elsaesser et al., 1998). Belayev and colleagues coated a filament with poly-L-lysine which increased their success rate of infarction after 1 or 2 hrs of ischaemia and 3 days of reperfusion, from 42% (uncoated filament) to 100% (poly-L-lysine-coated filament) and greatly lowered the intra-animal variability (Belayev et al., 1996). The success of coated filaments may be contributed to the filament's adherence qualities. By adhering to the blood vessel endothelium, the filament prevents any residual blood flow past it. However, when reperfusion is instigated by withdrawal of the filament, there is a higher chance of disruption to the vessel wall if the filament has attached to it (Nishigaya et al., 1991, Rabb, 1996). This could result in blood brain barrier permeability and additional injury found in the animal, which is not purely a result of cerebral ischaemia, but may be a consequence of the method of vessel occlusion itself. Therefore, several groups have redesigned the filament to improve the number of successful occlusions but also to reduce the amount of unrelated blood vessel damage (Touzani et al., 2002, Clark et al., 1997). In these reports, the tip of the filament was coated with a resin-like substance. This was used instead of coating the filament with poly-L-lysine or the traditional method of blunting the tip with heat until it is a specific diameter. This resin-style of filament may have a better chance of successfully occluding the MCA since the coated tip is longer than the length of the bulb in heat-blunted filaments. In contrast more recently, Shah et al., in 2006 showed that the silicone-coated 8-0 filament was a better choice for MCAO than the resin-coated filament in mice because of its flexibility. The flexible filament considerably increased the rates of successful strokes and survival in the study (Shah et al., 2006) (see **Figure 4.1**).

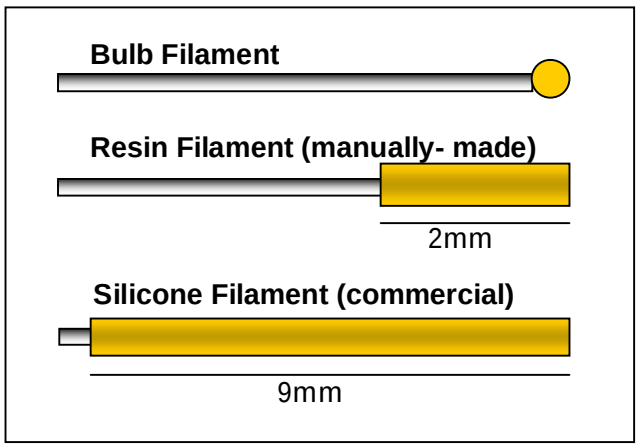

Figure 4.1: Diagram of traditional heat blunted blub, resin and commercially available silicon coated types of filament.

Physiological parameters- Temperature is an essential parameter to monitor and control during an animal experiment. In suture occlusion of 60 min duration or greater, hypothalamic damage is robust and occurs early in rodents (Carmichael, 2005, Garcia et al., 1995, Reglodi et al., 2000). Hypothalamic ischemia generates a hyperthermic response in rats that persists for at least 1 day after the animal has recovered (Li et al., 1999) and is often unmonitored. Both hyperthermia and hypothermia affect ischaemia lesion size. Hyperthermia exacerbates cell death, while mild to moderate hypothermia confers marked neuroprotection (McIlvoy, 2005) and this means that temperature fluctuations themselves may be a source of variability for ischemic cell death in MCAO.

Evidence is abundant suggesting the role of strain and of vendor on the reproducibility of infarct size after ischaemia (Bardutzky et al., 2005, Oliff et al., 1995, Walberer et al., 2006). Oliff and group showed that infarct size varied dramatically depending on not only the strain of rat used but also where a particular strain of rat was purchased. The variation may have resulted from

genetic variation or differences in the blood pressure of the rats The same strain of rat was found to have different resting blood pressures depending on the vendor and high blood pressure resulted in lower infarct volumes by enriching the collateral flow to the ischaemic area (Oliff et al., 1995). Though recently, evidence is growing showing systemic blood pressure, body temperature and blood gases do not differ between investigated groups and hence are unlikely to be responsible for the observed inter-model variations in CBF (Bardutzky et al., 2005, Walberer et al., 2006). Furthermore, since it is technically difficult to perform the suture insertion and to monitor physiological parameters in mice, monitoring blood pressure or blood gases was not included in the experiments.

Due to the discrepancies in literature regarding the use of the filament type or time of occlusion in the ILT model setup and in view of success of Shah et al. (Shah et al., 2006), this present study established the occlusion model that yielded highly consistent results in mice, using two types of filaments namely; the resin and Doccol filaments and two times of occlusion namely; 45 mins and 60 mins. The experiments described in this chapter were carried out to establish the ILT model of transient MCAO in mice. The immediate aim was to establish an optimal model that resulted in an infarct size where the peri-infarct is accessible by stereotaxic injection, an infarct size large enough to allow attenuation of infarct and small enough to allow exacerbation of infarct, the infarct should show cortical involvement (as sensorimotor function was to be used in behavioural outcome; discussed in **Chapter 5**) and the model should achieve a low mortality rate, with good reproducibility.

4.2 | Methods

4.2.1 | Surgical Procedures

Animals- Male C57Bl/6J mice (~11 to 13 weeks old, Charles River, UK and in-house) were group housed in conditions of a 12-hour light-dark cycle with free access to food and water. The animals weighed between 25- 30g at the time of MCAO surgery.

Transient MCAO and laser Doppler flowmetry- Mice were anaesthetised and underwent transient MCAO as described in section **2.2.10**. Cerebral blood flow was measured in animals before, during and after occlusion using laser Doppler flowmetry as described in section **2.2.10.3**. The method of occlusion used two of the types of intraluminal filament, the manually made resin coated filament and commercially available silicone coated monofilaments from Doccol, USA (see **Figure 4.1**) and time of occlusion - 60mins with 24hrs reperfusion, 45mins with 24 hrs of reperfusion and 45mins with 72 hrs of reperfusion.

Experimental conditions of the 3 studies used in this chapter are tabulated below.

Study Number	Mouse Strain	Surgery	Filament	Occlusion time	Recovery time	Laser Doppler	Clark's Score
1 (n=19)	C57	MCAO	Resin	60 and 45 mins	24 hrs	No	No
2 (n=6)	C57	MCAO	Resin and Doccol	45 mins	24 hrs	Yes	No
3 (n=9)	C57	Sham surgery	Doccol	45 mins	72 hrs	Yes	Yes

Table 4.1: Details of experimental conditions for all studies.

Termination of the Experiment- After a reperfusion period, the experiment was terminated and the brain was fresh frozen (see **section 2.2.12.1)** in all cases. The brains were processed

appropriately and coronal sections were cut at 20μm and collected on slides to measure infarct volumes (detailed in **section 2.2.13.1**).

4.2.2 | Measurement of Infarct

Eight coronal levels were selected from the atlas of mouse by Franklin and Paxino (+6.02, +4.66, +3.94, +3.34, +2.86, +1.98, +1.00, +0.16 with respect to interaural line). These sections were stained with haematoxylin and eosin to determine ischaemic damage and volume of infarct was derived for the fresh frozen tissue as described in **sections 2.2.13**. In addition co-efficient of variance (%CV) was calculated using formula; SD/mean*100.

During the establishment of the MCAO model in study 3, sham operated mice were used as controls. Sham surgery was conducted as described in **section 2.2.10.2** in Chapter 2.

4.2.3 | Clark's Deficit Score (CDS)

After 2, 24, 48 and 72 hrs after the induction of ischemia, each mouse was rated on two neurologic function scales unique to the mouse (Clark et al., 1997) to establish severity of deficit in each mouse (see **section 2.2.14.1**). No animal was excluded in any of the study discussed in this Chapter.

4.2.4 | Statistics

Statistical evaluations between oedema corrections in Study 1 were carried out using paired t-test unless otherwise stated. In the Clark's deficit score data was analysed using two-way ANOVA with repeated measures. Post hoc analyses were conducted using Bonferroni's test. A p-value of less that 0.05 was chosen as the significance level for all statistical analyses. The data are presented as mean ± SEM, n= number of animals per group.

4.3 | Results

4.3.1 | Study 1: Establishment of occlusion time for MCAO

Animals used in this study were C57BL/6 male mice. Nineteen animals underwent the MCAO surgery (different occlusion times; 60 mins (n=12) and 45 mins (n=7)) and were monitored during their recovery for 24 hrs (**Table 4.1**).

60 mins occlusion: Out of the 12 animals, 3 died during surgery which could be due to over dose of anaesthesia (each surgery lasted approximately three and half hrs; in the early stages of MCAO setup) or damage to the vagus nerve (control cardiac function) and 2 were close to the severity limits set on the Home Office Project Licence during recovery and thus were put down. 7 animals that survived the procedure and recovered were analysed for infarct (**Figure 4.2 and Table 4.2**). 5 animals showed infarct and 2 animals (SP27 and SP29) did not show any infarct, thus were excluded from the study. This could be because the filament was not been placed at the right position. All the results discussed below are of the 5 animals that suffered from stroke.

45 mins occlusion: No animal died during surgery and out of the 7 animals, 1 animal was close to the severity limits set on the Home Office Project Licence during recovery and thus was put down. 6 animals that survived the procedure and recovered were analysed for infarct (**Figure 4.2 and Table 4.3**). 5 animals showed infarct and 1 animal (SP36) did not show any infarct, thus was excluded from the study. All the results discussed below are of the 5 animals that suffered from stroke. Use of laser Doppler flowmetry demonstrated that the filaments were positioned correctly at the origin of the MCA. Thus it was used in the following optimising study to reduce the variability in achieving stroke.

A

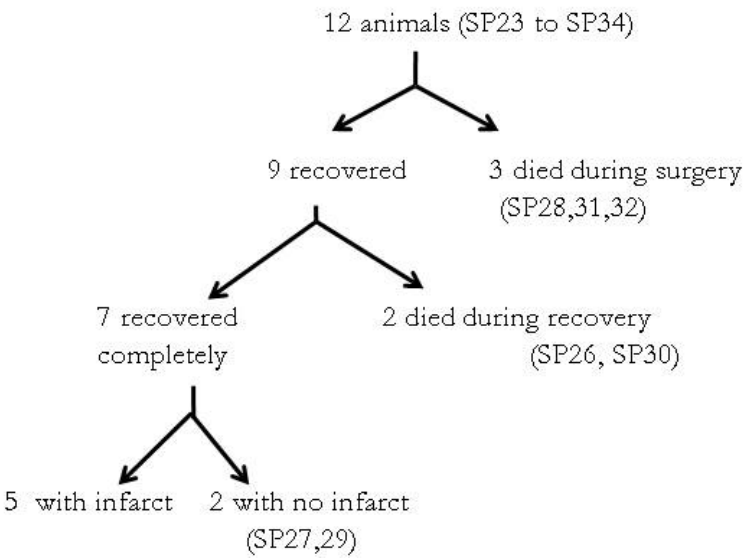

B

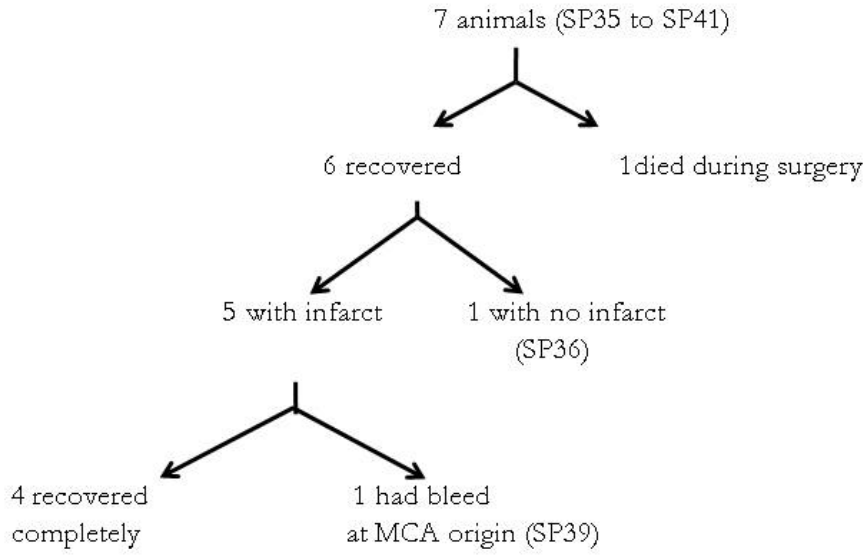

Figure 4.2: The outcome of all animals in Study 1.

(A) Animals undergoing 60 mins of occlusion and (B) Animals undergoing 45 mins of occlusion.

In the 60 mins occlusion group, there was a 40% mortality rate and this was supported by evidence of large volumes of infarct. SP26 was one of the 2 animals that died during recovery (**see table 4.2**) and it was observed that the animal suffered from a massive stroke (volume of lesion, circled red in table 4.2). **Figure 4.3** shows the area of infarct across the 8 pre-determined levels of the mouse brain which involves both the cortex and sub-cortical areas. A peak area of infarct was observed at level 5 which accorded to previous studies by McColl and colleagues (McColl et al., 2004) involving territories outside the MCA supply.

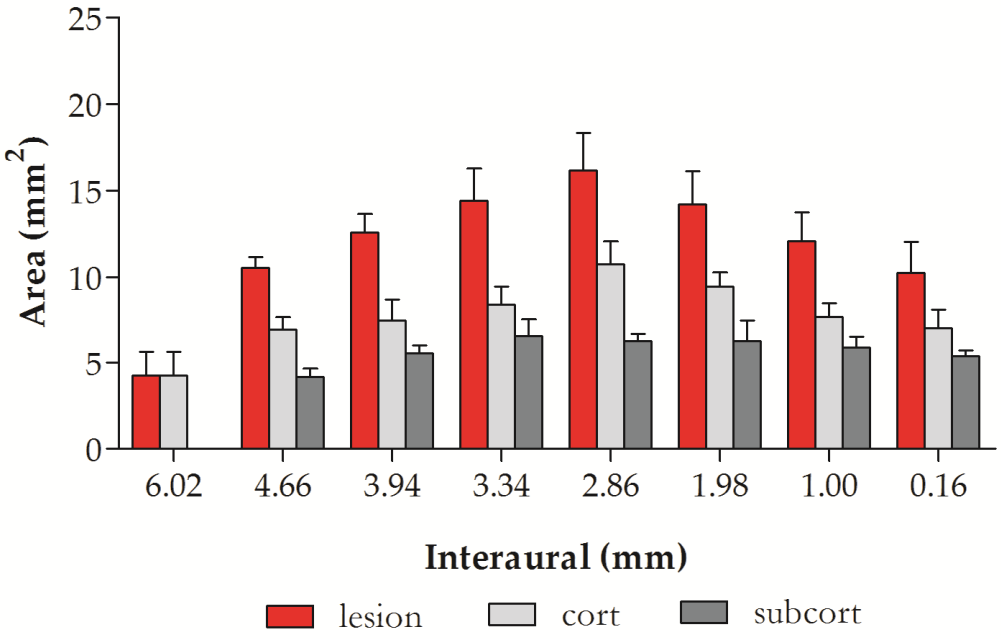

Figure 4.3: Area of cortical (cort), sub cortical (subcort) and total lesion (lesion) plotted at 8 coronal levels in mice occluded for 60 mins using the resin filament.

Cortical and sub-cortical areas were measured throughout the 8 levels. Area-wise cortical regions affected was more than the sub-cortical regions at all levels. A peak area of infarct was observed at level 5. The data is represented as (mean± SEM, n=5) Levels 1 through 8 correspond to atlas levels of +6.02, +4.66, +3.94, +3.34, +2.86, +1.98, +1.00, +0.16 with respect to interaural distance, respectively.

No	Strain	Weight		Volume (mm^3)		
		Pre	% loss	contra	ipsi	lesion
SP23	C57/mice	24.0	8.3	126.4	144.1	58.53
SP24	C57/mice	25.5	9.0	138.0	155.1	55.10
SP25	C57/mice	27.0	8.5	138.7	161.9	62.37
SP26	C57/mice	26.1	8.9	139.1	177.5	101.0
SP27	C57/mice	26.4	4.5	-	-	-
SP29	C57/mice	27.3	4.7	-	-	-
SP30	C57/mice	27.0	8.9	140.5	180.5	95.0
SP33	C57/mice	24.7	8.0	134.1	161.3	64.27
SP34	C57/mice	24.8	11	140.3	169.4	75.53

Table 4.2: The volume of lesion observed in mice used in study 1 with 60 mins occlusion and 24 hrs of recovery.

This table includes the volume of the hemispheres (contralateral and ipsilateral) and lesion before oedema correction. Furthermore, percent weight loss of the animal is indicated alongside the animal ID. MCAO- transient middle cerebral artery occlusion.

In the 45 mins occlusion group, there was a 15% mortality rate. SP39 was the animals that died during recovery (**see table 4.3**) and it was observed that the animal suffered from a massive stroke (volume of lesion, circled red in table 4.2). **Figure 4.4** shows the area of infarct across the 8 pre-determined levels of the mouse brain which involves both the cortex and sub-cortex. A peak area of infarct was observed at level 3 involving the sensorimotor cortex.

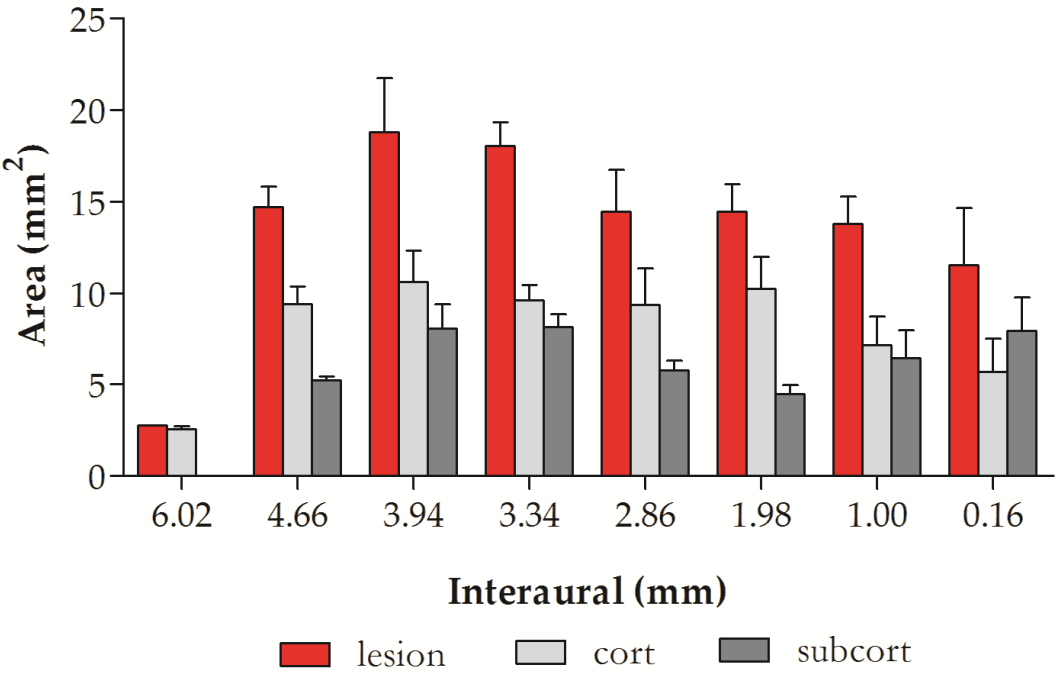

Figure 4.4: Area of cortical, sub cortical, and total lesion plotted at 8 coronal levels in animals occluded for 45 mins using the resin filament.

Cortical and sub-cortical areas were measured throughout the 8 levels. Area-wise cortical regions affected was more than the sub-cortical regions at all levels. A peak area of infarct was observed at level 3. The data is represented as (mean± SEM, n=5) Levels 1 through 8 correspond to atlas levels of +6.02, +4.66, +3.94, +3.34, +2.86, +1.98, +1.00, +0.16 with respect to interaural distance, respectively.

No	Strain	Weight		Volume (mm^3)		
		Pre	% loss	contra	ipsi	lesion
SP35	C57/mice	27.5	10.0	148.5	151.6	69.82
SP36	C57/mice	28.7	8.5	-	-	-
SP37	C57/mice	25.8	11.0	152.6	147.3	33.98
SP38	C57/mice	26.4	8.0	138.7	151.9	61.4
SP39	C57/mice	26.0	10.0	164.2	189.7	106.8
SP40	C57/mice	27.0	12.5	146.8	166.1	74.65

Table 4.3: The volume of lesion observed in animals used in study 1 with 45 mins occlusion after 24 hrs of recovery.

This table includes the volume of the hemispheres (contralateral and ipsilateral) and lesion before oedema correction. Furthermore, percent weight loss of the mice is included along side with the animal ID. MCAO- transient middle cerebral artery occlusion

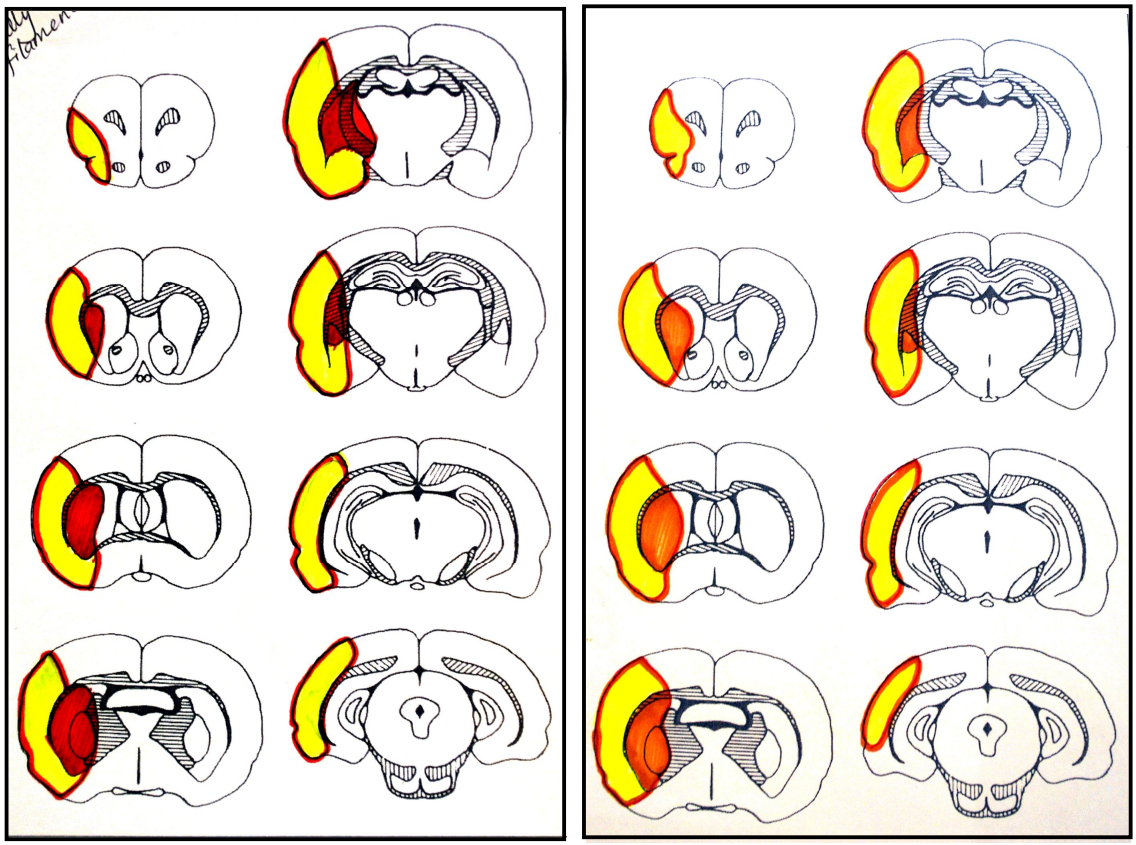

Figure 4.5: Distribution of infarct over 8 coronal levels after 60 mins (left) and 45 mins (right) MCAO after 24 hrs of reperfusion.

Shaded areas represent areas of infarction in one representative animal from each group (yellow- cortical and red- sub-cortical).

Figure 4.5 shows median representative distribution of infarct over the 8 pre-determined coronal sections in mice occluded for 60 mins (**Figure 4.5** left) and 45 mins (**Figure 4.5** right). Both cortex and sub-cortical areas were damaged and extent of damage was not significantly different.

In this study, the infarcted histopathology was measured by separately measuring the cortical and sub-cortical regions. This analysis indicates that structures not consistently infarcted following MCAO in rats (Kanemitsu et al., 2002) such as the hippocampus and thalamus are also not consistently damaged in the mice (**Figure 4.5**).

Previous studies in rodents have, in general, relied upon the use of the triphenyltetrazolium (TTC staining method) at relatively few coronal levels (Bederson et al., 1986, Tureyen et al.,

2004). While the TTC method is quicker and hence easier, the present study used haematoxylin and eosin staining (H&E) - a clear demarcation line was seen between the ischaemia and normal area. One advantage of H&E staining, compared to TTC staining, is the ability to see detailed cellular morphology. The histological appearance of the infarct regions was consistent in both groups, the most remarkable features being the overall pale staining of the neuropil and the generalized presence of 'triangular' cells, indicated by a vacuolated cytoplasm and early stages of nuclear disintegration with neuronal shrinkage (**Figure 4.6**).

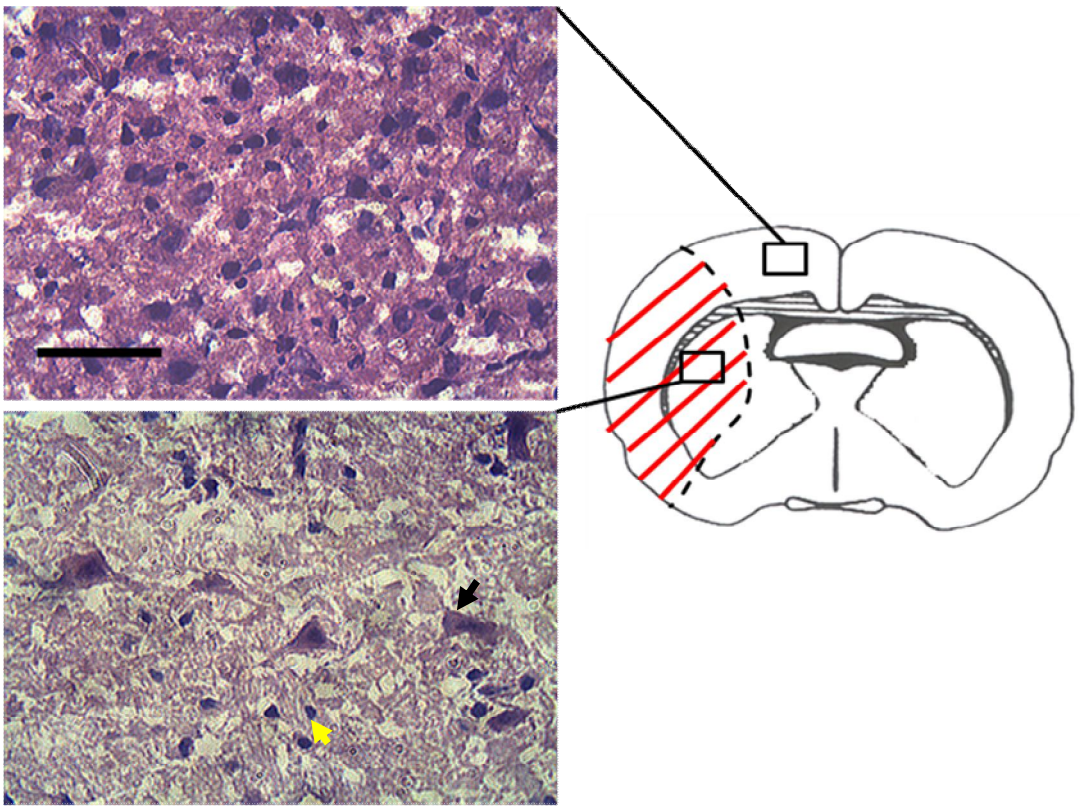

Figure 4.6: Haematoxylin and eosin staining after 60 mins of occlusion and 24 hrs of recovery

Normal tissue (top) and infarct tissue (bottom) showing triangular cells (black arrow) and shrunken cell (yellow arrows) in the infarcted area when compared to the healthy region. The coronal section from the atlas of the mouse brain (line diagram on the right) used as a reference to illustrate the regions measured (Bar scale = 50µm).

A

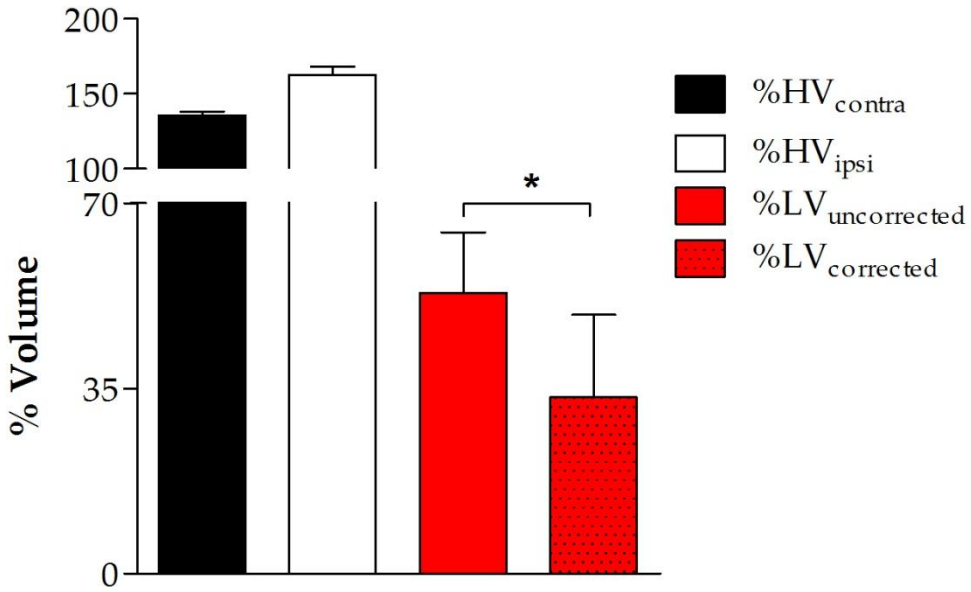

B

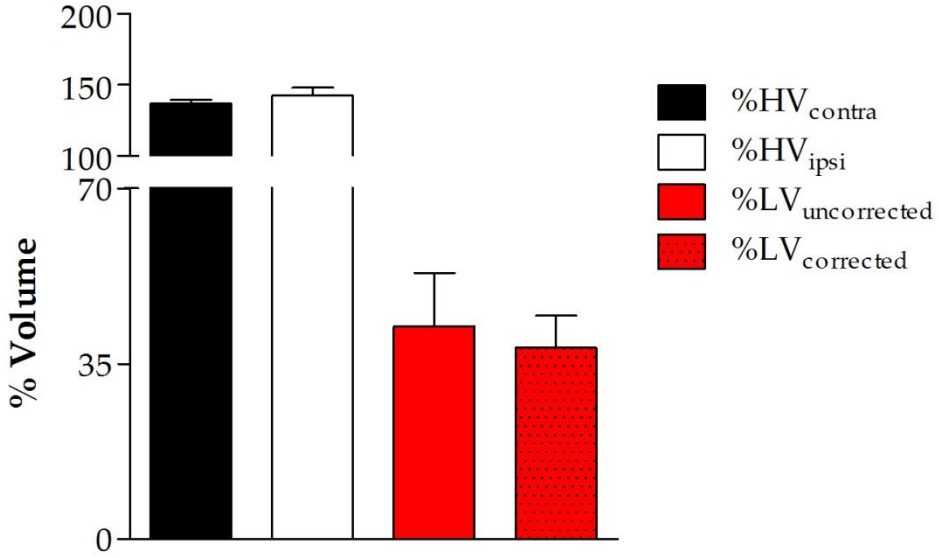

Figure 4.7: Impact of oedema correction on percent Lesion Volume (%LV) calculation induced by resin filaments and recovered for 24 hrs.

The difference in uncorrected and corrected hemispheric LV is demonstrated. (A) after 60 mins occlusion and 24 hrs recovery, oedema correction leads to a significant reduction of %LV by 20%. (B) After 45 mins occlusion and 24 hrs recovery, oedema correction lead to a non-significant reduction (Mean± SEM, n=5).

Post-ischaemia brain oedema is a common feature. Measurements of infarct volume in experimental brain research without correction for oedema increases the volume of the affected tissue and leads to an overestimation of lesion size (Park and Kang, 2000). Thus for accurate measurements lesion volume is corrected for oedema in this study (see **section 2.2.13.5** for calculation).

Percent contralateral hemispheric volume ($\%HV_{contra}$) (135.78 ± 2.50, n=5), percent ipsilateral hemispheric volume ($\%HV_{ipsi}$) (162.84 ± 5.53, n=5), percent lesion volume ($\%LV_{uncorrected}$) (53.1 ± 5.1, n=5) were calculated after 60 mins of occlusion (**Figure 4.7A**). The mean data of $\%HV_{contra}$ (137.0 ± 2.4, n=5), $\%HV_{ipsi}$ (142.6 ± 5.5, n=5), $\%LV_{uncorrected}$ (42.4 ± 10.7, n=5) were obtained from the area under the curve after 45 mins of occlusion. Furthermore, after correction for oedema % lesion volume was estimated ($\%LV_{corrected}$) (60 mins: 33.28 ± 7.0, n=5; 45 mins: 38.2 ± 6.4, n=5) (see **section 2.2.13.5** for calculation) (**Figure 4.7B**). Both the infarcts were fairly reproducible (co-efficient of variance, 23% with 60 min occlusion; co-efficient of variance, 20% with 45 min occlusion).

The present study indicates that after 60 mins occlusion and 24 hrs of recovery, % lesion volume (%LV) determined by H&E was calculated to be 53 ± 11.2% without oedema correction and 33.3 ± 6.9% with oedema correction . %LV was therefore overestimated by 20% without oedema correction. This finding is in accordance with MRI studies from Loubinoux et al, which demonstrated a 25% increase in LV due to brain oedema 24 hrs after ischaemia (Loubinoux et al., 1997). In addition, 45 mins occlusion and 24 hrs of recovery resulted in a non-significant reduction of oedema and %LV was overestimated by ~10% without oedema correction (**Figure 4.7**).

4.3.2 | Study 2: Establishment of filament type for the MCAO

Animals used in this study were C57BL/6 male mice. Six animals underwent the MCAO surgery (filament type; commercially available silicone coated filament, Doccol) for 45 mins occlusion time and were monitored during their recovery for 24 hrs (**Table 4.1**).

Silicone coated filaments: No animal died during surgery and all 6 animals recovered. All 6 animals suffered from stroke and no bleed at the MCAO origin was observed post mortem. All 6 animals recovered were well within the severity limits set on the Home Office Project Licence during recovery (**Table 4.4**). All the results discussed below are of the 6 animals that exhibited infarcts. Furthermore, laser Doppler flowmetry was used in this study to reduce intra-variability in establishing the model. This revealed a rapid and sustained reduction in cortical cerebral blood flow when the silicone filament was inserted, detected by the laser Doppler flow probe, sited on the temporal-parietal region of the cortex. The mean decrease in cortical blood flow induced by clipping the CCA was 62.3 ± 5.53%; furthermore, insertion of the silicone filament dropped the flow to 12.50 ± 1.32% which was sustained for the time of occlusion. The animal reperfused to almost baseline levels within 15 mins of removal of filament (see **Figure 4.8**).

No	Strain	Weight		Volume (mm^3)		
		Pre	% loss	contra	ipsi	lesion
SP42	C57/mice	25.2	9.0	138.5	155.6	49.82
SP43	C57/mice	25.8	10.0	137.7	147.6	19.69
SP44	C57/mice	27.8	8.5	146.7	159.3	52.31
SP45	C57/mice	27.7	10.5	132.4	153.3	63.77
SP46	C57/mice	26.7	9.0	141.1	148.8	24.4
SP47	C57/mice	28.7	12.0	145.2	162.2	70.8

Table 4.4: The volume of lesion observed in mice used in study 2 with 45 mins occlusion, commercially available silicone filaments and 24 hrs of recovery

This table includes the volume of the hemispheres (contralateral and ipsilateral) and lesion before oedema correction. Furthermore, percent weight loss of the mice is included along side with the animal ID. MCAO- transient middle cerebral artery occlusion.

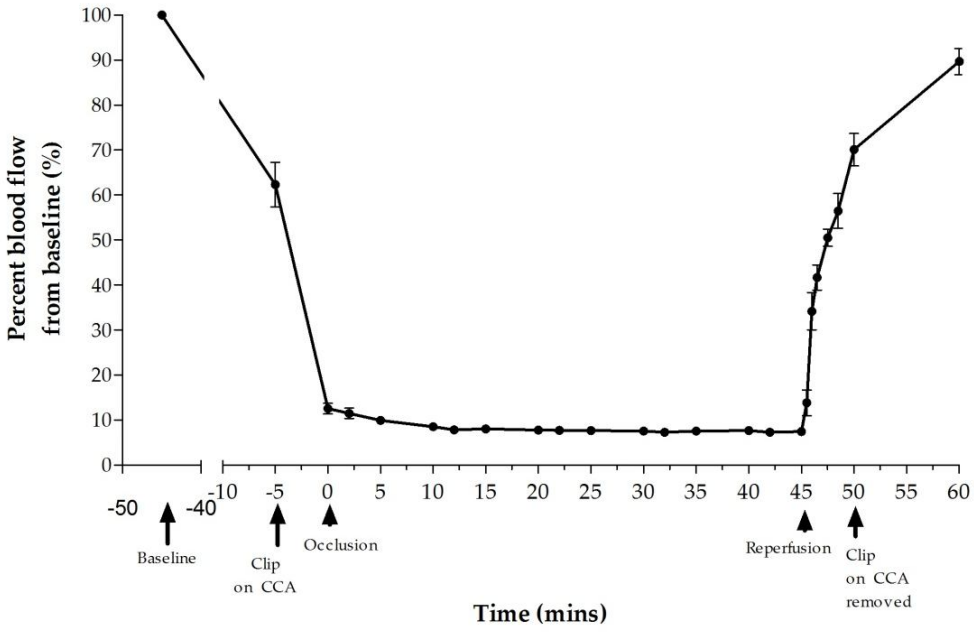

Figure 4.8: Laser Doppler flowmetry measurement in study 2

Cortical blood flow measured before, during and after insertion of the silicone filament to occlude the MCA, using laser Doppler flowmetry. Data are presented as a percentage change from baseline blood flow (100%) and represented as mean ± SEM, n=6. CCA= common carotid artery.

Figure 4.9 shows the area of infarct across the 8 pre-determined levels of the mouse brain which involves both the cortex and sub-cortex. Peak area of infarct observed was at level 3 and was not significantly different to the resin filament group (See **Figure 4.9**).

$\%HV_{contra}$ (142.6 ± 3.10, n=6), $\%HV_{ipsi}$ (154.9 ± 2.80, n=6) and $\%LV_{uncorrected}$ (32.6 ± 8.4, n=6) were calculated as described earlier (see **section 2.8.4**) and were obtained from the area under the curve after 45 mins of occlusion using the silicone filament (**Figure 4.10**). Infarcts were fairly reproducible when compared across different filament types measured directly from the section (**Table 4.3 & 4.4**). Furthermore, % lesion volume (%LV) determined by H&E was calculated to be (resin: 42.4 ± 10.7%; silicone: 32.6 ± 8.4, n=6) without oedema correction and after % lesion volume was corrected for oedema $\%LV_{corrected}$ (resin: 38.2 ± 6.4, n=5; silicone: 24.0 ± 6.0, n=6) (**Figure 4.10**).

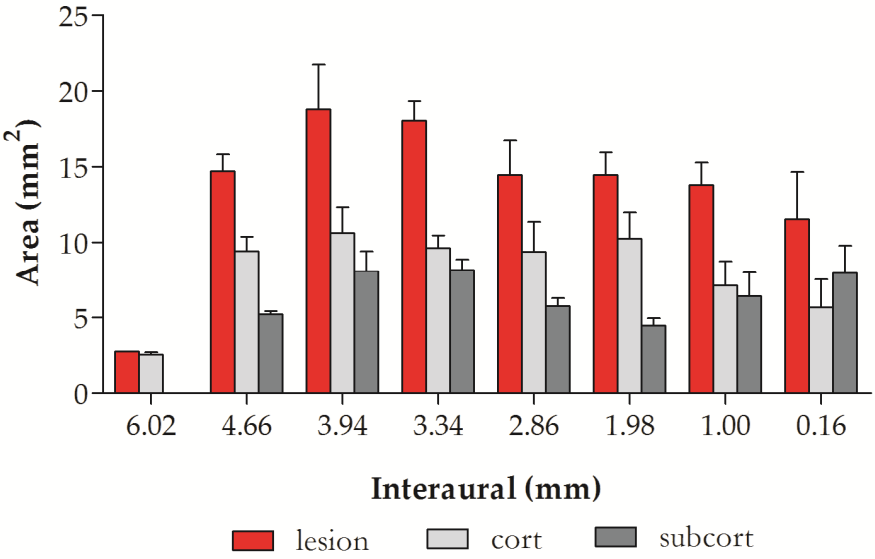

Figure 4.9: Area of cortical, sub cortical, and total lesion plotted at 8 coronal levels in animals occluded for 45 mins using the silicone filament.

Cortical and sub-cortical areas were measured throughout the 8 levels. Area-wise cortical regions affected was more than the sub-cortical regions at all levels except level 8. A peak area of infarct was observed at level 3 similar to study 2. The data is represented as mean ± SEM, n=6.

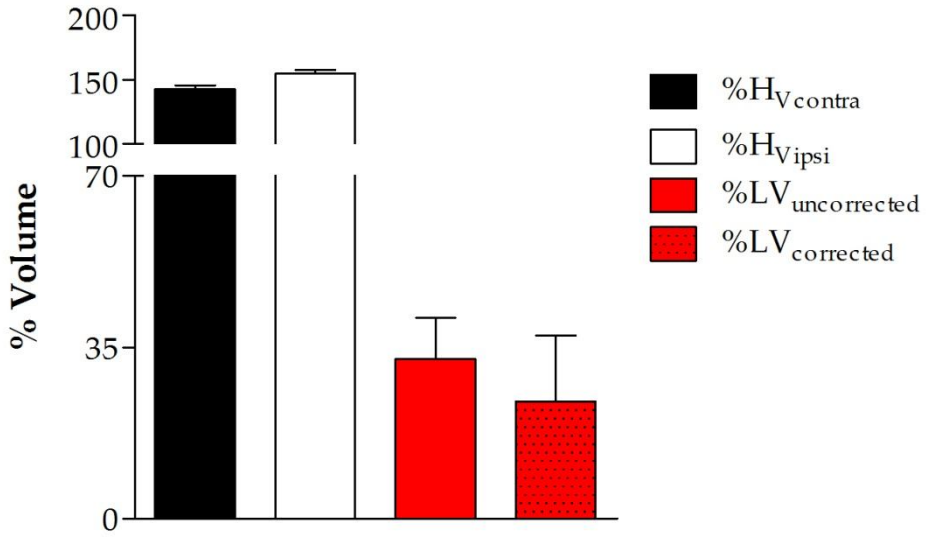

Figure 4.10: Impact of oedema correction on percent Lesion Volume (%LV) calculation induced by silicone coated filaments for 45 mins and recovered for 24 hrs.

The difference in uncorrected and corrected hemispheric LV is demonstrated. After 45 mins occlusion and 24 hrs recovery, oedema correction lead to a non-significant reduction (mean± SEM, n=5). %HV= percent hemispheric volume, % LV= percent lesion volume.

4.3.3 | Study 3: Establishment of sham surgery and complete evolvement of infarct measured after 72 hrs recovery

Animals used in this study were C57BL/6 male mice. Nine animals underwent either sham surgery (CCAO), (no CCAO) or MCAO surgery (n=3 in each group) (filament type; commercially available silicone coated filament, Doccol; 45 mins occlusion) and were monitored during their recovery for 72 hrs (**Table 4.1**). Laser Doppler flowmetry was used in this study to observe the reduction in blood flow and optimise the sham surgery plus reduce intra-variability in the MCAO model. The Doppler readings during the MCAO were reproducible to study 2. During CCAO sham surgery, almost a 50% reduction was observed in blood flow after clipping the CCA for the time of occlusion. On the other hand, no reduction was observed after ligatures of ECA (involved during the MCAO procedure) in the sham surgery involving no CCAO. The animal reperfused immediately to almost baseline levels monitored for 15 mins after unclipping the CCA or removal of filament (see **Figure 4.11**).

A similar observation was made with the % LV as made in Study 2. % LV was not significantly different after recovering animals for 72 hrs versus 24 hrs (24 hrs: 24.0 ± 6.0, n=6; 72 hrs: 22.8 ± 9.7, n=3) (**Figure 4.12**). In addition, to the post-mortem H&E evaluation of ischaemic damage, behavioural neurologic scores were evaluated using the Clark's deficit score. Post-MCAO animals showed a significant deficit in both the general and focal score when compared to animals that underwent no CCAO sham surgery at all time-points (**Figure 4.13A & B**). Sham animals undergoing CCAO suffered significant deficits observed at 24 hrs using the Clark's general deficit score which was sustained till 48 hrs. Furthermore, at 2 hrs a significant deficit was observed in focal scores when animals underwent CCAO when compared to no CCAO surgery.

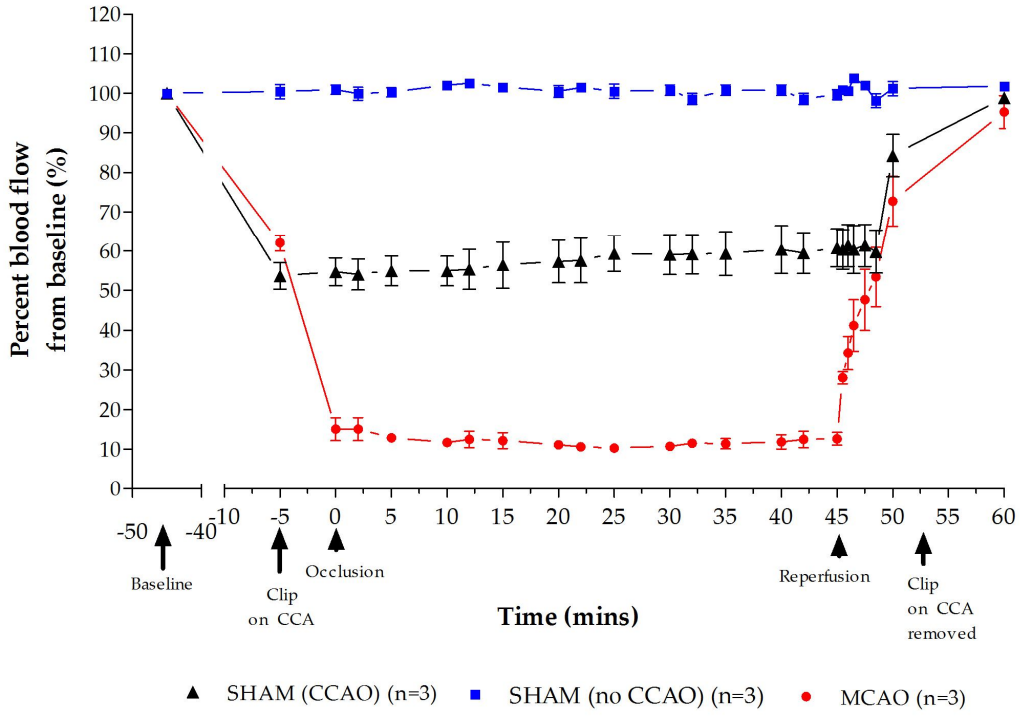

Figure 4.11: Laser Doppler flowmetry measurement in study 3.

Cortical blood flow measured before, during and after insertion of the silicone filament to occlude the MCA, using laser Doppler flowmetry. Data are presented as a percentage change from baseline blood flow (100%) and represented as mean ± SEM, n=3 in each group. CCA= common carotid artery.

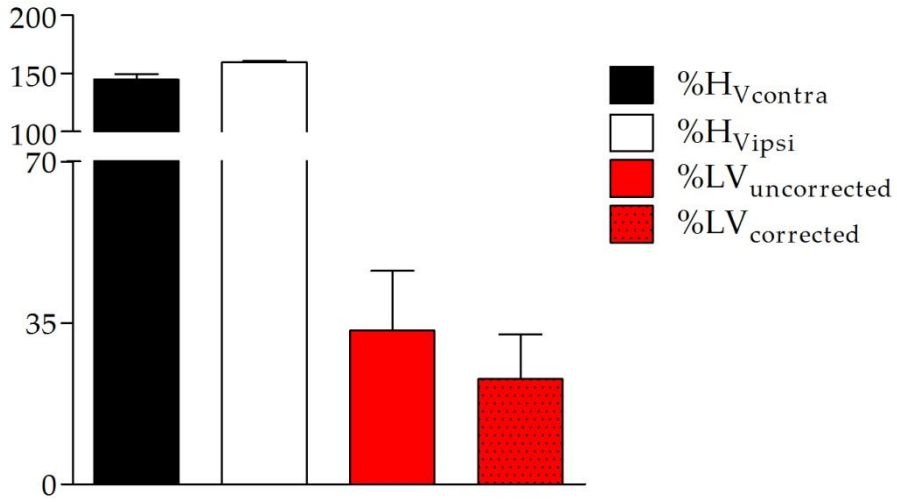

Figure 4.12: Impact of oedema correction on percent Lesion Volume (%LV) calculation induced by silicone coated filaments for 45 mins and recovered for 72 hrs.

The difference in uncorrected and corrected hemispheric LV is demonstrated. After 45 mins occlusion and 72 hrs recovery, oedema correction lead to a non-significant reduction (mean± SEM, n=5). %HV= percent hemispheric volume, % LV= percent lesion volume.

A

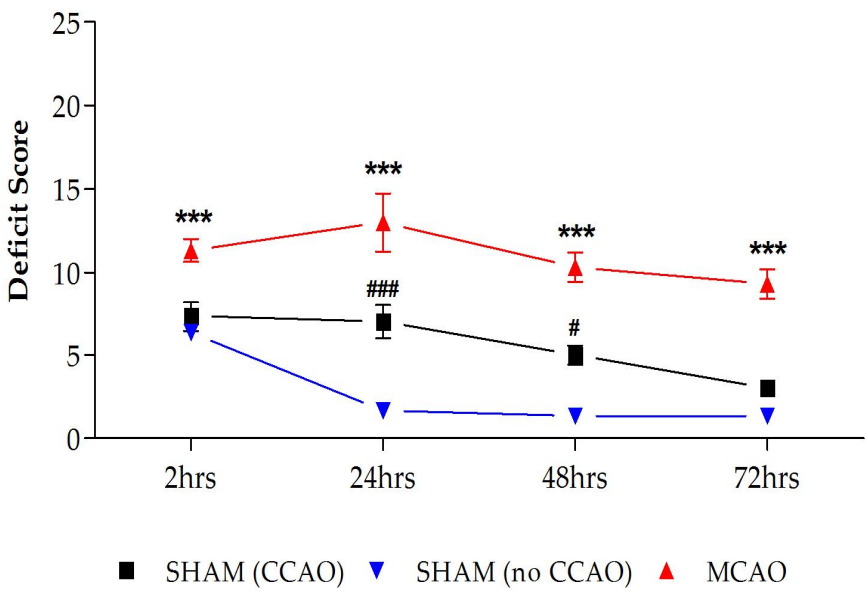

B

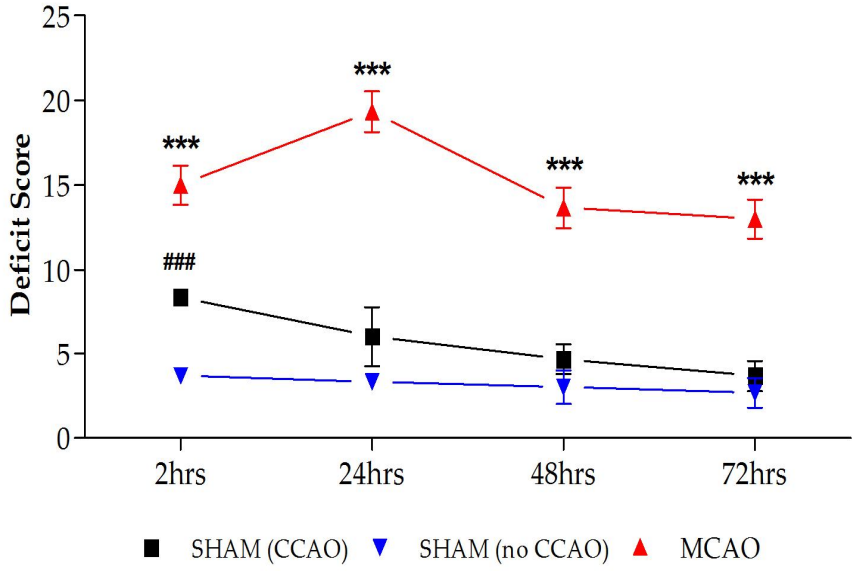

Figure 4.13: General and focal neurologic Clark's deficit score evaluation assessed at 2, 24, 48 and 72 hrs post-MCAO in mice

Sham (CCAO) (black) or (no CCAO) (blue) and MCAO (red) surgery. Neurologic deficits were assessed on a scale ranging from 0 (healthy) to 28. Data represented as mean ± SEM, n=3. Asterisks indicate *** $p \geq 0.001$ no CCAO sham surgery versus MCAO, ### $p \geq 0.001$ no CCAO sham surgery versus CCAO sham surgery.

4.4 | Discussion

The major utility of the intraluminal filament occlusion technique is the ability to induce a transient period of ischaemia followed by restoration of blood flow through the artery, which replicates the sequence of events in human stroke. However, limitations of this model include the widely reported high mortality rate, observed in rats and mice and variability in extent of damage.

The aim of the present study was to establish a MCAO model of ischaemia in mice with reproducible infarct volumes involving cortical and sub-cortical regions and reduced mortality rate. In Study 1, two different times of occlusion (60 and 45 mins), high mortality rate was observed during surgery (which could be due to process of establishing the model and inexperienced surgeon) and recovery (due to increased oedema which led to increased intracranial pressure). Brain oedema may develop when CBF decreases below a threshold of about 10 ml/100 g/min (Unterberg et al., 2004). In this study, CBF was not measured but the mortality may indeed have been due to increased oedema (observed by 20% over estimation of LV for oedema). At this "low flow status," ion exchange pumps break down (cytotoxic (cellular) oedema). Subsequently, blood brain barrier (BBB) breakdown occurs allowing extravasation of serum proteins and vasogenic brain oedema to develop. However, it has to be mentioned that after onset of ischemia-in spite of cell swelling-no net increase of water is present. Only after reperfusion there is a rapid increase in extracellular fluid and a corresponding rise in intracranial pressure as well as brain water content which is detrimental for stroke outcome (Unterberg et al., 2004). However, the volumes of ischaemic damage achieved were consistent (exception of SP26) using a monofilament coated with resin. Two possible factors underlying this reproducibility are proposed. Firstly, this study used different sizes of filaments depending upon the size of mice. It has been shown previously that the size of filament is an important determinant for successful occlusion and

that the appropriate diameter of filament varies according to the animal's weight (Shah et al., 2006). Secondly, to occlude the MCA, a technique that does not require interference with the pterygopalatine artery (pterygoA), a branch of the ICA was used. In many studies, the pterygoA is ligated or electro-coagulated. However, due to its small size, deep position and proximity to the vagus nerve, gaining access to this artery may produce inadvertent damage to the vagus nerve or one of its smaller branches with detrimental effects on the cardiovascular and/or respiratory system(s) (McColl et al., 2004). Ischaemic lesion observed with 60mins of occlusion was due to development of damage in MCA territory (e.g. cortical and sub-cortical region). The volume of lesion (LV_{un}) (72.34 ± 7.7) obtained in this study are similar to a study carried out by McColl and colleagues in mice (Belayev et al., 1999, McColl et al., 2004) in which C57 mice underwent a 60min occlusion and 24 hrs reperfusion. Without correction for oedema, lesion size is overestimated by almost 20% after 24 hrs of MCAO. These findings emphasize that oedema correction is important for the exact determination of lesion size (Gerriets et al., 2004).

Study 1 (establishment of occlusion time for the MCAO) showed that infarction was massive and the severity of stroke was high. As one of the aims stated in this Chapter was to produce a sufficient size of infarct and reduce mortality rate, the model needed to be redesigned. Furthermore, since 2 out of 9 animals were close to the severity limits set on the Home Office Project Licence during recovery requiring the animals to be put down. The high mortality rate associated in the study 1 may not be due simply to use of the resin filament as other groups have used it successfully to occlude the MCA (Clark et al., 1997, Touzani et al., 2002). It is more likely that the complications arose from a combination of experimenter technique, mouse vasculature, preparation of the resin filament; all of which were likely to be very different to the conditions of previous studies using the resin filament successfully.

Previously, Belayev and colleagues reported that mice after 30 mins of occlusion and 24 hrs recovery showed a variable cortical and consistent sub-cortical lesion (Belayev et al., 1999). Furthermore, McColl and colleagues demonstrated that ILT model of occlusion in mice lead to an occlusion duration-dependent increase in severity of cerebral hypoperfusion and extension of ischaemic pathology beyond the MCA territory (McColl et al., 2004). To avoid being at the threshold for cortical and sub-cortical lesion this led to a reduction in the occlusion time to 45 mins. Reducing the occlusion time to 45 mins reduced the mortality, which was related to the reduced oedema formation (**Figure 4.7**). In contrast, to 60 mins occlusion, a bleed at the MCA origin was observed. The method of coating the filament with resin and by increasing the length of tip at the correct diameter (as opposed to heat blunter bulb filament) to occlude the MCA was proposed to increase the number of successful occlusions and reduce the damage caused to the lining of the arterial wall when a fully coated filament was withdrawn. However, this style of filament was unable to easily pass through the ICA at the point of the temporal bone of the skull. Problems pushing the filament past this point were a common problem throughout the study and were sometimes associated with haemorrhage in this area and the subsequent death of animals. SAH resulting from excessive insertion pressure of the intraluminal filament also has been documented. Thus, 45 mins of occlusion was observed to be better than the 60 mins and was used for future experiments. A study (Tsuchiya et al., 2003) showed that using heat-blunted monofilaments for inducing MCA occlusion caused 40% occurrence of SAH. Another study particularly compared the effects of suture types on the infarct stability and showed that silicone coated monofilaments were superior to heat-blunted ones, producing consistent infarction and this was true even with inexperienced surgeons (Shimamura et al., 2006). In the mouse intraluminal model, SAH rate could reach 40% if uncoated heat-blunted monofilaments were used (Tsuchiya et al., 2003) and use of poly-L-lysine coated monofilament only increased the mortality (to a rate of 60%), without any benefits for

reducing infarct variation (Huang et al., 1998). To reduce the mortality rate caused by haemorrhage and have a reproducible infarct involving regions (cortical and sub-cortical) Study 2 (establishment of filament type for MCAO) was devised in which the occlusion time was fixed to 45 mins but instead of resin filaments, the use of commercially available silicone coated filaments from Doccol were chosen. The commercially available silicone coated Doccol MCAO sutures were used for the following two reasons. 1) They have a sufficient length of coated surface, which is cylindrical in shape, elastic, and smooth (such a physical property of Doccol MCAO sutures is significantly effective in reducing the occurrence of the insufficient occlusion, the premature reperfusion, and the mono filament dislodgement). 2) The standard deviation for infarction volume, when home-made silicon rubber-coated monofilaments are being used, is around 30% of its corresponding mean value both in rats (Schmid-Elsaesser et al., 1998) and in mice (Shah et al., 2006).

The 45mins occlusion peroid using Doccol filaments (study 2; used resin coated and silicone coated filament)) reduced the mortality to 0% during surgery, reduced the mortality during recovery when compared to 45mins occlusion using resin in Study 1 as well as reduced the number of animals with no infarct (employed by the use of laser doppler). Furthermore, the infarct volumes did not significantly change when compared to the counterpart group (Study 1 used 45 mins occlusion time and resin coated filament). The infarct volumes observed were fairly reproducible (**Table 4.3**). Additionally, McColl in 2004 have been successful in demonstrating the integrity of the circle of Willis in C57Bl/6J mice and they state that 10% (n=10 animals used in the study) had a complete circle of Willis and 60% had an incomplete circle of Willis thus suggesting some intra animal variability which is unavoidable (McColl et al., 2004). Thus, the commercially available silicone coated filaments were better than the resin coated filaments and used in future experiments.

Study 3 (45 mins occlusion time; silicone coated filament with 72 hrs recovery and sham CCAO versus sham with no CCAO) was devised to measure the development of infarct over 72 hrs of recovery and establish the sham surgery for future experiments. This study included use of 45 mins occlusion and silicone coated Doccol filaments (**Table 4.1**). The infarct is believed to evolve and mature by 72 hrs (Garcia et al., 1993) and to choose stereotaxic co-ordinates for the injection of stem cells in the ipsilateral hemisphere of the brain, the infarct regions damaged were measured by recovering the animals for 72 hrs. It was observed that the infarct did not change significantly when compared to the infarct observed with 24 hrs recovery. The infarct volume data will be used in Chapter 5 to decide the co-ordinates. In addition, sham surgeries were established in this chapter. It was noted that carrying out the complete procedure for MCAO except for inserting the filament which involved clipping the CCA led to a significant deficit observed using Clark's deficit score scale at 2hrs and 24 hrs in the mice. Furthermore, using laser Doppler indicated a 50% reduction in blood flow, which could have resulted in the observed neurologic deficit and therefore cannot be used as a control since it is a part of ischaemia. Thus, sham with no CCAO (no CCAO sham surgery) resulted in no neurologic deficits and thus was used in future experiments.

In conclusion, these studies have shown that in C57 mice, the optimal model of ILT MCAO uses a silicone coated commercially available Doccol filament and 45 mins of occlusion with sham surgery being performed with no CCAO. This method maintains mortality rate at a low level and when laser doppler flowmetry is used, produces 100% stroke outcome with reproducible infarctions in terms of cortical and striatal involvement. These conditions were adopted for the future studies involving effects of stem cells after MCAO on behaviour and histology discussed in **Chapter 5** and **6**.

CHAPTER 5

EFFECTS OF MHP36 NEURAL STEM CELLS ON BRAIN REPAIR AFTER MCAO IN MICE

5.1 | Introduction

Cell-based therapies are of particular interest in the central nervous system, because the mature brain has little capacity for self-repair. The plasticity exhibited by stem cells raises the possibility that they can be used to restore function compromised by brain insults, such as stroke (Lindvall and Kokaia, 2004, Savitz et al., 2002, Makinen et al., 2006). Initial studies using foetal tissue transplantation have been successful in ameliorating neurodegenerative deficits in animal experiments (Isacson et al., 1984) and this has been translated with some success demonstrated from clinical trials in humans with intrastriatal transplantation of human embryonic mesencephalic tissue, rich in post-mitotic dopamine neurons, in Parkinson's disease patients (Lindvall and Kokaia, 2005). However, further use of foetal tissue in treating human disease is problematic due to ethical considerations and a limited supply of tissue. In order to combat these problems, a variety of neural stem cell lines have been investigated for their potential in improving recovery in animal models of neurodegenerative disease. These include human bone marrow stromal cells (Chen et al., 2001a), human neuroteratocarcinoma cells (Saporta et al., 1999) and conditionally immortalised murine stem cells (Sinden et al., 1997) (discussed in Chapter 1). The Maudsley hippocampal stem cell line clone 36 (MHP36) grafts are well suited to repair the indiscriminate cell loss that occurs with middle cerebral artery occlusion because previously, they have been shown to have the capacity to develop into neurons, glia, or

oligodendrocytes in response to host signals (Hodges et al., 2000b, Gray et al., 2000) and migrate to and engraft areas of damage in the host brain (Gray et al., 1999, Veizovic et al., 2001). Furthermore, they have been shown to reduce damage in several models of neurological impairment, including global ischaemia in mice (Wong et al., 2005), transient intraluminal middle cerebral artery occlusion (tMCAO) (Hodges et al., 2000a) and lesions to cholinergic forebrain projections in rats (Gray et al., 2000). In addition, MHP36 cells reverse age-associated deficits in spatial learning and memory as assessed by the water maze and resolve motor associated deficits (Veizovic et al., 2001, Hodges et al., 2000b). MHP36 cells have been shown to migrate across the corpus callosum towards an ischaemic lesion induced by tMCAO (Veizovic et al., 2001) and differentiate into site appropriate phenotypes (Modo et al., 2002b, Wong et al., 2005), but mechanisms involved still need to be clarified. Previous MCAO studies of MHP36 cells have used rats subjected to focal cerebral ischaemia and assessed functional recovery using behavioural tasks (e.g. neurological severity score, rotational bias, spontaneous activity, bilateral asymmetry test, water maze). Improvement within six weeks after administration has been demonstrated using the bilateral asymmetry test (Modo et al., 2002b). To study the effect of over-expressed oestrogen in the MHP36 cells (discussed in **Chapter 6**), firstly MHP36 cells were investigated for promoting functional recovery after MCAO in mice using sensorimotor function tests known to assess spontaneous forelimb use asymmetry (Baskin et al., 2003, Fleming et al., 2004, Schallert et al., 2000, Li et al., 2004, Starkey et al., 2005) and foot faults (Farr et al., 2006, Metz and Whishaw, 2002, Riek-Burchardt et al., 2004) and to investigate the mechanisms involved. The use of robust markers of neural stem cells (NSCs) helps us to understand the behaviour of the transplanted cells in the host brain. One of the most robust markers of NSCs is the intermediate filament protein, nestin. Nestin is a major cytoskeletal protein present in neural precursors in the mammalian CNS. Cells exiting the cell

cycle at the commencement of differentiation have been shown to down-regulate nestin and subsequently up-regulate alternative intermediate filaments during both neuronal (microtubule-associated protein : MAP-2) and glial (glial fibrillary acidic protein: GFAP) differentiation (Reynolds and Weiss, 1992). The loss of nestin expression is currently accepted as one of the earliest significant indicators of the progression from precursor to differentiated phenotypes. Furthermore, Mellodew and colleagues showed that nestin expression is lost immediately, 1-4 hrs post-transplantation (Mellodew et al., 2004).

In addition to testing the effects of MHP36 cells on sensorimotor function and to investigate the mechanisms involved, this Chapter will also briefly focus on 1) A pilot study carried out in the process of establishing stereotaxic injections in the mice brain. The technique was performed on live animals using MHP36 NSC labelled with PKH26 dye initially at Dr Mike Modo's laboratory in Kings College London, UK. 2) Whether expression of nestin by MHP36 cells is observed 24 hrs post-transplantation. 3) Whether expression of differentiation markers is observed 24 hrs after transplantation in the mouse brain.

5.2 | Methods

5.2.1 | Establishment of MHP36 cell stereotaxic injections in mice

5.2.1.1| Subjects

C57BL/6 male mice, 12-14 weeks old were used from the in-house supply at King's College, London (n=2), weighing 30 g with local ethical review permission.

5.2.1.2| Cell transplantation surgery

Normal mice were anaesthetised and mounted on the frame for stereotaxic injections (as described in **section 2.2.10** and **2.2.11**, respectively). The following coordinates (Medial/Lateral + 2 mm, Anterior/Posterior - 0.50 mm and Ventral – 3 mm from the surface of the brain) were used in this experiment. Pre-labelled cell suspension (12,500 cells/0.5 µl) or vehicle (0.5 µl) was injected over 2 min, and the syringe was left in place for another 2 min.

5.2.1.3| Histology

Twenty-four hrs following the completion of injection, mice were perfused through the heart with 0.9% physiological saline followed by 4% paraformaldehyde. The brains were processed appropriately and coronal sections were cut at 20µm and collected on slides to measure lesion volumes (detailed in **section 2.2.13.1**).

5.2.1.3.1 | Assessment of neural stem cell marker 24hrs post-transplantation

Serial 20 µm coronal sections were processed for immunostaining (see **section 2.2.3**) (three sections were stained in each animal) with mouse anti-Nestin (1:200, Chemicon, UK) and mouse anti-GFAP (1:200, Sigma, UK) to identify neural markers in PKH26 labelled MHP36 cells after

24 hrs. The coronal level, bregma -0.5± 0.02 mm (injection site), was used for staining in order to visualise the labelled PKH26 cells 24 hrs post-transplantation.

5.2.2 | Effects of MHP36 cells in mice 28 days post-MCAO

5.2.2.1| Subjects

Forty-two, C57BL/6 male mice, 12-14 week old, were used from Charles River, UK (n=42), weighing between 25 and 30 g.

5.2.2.2| Experimental design

The mice were handled extensively and habituated to the testing location and apparatus prior to training and testing. Baseline behavioural testing was performed by placing the animals for two crossings on the ladder rung task with a set rung arrangement pattern (irregular). Two days following completion of baseline behavioural testing the mice underwent tMCAO and were recovered for 28 days. Post-MCAO testing and video recording of both ladder test and cylinder test occurred on 2, 7, 14 and 28 days post-MCAO (**Figure 5.1**). Each post-MCAO test session included two crossings on the ladder rung task with set rung arrangement pattern. It is important to note that throughout the experimental plan and during behavioural analysis, the experimenter was blind as to which treatment the mice received.

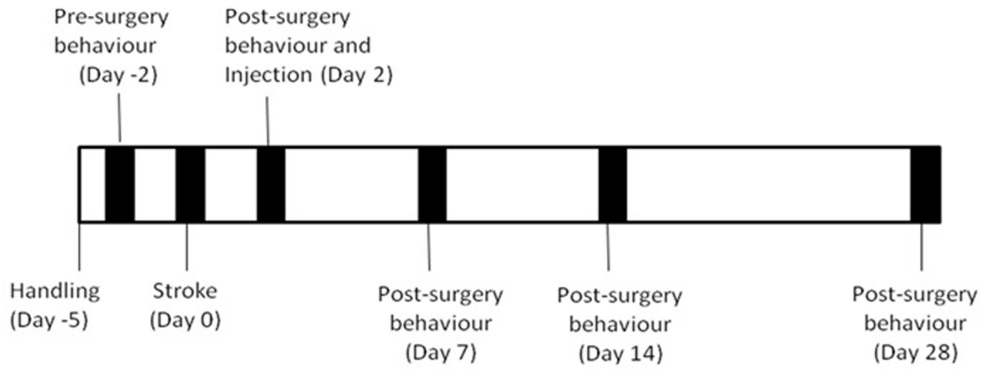

Figure 5.1- Experimental regime used for the behavioural study

Mice were first handled before testing for 3 days each. The following day pre-surgery testing occurred for both tasks. Mice received a focal tMCAO lesion or underwent sham surgery on day 0 and were tested post-MCAO on day 2 before receiving an injection. Behaviour post-injection was filmed on days 7, 14 and 28.

5.2.2.3| Surgery and measurement of cerebral blood flow

Following completion of baseline behavioural testing, animals were anaesthetised and focal ischaemia was induced within the left hemisphere by transient (45 min) MCAO as described in **section 2.2.10**. The core body temperature was regulated at 37 ± 0.5°C and a 7-0 silicone monofilament (Doccol, Ltd., USA) was used for occlusion. Sham-operated mice underwent the no CCAO procedure described in Chapter 4.

In each animal, laser Doppler flowmetry (Moor Instruments, UK) was used to monitor cerebral blood flow (CBF) continuously, before and during MCAO as well as during reperfusion as described in **section 2.2.10.3**. Animals were included only when CBF was reduced by ≥ 85% during ischaemia, and successful reperfusion was subsequently achieved.

5.2.2.4| Cell maintenance and transplantation

MHP36 cells were cultured from frozen stock and maintained in an undifferentiated state at 33 °C (passage number 53–65) (Sinden et al., 1997) as described in detail in **section 2.2.1**. Two days post-MCAO or sham surgery, mice were randomly selected (suggested in STAIR; (Saver et al., 2009) to receive a unilateral cortical and striatal graft of either PKH26 pre-labelled MHP36 stem cells (n = 8) or vehicle (NAC solution) (n = 8) as described in **section 2.2.11.2**. The following coordinates (Medial/Lateral + 2 mm, Anterior/Posterior - 0.26 mm, Ventral -1.5 and -3.0 mm from the surface of the brain) were used. Cell suspension (12,500 cells/0.5 µl) or vehicle (0.5 µl) was injected over 2 min, and the syringe was left in place for another 2 min.

5.2.2.5| Clark's Deficit Score (CDS)

After 24, 72 and 96 hours after the induction of ischaemia, each mouse was rated on two neurologic function scales unique to the mouse (Clark et al., 1997) (see **section 2.2.14.1**). Out of the 42 animals that underwent MCAO, 10 were excluded on this criteria (all exclusion were made before 2 days post MCAO injection).

5.2.2.6| Ladder rung task apparatus and analysis

The ladder rung task was adapted from the ladder rung walking task used previously in rats (Metz and Whishaw, 2002) and is described in **section 2.2.14.2**. Each step was scored according to the quality of limb placement based on the scale adapted from (Metz and Whishaw, 2002).

5.2.2.7| Cylinder task apparatus and analysis

The cylinder or spontaneous forelimb test modified for mouse (Baskin et al., 2003) measures the spontaneous activity of the mouse to rear up on its hind limbs and explore the vertical surface with its forelimbs was observed as described in **section 2.2.14.3**.

5.2.2.8| Video recording and analysis equipment

Post-MCAO measurements were taken at 2, 7, 14 and 28 day time points. The mice were filmed with a high speed Panasonic digital camcorder (30 frames/s; shutter speed of 1/1000). The digital videotapes were analyzed using a HP Pavilion DV2000 laptop. Single frames were imported from the digital video records using Windows media player on a Windows operating system.

5.2.2.9| Histology

Twenty-eight days following the completion of behavioural testing, the mice were perfused through the heart with 0.9% physiological saline followed by 4% paraformaldehyde. The brains were processed appropriately and coronal sections were cut at 20µm and collected on slides for further analysis (detailed in **section 2.2.13**). For immunofluorescence staining, n=3 animals were chosen randomly; after analysis of staining, lesion volumes were revealed to experimenter, to avoid bias during the random selection.

5.2.2.9.1 | Measurement of lesion

Sections were stained with haematoxylin and eosin to determine lesion (tissue loss) and measure volume as described in **sections 2.2.13**.

5.2.2.9.2 | *Assessment of differentiation*

Serial 20 µm coronal sections were used for immunostaining (refer to **section 2.2.3**) using chicken anti- MAP-2 (1:500, Chemicon, UK), mouse anti-GFAP (1:200, Sigma, UK), mouse anti-CNPase (2', 3'-Cyclic Nucleotide 3'-Phosphodiesterase) (1:200, Chemicon, UK) and goat anti-IBA-1 (1:500, Abcam Plc., UK) to identify differentiated cells. The coronal levels used for staining ranged between bregma -0.38 ± 0.10 mm in order to visualise labelled PKH26 MHP36 cells close to the injection site to promote differentiation 28 days post-transplantation.

5.2.2.9.3 | *Assessment of synaptic plasticity*

Mouse anti-synaptophysin (Syn, 1:200, Abcam Plc., UK) was used to investigate synaptogenesis. PKH26/anti-Syn (1:200) double-label immunofluorescence was used to relate synaptogenesis to transplanted cells. The coronal levels used for staining ranged between bregma -0.38 ± 0.10 mm in order to visualise labelled PKH26 MHP36 cells that migrated to promote synaptic connection at 28 days post-transplantation.

Using Image-J system software, the obtained images were semi-quantified by acquiring the intensity of fluorescence across a set area for each region of interest (ROI). The obtained values used for graphical representation are a ratio of intensity over area (as described in **section 2.2.3.1**).

5.2.2.10 | Statistical analysis

In the main study, statistical comparisons in all behavioural tests were made using one-way ANOVA with repeated measures (comparisons between pre- versus post-MCAO and pre-MCAO versus 28 day post-MCAO in each treatment was performed). In the Clark's deficit score data was analysed using two-way ANOVA with repeated measures. Post hoc analyses were

conducted using Bonferroni's test. Histology data was analysed using unpaired t-test unless otherwise stated. A p-value of less that 0.05 was chosen as the significance level for all statistical analyses. All data are presented as mean ± SEM, n=8.

5.3 | Results

5.3.1 | Establishment of stereotaxic injections

5.3.1.1| Cell transplantation after 24 hrs in mice

In two pilot studies, transplanted cells were clearly detectable by PKH26 fluorescence 24 hrs post–transplantation in mice (both pilot studies do not involve animals undergoing prior MCAO) (**Figure 5.2**). Injection tracts of the transplants were clearly visible and suggested that graft placement was in the striatum close to the ventricle (F**igure 5.2A**). The macroscopic appearance of the graft, i.e. the distribution of cells labelled with PKH26, indicated that grafted cells resided in the striatum and overlying cortex (around the injection site) with cells migrating out from the implantation site (**Figure 5.2C**).

5.3.1.2| Histology

5.3.1.2.1 | Assessment of NSC expression after 24 hrs post-transplantation

The PKH26 labelled MHP36 cells did not express nestin (green; endogenous neural stem cells positive for nestin visualised near the ventricle) at 24 hrs post- transplantation (**Figure 5.3**). This finding is similar to the study conducted by Mellodew and colleagues, where they showed that nestin expression is lost quickly, within 1-4 h of transplantation in the brain (Mellodew et al., 2004). In addition, GFAP (astrocytic marker) was not co-localised with PKH26 labelled MHP36 cells (**Figure 5.3 & 5.4**) as expected since differentiation would not take place by 24 hrs post-tranplantation (Mellodew et al., 2004). GFAP expression of reactive endogenous astrocytes was observed at the injection site (**Figure 5.3 & 5.4**). **Figure 5.4** summarises the results shown in

Figure 5.2 with a line diagram to show the site of injection (including stereotaxic co-ordinates) and series of images taken at sites of injection.

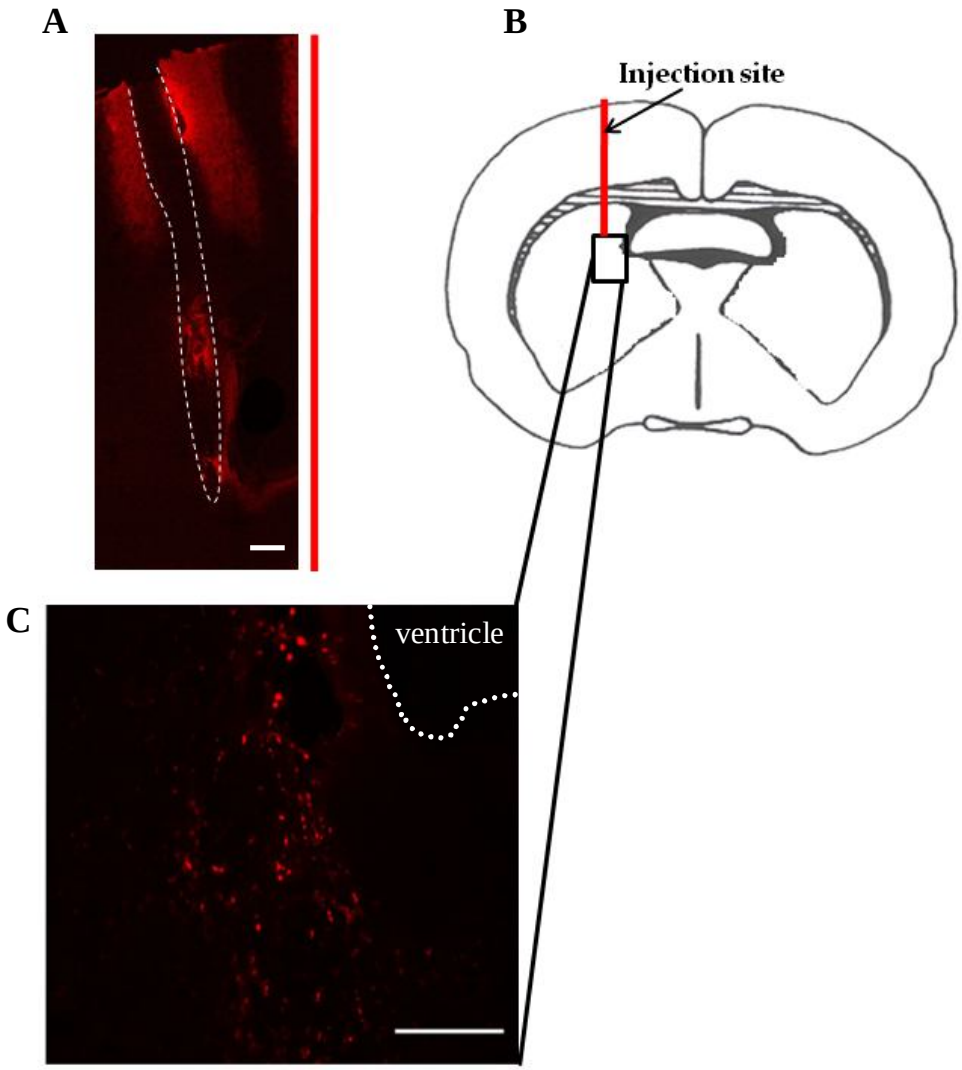

Figure 5.2: Injection of PKH26 labelled MHP36 cells in mice brain 24 hrs post-transplantation

(**A**) PKH26 labelled MHP36 cells transplanted stereotaxically into the right striatum of C57 male mouse brain. The dotted line marks the injection site. (**B**) Representative mouse brain coronal section used as reference for area used in imaging (Bregma: -0.5mm). (**C**) Higher magnification of the same section; dotted line marks the ventricles (Bars represent 50µm).

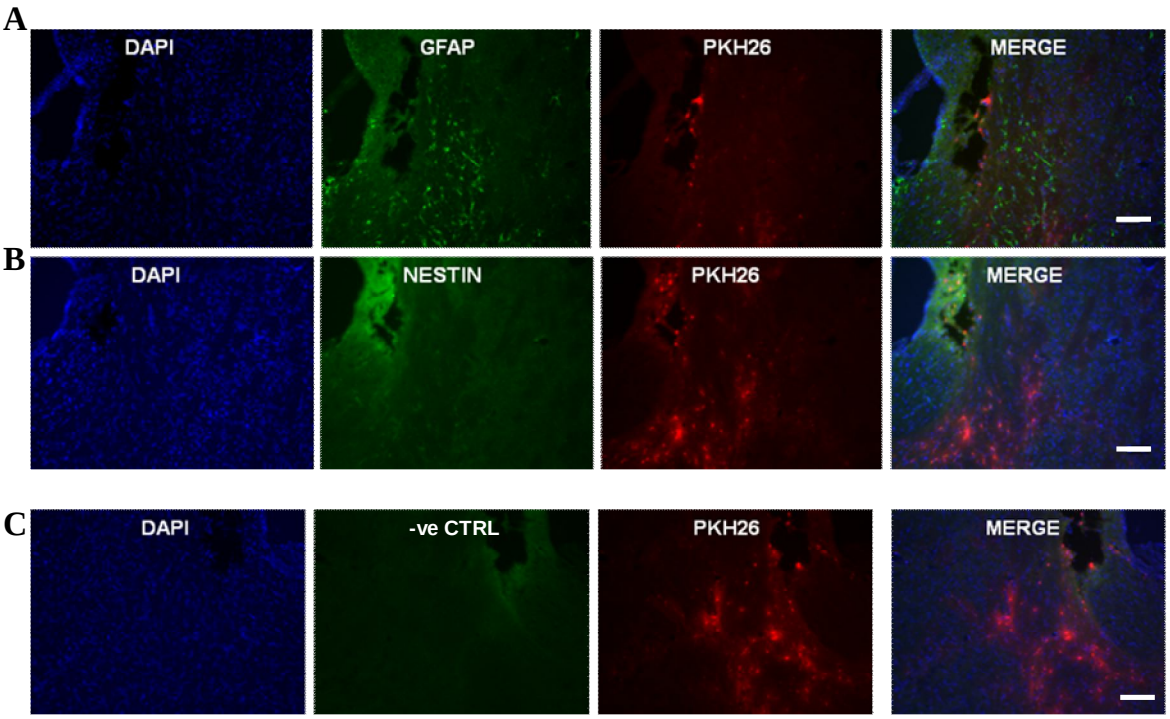

Figure 5.3: Immunofluorescence staining of C57 mice brain 24 hrs post-transplantation.

(**A**) DAPI (blue) stained nucleus, GFAP (green) stained reactive endogenous astrocytes as compared to no co-localised PKH26 labelled (red) transplanted stem cells. (**B**) DAPI (blue) stained nucleus, no Nestin (green) positive PKH26 labelled (red) stem cells 24 hrs post transplantation into the brain. (**C**) Negative control for GFAP/ nestin (no primary antibody) (20µm thick; n=3) (Bars represent 50µm).

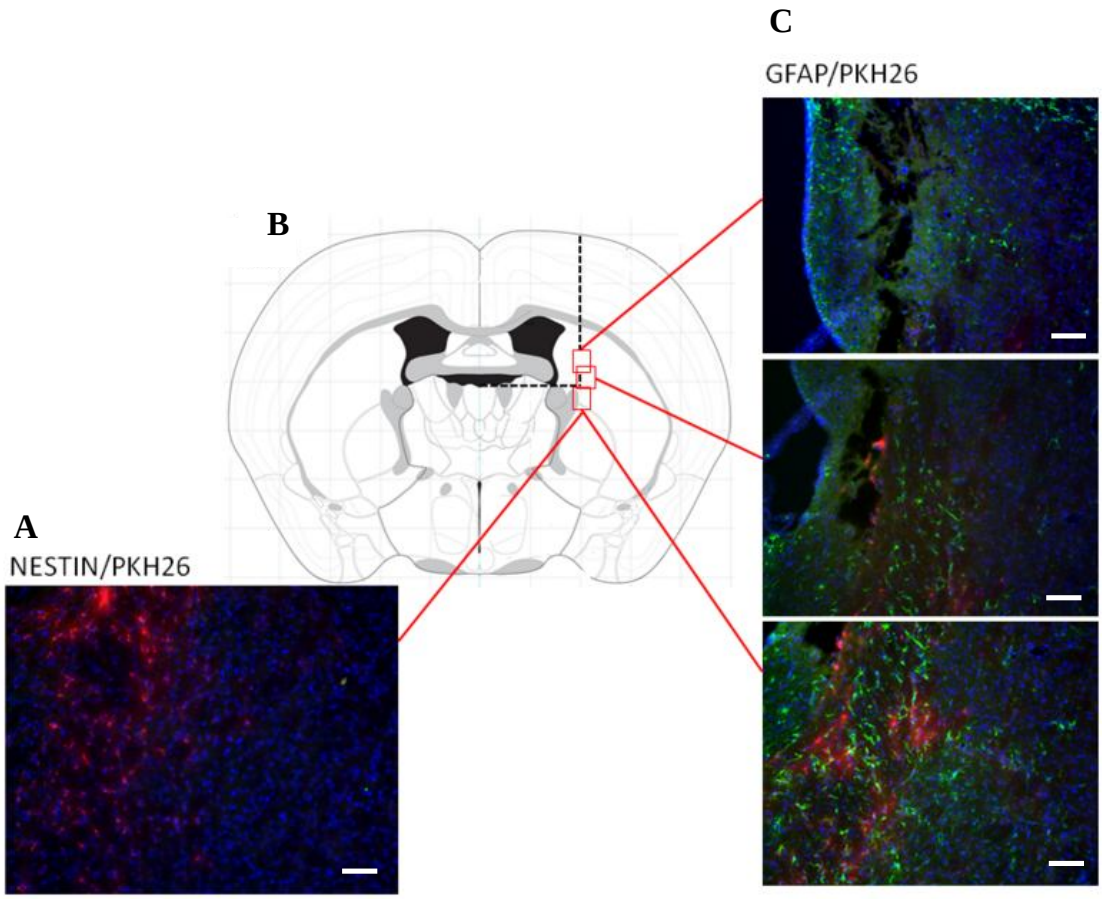

Figure 5.4: Summary of immunofluorescence staining of PKH26 labelled MHP36 cells 24 hrs post-transplantation.

(**A**) PKH26 labelled (red) stem cells with no nestin (green) expression 24 hrs post transplantation into the brain. (**B**) Representative mouse brain coronal section from the atlas used as reference for injection site (dotted line) and areas used for imaging (red box) (Bregma: -0.5mm). (**C**) GFAP (green) stained reactive endogenous astrocytes with PKH26 labelled (red) transplanted stem cells. (20 µm thick; n=3) (Bars represent 50 µm).

5.3.2 | Effects of MHP36 cells in mice 28 days post-MCAO

5.3.2.1| Cerebral blood flow

Analysis of CBF did not show any difference between different groups that were later to receive either vehicle or MHP36 stem cells, CBF was reduced by >85-90% in all groups during MCAO when compared to pre-occlusion baseline values (**Figure 5.5**).

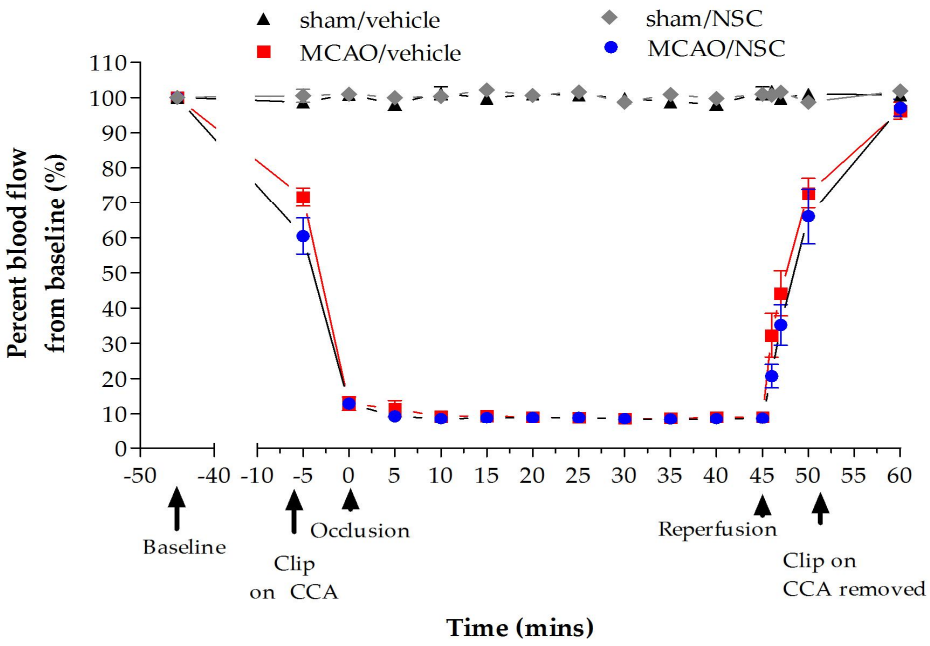

Figure 5.5: Laser Doppler flowmetry in mice undergoing MCAO or sham surgery.

Cortical blood flow measured before, during and after insertion of the silicone filament to occlude the MCA, using laser Doppler flowmetry. Data are presented as a percentage change from baseline blood flow (100%) and represented as mean ± SEM, n=3 in each group. CCA= common carotid artery.

5.3.2.2 | Clark's deficit score

Neurological deficit was evaluated using Clark's deficit score. Animals at 24 hrs post-MCAO showed a significant increase in general and focal deficit score when compared to sham animals

which was followed by either vehicle or MHP36 cell injection at 48 hrs. The deficit was not affected by either vehicle or MHP36 cells as observed at 72 and 96 hrs post-MCAO (**Figure 5.6A and B**).

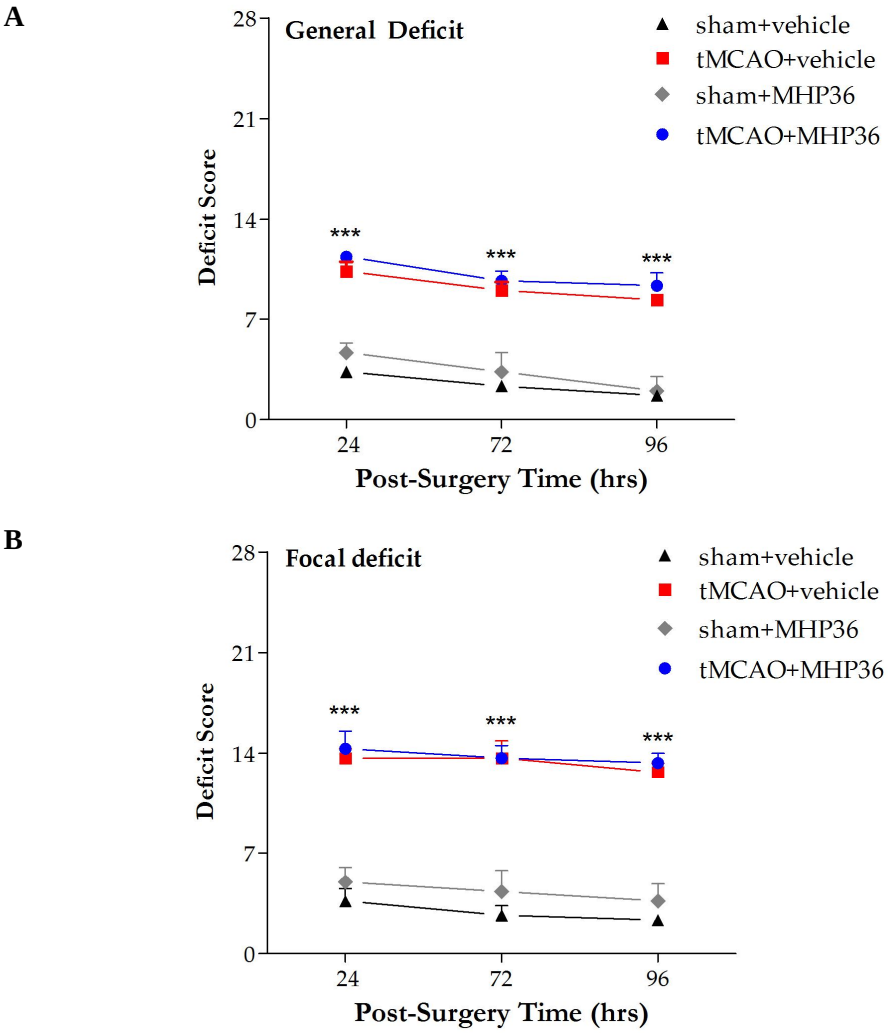

Figure 5.6: Assessment of neurological deficit score across time using Clark's deficit score.

(**A**) General and (**B**) focal neurologic Clark's deficit score evaluation assessed 24, 72 and 96 hrs post-MCAO in mice receiving either vehicle or MHP36 stem cells at 48 hrs post-MCAO; (mean ± S.E.M., n = 8 mice per experimental group). Asterisks indicate *** p≥ 0.001 sham versus tMCAO (different injection).

5.3.2.3| Ladder rung test

There were no significant placement errors noted on the ladder test in sham-treated animals, regardless of either vehicle or MHP36 cell injection (**Figure 5.7**). Prior to MCAO, mice performed mainly correct placements with all four limbs. There was a significant increase in placement errors of the contralateral forelimb in MCAO mice at 2 days post MCAO scores (vehicle, 4.03 ± 0.19; MHP36, 4.07 ± 0.13) when compared to pre-MCAO scores (vehicle, 5.77 ± 0.05; MHP36, 5.73 ± 0.04) in both MCAO injection groups. There was a highly significant deficit at 28 days post-MCAO in vehicle group (4.03 ± 0.19) when compared to pre-MCAO scores (vehicle, 5.77 ± 0.05) which was improved in the animals receiving the MHP36 cells (pre: 5.73 ± 0.04; 28 days: 4.95 ± 0.12) (**Figure 5.7**). Data of all four limbs at pre-MCAO and 28 days post-MCAO are displayed below (**Table 5.1**).

A

	Sham+vehicle				**Sham+MHP36 cells**		
Pre-scores	Mean	SEM	n		Mean	SEM	n
Ipsi H	5.78	0.14	8		5.85	0.02	8
Ipsi F	5.70	0.11	8		5.76	0.16	8
Contra H	5.88	0.07	8		5.84	0.07	8
Contra F	5.71	0.02	8		5.68	0.04	8

B

	tMCAO+vehicle				**tMCAO+MHP36 cells**		
Pre-scores	Mean	SEM	n		Mean	SEM	n
Ipsi H	5.93	0.02	8		5.89	0.03	8
Ipsi F	5.77	0.05	8		5.75	0.09	8
Contra H	5.91	0.02	8		5.86	0.01	8
Contra F	5.77	0.05	8		5.73	0.04	8

C

	Sham+vehicle				Sham+MHP36 cells		
28 days score	Mean	SEM	n		Mean	SEM	n
Ipsi H	5.82	0.17	8		5.88	0.05	8
Ipsi F	5.72	0.18	8		5.75	0.02	8
Contra H	5.77	0.02	8		5.83	0.06	8
Contra F	5.7	0.13	8		5.67	0.01	8

D

	tMCAO+vehicle				tMCAO+MHP36 cells		
28 days score	Mean	SEM	n		Mean	SEM	n
Ipsi H	5.90	0.03	8		5.84	0.01	8
Ipsi F	5.76	0.02	8		5.72	0.08	8
Contra H	5.38	0.09	8		5.46	0.11	8
Contra F	4.52	0.10	8		4.95	0.12	8

Ipsi= Ipsilateral; Contra= Contralateral; H= Hind Limb; F= Fore limb

Table 5.1: Displaying data of all four limbs pre- and 28 days post-tMCAO

(**A & B**) Pre and (**C & D**) 28 days post MCAO scores of sham versus tMCAO animals receiving vehicle or MHP36 cells.

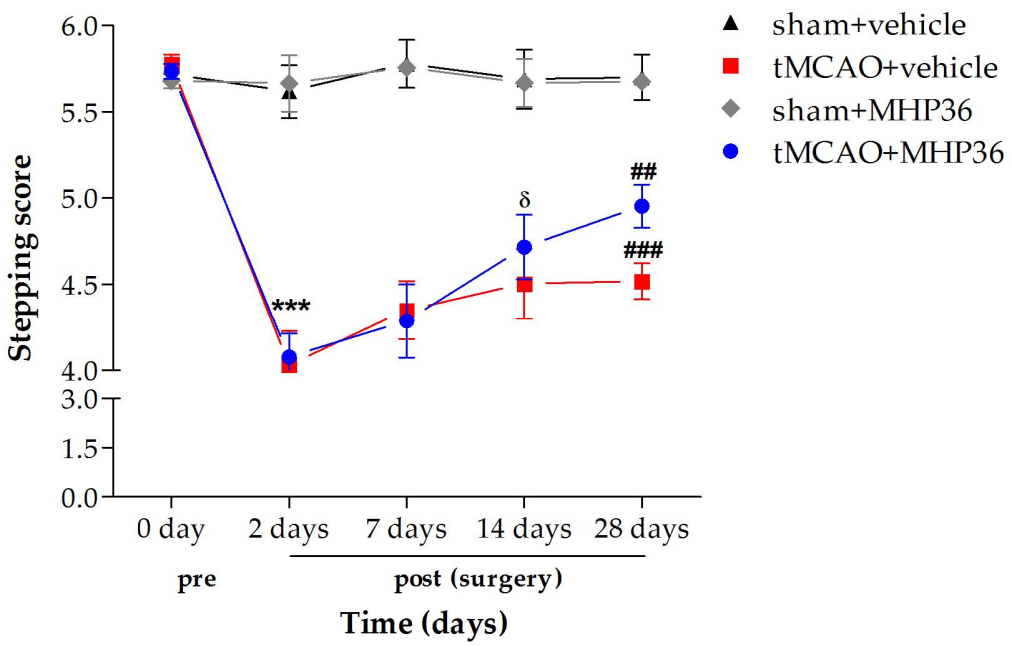

Figure 5.7: Assessment of behavioural outcome using the ladder rung test (contralateral forelimb use).

Sham operated mice and tMCAO receiving either vehicle or MHP36 cells for five time points indicated as pre-MCAO, 2, 7, 14 and 28 days post-MCAO (mean ± S.E.M., n=8 each group). A score of 6 indicated correct placements. Asterisks indicate *** p< 0.001 (pre- versus 2 days post-MCAO in all groups), ## p<0.01, ### p<0.001 (pre-MCAO versus 28 days), δ p<0.05 (2 days post-MCAO versus 28 days post-MCAO), one-way ANOVA with repeated measure. Scores at 28 days post-MCAO were not significant between mice receiving vehicle or MHP36 cells that underwent tMCAO

5.3.2.4| Cylinder test

Spontaneous forelimb (cylinder) task results are shown in **Figure 5.8**. In this task, the mean laterality score of the injured group, which measures preference for the forelimb unaffected by (ipsilateral to) the injury, peaked at 2 days post-MCAO time point. There were no significant asymmetries noted in the cylinder test in sham-treated animals, regardless of either vehicle or MHP36 cell injection (**Figure 5.8**). There was a significant increase in left forelimb (ipsilateral) usage in tMCAO animals at 2 days post-MCAO (vehicle, 0.810 ± 0.19; MHP36, 0.767 ± 0.26)

when compared to pre-MCAO (vehicle, -0.021 ± 0.15; MHP36, 0.024 ± 0.12) in both injection groups. There was a highly significant deficit from pre-MCAO scores (vehicle, -0.021 ± 0.15; MHP36, 0.024 ± 0.12) and at 28 days post-MCAO in the vehicle (0.46 ± 0.1) which improved in the group of animals receiving MHP36 cells (-0.3 ± 0.16, ns) (**Figure 5.8**). Asterisks indicate ***p< 0.001 (pre- versus 2 days post-MCAO), ns= not significant (pre-MCAO versus 28 days post-MCAO), repeated measure ANOVA.

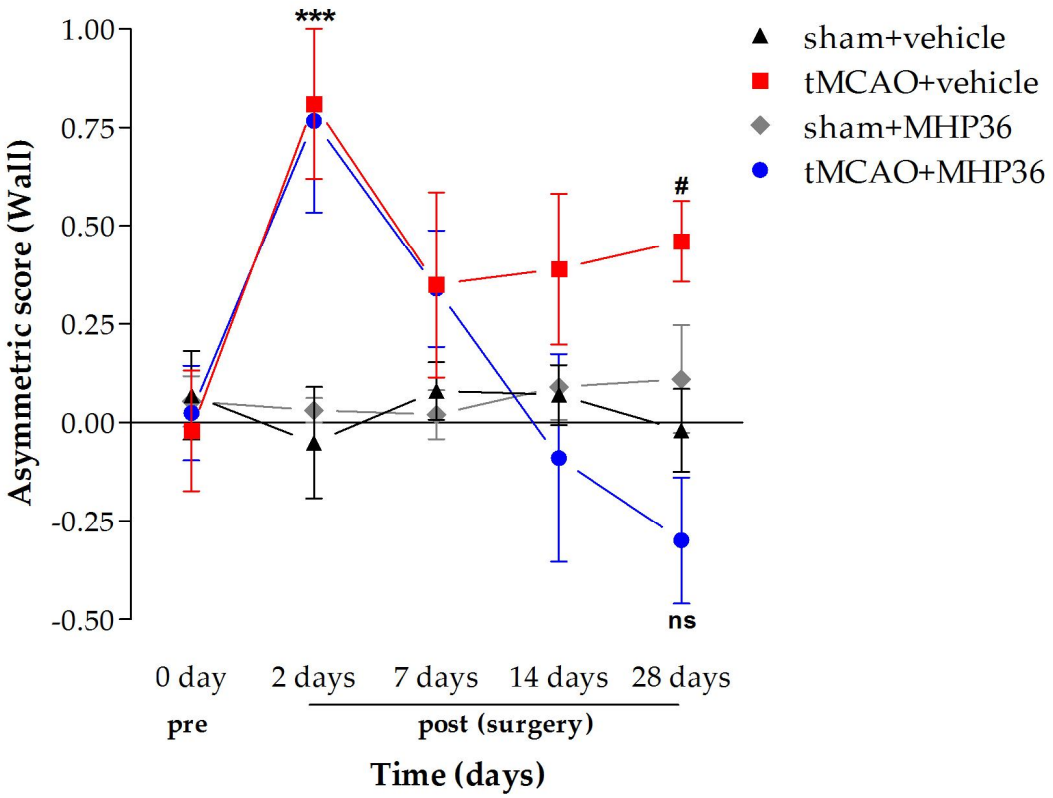

Figure 5.8: Assessment of spontaneous exploration of fore-limb in cylinder test.

Sham operated and tMCAO mice receiving either vehicle or MHP36 cells for five test conditions are indicated: pre-MCAO, 2, 7, 14 and 28 days post-MCAO (mean ± S.E.M., n=8 each group). MCAO animals have significant asymmetry at 2 days post-MCAO time point that improved significantly over time in animals receiving MHP36 cells (blue) but not vehicle (red). Asterisks indicate ***p< 0.001 (pre- versus 2 days post-MCAO), ###p<0.001 (pre-MCAO versus 28 days post-MCAO), one-way ANOVA with repeated measure. ns= not significant.

5.3.2.5 | Histology

5.3.2.5.1 | Measurement of lesion (tissue loss) after 28 days post-MCAO

At 28 days post-transplantation there was no significant difference in tissue loss volume between the MHP36 (13.08 ± 1.3 mm^3; n=8) and vehicle (13.2 ± 1.97 mm^3, n=8) grafted mice (**Figure 5.9**).

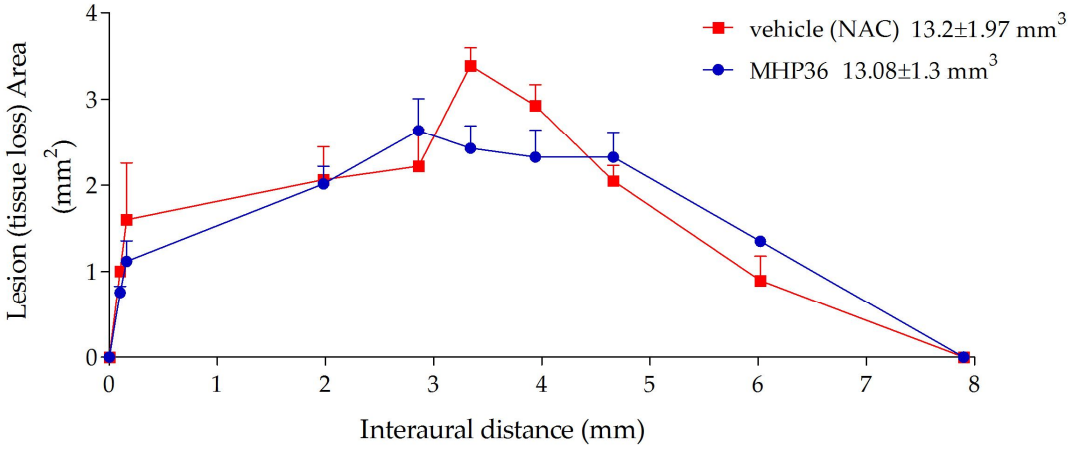

Figure 5.9: Assessment of lesion (tissue loss) after either vehicle or MHP36 cell transplantation 28 days post-MCAO

No significant difference in lesion (tissue loss) between MHP36 and vehicle treatment as displayed over 8 pre-determined coronal levels (mean ± SEM, n=8, each group).

Figure 5.10 shows the distribution of lesion across the 8 pre-determined levels acquired from the atlas of mouse brain. The lesion involves both sensorimotor cortex and striatal damage.

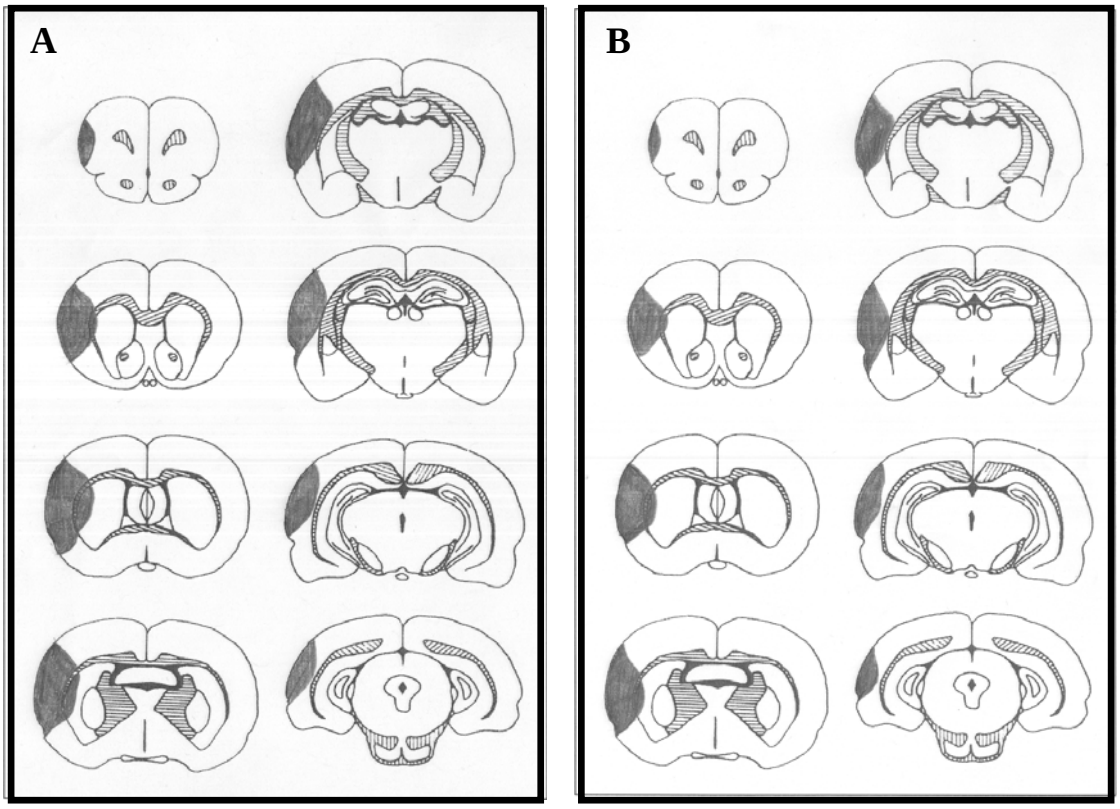

Figure 5.10: Distribution of lesion over 8 coronal levels after 28 days post-MCAO in mice receiving (A) vehicle and (B) MHP36 cells.

Shaded areas represent areas of lesion in one representative animal from each group.

5.3.2.5.2 | Assessment of differentiation after 28 days post-MCAO

At 28 days post-MCAO, staining of brain sections with neuronal marker MAP-2 revealed no significant increase in expression in the MHP36 group of animals when compared to the vehicle group of animals. Furthermore, no PKH26 labelled MHP36 cells differentiated into neurons (**Figure 5.11A-F**) (Bregma: -0.38± 0.10mm). GFAP-positive astrocytes in the peri-lesion which included the cortex and striatum showed a non-significant trend to decrease in the MHP36 group of animals when compared to vehicle (**Figure 5.12A-C**). Oligodendrocytes showed a trend to

increase in the MHP36 group of animals versus vehicle, detected using CNPase antibody (**Figure 5.12D-F**) and there was no difference in IBA-1 positive activated microglial cells in MHP36 versus vehicle groups (**Figure 5.13A-C**). Sections from sham group were stained and showed no statistical difference in mean intensity between injections (data not shown).

5.3.2.5.3 | Assessment of synaptic plasticity after 28 days post MCAO

At 28 days post-MCAO using the mouse anti-Synaptophysin (Syn) antibody, a dense Syn positive immunostaining within the grafts was revealed (**Figure. 5.14A and B**) in the MHP36 receiving animals when compared to vehicle group. PKH26/Syn co-localised MHP36 cells were observed in the cortex within the peri-lesion (Bregma: -0.38± 0.10 mm) (**Figure 5.14D**). A significant increase in Syn expression was observed in the ipsilateral cortex when compared to contralateral cortex in the MHP36 receiving animals (**Figure 5.14E**). Sections from sham group were stained and showed no statistical difference in mean intensity between injections (data not shown).

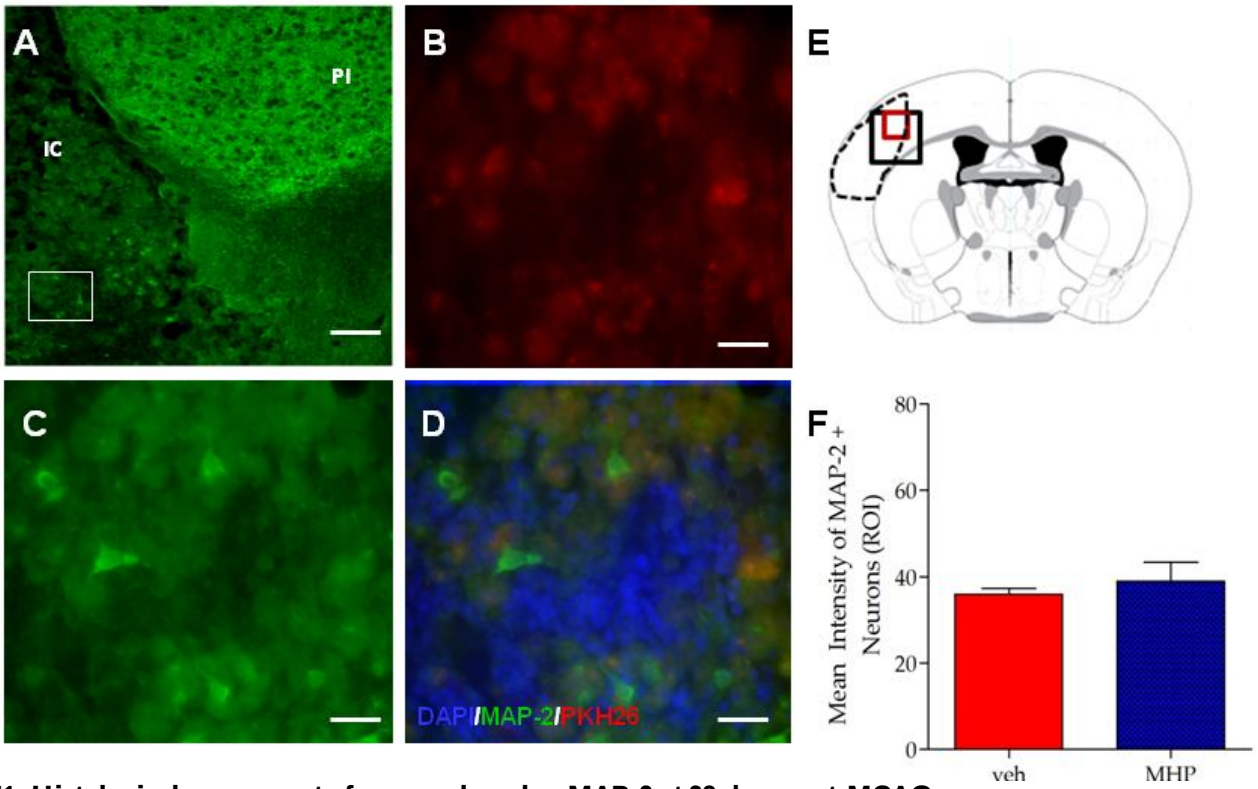

Figure 5.11: Histological assessment of neuronal marker MAP-2 at 28 days post-MCAO

(**A**) Peri-lesion in mice receiving MHP36 cells stained for microtubule-associated protein-2 (MAP-2) expression; (scale bar = 100 µm), showing the IC: lesion core; PI: peri-lesion. (**B**) A higher magnification in the same section (white box enlarged), MHP36 cells labelled with PKH26 dye, (**C**) MAP-2 positive neurons observed in the lesion at 28 days post-MCAO and (**D**) merged image indicating that the MHP36 cells do not co-localise with MAP-2 (B-D: scale bar = 20 µm). (**E**) Representative mouse brain coronal section used as a reference for imaging (Bregma: -0.40 mm). (**F**) Graphical representation of mean average intensity staining for MAP-2 positive cells (not significant; versus vehicle) (Bregma: -0.38 ± 0.10 mm). Data represented as mean ± SEM, n=3, unpaired Student's t-test.

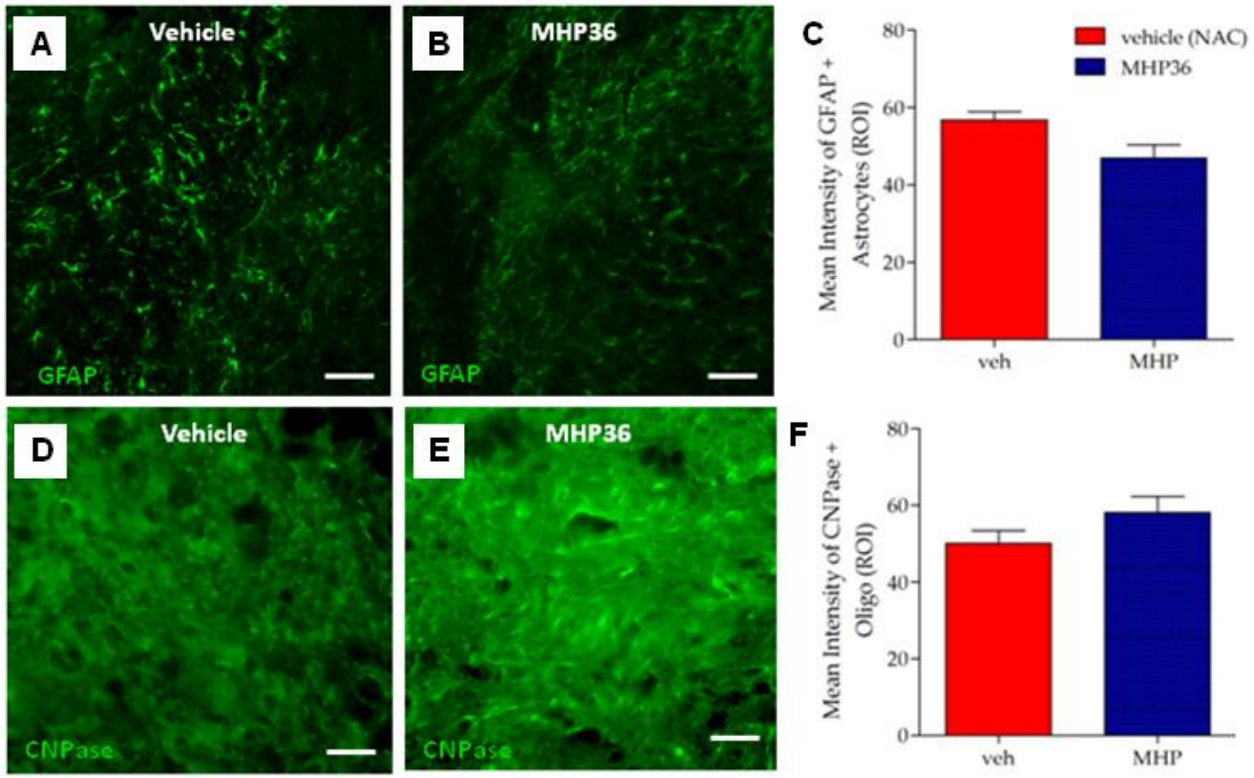

Figure 5.12: Histological assessment of glial marker GFAP and CNPase at 28 days post-MCAO

Peri-lesion stained in mice receiving (**A**) vehicle versus (**B**) MHP36 cells for GFAP; (scale bar = 100µm). (**C**) Graphical representation of mean average intensity staining for GFAP positive cells. Peri-lesion stained in mice receiving (**D**) vehicle versus (**E**) MHP36 cells with CNPase; (scale bar = 50 µm). (**F**) Graphical representation of mean average intensity staining for CNPase positive cells (not significant; versus vehicle for both markers) (Bregma: -0.38 ± 0.10 mm). Data represented as mean ± SEM, n=3, unpaired Student's t-test.

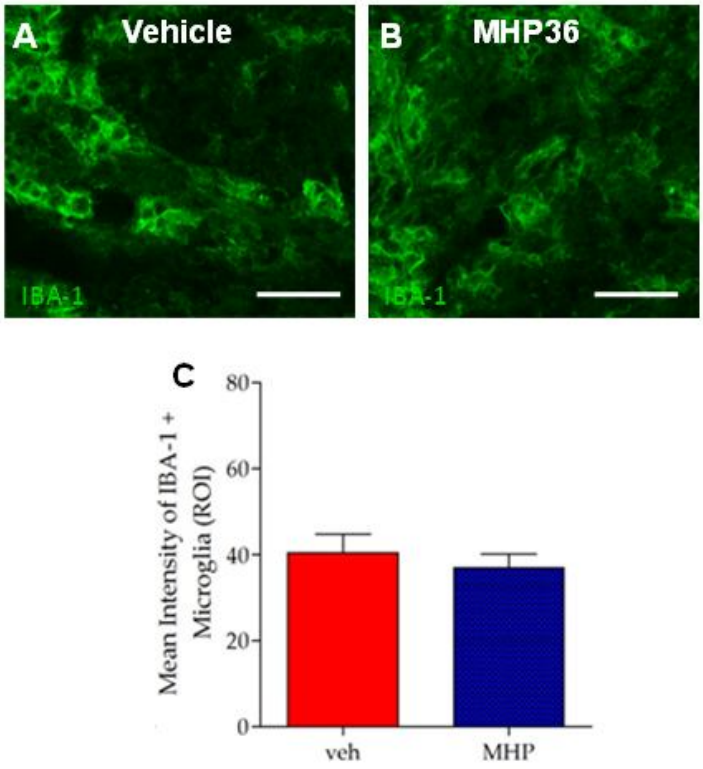

Figure 5.13: Histological assessment of glial marker IBA-1 at 28 days post-MCAO

Peri-lesion stained in mice receiving (**A**) vehicle versus (**B**) MHP36 cells for IBA-1; (scale bar = 20µm). (**C**) Graphical representation of mean average intensity staining (Bregma: -0.38 ± 0.10 mm) for IBA-1 (microglia) positive cells (not significant; versus vehicle). Data represented as mean ± SEM., n=3, unpaired Student's t-test.

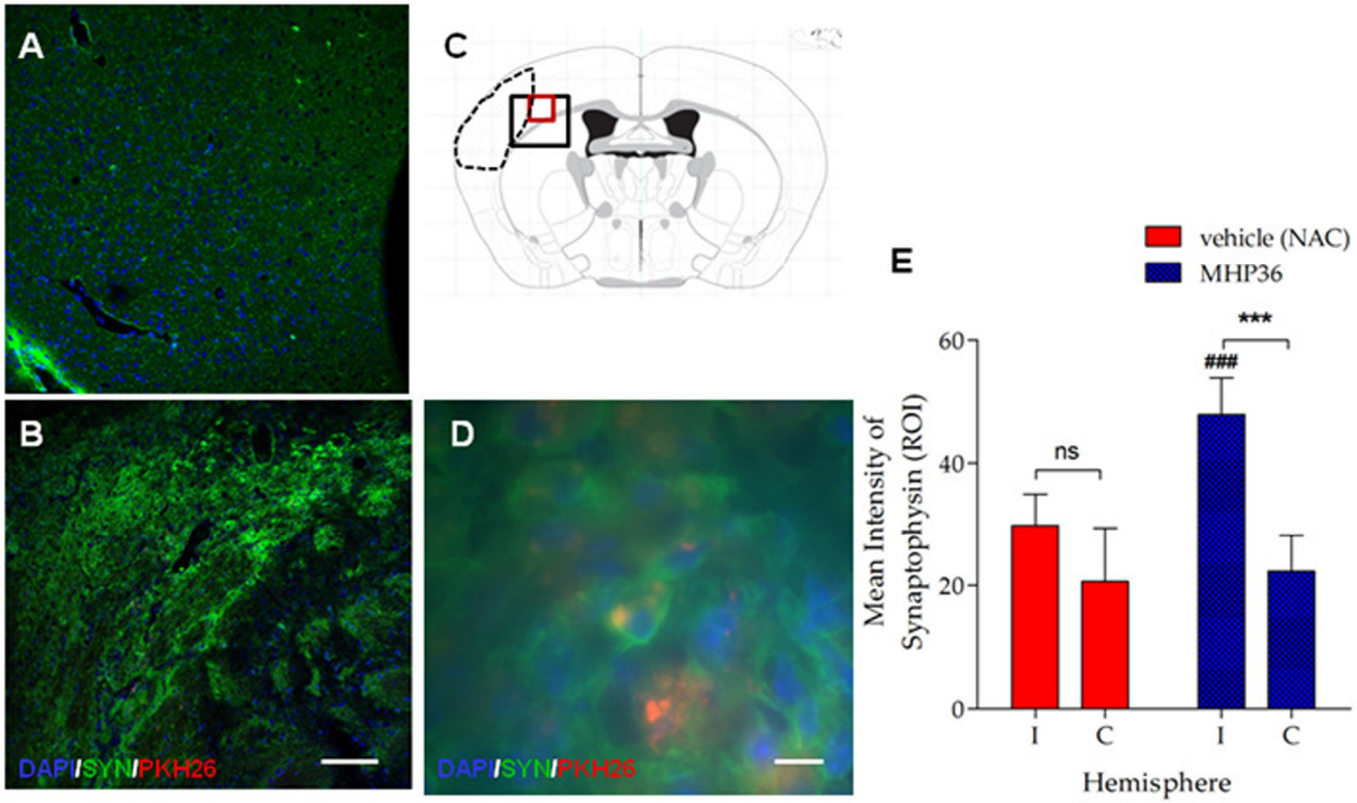

Figure 5.14: Histological assessment of synaptogenesis at 28 days post-MCAO

Region of interest, peri-lesion cortex stained for synaptophysin in animals receiving (**A**) vehicle and (**B**) MHP36 cells (view black box) (scale bar = 100 µm). (**C**) Representative mouse brain coronal section used as reference for area used for imaging (Bregma: -0.38 mm). (**D**) A higher magnification in the same section (red box), MHP36 cells labelled with PKH26 dye (red) co-localised with Syn positive cells (green) (scale bar = 20µm). (**E**) Graphical representation of mean average intensity of Syn in vehicle and MHP36 receiving animals. Data represented as mean ± S.E.M., n=3, two-way ANOVA with a post hoc Bonferroni's test. Asterisks indicate *** p>0.001 contralateral vs. ipsilateral hemisphere; ### p>0.001 vehicle vs. MHP36 in ipsilateral hemisphere. (I= ipsilateral; C= contralateral).

5.4 | Discussion

Cell transplantation therapy for stroke has tremendous potential; however certain limitations are delaying their success in humans. Cell types that have been shown to improve behavioural function after experimental stroke include neural stem/progenitor cells cultured from fetal tissue (Borlongan et al., 1998), hematopoietic/endothelial progenitors and stromal cells from bone marrow (Chen et al., 2003a, Zhang et al., 2002), umbilical cord blood (Chen et al., 2001b), peripheral blood (Willing et al., 2003), adipose tissue (Kang et al., 2003) and immortalized neural cell lines (Park, 2000, Veizovic et al., 2001). Limitations include potential hazards of tumour formation using embryonic stem cells (Erdo et al., 2003) and availability of cell numbers from hematopoietic/endothelial sources (Carmeliet, 2003, Rouhl et al., 2008). In this Chapter, we have shown that the MHP36 cells following transplantation *in vivo* lose nestin immunoreactivity rapidly and completely. This regulation is an early event in the differentiation process. Thus, the host cells must be transmitting a signal to the MHP36 cells, which results in them entering the initial stages of differentiation, beginning with the degradation of nestin protein. Interestingly, this loss of nestin does not lead to an equally rapid appearance of markers of differentiation (GFAP staining does not co-localise with labelled PKH26 MHP36 cells) in the MHP36 cells at least under conditions where there is no MCAO (**Figure 5.3**). Mellodew and colleagues have shown that nestin regulation is an early step in the process of neural stem cell differentiation, and is mediated by the rapid degradation of the nestin protein, probably via the ubiquitin-proteasome pathway. Furthermore, the Notch signalling pathway could be involved in the modulation of nestin degradation during stem cell differentiation (Mellodew et al., 2004). Endogenous astrocytes (reactive) were also observed using a marker for astrocytes (GFAP) and this was confirmed by the lack of co-localisation with the PKH26 labelled MHP36 cells.

Reactive astrocytes in this experiment are probably present as a result of local injury due to injection. Of relevance to stroke, reactive astrocytes are thought to protect the penumbra during brain ischaemia (Li et al., 2008), but direct evidence has been lacking due to the absence of suitable experimental models. These experiments were designed to establish the stereotaxic surgery and immunostaining (preparation of brain tissue for visualizing the stem cells *in vivo*) post transplantation. The key findings of the main study in the present chapter are that conditionally immortalised neural stem cells MHP36 restore lost sensorimotor function after transient MCAO in mice as demonstrated in both the cylinder and ladder rung tests. The observed improved function is not due to reduced lesion size or increased cellular differentiation but perhaps due to increased synaptic plasticity.

Improved functional recovery after transient MCAO by MHP36 cells has been shown in a previous study but in that study grafting was done in rats, at 8 distinct contralateral sites and at 2 to 3 weeks after MCAO (Veizovic et al., 2001). This study extends previous work showing success of MHP36 cells after transient MCAO when grafted in mice in 2 ipsilateral sites 2 days post-MCAO. Furthermore, updated STAIR preclinical recommends using a time window (at least 2-3 weeks post MCAO recovery) with both histological and functional outcomes in multiple animal species (Fisher et al., 2009). Other previous studies have shown MHP36 cell survival, migration, differentiation, and efficacy in cognitive tasks after four-vessel occlusion in rats (Gray et al., 2000, Gray et al., 1999, Sinden et al., 1997), motor and cognitive recovery after MCAO in rats (Veizovic et al., 2001) and hippocampal lesions in the marmoset (Hodges et al., 2000b), which resulted in circumscribed CA1 cell loss. MHP36 cells have been tested in mice after 2 vessel global ischaemia and were found to reduce ischaemic damage with 50% of cells having neuronal phenotype though no functional recovery was assessed (Wong et al., 2005).

Improving functional outcome after stroke is the ultimate goal of stroke treatment. The detection of functional deficits and potential therapies that restore these is essential for potential translational applications. Mice, due to their small size and quick movements, can be perceived as more challenging to handle and train than rats (Wahlsten et al., 2003). Thus, test strategies for mice are frequently based on evaluation of simple motor behaviour in standard test batteries (Cook et al., 2002, Lalonde et al., 2003, Li et al., 2004) or neurological score such as Clark's deficit score (Clark et al., 1997, De Simoni et al., 2003). The Clark's deficit score was used in this study to allow assessment of significant deficit in MCAO animals as opposed to animals undergoing sham surgery. Importantly, the Clark's score was not designed in the present study to test the efficacy of stem cells given at acute time points (72 and 96 hrs post MCAO). While these tests evaluate gross behaviour, they lack resolution when rather specific chronic deficits need to be identified (Brambilla and Martelli, 2004, Farr et al., 2006). Numerous studies have reported behavioural deficits in rodents after focal stroke (DeVries et al., 2001, Hatcher et al., 2002, Hunter et al., 1998, Li et al., 2004). Often, these tasks show remarkable degrees of spontaneous recovery in the first week after stroke, making them less useful for chronic testing. In the rat, there are several well-established behavioural tests such as the sticky tape test, corner test, rotarod tests that continue to show deficits for several weeks after ischaemic damage (Cenci et al., 2002, Modo et al., 2000, Reglodi et al., 2003, Schallert et al., 1982). Much less has been described regarding the recovery of sensorimotor deficits in the mouse. In one of the more extensive studies in mice, deficits on a large number of behaviours including locomotor activity, gait, limb tone and negative geotaxis was demonstrated; however animals were only tested for 24 hrs after stroke (Hunter et al., 2000). Moreover, clear differences exist in the behavioural deficits seen in rats versus those seen in mice after stroke. For example in mice, the rotarod test was unable to distinguish sham and MCAO animals even 1 day after MCAO; in rats rotarod

testing has been used extensively to distinguish infarcted animals from sham (Hunter et al., 2000). The “adhesive tape test’’ originally described by Schallert and colleagues (Schallert et al., 1982) has been used in countless experiments and is sensitive to the degree of ischaemic damage in rat (Karhunen et al., 2003); however, this test is difficult to perform reliably in mice due to their small size (Li et al., 2004).

Tests that have shown successful recovery after MCAO with MHP36 include bilateral asymmetry and amphetamine rotation (Veizovic et al., 2001, Modo et al., 2002b), cognitive function (Gray et al., 2000) and simple and conditioned discrimination (Virley et al., 1999), whereas no recovery was observed using Morris water-maze (Veizovic et al., 2001). Unilateral brain damage in human and rodents results in deficits of symmetry and tests that detect asymmetries such as the cylinder test, which can detect even mild neurological impairments, (Hua et al., 2002) help factor out confounding variables such as an overall decrease in activity after surgical induction of stroke, as additional trials can be performed until the desired number of rearing observations are made (Onyszchuk et al., 2007). This is the first time the cylinder test has been used to assess the potential of MHP36 cells. We observed symmetrical use of both paws in sham animals and a marked preference for use of the non-impaired (ipsilateral) paw after tMCAO. Importantly, treatment with MHP36 not only reduced this asymmetry [by >70%] but also induced a marked preference for use of the impaired paw. The reasons for this are unclear but may be related to compensatory effects or increased activity of neurons which are discussed later.Since topography of our lesion includes cortical and subcortical areas, motor impairments of limb functioning and placing deficits were evaluated in the present study by the foot fault test which has commonly been used to demonstrate motor coordination deficits in rats (Stroemer et al., 1995). Recently, Farr and colleagues (Farr et al., 2006) have developed an

efficient and sensitive test strategy for chronic assessment of skilled fore- and hind-limb stepping in mice. Performance in the ladder rung task requires fine muscle and limb coordination as well as the ability for balanced weight-supported stepping movements. The stepping movements are usually accompanied by body weight shifts to maintain a balanced and undisrupted walking pattern. In order to adapt limb coordination to the irregular rung positions, animals are required to control their weight support and quickly correct for a limb placement error (Farr et al., 2006). The ladder rung test in the present study revealed impairments in limb stepping patterns post-MCAO when compared to pre-MCAO that were likely caused by loss of refined motor control. These deficits may be due to absence of the arpeggio movement in contralateral fore- and hind-limbs (Farr et al., 2006), which involves successive placement of digits 1–5 when palpating the surface and finely adjusting the paw position relative to the surface (Whishaw et al., 2003) (see **Table 5.1** for fore and hind limb scores for this study). Previous studies in rats have indicated that arpeggio movements of fore- and hind-limbs are impaired after dopamine depletion (Miklyaeva et al., 1994, Whishaw et al., 2003) and in mice with motor cortex lesions (Farr et al., 2006). This is the first study to show a lesser significant deficit in the MHP36 group when compared to vehicle group by 28 days post MCAO and that this improvement is accelerated by 14 days in mice receiving MHP36 cells.

The tests used in this study are convenient and reliably detect motor deficits independent of the influence of repeated testing, which is essential for investigating the recovery process at any time points. It is important to understand however, that both plasticity and degenerative events may co-occur over long periods of time. The extent to which delayed degeneration and plasticity events tend to cancel each other is not easily investigated, but should be kept in mind particularly when making decisions about the optimal timing of an intervention (Schallert et al.,

2000). The functional recovery after implantation of MHP36 cells observed in this study provides some pointers to the possible mechanisms involved. Three possibilities for the observed functional outcome using MHP36 cells are that 1) it is unlikely to be compensatory effects or it would be evident in MCAO/vehicle group. 2) grafted MHP36 cells promoted neuroprotection by migrating to the area of damage and reconstituting local circuits that were sufficient to sustain some functions and 3) grafted MHP36 cells promote plasticity by augmenting spontaneous reorganization within the host environment sufficient to undertake, or compensate for, some lost function by release of nerve growth factors; neurotrophins. Evidence from imaging studies suggests that both possibilities are reasonable (Cramer et al., 1997).

Whether transplanted cells reduce death of host cells is an important observation as enhanced recovery of function could result from neuroprotection (Shen et al., 2010). The lesion volume in the present study was not significantly reduced by MHP36 cell which was in agreement with Modo et al., (2002) (Modo et al., 2002a) where they showed no difference in infarct when transplantation was 2-3 weeks post-MCAO and lesion was assessed at 14 weeks. In other studies, MHP36 cells have been shown to reduce infarct size in rats (Modo et al., 2009, Veizovic et al., 2001). This was observed 11 months after transplantation possibly due to a reduction of secondary degeneration and atrophy (Schallert et al., 1982). Furthermore, they suggest the reduction in lesion volume appears to be a delayed effect because they did not observe a reduction in lesion in rats examined 3 months after transplantation of MHP36 grafts, which already exerted positive effects on bilateral asymmetry. Thus, a time course study is essential to compare the evolution of lesion size in grafted and non grafted animals after MCAO and to relate volume change to behavioural outcome. Other stem cell sources and their outcomes after MCAO promoting neuroprotection are discussed in **section 1.2.2** & **1.2.3**. Other mechanisms of

action of MHP36 could include filling out of cavities, replacing lost circuitry and integration of MHP36 cells into host circuitry. In the present study it would not be possible for injections of 1 µl (25,000 cells) to fill out cavities averaging ~2-3 mm^3, particularly since only a third of the cells migrate to the lesion site (Veizovic et al., 2001). In our study, at 28 days post-MCAO, there were fewer MHP36 cells present in the injection tract, with increased numbers of cells in the surrounding areas at 28 days post-transplantation. Cells were observed in the peri-lesion cortex and caudate nucleus, regions that undergo neuronal damage after transient MCAO, suggesting that the grafts were migrating in response to damage.

MHP36 cells are unlikely to be improving functional recovery after stroke via replacing lost circuitry or integration of MHP36 cells into host circuitry in the present study. This is due to a non-significant trend to increased expression of MAP-2 (neuronal), CNPase (oligodendrocytes) and decreased expression of GFAP (astrocytes) in the MHP36 group when compared to vehicle at 28 days was observed. Conversely, Hodges and colleagues have shown that astrocytes may play an important role in the functional recovery induced by MHP36 grafts, since grafted cells readily adopted this phenotype (Hodges et al., 2000b). Furthermore, Bradbury and colleagues found that astrocytes grafts elevate recovery from deficits induced by cholinergic lesions as effectively as primary foetal tissue (Bradbury et al., 1995). In the present study a decreased expression of GFAP was observed which can be supported by a recent finding by Järlestedt and colleagues that states attenuation of reactive gliosis, using GFAP and vimentin knock-out mice in the developing brain does not affect infarct volume after hypoxic-ischaemia, but increases the number of surviving newborn neurons (Jarlestedt et al., 2010). Nevertheless glial contributions are important and might include: 1) provision of a matrix to support the survival and integration of the neuronal population of grafted cells; 2) promote local remyelinization; 3) release of

transmitter substances to supplement the activity of host cells or 4) release of trophic factors that sustain damaged host or grafted neurons (Hodges et al., 2000b). Furthermore, IBA-1 positive microglia were also observed after 28 days post-MCAO. Our findings are similar to Lambertsen and colleagues that showed microglia and microglial-derived TNF played a key role in determining the survival of endangered neurons in cerebral ischaemia (Lambertsen et al., 2009). Attenuation of a stroke-induced inflammatory/immune response after cell replacement has also been observed (Wong et al., 2005). However, we did not observe any significant effect of MHP36 on microglia when compared to vehicle. In agreement, Wong and colleagues showed a marked increase in microglia/macrophage in MHP36 grafted mice as compared to vehicle mice at 1 week post transplantation indicating that the MHP36 cells further evoked an inflammatory response. This vast inflammatory response decreased dramatically at 4 weeks post-transplantation to levels approaching that of vehicle mice (Wong et al., 2005). This suggests that the MHP36 cells are no longer recognised as foreign by host microglia and macrophages. In addition, there was no co-localisation of microglia with MHP36 cells indicating that these cells were not being phagocytosed. Microglial inflammation has been shown to have a varying effect on neural stem cell grafts. The pro-inflammatory effects of microglia have been well documented (Vilhardt, 2005) with graft rejection strongly associated with macrophage and microglial infiltration (Duan et al., 1995). Microglia can also have a beneficial effect on NSC grafts, aiding in migration, axonal growth and differentiation, possibly by secretion of growth factors or through cell–cell contact (Vilhardt, 2005, Lambertsen et al., 2009).

Brain plasticity is promoted by neuronal connections that are continuously remodelled and suffer intense adaptive functional and structural reorganisation after lesions (Carmichael, 2003, Giraldi-Guimaraes et al., 2009, Rossi et al., 2007). This restorative reorganisation promoting

endogenous brain plasticity (Modo et al., 2003, Minger et al., 2007) is one of the most important mechanisms underlying functional recovery. The functional recovery observed in the present work might be explained in part by a positive effect of the MHP36 cells in the structural plasticity induced by ischaemia. To analyse this hypothesis, we studied the expression of synaptophysin protein, related to structural plasticity, in the periphery of the lesion and in the contralateral (homologous) cortex. Our results showed a significant effect of the MHP36 treatment in the expression of synaptophysin in the ipsilateral cortex suggesting that the observed recovery might be attributed to significant plastic structural changes involving synaptogenesis. In agreement, Shen and co-workers showed an increase of the synaptophysin expression in the periphery of the ischaemic lesion in rats treated with bone-marrow stromal cells one day after MCAO (Shen et al., 2006).

Other mechanisms that may lead MHP36 cells to improve functional recovery include enhancing angiogenesis (Carmeliet, 2003, Chen et al., 2005, Chen et al., 2003b, Zhang et al., 2002, Krupinski et al., 1994) and motor remapping (Carmichael, 2003, Li et al., 2005, Shen et al., 2006). Future studies would be required to elucidate these functions. In conclusion, the pilot study showed firstly that, the PKH26 labelled MHP36 cells migrated out of the implanted site. Secondly, these PKH26 labelled NSC lost nestin expression but did not differentiate into astrocytes after 24 hours in the host brain. Thirdly, GFAP-positive cells were observed near the injection site suggesting that endogenous reactive astrocytes were attracted near the site of injection possibly to protect the brain from the injury caused by the injection. Key findings from the main study suggest that MHP36 grafts ipsilateral to the lesion exert a positive functional effect as observed using the ladder and cylinder test which is probably mediated by promoting synaptogenesis rather than via neurogenesis or neuroprotection. Enhanced or accelerated

improvement of behaviour on these tests may be a useful marker of functional reorganization in the damaged brain. Thus, the same experimental plan was used to test our hypothesis, whether NSCs over-expressing oestrogen enhanced or accelerated improvement, see Chapter 6.

CHAPTER 6

EFFECTS OF MHP36 NEURAL STEM CELLS OVER-EXPRESSING OESTROGEN ON BRAIN REPAIR AFTER MCAO IN MICE

6.1 | Introduction

In the previous Chapter it was demonstrated that MHP36 cells have the capacity to exert a positive functional recovery using sensorimotor tasks after tMCAO in mice likely linked to increased synaptogenesis. In that study, grafted MHP36 cells migrated to the area of damage and reconstituted local endogenous circuits that were sufficient to promote synaptogenesis and sustain some functions rather than by replacing host cells. One possible way to promote survival, integration and enhancement of functional recovery is via neurorestoration and re-modelling of animal brain; by modulating properties of the MHP36 cells to promote success of stem cells.

Oestrogen regulates the development, maturation, survival and function of multiple types of neurons in multiple brain regions (McEwen and Alves, 1999, Simpkins et al., 1997, Toran-Allerand, 2004, Brinton, 2004). Recent advances in our understanding of oestrogen action in brain are that 17β-oestradiol (E2) can promote neurogenesis in rat brain *in vivo* and proliferation of neural progenitor cells (NPCs) *in vitro* (Brannvall et al., 2005, Brannvall et al., 2002, Tanapat et al., 2005, Tanapat et al., 1999). Oestrogen can act as a neuroprotective agent (Behl, 2002, Dubal and Wise, 2001, Hurn and Macrae, 2000), promoting synaptic plasticity and growth of nerve processes (Bi et al., 2001, McEwen, 2002), attenuates programmed cell death (Rau et al., 2003) and modulates various synaptic markers that are associated with cognition (Gibbs and Gabor, 2003, Kim and Casadesus, 2010). Thus far, two

types of oestrogen receptors (ERs), ERα and ERβ are well characterized. ERα and ERβ reveal common feature of the nuclear receptor structure but are encoded by different genes located on different chromosomes, and, in addition, they exhibit different brain distribution profiles (for review, see (McEwen and Alves, 1999) and **section 1.3.3**). The brain region-specific distribution for these receptors is linked to functional distinctions between ERα and ERβ for oestrogen-induced neuroprotection, neurotrophic and neurogenic activities (Struble et al., 2003, Wang et al., 1994, Zhao et al., 2005). E2-induced neuroprotection and neurotrophism are regulated by a coordinated signalling cascade that involves ER protein interaction with the regulatory subunit (discussed in Chapter 1 **section 1.3.4**). Furthermore, Suzuki and colleagues have clearly demonstrated that both ER α and β play pivotal functional roles, insofar as knocking out either of these receptors blocks the ability of E2 to increase neurogenesis (Suzuki et al., 2007). Furthermore, ER- dependent E2-induced stem cell proliferation and differentiation has been shown *in vitro* (Brannvall et al., 2002).

Considering evidence of MHP36 cells to promote functional recovery in stroke animals following brain transplantation and of E2 to promote neurogenesis and synaptogenesis, this led to the hypothesis that over-expression of E2 in MHP36 (discussed in **Chapter 3**; Dax-1KD-MHP36 cells) can increase plasticity of grafted NSCs, enhance and accelerate functional recovery via neurogenesis and synaptogenesis in the mouse MCAO model.

6.2 | Methods

6.2.1 | Subjects

Thirty-two, C57BL/6 male mice, 12-14 weeks old (Charles River, UK), weighing between 25 and 30 g, were used complying with the UK Animals (Scientific Procedures) Act, 1986.

6.2.2 | Experimental design

The experimental design was similar to the one used in Chapter 5 (see **section 5.2.2.2**).

6.2.3 | Surgery and measurement of CBF

Following completion of baseline behavioural testing, focal ischaemia was induced within the left hemisphere by transient (45 min) tMCAO as described previously in **section 2.2.10.2**. In each animal, laser Doppler flowmetry (Moor Instruments, UK) was used to monitor cerebral blood flow (CBF) continuously, before and during MCAO as well as during reperfusion as described in **section 2.2.10.3**. Animals were included only when CBF was reduced by ≥ 85% during ischaemia, and successful reperfusion was subsequently achieved.

6.2.4 | Cell maintenance and transplantation

MHP36 and Dax-1KD-MHP36 cells were cultured from frozen stock and maintained in an undifferentiated state at 33 °C as described in **section 2.2.1**. Dax-1KD-MHP36 cells were cultured in the same media, which in addition contained puromycin.

Two days post-ischaemia, mice were randomly selected (suggested in STAIR; (Saver et al., 2009) to receive a unilateral cortical and striatal graft of either control vehicle (n = 4), MHP36 stem cells (n = 4), E2 (n = 4), MHP36 + E2 (n = 6), Dax-1KD-MHP36 (n = 6) (all treatments in presence of NAC and ethanol). Before grafting, cells were labelled with the

membrane bound fluorescent marker PKH26 (described in detail in **section 2.2.13.2)**. The following coordinates (Medial/Lateral + 2 mm, Anterior/Posterior - 0.26 mm, Ventral -1.5 and -3.0 mm from the surface of the brain) were used for injection.

6.2.5 | Clark's Deficit Score (CDS)

The CDS was similar to the one used in Chapter 5 (see **section 5.2.2.5**). Out of the 32 animals that underwent tMCAO, 8 were excluded according to the exclusion criteria (all exclusions were before 2 days post MCAO injection).

6.2.6 | Ladder rung task apparatus and analysis

The ladder rung test was similar to the one used in Chapter 5 (see **section 5.2.2.6**) and is described in detail in **section 2.2.14.2**.

6.2.7 | Cylinder task apparatus and analysis

The cylinder test was similar to the one used in Chapter 5 (see **section 5.2.2.7**) and is described in detail in **section 2.2.14.3**.

6.2.8 | Video recording and analysis equipment

Post-MCAO measurements were taken at 2, 7, 14 and 28 day time points. The mice were filmed with a high speed Panasonic digital camcorder (30 frames/s; shutter speed of 1/1000). The digital videotapes were analyzed using a HP Pavilion DV2000 laptop. Single frames were imported from the digital video records using Windows media player on a Windows operating system.

6.2.9 | Histology and infarct measurement

All histology and analysis for volumetric assessment of ischaemic damage, the observer was unaware of treatment (injection). Mice were perfused at 28 days following the completion of

behavioural testing. The brains were processed appropriately and coronal sections were cut at 20μm and collected on slides for further analysis (detailed in **section 2.2.13**).

6.2.9.1| Measurement of lesion

Sections were stained with haematoxylin and eosin to determine lesion (tissue loss) and measure volume as described in **sections 2.2.13**.

6.2.9.2| Assessment of differentiation

Serial 20μm coronal sections were processed (see **section 2.2.3**) and stained (see **section 5.2.2.9.2**) to identify differentiated cells.

6.2.9.3| Assessment of synaptic plasticity

Serial 20μm coronal sections were processed (see **section 2.2.3**) and stained (see **section 5.2.2.9.3**) to investigate synaptogenesis. PKH26/anti-Syn double-label immunofluorescence was used to relate synaptogenesis.

The coronal levels used for staining ranged between bregma -0.38 ± 0.10 mm. The analysis for immunofluorescence staining was carried out as described in **section 2.2.3.1**.

6.2.10 | Statistical analysis

Statistical comparisons in cylinder and ladder rung test were made using one-way ANOVA with repeated measures. Clark's deficit score was analysed using two-way ANOVA. A post hoc Bonferroni's test was applied to correct for multiple comparisons. In histology assessments, unpaired Student's t-test was performed unless otherwise stated. A p-value of less that 0.05 was chosen as the significance.

6.3 | Results

6.3.1 | Summary of characterisation of neural stem cells for oestrogen

Initially, we determined whether MHP36 cells express oestrogen receptors and aromatase for genetic modification (refer to **Chapter 3**). Furthermore, Dax-1KD-MHP36 cells were characterised for oestrogen after genetic modification (refer to **Chapter 3**).

6.3.2 | Cerebral blood flow

Analysis of CBF did not show any difference between different groups that were to later receive either vehicle or stem cells. CBF was reduced by >85-90% in all groups during MCAO when compared to pre-occlusion baseline values (**Figure 6.1**).

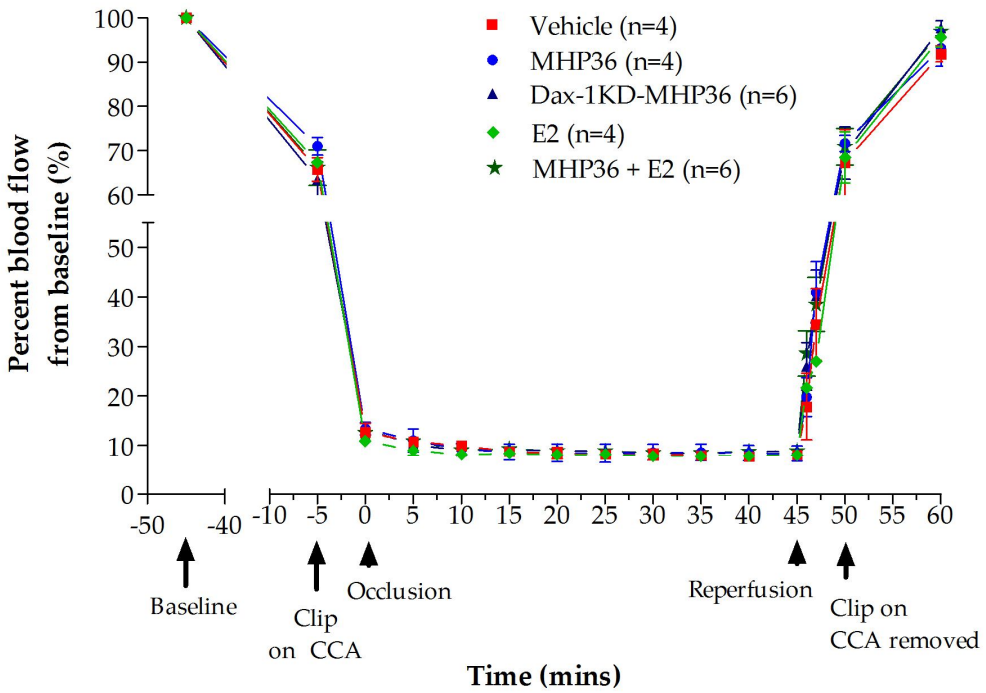

Figure 6.1: Laser Doppler flowmetry in mice undergoing MCAO.

Cortical blood flow measured before, during and after insertion of the silicone filament to occlude the MCA, using laser Doppler flowmetry. Data are presented as a percentage change from baseline blood flow (100%) and represented as mean ± SEM, n ≥ 4 in each group. CCA= common carotid artery.

6.3.3 | Clark's deficit score

Animals at 24 hrs post-MCAO showed a significant genral and focal deficits in all groups when compared to sham animals (data from Chapater 5). At 48 hrs post-MCAO animals recieved either vehicle or E2 or stem cells injection. The general and focal deficits were not affected by any of injections as observed at 72 and 96 hrs post-MCAO (**Figure 6.2**).

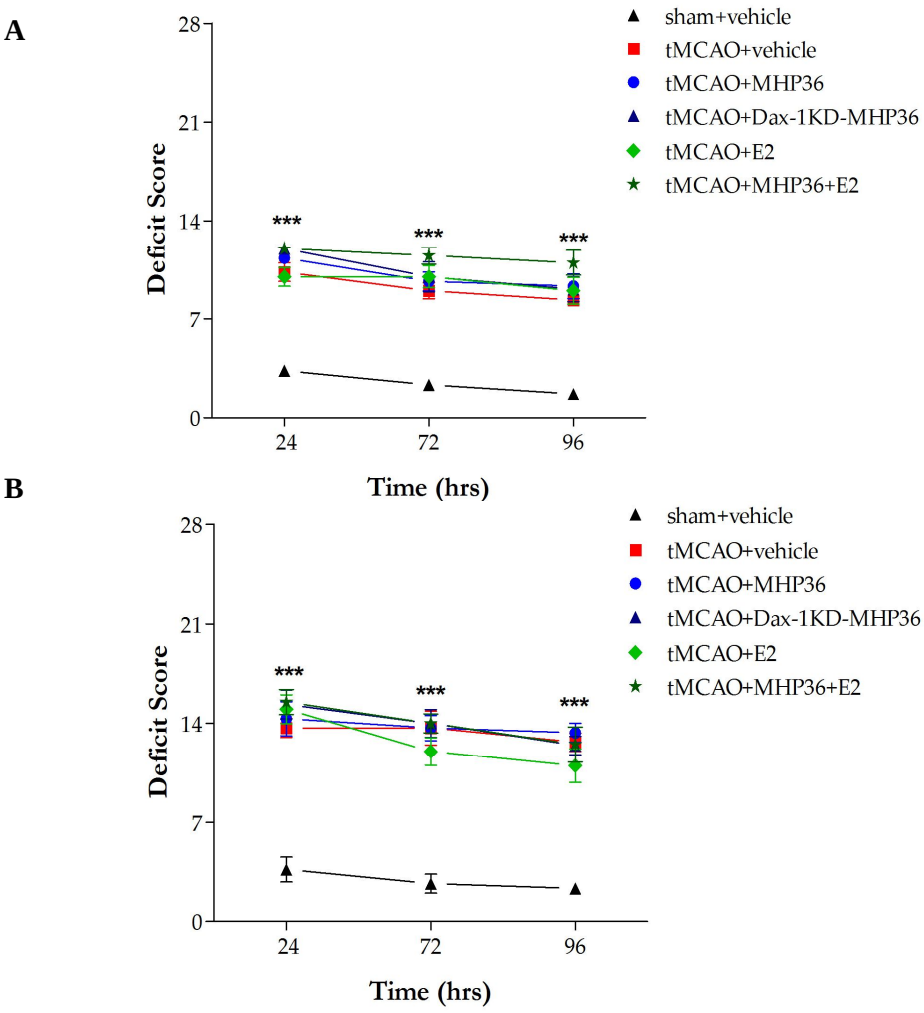

Figure 6.2: Evaluation of Neurological score using Clark's deficit Scale

(**A**) General and (**B**) focal neurologic Clark's deficit score evaluation assessed 24, 72 and 96 hrs post-MCAO in mice receiving either vehicle, MHP36, Dax-1KD-MHP36, E2 or MHP36 +E2 cells at 48 hrs post-MCAO, respectively. Significant deficit observed after tMCAO when compared to sham surgery animals at all 3 time points assessed. Data represented as mean ± S.E.M, n ≥ 4. Asterisks indicate *** p≥ 0.001 sham versus tMCAO (different injection).

6.3.4 | Effects of Dax-1KD-MHP36 cells on behavioural outcome using ladder rung test after tMCAO

Prior to MCAO, mice performed mainly correct placements with all four limbs (table 6.1). There was a significant increase in placement errors of the contralateral forelimb in all groups (**Figure 6.3**) at 2 days post MCAO (vehicle, 3.95 ± 0.39; MHP36, 3.82 ± 0.13; Dax-1KD-MHP36, 3.97 ± 0.23; E2, 4.02 ± 0.26; MHP36+E2, 4.09 ± 0.22) when compared to pre-MCAO scores for the same treatment (vehicle, 5.77 ± 0.1; MHP36, 5.71 ± 0.04; Dax-1KD-MHP36, 5.73 ± 0.08; E2, 5.75 ± 0.04; MHP36+E2, 5.79 ± 0.04). There was still a significant deficit from pre-MCAO scores at 28 days post-MCAO in all groups except animals receiving Dax-1KD-MHP36 cells (MHP36 and MHP36+E2, p= 0.05; E2 and vehicle, p= 0.01, one-way ANOVA repeated measures, Bonferroni's post test) (**Figure 6.3**). Dax-1KD-MHP36 completely reversed the functional deficit close to pre-MCAO scores (5.73 ± 0.08) by 28 days post-MCAO (5.07± 0.12, n.s., one-way ANOVA repeated measures, Bonferroni's post test) (**Figure 6.3**). Furthermore, Dax-1KD-MHP36 cells had the capacity to accelerate the functional recovery by 14 days which was not apparent in the other groups (MHP36, 4.33± 0.32; Dax-1KD-MHP36, 4.88 ± 0.12; MHP36 + E2, 4.52± 0.22) when compared with 2 days post-MCAO scores (**Figure 6.3**).

A Vehicle

Pre Scores	Mean	SEM	n	28 days score	Mean	SEM	n
Ipsi H	5.96	0.04	4	**Ipsi H**	5.90	0.05	4
Ipsi F	5.62	0.19	4	**Ipsi F**	5.71	0.08	4
Contra H	5.92	0.04	4	**Contra H**	5.52	0.05	4
Contra F	5.77	0.10	4	**Contra F**	4.57	0.14	4

B MHP36 cells

Pre Scores	Mean	SEM	n	**28 days score**	Mean	SEM	n
Ipsi H	5.90	0.04	4	**Ipsi H**	5.80	0.03	4
Ipsi F	5.80	0.07	4	**Ipsi F**	5.81	0.04	4
Contra H	5.90	0.03	4	**Contra H**	5.50	0.15	4
Contra F	5.71	0.07	4	**Contra F**	4.90	0.22	4

C E2

Pre Scores	Mean	SEM	n	28 days score	Mean	SEM	n
Ipsi H	5.85	0.06	4	**Ipsi H**	5.93	0.04	4
Ipsi F	5.78	0.04	4	**Ipsi F**	5.78	0.08	4
Contra H	5.89	0.08	4	**Contra H**	5.28	0.20	4
Contra F	5.75	0.04	4	**Contra F**	4.57	0.11	4

D MHP36 + E2

Pre Scores	Mean	SEM	n	28 days score	Mean	SEM	n
Ipsi H	5.86	0.04	6	**Ipsi H**	5.97	0.03	6
Ipsi F	5.69	0.09	6	**Ipsi F**	5.81	0.04	6
Contra H	5.87	0.06	6	**Contra H**	5.69	0.06	6
Contra F	5.79	0.04	6	**Contra F**	4.76	0.22	6

E Dax-1KD-MHP36 cells

Pre Scores	Mean	SEM	n	28 days score	Mean	SEM	n
Ipsi H	5.91	0.04	6	**Ipsi H**	5.93	0.07	6
Ipsi F	5.85	0.09	6	**Ipsi F**	5.88	0.03	6
Contra H	5.88	0.03	6	**Contra H**	5.47	0.14	6
Contra F	5.73	0.08	6	**Contra F**	5.07	0.12	6

Ipsi= Ipsilateral; Contra= Contralateral; H= Hind Limb; F= Fore limb

Table 6.1: Scores of all four limbs at pre- and 28 days post-tMCAO in the ladder test

(**A**) Vehicle, (**B**) MHP36 cells, (**C**) E2, (**D**) MHP36 cells + E2 and (**E**) Dax-1KD-MHP36 cells pre and 28 days post-MCAO scores.

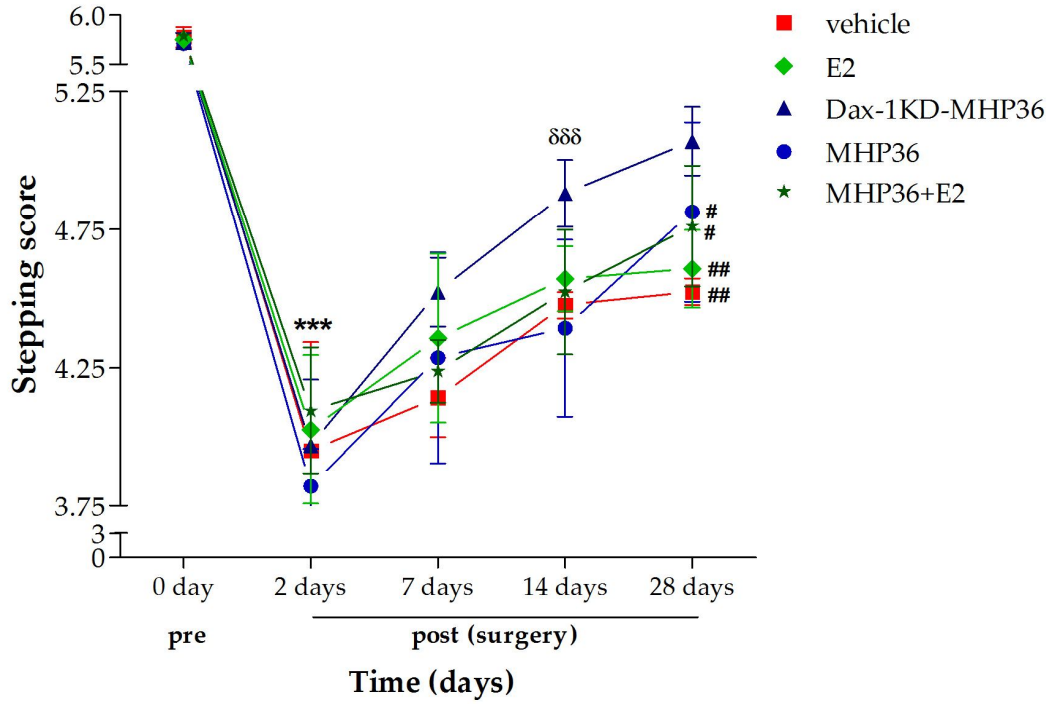

Figure 6.3: Average stepping score for contralateral fore-limb on the ladder rung task after MCAO

Mice receiving either vehicle, E2, MHP36, MHP36+E2 cells or Dax-1KD-MHP36 cells tested at four time points post-MCAO. A significant stepping deficit at 2 days post-MCAO was observed in all groups. Dax-1KD-MHP36 cells accelerated the functional recovery observed at 14 days post-MCAO when compared to 2 days post-MCAO score. Asterisks indicate ***p< 0.001 (pre- versus 2 days), # p<0.01, ## p<0.001 (pre-MCAO versus 28 days), δδδ p<0.001 (2 days versus 14 days) one-way ANOVA, repeated measures.

6.3.5 | Effects of Dax-1KD-MHP36 cells on behavioural outcome using cylinder test after tMCAO

In this task, the mean laterality score of the injured group, which measures preference for the forelimb unaffected by (ipsilateral to) the injury, peaked at 2 days post-MCAO time point. There was a significant increase in left (non-impaired) forelimb usage in tMCAO animals (**Figure 6.4**) at 2 days post-MCAO (vehicle, 0.83 ± 0.08; MHP36, 0.83 ± 0.06; Dax-1KD-MHP36, 0.7 ± 0.08; E2, 0.78 ± 0.07; MHP36+E2, 0.75 ± 0.06) when compared to pre-

MCAO scores in each injection groups (vehicle, 0.05 ± 0.09; MHP36, -0.06 ± 0.03; Dax-1KD-MHP36, 0.01 ± 0.13; E2, -0.04 ± 0.06; MHP36+E2, 0.04 ± 0.03). There was still a significant deficit at 28 days post-MCAO in the vehicle (0.38 ± 0.097, p= 0.04) and E2 alone groups (0.1 ± 0.094, p= 0.01) compared to pre-MCAO scores (**Figure 6.4**). However, a highly significant preference for the right (impaired) forelimb was observed at 28 days in the animals receiving MHP36 cells (-0.55 ± 0.12) and MHP36 cells suspended in oestrogen (-0.43 ± 0.035) when compared to pre-MCAO. On the other hand, Dax-1KD-MHP36 completely reversed the functional deficit to pre-MCAO scores (0.10 ± 0.13) by 28 days post-MCAO (-0.03±0.12, ns) (**Figure 6.4**).

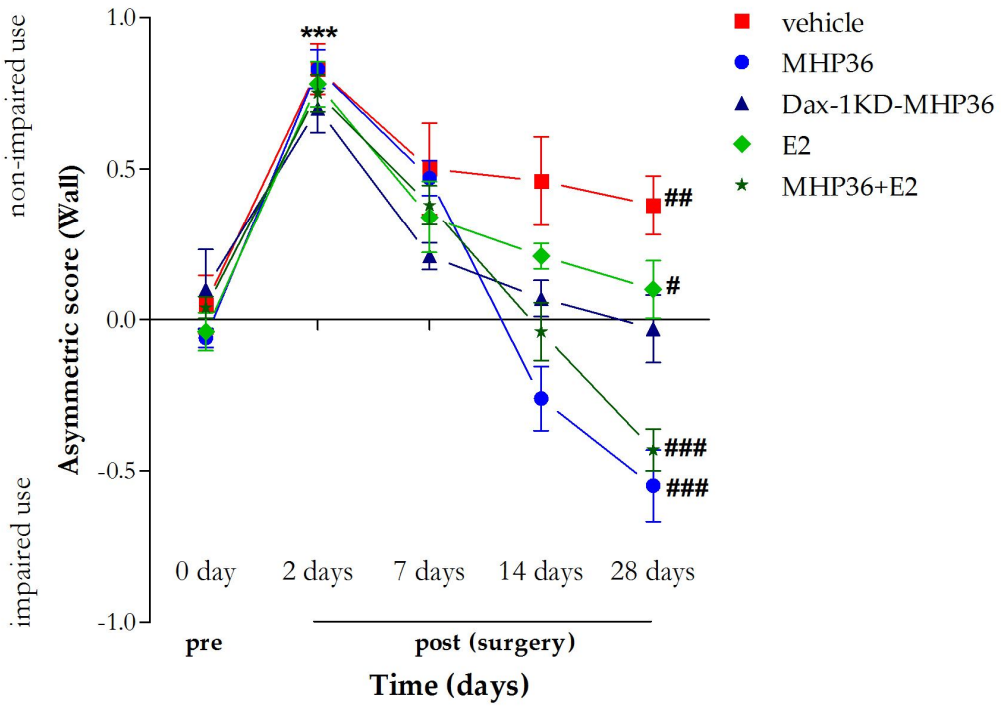

Figure 6.4: Spontaneous vertical exploration of fore-limb using cylinder test after MCAO

Mice receiving either vehicle, E2, MHP36, MHP36+E2 cells or Dax-1KD-MHP36 cells were tested at four time-points post-MCAO. A significant asymmetry on cylinder testing at post-MCAO time point was observed in all groups. Dax-1KD-MHP36 cells restored the functional deficit to pre-MCAO baseline score. Asterisks indicate ***p< 0.001 (pre- versus 2 days; all groups), # p<0.05, ## p<0.01, ### p<0.001 (pre-MCAO versus 28 days), one-way ANOVA with repeated measures.

6.3.6 | Histology

6.3.6.1 | Measurement of lesion (tissue loss) after 28 days post-MCAO

At 28 days post-transplantation there was a significant difference in lesion (tissue loss) between the vehicle (18.5 ± 1.34 mm^3; n=4) and Dax-1KD-MHP36 only (12.0 ± 1.66 mm^3, n=6) grafted mice (**Figure 6.5**). The lesion volume was not significantly reduced in any other group.

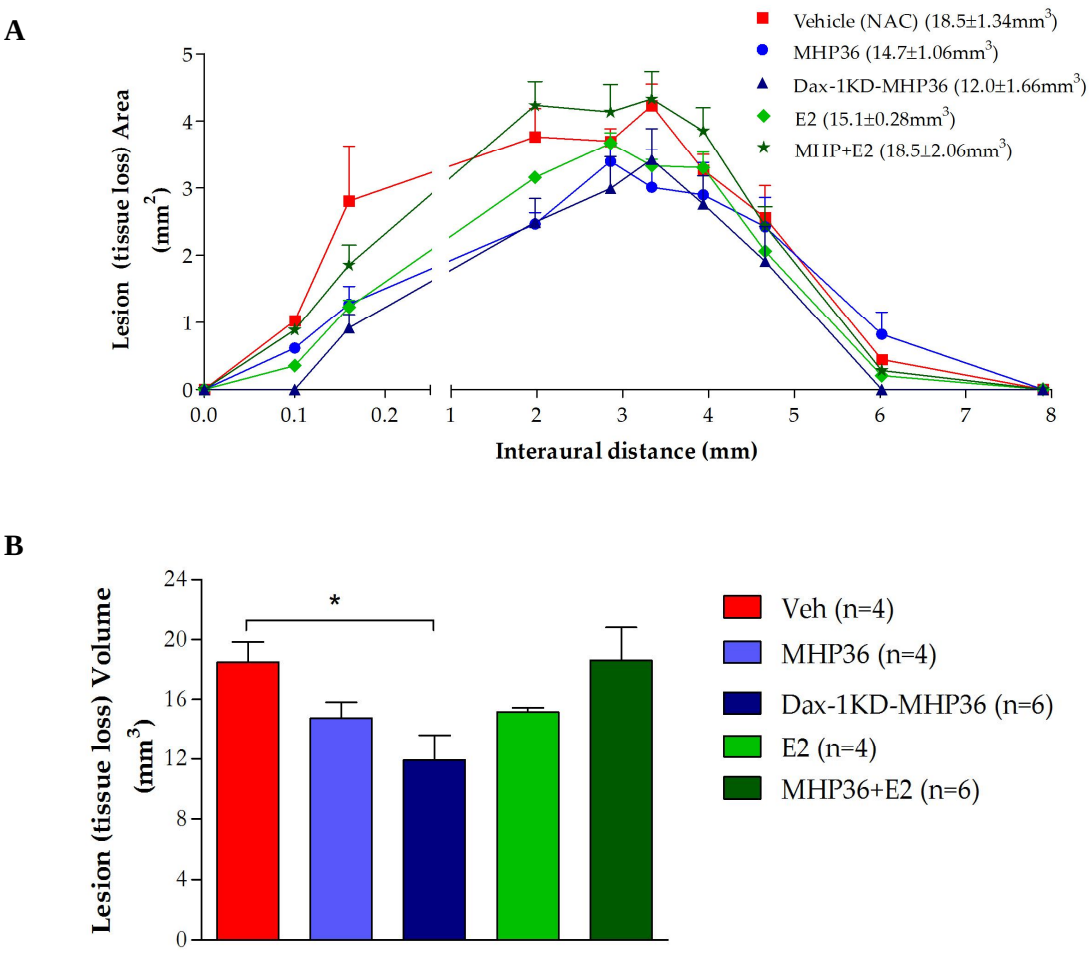

Figure 6.5: Measurement of lesion (tissue loss) post-MCAO in all experimental groups

(**A**) Topography of lesion (tissue loss) over eight coronal levels (with respect to interaural distance). (**B**) Bar graph representing infarct volumes measured in all experimental groups. A significant difference in infarct volume was observed between Dax-1KD-MHP36 and vehicle. Asterisks indicate *p<0.01 (vehicle versus Dax-1KD-MHP36 cells), one-way ANOVA, post hoc Bonferroni's test to correct for multiple comparisons.

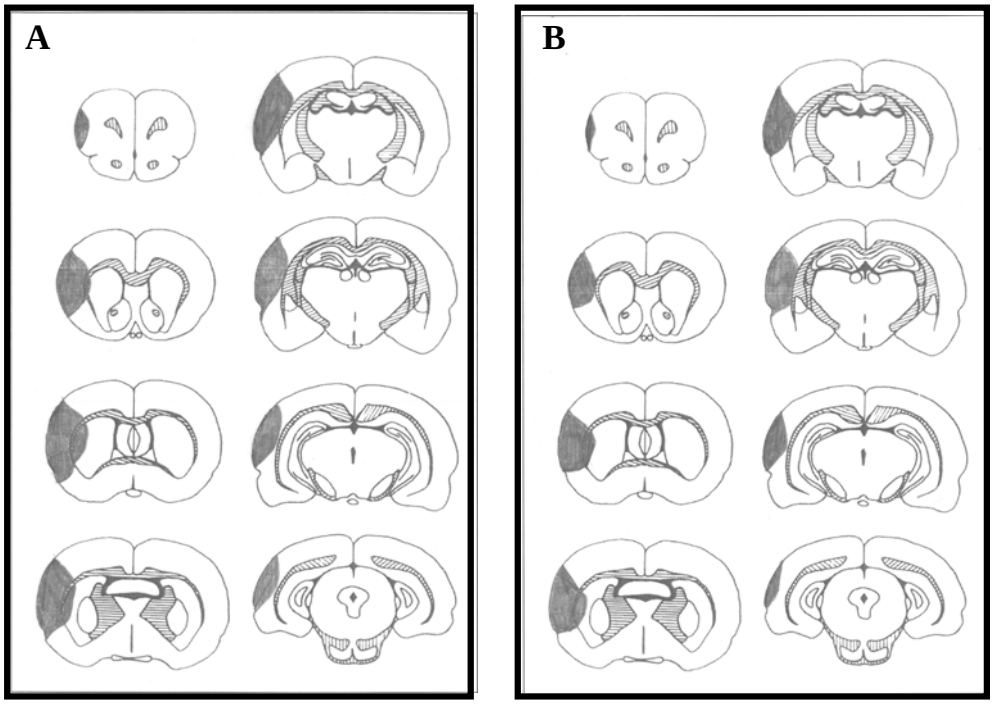

Figure 6.6: Distribution of lesion over 8 coronal levels after 28 days post-MCAO in mice receiving (A) vehicle and (B) Dax-1KD-MHP36 cells

Shaded areas represent areas of lesion in one representative animal from each group.

6.3.7 | Effects of Dax-1KD-MHP36 cells on differentiation

Staining of brain sections with neuronal marker MAP-2, revealed a significant increase in expression in the Dax-1KD-MHP36 group of animals when compared to the vehicle and MHP36 group of animals (**Figure 6.7A**) (Bregma: -0.38 ± 0.10mm). MAP-2 positive neurons were observed mainly in the cortex. No PKH26 labelled cells were observed positive for MAP-2 neurons in MHP36 or Dax-1KD-MHP36 group. There was no difference in intensity of IBA-1 positive activated microglial cells in MHP36 and Dax-1KD-MHP36 versus vehicle groups (**Figure 6.7C**). A graphical representation of the average mean intensity for MAP-2 positive and IBA-1 positive cells is shown in **Figure 6.7B & D** respectively. Highly populated GFAP-positive astrocytes were observed in the peri-lesion

versus vehicle groups (**Figure 6.7C**). A graphical representation of the average mean intensity for MAP-2 positive and IBA-1 positive cells is shown in **Figure 6.7B & D** respectively. Highly populated GFAP-positive astrocytes were observed in the peri-lesion which included the cortex and striatum (**Figure 6.8A**). The mean average intensity measurement showed a non-significant trend to decrease in the MHP36, MHP36+E2 and Dax-1KD-MHP36 group of animals when compared to vehicle (**Figure 6.8B**). Similarly, Oligodendrocytes were observed in the peri-lesion mainly the cortex (**Figure 6.8C**) and the mean intensity showed a trend to increase in the MHP36, MHP36+E2 and Dax-1KD-MHP36 group of animals versus vehicle (**Figure 6.8D**).

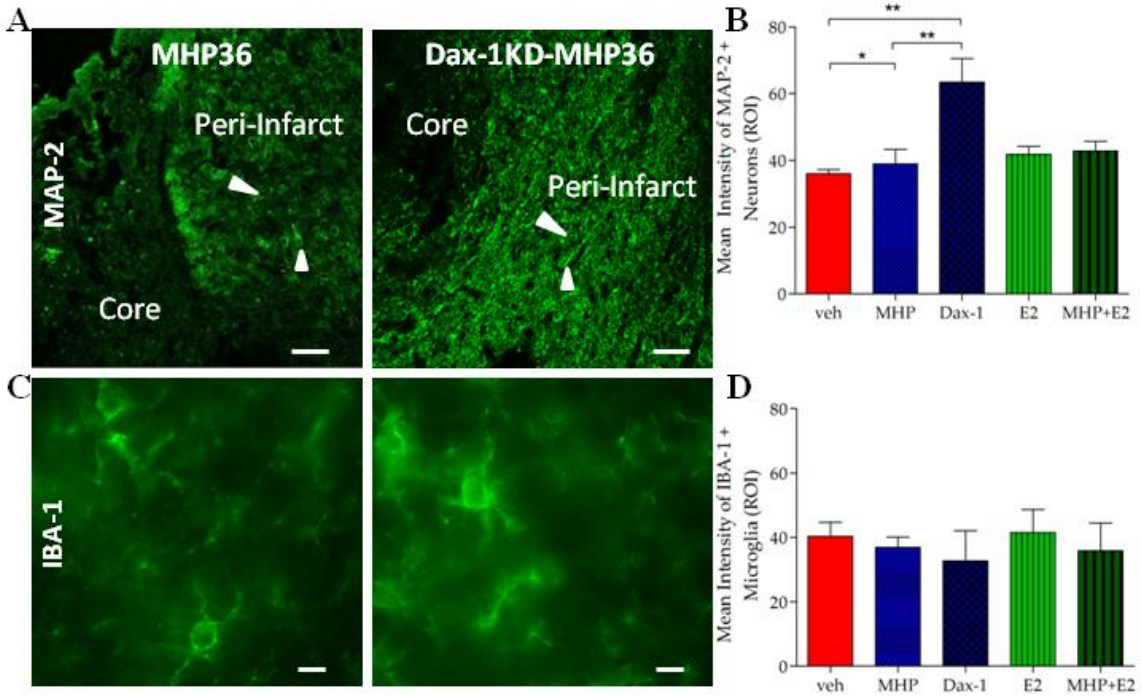

Figure 6.7: Effects of Dax-1KD-MHP36 cells on differentiation into neurons and microglia.

(**A**) Peri-lesion cortex in the mice recieving MHP36 and Dax-1KD-MHP36 cells demonstrating microtubule-associated protein-2 (MAP-2) expression; (scale bar = 100 µm) (white arrows indicate neurons stained with MAP-2). (**B**) Graphical representation of mean average intensity for MAP-2 expression in all experimental groups. (**C**) IBA-1 positive microglia observed in the peri-lesion cortex and striatum at 28days post-MCAO in mice receiving MHP36 and Dax-1KD-MHP36 cells (scale bar = 5 µm). (**D**) Graphical representation of mean average intensity for IBA-1 (microglia) expression in all experimental groups. Data represented as mean ± S.E.M., n=3, one-way ANOVA with a post hoc Bonferroni's test. Asterisks indicate * $p<0.05$, ** $p<0.001$ vehicle vs. treatment groups.

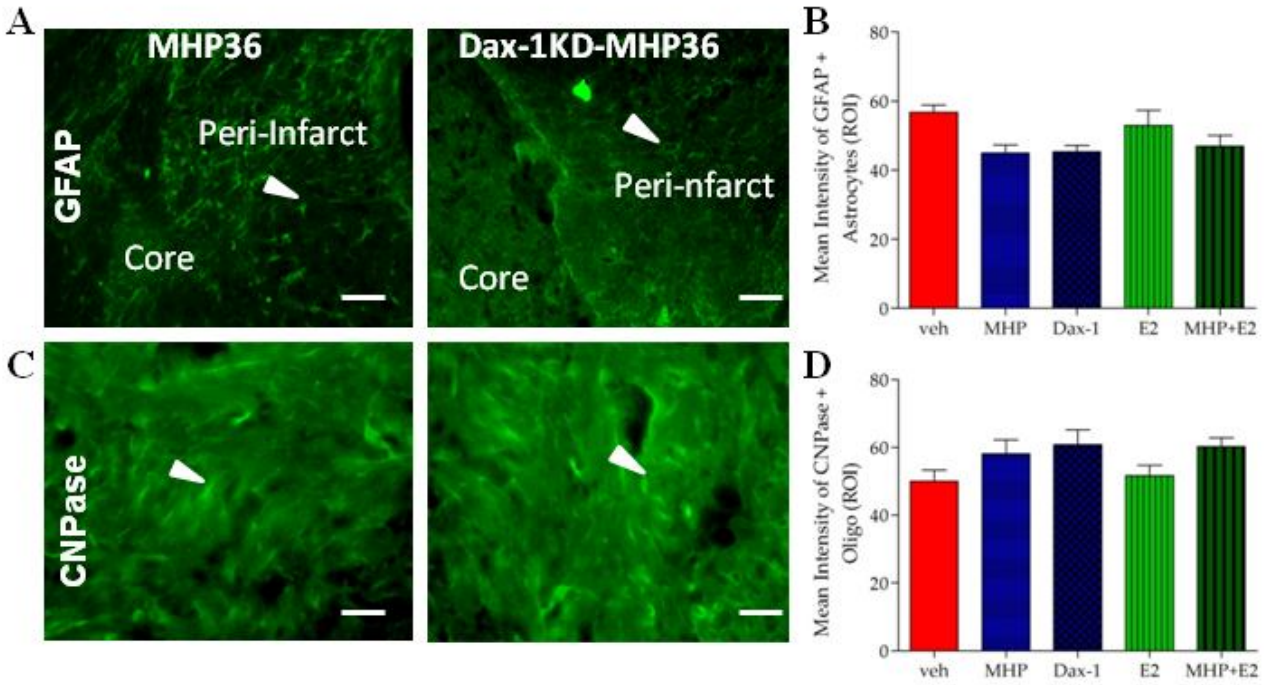

Figure 6.8: Effects of Dax-1KD-MHP36 cells on differentiation into astrocytes and oligodendrocytes.

(**A**) GFAP positive astrocytes observed in/close to the peri-lesion of mice receiving MHP36 and Dax-1KD-MHP36 at 28days post-MCAO (scale bar = 100 µm). (**B**) Graphical representation of mean average intensity for GFAP expression in all experimental groups. (**C**) CNPase positive oligodendrocytes observed in cortex at 28days post-MCAO in mice receiving MHP36 and Dax-1KD-MHP36 cells (scale bar = 100 µm). (**D**) Graphical representation of CNPase in all experimental groups. Data represented as mean ± SEM, n=3, one-way ANOVA with a post hoc Bonferroni's test.

6.3.8 | Effects of Dax-1KD-MHP36 cells on synaptic plasticity

At 28 days post-MCAO a dense Syn positive immunostaining within the grafts was revealed (**Figure. 6.9A**) in all treatment groups when compared to vehicle group (representative graph is shown in **Figure 6.9B**). PKH26/Syn co-localised cells were observed in the cortex within the peri-lesion region in all groups receiving cells MHP36, MHP36 + E2 and Dax-1KD-MHP36 groups (Bregma: -0.38± 0.10mm) (**Figure 6.9D**) (MHP36 and Dax-1KD-MHP36 data shown as images). There was a significant difference between the numbers of co-localised cells in mice receiving Dax-1KD-MHP36 cells when compared to controls. The other groups were not significantly different when compared to controls. A significant increase in Syn expression was observed in the ipsilateral cortex when compared to contralateral cortex and vehicle in all animals treatment groups (**Figure 6.9C**). A higher magnification demonstrating PKH26- labelled MHP36 and Dax-1KD-MHP36 co-localised with Syn positive staining in the cortex at 28 days post-MCAO (**Figure 6.10**).

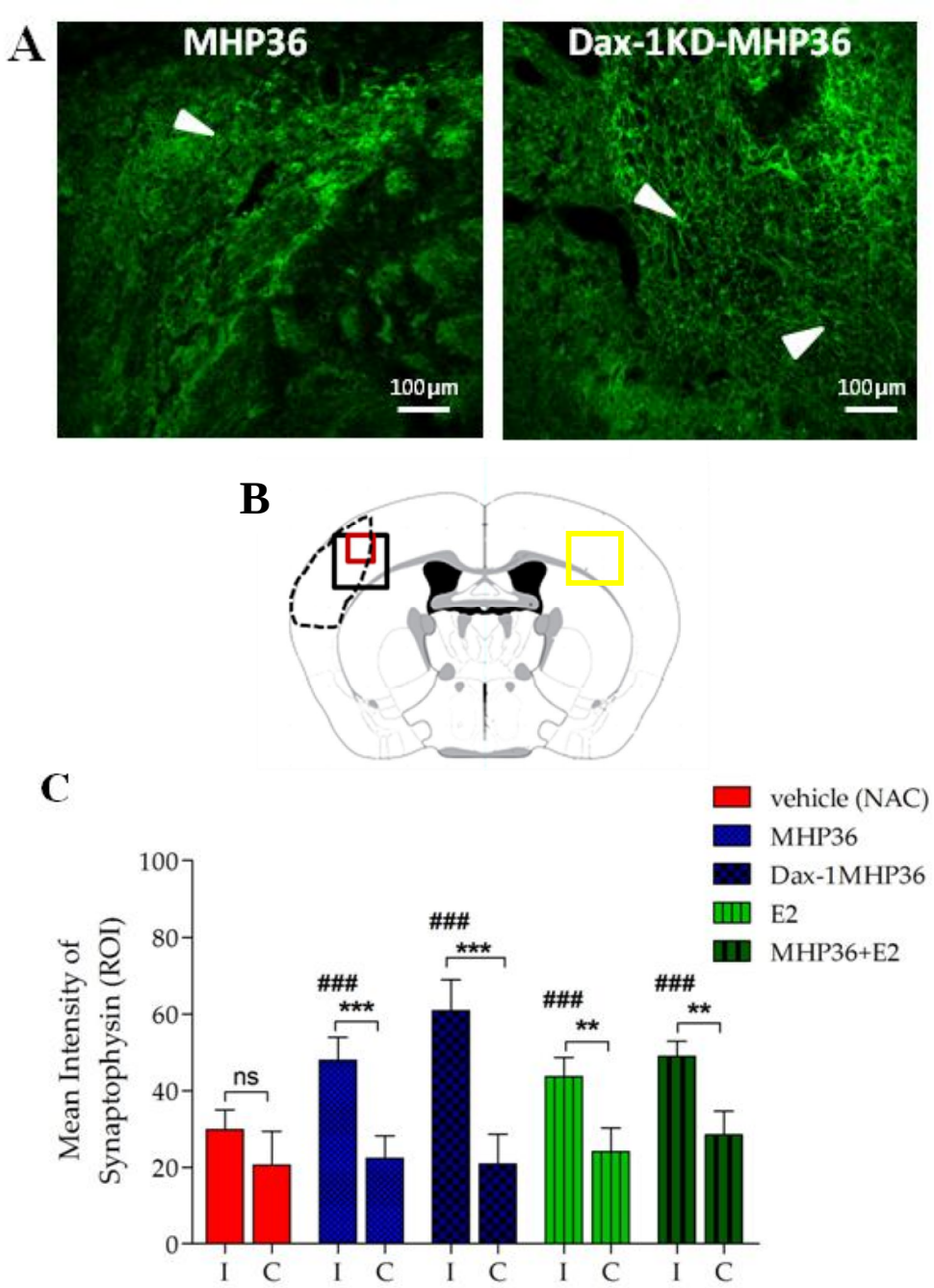

Figure 6.9: Effects of Dax-1KD-MHP36 cells on synaptic plasticity

(**A**) Peri-lesion cortex in the mice receiving MHP36 and Dax-1KD-MHP36 cells stained for synaptophysin (arrows indicate positive Syn staining; scale bar = 100µm). (**B**) Representative coronal section from the mouse atlas used for imaging (Bregma: -0.38). (**C**) Graphical representation of intensity of Syn observed in all experimental groups (Bregma: -0.38 ± 0.10mm). Data represented as mean ± SEM, n=3, two-way ANOVA with a post hoc Bonferroni's test. Asterisks indicate *** $p<0.001$ contralateral (yellow box) vs. ipsilateral hemisphere (black box); ### $p<0.001$ versus vehicle in ipsilateral hemisphere. (I= ipsilateral; C= contralateral).

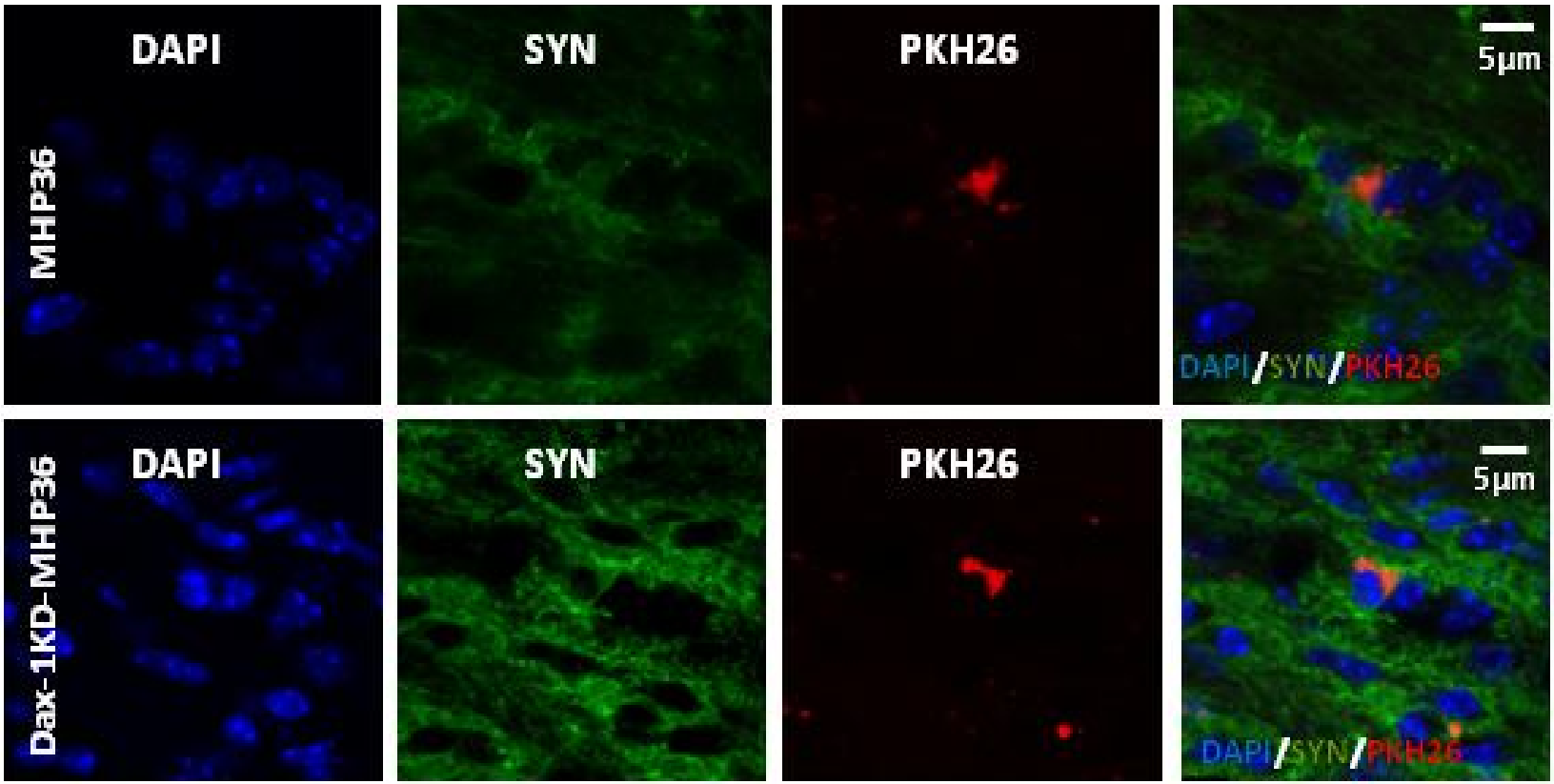

Figure 6.10: Co-localisation of pre-labelled stem cells and synaptophysin at 28 days post-MCAO.

A higher magnification of the previous section demonstrating PKH26- labelled MHP36 and Dax-1KD-MHP36 co-localised with Syn positive staining in the cortex at 28 days post-MCAO (scale bar = 5 µm).

6.4 | Discussion

Over the last three decades, intense pre-clinical and clinical studies of the role of E2 on neuroprotection and cognition have been undertaken to elucidate the significance of oestrogen in the brain. Oestrogen can act as a neuroprotective agent (Behl, 2002, Dubal and Wise, 2001, Hurn and Macrae, 2000), promotes synaptic plasticity, neurogenesis (Suzuki et al., 2007) and growth of nerve processes (Bi et al., 2001, McEwen, 2002), attenuates programmed cell death (Rau et al., 2003) and modulates various synaptic markers that are associated with cognition (Gibbs and Gabor, 2003, Kim and Casadesus, 2010). However detrimental and adverse effects of oestrogen in ischaemic brain have become apparent both in the pre-clinic as well as clinic (as described in **section 1.3.5**). We therefore seek new strategies to harness the beneficial effects of oestrogen.

This is the first study to show that stem cells over-expressing oestrogen have improved plasticity. It is based on three findings showing that MHP36, a conditionally immortalised neural stem cell line genetically modified to over-express oestrogen (Dax-1KD-MHP36) 1) completely restore lost sensorimotor function after transient MCAO to pre-MCAO baseline values in mice as demonstrated in both the cylinder and ladder rung tests, 2) accelerated the functional recovery to 14 days post-MCAO and 3) reduced tissue loss, increased cellular differentiation and increased synaptic plasticity. Other key findings of the present study indicate that oestrogen needs to be expressed by the stem cells since oestrogen administered alone into the brain parenchyma or administered with MHP36 cell did not restore brain function to pre-MCAO baseline values, accelerate function, increase differentiation or reduce lesion size. In addition we found that, to our surprise, MHP36 cell co-administered with or without E2 induced over usage of the impaired (right) limb.

Motor impairments of limb functioning and placing deficits were evaluated in the present study by foot fault test using the ladder rung test which has commonly been used as an efficient and sensitive test strategy for chronic assessment of skilled fore- and hind-limb stepping in mice (Farr et al., 2006). Furthermore, since unilateral brain damage in human and rodents results in deficits of symmetry another test that detects asymmetries, namely the cylinder test was used. The advantage of the cylinder test is that it can detect even mild neurological impairments (Hua et al., 2002) and factors out confounding variables such as overall decrease in activity after surgical induction of stroke as additional trials can be performed. In both tests, a marked functional deficit was observed in all experimental groups measured at 2 days post-MCAO displayed by an increase in step errors in the ladder and a marked preference for use of the non-impaired (ipsilateral) paw in the cylinder test.

In the present study functional recovery by MHP36 cells was not complete by 28 days post-MCAO given that in the ladder test there was still a significant difference from pre-MCAO scores. Importantly, treatment with MHP36 not only reduced asymmetry [by >70%] in the cylinder test, but surprisingly also induced a marked preference for use of the impaired paw. The reasons for over usage of the impaired limb are unclear but, as discussed in Chapter 5, could be speculated as 1) unlikely to be compensatory effects or it would be evident in MCAO/vehicle group and 2) an increased activity of neurons in the ipsilateral cortex which is addressed below. Of interest is that similar results on functional outcome were shown when E2 was co-administered with MHP36 cell. On the other hand a complete restoration of foot faults to baseline scores, by 28 days post MCAO in mice receiving the genetically modified MHP36 cell for oestrogen (Dax-1KD-MHP36 cell) was achieved. In addition, this restoration was further accelerated as observed at 14 days post-MCAO in Dax-1KD-MHP36 cell group. These findings possibly indicate an effect of local E2 released by the stem cells after migrating to the injury site.

Neuronal connections are continuously remodelled and suffer intense adaptive functional and structural reorganization after lesions (Carmichael, 2003, Giraldi-Guimaraes et al., 2009, Rossi et al., 2007). This restorative reorganization is one of the most important mechanisms underlying functional recovery as described below. The restoration of functional recovery observed in the present study might be explained in part by a positive effect of the Dax-1KD-MHP36 cells on the structural plasticity. To analyse this hypothesis, we studied the expression of synaptophysin protein, related to structural plasticity, in the periphery of the lesion and in the contralateral (homologous) cortex. The results showed that MHP36 cells with or without administration of E2 had an increased expression of synaptophysin in the ipsilateral cortex when compared to vehicle group. However the increased synaptogenesis was augmented when the stem cells were genetically modified to increase oestrogen production and this likely at least in part explains the restoration of functional outcome in this treatment group. Whether such structural changes are in place by 14 days to explain the accelerated recovery would require future elucidation using time course studies. Beneficial effects of oestrogen have been shown in other studies in promoting brain plasticity where ovariectomy reduced synaptic remodelling via the reduction in spine density in the CA1 region and that this effect could be rescued by E2 replacement in rodents (Gould et al., 1990, Woolley et al., 1990) and in primates (Leranth et al., 2002, Woolley et al., 1990). Likewise, various synaptic markers are up-regulated after systemic E2 application (Flynn et al., 2008), namely, synaptophysin and synaptophilin. In terms of mechanisms involved in increased synaptogenesis there at least two possibilities: 1) that grafted MHP36 cells migrate to the area of damage and reconstitute local circuits that are sufficient to promote synaptogenesis and sustain some functions and 2) that grafts augment spontaneous reorganization within the host environment sufficient to undertake, or compensate for, some lost function. Evidence from imaging studies suggests that both possibilities are reasonable (Cramer et al., 1997).

Whether transplanted cells reduce death of host cells is an important observation as enhanced recovery of function could result from neuroprotection (Shen et al., 2010). There are reports that suggest infarct volumes can take upto 72 hrs (Garcia et al., 1993) or even 5 days (Swanson et al., 1990) to mature. In the present study, the significant reduction of lesion by the Dax-1KD-MHP36 cells can be accounted for reduction in secondary damage growth. Secondary neuronal cell death occurs in the lesion and adjacent tissue (the peri-lesion) and is considered largely apoptotic (Sribnick et al., 2003). Taken together with the lack of effect of E2 administered alone this suggests an effect of local E2 released by the stem cells after migrating to the injury site. Lesion volume was not reduced in animal groups receiving E2 alone or MHP36 administered with or without E2. Several studies have shown E2 pre-treatment, for days to weeks before brain insult, is neuroprotective in several models of focal and global ischaemia irrespective of sex, age and method of hormone administration (for review see Strom et al., 2009). There are fewer reports on the ability of E2 to attenuate neuronal death when given after ischaemia (Lebesgue et al., 2010) and there are no reports to our knowledge on effects of E2 administered into the brain in the lesion side.

Other mechanisms of reconstituting local circuits by MHP36 as discussed in detail in Chapter 5 could include filling out of cavities however in the present study this is not the case, particularly since only a third of the cells migrate to the lesion side (Veizovic et al., 2001). In the present study, by 28 days post-MCAO there were fewer Dax-1KD-MHP36 cells present in the injection tract, with increased numbers of cells in the surrounding areas. Cells were observed in the peri-lesion cortex and caudate nucleus, regions that undergo neuronal damage after transient MCAO, suggesting that the grafts were migrating in response to damage.

Higher than physiological concentration of E2 (100nM) was used in this study for co-administration and no beneficial effect of E2 was observed as discussed in this Chapter in any of the outcomes measured. However, the dose used has been tested and there are studies reporting a neuroprotective effect *in vitro* after neurotoxicity. For example, Goodman and colleagues have used μM concentrations of E2 to protect hippocampal cell cultures against glutamate (Goodman et al., 1996). Furthermore, (lower) nM concentrations of E2, are also effective in protecting cortical neurones against glutamate (Singer et al., 1996). Although the lowest concentration of E2 required for neuroprotection varies between studies, neuroprotection against glutamate is always present, indicating that there is a threshold of E2 concentration that must be exceeded for neuroprotection against glutamate. In addition, Kajta and colleagues demonstrated that pre-treatment with E2 (100 nM) prevented the NMDA-induced apoptosis in rat primary cortical neurons (Kajta et al., 2001). Few studies have examined the effect of oestrogen on non-neuronal brain cells. Bruce-Keller and colleagues showed E2 at high concentrations protects microglia from lipopolysaccharide-induced superoxide production (Bruce-Keller et al., 2000). Furthermore, as reported in Chapter 3 using ELISA, concentration of E2 released into the media is in unison with study performed by Suzuki and colleagues that showed low physiological concentrations of E2 (25 pg/ml) given systemically to ovariectomized mice increases the number of proliferating cells in the sub-ventricular zone (SVZ) after stroke. In addition, E2 exclusively increases the number of newborn cells that are destined to become neurons and does not influence gliosis (Suzuki et al., 2007).

Another important mechanism underlying the observed functional recovery is improved neurogenesis. In the present study no significant effect of MHP36 on expression neurons (MAP-2), astrocytes (GFAP), oligodendrocytes (CNPase) and microglia (IBA-1) was observed when compared to vehicle at 28 days post-MCAO (reproduced as observed in

Chapter 5). However, Dax-1KD-MHP36 (over-expressing E2) cells revealed a significant increase in expression of MAP-2 when compared to vehicle or MHP36 cells. Given that E2 administered with or with MHP36 cells did not increase MAP-2 expression, it is likely that local E2 from migrated stem cells is promoting neurogenesis. Whether E2 is promoting exogenous stem cell differentiation or promoting proliferation and differentiation of endogenous new born stem cells is yet to be determined. Furthermore, recently Yamashita and colleagues (Yamashita et al., 2006) have demonstrated that a proportion of the SVZ-derived neuroblasts differentiate into mature neurons and starts to express NeuN at the sites of injury, where they begin to incorporate into the existing neuronal circuit by forming synapses with neighbouring cells (Yamashita et al., 2006). However, although the SVZ is a promising therapeutic target for neuronal replacement therapy, the numbers of newborn neurons migrating to the sites of injury are believed to be inadequate for the functional recovery of the ischemic brain (Arvidsson et al., 2002, Yamashita et al., 2006). Therefore, the identification of an endogenous factor such as E2 that can stimulate neurogenesis in the face of brain insults, as well as understanding the underlying mechanisms of its action may lead to the progress of neuronal restorative therapies against neurodegenerative diseases and injury.

In contrast, there was a trend for the expression of CNPase (oligodendrocytes) to increase and for GFAP (astrocytes) to decrease in the Dax-1KD-MHP36 cell group and MHP36 cell group administered with or without E2 and when compared to vehicle group at 28 days post-MCAO. The potential increase in CNPase expression suggests that endogenous or transplanted stem cells differentiate into new oligodendrocytes to promote local remyelinisation of the newly born or damaged neurons (co-localisation could not be demonstrated because it was hard to identify auto-fluorescence of the brain from the PKH26 labelled cells). Furthermore, a possible reduced expression of GFAP can be supported by a

recent finding by Järlestedt and colleagues that states attenuation of reactive gliosis, using GFAP and vimentin knock-out mice in the developing brain does not affect infarct volume after hypoxic-ischaemia, but increases the number of surviving newborn neurons (Jarlestedt et al., 2010). These effects by the glial cells on the host brain could be achieved by providing a matrix to support the survival and integration of the neuronal population of grafted cells or release trophic factors and or transmitter substances to supplement the activity of host cells (Hodges et al., 2000). In the present study, IBA-1 positive microglia were also observed after 28 days post-MCAO which was not affected in the Dax-1KD-MHP36 cell group. This suggests that the stem cell were no longer recognised as foreign by host microglia and macrophages. In addition, there was no co-localisation of microglia with either the MHP36 cell with or without E2 and Dax-1KD-MHP36 cell indicating that these cells were not being phagocytosed. Microglial inflammation has been shown to have a varying effect on neural stem cell grafts. The pro-inflammatory effects of microglia have been well documented (Vilhardt, 2005) with graft rejection strongly associated with macrophage and microglial infiltration (Duan et al., 1995). Microglia can also have a beneficial effect on NSC grafts, aiding in migration, axonal growth and differentiation, possibly by secretion of growth factors or through cell–cell contact (Vilhardt, 2005, Lambertsen et al., 2009). Whether microglia play either of these roles in the present study have yet to be studied.

In conclusion, the key findings from this study suggest that used MHP36 grafts due to their genetic modification to over-express oestrogen completely restored functional recovery to pre-MCAO baseline values as observed using the ladder and cylinder test. This may be directly or indirectly mediated by promoting neurogenesis and elevating the process of synaptic remodelling. It is important to note that E2 administered with or without stem cells did not fully replicate these results. It is also important to note that like any steroid hormone E2 readily diffuses in the parenchyma once transplanted and thus it is proposed that there is

not enough local E2 at the site of lesion and thus cannot exert the effects that are observed in the group of animals receiving the Dax-1KD-MHP36 cell. Thus stem cells carrying E2 and migrating using cues such as chemokines to areas of insult and releasing E2 locally seems to be a more promising approach to understand the mechanisms exerted by E2 in the brain after injury.

CHAPTER 7

GENERAL DISCUSSSION

Acute ischemic stroke caused by cerebral artery occlusion leading to infarction of brain tissue with acute loss of neurons, astroglia and oligodendroglia, is the most important vascular central nervous system (CNS) disorder and remains a leading cause of death and disability (Feigin et al., 2003). Despite significant clinical benefits after systemic thrombolysis, only a minority of patients have timely access to this therapy. Therefore, it is crucial to develop new alternative therapeutic strategies with less time constraints. Animal models of cerebral ischaemia are crucial for understanding the mechanism of neuronal survival and death following cerebral ischaemia. This understanding further helps in development of therapeutic interventions for patients suffering from stroke. Many different species, especially rodents have been used to obtain further knowledge in this area of research. The most encouraging approach to treat stroke is directed towards cell replacement in the ischemic regions. Furthermore, the ability of the brain to regenerate neural elements to restore function was thought to be nonexistent. It is now known that not only does regenerative capacity exist, but transplanted cells can integrate into the host brain, survive, and reverse neurological deficits (Wechsler and Kondziolka, 2003).

Transplanted cells may preserve existing host cells and connections through secretion of trophic factors, replace cellular elements; or establish local connections that improve synaptic activity (Wechsler and Kondziolka, 2003). The challenge of cell replacement for treatment of stroke is in some ways similar to that for Parkinson's disease but in other ways is very different. Like Parkinson's disease, the injury is focal but the neuronal loss mostly involves many more cell

types. Neural pathways are more complex, and the likelihood of implanted cells forming exact and appropriate connections to restore function seems remote, unless directed by the host brain. Furthermore, results obtained from cell transplantation in animal models of stroke are difficult to extrapolate to humans, particularly because of the lack of adequate primate stroke models. The typical therapies available for stroke seek (1) to interrupt the cascade of events that lead to cell death and (2) to harness the substantial intracerebral reorganization after stroke to functional recovery by rehabilitation therapies (Dirnagl et al., 1999).

This study has used MHP36 grafts due to its ability to (1) to develop into neurons, glia, or oligodendrocytes in response to host signals and (2) to improve outcomes shown in several models of impairment (Gray et al., 2000, Gray et al., 1999, Hodges et al., 2000a, Hodges et al., 2000b, Sinden et al., 1997) but further research is needed to understand the mechanism involved to explain, if not completely, the observed improved outcome. Demonstrated in Chapter 5, MHP36 graft ipsilateral to the lesion exerted a positive functional effect as observed using the ladder and cylinder test when compared to vehicle group. This improvement in behaviour could partly be mediated by promoting synaptogenesis rather than via neurogenesis or neuroprotection. Enhanced or accelerated improvement of behaviour on these tests may serve as a useful marker of functional reorganization in the damaged brain. Thus, the same experimental plan was used to test the hypothesis, whether NSCs over-expressing oestrogen enhanced or accelerated improvement observed using naïve MHP36 cells.

McEwen and colleagues have reviewed, that oestrogen influences synaptogenesis and contributes to synaptic plasticity (McEwen, 2001). Oestrogen could also modulate processes ranging from adhesion and migration to survival and proliferation, cardiovascular and neuroprotection, angiogenesis and cancer. In addition, neurological processes such as stress

responses, feeding patterns, sleep cycles and temperature regulation have been shown to be modulated by oestrogen. Against this background, as described in Chapter 3, these MHP36 cell were characterised for oestrogen first before they could be genetically modified to over-express oestrogen. Using the genetically modified MHP36 cell (Dax-1KD-MHP36) in Chapter 6 it has demonstrated the beneficial effects of locally produced oestrogen by the cell, on behaviour, when compared to oestrogen that was co-administered with MHP36 cell or alone. Furthermore, the behavioural improvement observed in the MHP36 cell (Chapter 5) was enhanced and accelerated in the animals receiving the Dax-1KD-MHP36 cell. This enhanced and accelerated improvement in behaviour could partly be mediated by promoting neurogenesis and brain plasticity. This is only one of many proposed actions of oestrogen in the stroke-injured brain.

The MHP36 cells cannot indeed be used in the clinic due to their genetic modification and murine source. Nevertheless, this fact alone should not detract from their potential use in *in vivo* for a more mechanistic outcome. Their ability to be maintained easily *in vitro* and obtain a large cell number for transplantation is of great benefit. In addition given the migratory potential of many stem cells toward areas of injury as described in Chapter 1, they may serve as appropriate vehicles for delivery of specific molecules that may be difficult to deliver at adequate concentration into the ischemic area via systemic administration (Muller et al., 2006). Candidates for such *ex vivo* gene therapy may include anti-inflammatory, pro-angiogenic and pro-survival molecules. This study tests the effects of oestrogen using the same principle. Molecules that promote endogenous neurogenesis may also prove to be useful. In fact, given the low percentage of adult-born neurons that survive, delivery of pro-angiogenic and pro-survival drugs might indirectly promote the survival of migrating neuroblasts that discover themselves at the infarct site. Many of the trophic effects displayed by stem cells are poorly understood;

therefore the delivery of such stem cells in conjunction with specific gene delivery may provide additional benefit (Burns et al., 2009, Horita et al., 2006, Lee et al., 2007).

For the purpose of this study it is evident that further work is needed to clarify the involvement of oestrogen and its beneficial role in integration of the neural stem cells. Future studies directed towards 1) the use of aromatase inhibitors or 2) specific oestrogen receptor antagonists to abolish the effects of Dax-1KD-MHP36 to promote synaptic plasticity, differentiation and functional outcome will elucidate the beneficial role of E2. 3) Use of growth factor inhibitors for example; VEGF or IGF inhibitors can elucidate if Dax-1KD-MHP36 did indeed increase growth factor secretion. 4) investigating earlier (24, 72 hrs and 1 week post-transplantation) time points will elucidate acute role of oestrogen *in vivo* and 5) to investigate the mechanism of acceleration observed at 14 days post-MCAO will be of exceptional value to refine our knowledge of the significance of oestrogen in the brain and to maximize the potential of this protein as a therapeutic agent.

Finally, the clinical use of neural stem cells will mainly depend on the behavioural improvements that can be achieved and the present findings provoke an investigation of novel graft mechanisms, which will increase our knowledge of how grafts may be used to harness and augment brain plasticity in response to stroke damage. Therefore this approach of genetic modification will allow future exploitation in transgenic mice for genetic dissection of mechanisms of stem cell based therapy as well as gene therapy.

CHAPTER 8

REFERENCES

AASEN, T., RAYA, A., BARRERO, M. J., GARRETA, E., CONSIGLIO, A., GONZALEZ, F., VASSENA, R., BILIC, J., PEKARIK, V., TISCORNIA, G., EDEL, M., BOUE, S. & IZPISUA BELMONTE, J. C. (2008) Efficient and rapid generation of induced pluripotent stem cells from human keratinocytes. *Nat Biotechnol,* 26**,** 1276-84.

ADAMS, H. P., JR., BENDIXEN, B. H., KAPPELLE, L. J., BILLER, J., LOVE, B. B., GORDON, D. L. & MARSH, E. E., 3RD (1993) Classification of subtype of acute ischemic stroke. Definitions for use in a multicenter clinical trial. TOAST. Trial of Org 10172 in Acute Stroke Treatment. *Stroke,* 24**,** 35-41.

ADAMS, H. P., JR., DEL ZOPPO, G., ALBERTS, M. J., BHATT, D. L., BRASS, L., FURLAN, A., GRUBB, R. L., HIGASHIDA, R. T., JAUCH, E. C., KIDWELL, C., LYDEN, P. D., MORGENSTERN, L. B., QURESHI, A. I., ROSENWASSER, R. H., SCOTT, P. A. & WIJDICKS, E. F. (2007) Guidelines for the early management of adults with ischemic stroke: a guideline from the American Heart Association/American Stroke Association Stroke Council, Clinical Cardiology Council, Cardiovascular Radiology and Intervention Council, and the Atherosclerotic Peripheral Vascular Disease and Quality of Care Outcomes in Research Interdisciplinary Working Groups: the American Academy of Neurology affirms the value of this guideline as an educational tool for neurologists. *Stroke,* 38**,** 1655-711.

ALBERTS, M. J. (1993) Tissue plasminogen activator in acute stroke. *AJNR Am J Neuroradiol,* 14**,** 1448-9.

ALI, S. H. & DECAPRIO, J. A. (2001) Cellular transformation by SV40 large T antigen: interaction with host proteins. *Semin Cancer Biol,* 11**,** 15-23.

ALKAYED, N. J., GOTO, S., SUGO, N., JOH, H. D., KLAUS, J., CRAIN, B. J., BERNARD, O., TRAYSTMAN, R. J. & HURN, P. D. (2001) Estrogen and Bcl-2: gene induction and effect of transgene in experimental stroke. *J Neurosci,* 21**,** 7543-50.

ANDERSON, D. J. (2001) Stem cells and pattern formation in the nervous system: the possible versus the actual. *Neuron,* 30**,** 19-35.

ANDERSON, G. L., LIMACHER, M., ASSAF, A. R., BASSFORD, T., BERESFORD, S. A., BLACK, H., BONDS, D., BRUNNER, R., BRZYSKI, R., CAAN, B., CHLEBOWSKI, R., CURB, D., GASS, M., HAYS, J., HEISS, G., HENDRIX, S., HOWARD, B. V., HSIA, J., HUBBELL, A., JACKSON, R., JOHNSON, K. C., JUDD, H., KOTCHEN, J. M., KULLER, L., LACROIX, A. Z., LANE, D., LANGER, R. D., LASSER, N., LEWIS, C. E., MANSON, J., MARGOLIS, K., OCKENE, J., O'SULLIVAN, M. J., PHILLIPS, L., PRENTICE, R. L., RITENBAUGH, C., ROBBINS, J., ROSSOUW, J. E., SARTO, G., STEFANICK, M. L., VAN HORN, L., WACTAWSKI-WENDE, J., WALLACE, R. &

WASSERTHEIL-SMOLLER, S. (2004) Effects of conjugated equine estrogen in postmenopausal women with hysterectomy: the Women's Health Initiative randomized controlled trial. *JAMA,* 291**,** 1701-12.

ANJOS-AFONSO, F. & BONNET, D. (2007) Nonhematopoietic/endothelial SSEA-1+ cells define the most primitive progenitors in the adult murine bone marrow mesenchymal compartment. *Blood,* 109**,** 1298-306.

AREVALO, M. A., SANTOS-GALINDO, M., BELLINI, M. J., AZCOITIA, I. & GARCIA-SEGURA, L. M. (2010) Actions of estrogens on glial cells: Implications for neuroprotection. *Biochim Biophys Acta,* 1800**,** 1106-12.

ARIEN-ZAKAY, H., LECHT, S., BERCU, M. M., TABAKMAN, R., KOHEN, R., GALSKI, H., NAGLER, A. & LAZAROVICI, P. (2009) Neuroprotection by cord blood neural progenitors involves antioxidants, neurotrophic and angiogenic factors. *Exp Neurol,* 216**,** 83-94.

ARONICA, S. M., KRAUS, W. L. & KATZENELLENBOGEN, B. S. (1994) Estrogen action via the cAMP signaling pathway: stimulation of adenylate cyclase and cAMP-regulated gene transcription. *Proc Natl Acad Sci U S A,* 91**,** 8517-21.

ARVANITIS, D. N., WANG, H., BAGSHAW, R. D., CALLAHAN, J. W. & BOGGS, J. M. (2004) Membrane-associated estrogen receptor and caveolin-1 are present in central nervous system myelin and oligodendrocyte plasma membranes. *J Neurosci Res,* 75**,** 603-13.

ARVIDSSON, A., COLLIN, T., KIRIK, D., KOKAIA, Z. & LINDVALL, O. (2002) Neuronal replacement from endogenous precursors in the adult brain after stroke. *Nat Med,* 8**,** 963-70.

BAI, G. & KUSIAK, J. W. (1997) Nerve growth factor up-regulates the N-methyl-D-aspartate receptor subunit 1 promoter in PC12 cells. *J Biol Chem,* 272**,** 5936-42.

BAKER, A. E., BRAUTIGAM, V. M. & WATTERS, J. J. (2004) Estrogen modulates microglial inflammatory mediator production via interactions with estrogen receptor beta. *Endocrinology,* 145**,** 5021-32.

BAKONDI, B., SHIMADA, I. S., PERRY, A., MUNOZ, J. R., YLOSTALO, J., HOWARD, A. B., GREGORY, C. A. & SPEES, J. L. (2009) CD133 identifies a human bone marrow stem/progenitor cell sub-population with a repertoire of secreted factors that protect against stroke. *Mol Ther,* 17**,** 1938-47.

BAMFORD, J., SANDERCOCK, P., DENNIS, M., BURN, J. & WARLOW, C. (1990) A prospective study of acute cerebrovascular disease in the community: the Oxfordshire Community Stroke Project--1981-86. 2. Incidence, case fatality rates and overall outcome at one year of cerebral infarction, primary intracerebral and subarachnoid haemorrhage. *J Neurol Neurosurg Psychiatry,* 53**,** 16-22.

BAMFORD, J., SANDERCOCK, P., DENNIS, M., BURN, J. & WARLOW, C. (1991) Classification and natural history of clinically identifiable subtypes of cerebral infarction. *Lancet,* 337**,** 1521-6.

BARBER, P. A., HOYTE, L., COLBOURNE, F. & BUCHAN, A. M. (2004) Temperature-regulated model of focal ischemia in the mouse: a study with histopathological and behavioral outcomes. *Stroke,* 35**,** 1720-5.

BARDONI, B., ZANARIA, E., GUIOLI, S., FLORIDIA, G., WORLEY, K. C., TONINI, G., FERRANTE, E., CHIUMELLO, G., MCCABE, E. R., FRACCARO, M. & ET AL. (1994) A dosage sensitive locus at chromosome Xp21 is involved in male to female sex reversal. *Nat Genet,* 7**,** 497-501.

BARDUTZKY, J., SHEN, Q., HENNINGER, N., BOULEY, J., DUONG, T. Q. & FISHER, M. (2005) Differences in ischemic lesion evolution in different rat strains using diffusion and perfusion imaging. *Stroke,* 36**,** 2000-5.

BARHA, C. K., DALTON, G. L. & GALEA, L. A. (2010) Low doses of 17alpha-estradiol and 17beta-estradiol facilitate, whereas higher doses of estrone and 17alpha- and 17beta-estradiol impair, contextual fear conditioning in adult female rats. *Neuropsychopharmacology,* 35**,** 547-59.

BARREIRO, O., MARTIN, P., GONZALEZ-AMARO, R. & SANCHEZ-MADRID, F. (2010) Molecular cues guiding inflammatory responses. *Cardiovasc Res,* 86**,** 174-82.

BASKIN, Y. K., DIETRICH, W. D. & GREEN, E. J. (2003) Two effective behavioral tasks for evaluating sensorimotor dysfunction following traumatic brain injury in mice. *J Neurosci Methods,* 129**,** 87-93.

BAULIEU, E. E. (1997) Neurosteroids: of the nervous system, by the nervous system, for the nervous system. *Recent Prog Horm Res,* 52**,** 1-32.

BEDERSON, J. B., PITTS, L. H., GERMANO, S. M., NISHIMURA, M. C., DAVIS, R. L. & BARTKOWSKI, H. M. (1986) Evaluation of 2,3,5-triphenyltetrazolium chloride as a stain for detection and quantification of experimental cerebral infarction in rats. *Stroke,* 17**,** 1304-8.

BEHL, C. (2002) Oestrogen as a neuroprotective hormone. *Nat Rev Neurosci,* 3**,** 433-42.

BEHL, C., SKUTELLA, T., LEZOUALC'H, F., POST, A., WIDMANN, M., NEWTON, C. J. & HOLSBOER, F. (1997) Neuroprotection against oxidative stress by estrogens: structure-activity relationship. *Mol Pharmacol,* 51**,** 535-41.

BELAYEV, L., ALONSO, O. F., BUSTO, R., ZHAO, W. & GINSBERG, M. D. (1996a) Middle cerebral artery occlusion in the rat by intraluminal suture. Neurological and pathological evaluation of an improved model. *Stroke,* 27**,** 1616-22; discussion 1623.

BELAYEV, L., BUSTO, R., ZHAO, W., FERNANDEZ, G. & GINSBERG, M. D. (1999) Middle cerebral artery occlusion in the mouse by intraluminal suture coated with poly-L-lysine: neurological and histological validation. *Brain Res,* 833**,** 181-90.

BELAYEV, L., BUSTO, R., ZHAO, W. & GINSBERG, M. D. (1996b) Quantitative evaluation of blood-brain barrier permeability following middle cerebral artery occlusion in rats. *Brain Res,* 739**,** 88-96.

BELCREDITO, S., VEGETO, E., BRUSADELLI, A., GHISLETTI, S., MUSSI, P., CIANA, P. & MAGGI, A. (2001) Estrogen neuroprotection: the involvement of the Bcl-2 binding protein BNIP2. *Brain Res Brain Res Rev,* 37**,** 335-42.

BENNINGER, F., BECK, H., WERNIG, M., TUCKER, K. L., BRUSTLE, O. & SCHEFFLER, B. (2003) Functional integration of embryonic stem cell-derived neurons in hippocampal slice cultures. *J Neurosci,* 23**,** 7075-83.

BI, R., BROUTMAN, G., FOY, M. R., THOMPSON, R. F. & BAUDRY, M. (2000) The tyrosine kinase and mitogen-activated protein kinase pathways mediate multiple effects of estrogen in hippocampus. *Proc Natl Acad Sci U S A,* 97**,** 3602-7.

BI, R., FOY, M. R., VOUIMBA, R. M., THOMPSON, R. F. & BAUDRY, M. (2001) Cyclic changes in estradiol regulate synaptic plasticity through the MAP kinase pathway. *Proc Natl Acad Sci U S A,* 98**,** 13391-5.

BILLECI, A. M., PACIARONI, M., CASO, V. & AGNELLI, G. (2008) Hormone replacement therapy and stroke. *Curr Vasc Pharmacol,* 6**,** 112-23.

BINGHAM, D., MACRAE, I. M. & CARSWELL, H. V. (2005) Detrimental effects of 17beta-oestradiol after permanent middle cerebral artery occlusion. *J Cereb Blood Flow Metab,* 25**,** 414-20.

BINKO, J. & MAJEWSKI, H. (1998) 17 beta-Estradiol reduces vasoconstriction in endothelium-denuded rat aortas through inducible NOS. *Am J Physiol,* 274**,** H853-9.

BJORKLUND, L. M., SANCHEZ-PERNAUTE, R., CHUNG, S., ANDERSSON, T., CHEN, I. Y., MCNAUGHT, K. S., BROWNELL, A. L., JENKINS, B. G., WAHLESTEDT, C., KIM, K. S. & ISACSON, O. (2002) Embryonic stem cells develop into functional dopaminergic neurons after transplantation in a Parkinson rat model. *Proc Natl Acad Sci U S A,* 99**,** 2344-9.

BOGOUSSLAVSKY, J. & REGLI, F. (1986) Borderzone infarctions distal to internal carotid artery occlusion: prognostic implications. *Ann Neurol,* 20**,** 346-50.

BOLAND, M. J., HAZEN, J. L., NAZOR, K. L., RODRIGUEZ, A. R., GIFFORD, W., MARTIN, G., KUPRIYANOV, S. & BALDWIN, K. K. (2009) Adult mice generated from induced pluripotent stem cells. *Nature,* 461**,** 91-4.

BONITA, R. (1992) Epidemiology of stroke. *Lancet,* 339**,** 342-4.

BORLONGAN, C. V., TAJIMA, Y., TROJANOWSKI, J. Q., LEE, V. M. & SANBERG, P. R. (1998) Transplantation of cryopreserved human embryonal carcinoma-derived neurons (NT2N cells) promotes functional recovery in ischemic rats. *Exp Neurol,* 149**,** 310-21.

BOULEY, J., FISHER, M. & HENNINGER, N. (2007) Comparison between coated vs. uncoated suture middle cerebral artery occlusion in the rat as assessed by perfusion/diffusion weighted imaging. *Neurosci Lett,* 412**,** 185-90.

BOWMAN, R. E., FERGUSON, D. & LUINE, V. N. (2002) Effects of chronic restraint stress and estradiol on open field activity, spatial memory, and monoaminergic neurotransmitters in ovariectomized rats. *Neuroscience,* 113**,** 401-10.

BRADBURY, E. J., KERSHAW, T. R., MARCHBANKS, R. M. & SINDEN, J. D. (1995) Astrocyte transplants alleviate lesion induced memory deficits independently of cholinergic recovery. *Neuroscience,* 65**,** 955-72.

BRADFORD, M. M. (1976) A rapid and sensitive method for the quantitation of microgram quantities of protein utilizing the principle of protein-dye binding. *Anal Biochem,* 72**,** 248-54.

BRAMBILLA, G. & MARTELLI, A. (2004) Failure of the standard battery of short-term tests in detecting some rodent and human genotoxic carcinogens. *Toxicology,* 196**,** 1-19.

BRANN, D. W., ZAMORANO, P. L., CHORICH, L. P. & MAHESH, V. B. (1993) Steroid hormone effects on NMDA receptor binding and NMDA receptor mRNA levels in the hypothalamus and cerebral cortex of the adult rat. *Neuroendocrinology,* 58**,** 666-72.

BRANNVALL, K. (2004) Hormonal regulation ofneural stem cell proliferation and fate determination. *Uppsala University, Medicinska vetenskapsområdet, Faculty of Medicine, Department of Neuroscience, Neurobiology***,** 63.

BRANNVALL, K., BOGDANOVIC, N., KORHONEN, L. & LINDHOLM, D. (2005) 19-Nortestosterone influences neural stem cell proliferation and neurogenesis in the rat brain. *Eur J Neurosci,* 21**,** 871-8.

BRANNVALL, K., KORHONEN, L. & LINDHOLM, D. (2002) Estrogen-receptor-dependent regulation of neural stem cell proliferation and differentiation. *Mol Cell Neurosci,* 21**,** 512-20.

BRATTON, M. R., DUONG, B. N., ELLIOTT, S., WELDON, C. B., BECKMAN, B. S., MCLACHLAN, J. A. & BUROW, M. E. (2010) Regulation of ERalpha-mediated transcription of Bcl-2 by PI3K-AKT crosstalk: implications for breast cancer cell survival. *Int J Oncol,* 37**,** 541-50.

BRICKNER, M. E. (1996) Cardioembolic stroke. *Am J Med,* 100**,** 465-74.

BRINKER, G., FRANKE, C., HOEHN, M., UHLENKUKEN, U. & HOSSMANN, K. A. (1999) Thrombolysis of cerebral clot embolism in rat: effect of treatment delay. *Neuroreport,* 10**,** 3269-72.

BRINTON, R. D. (2001) Cellular and molecular mechanisms of estrogen regulation of memory function and neuroprotection against Alzheimer's disease: recent insights and remaining challenges. *Learn Mem,* 8**,** 121-33.

BRINTON, R. D. (2004) Impact of estrogen therapy on Alzheimer's disease: a fork in the road? *CNS Drugs,* 18**,** 405-22.

BROWN, C. M., SUZUKI, S., JELKS, K. A. & WISE, P. M. (2009) Estradiol is a potent protective, restorative, and trophic factor after brain injury. *Semin Reprod Med,* 27**,** 240-9.

BRUCE-KELLER, A. J., KEELING, J. L., KELLER, J. N., HUANG, F. F., CAMONDOLA, S. & MATTSON, M. P. (2000) Antiinflammatory effects of estrogen on microglial activation. *Endocrinology,* 141**,** 3646-56.

BUCCI, M., ROVIEZZO, F., CICALA, C., PINTO, A. & CIRINO, G. (2002) 17-beta-oestradiol-induced vasorelaxation in vitro is mediated by eNOS through hsp90 and akt/pkb dependent mechanism. *Br J Pharmacol,* 135**,** 1695-700.

BUHNEMANN, C., SCHOLZ, A., BERNREUTHER, C., MALIK, C. Y., BRAUN, H., SCHACHNER, M., REYMANN, K. G. & DIHNE, M. (2006) Neuronal differentiation of transplanted embryonic stem cell-derived precursors in stroke lesions of adult rats. *Brain,* 129**,** 3238-48.

BULUN, S. E., ROSENTHAL, I. M., BRODIE, A. M., INKSTER, S. E., ZELLER, W. P., DIGEORGE, A. M., FRASIER, S. D., KILGORE, M. W. & SIMPSON, E. R. (1993) Use of tissue-specific promoters in the regulation of aromatase cytochrome P450 gene expression in human testicular and ovarian sex cord tumors, as well as in normal fetal and adult gonads. *J Clin Endocrinol Metab,* 77**,** 1616-21.

BURNS, T. C., ORTIZ-GONZALEZ, X. R., GUTIERREZ-PEREZ, M., KEENE, C. D., SHARDA, R., DEMOREST, Z. L., JIANG, Y., NELSON-HOLTE, M., SORIANO, M., NAKAGAWA, Y., LUQUIN, M. R., GARCIA-VERDUGO, J. M., PROSPER, F., LOW, W. C. & VERFAILLIE, C. M. (2006) Thymidine analogs are transferred from prelabeled donor to host cells in the central nervous system after transplantation: a word of caution. *Stem Cells,* 24**,** 1121-7.

BURNS, T. C., VERFAILLIE, C. M. & LOW, W. C. (2009) Stem cells for ischemic brain injury: a critical review. *J Comp Neurol,* 515**,** 125-44.

CADILHAC, D. A., CARTER, R., THRIFT, A. G. & DEWEY, H. M. (2009) Estimating the long-term costs of ischemic and hemorrhagic stroke for Australia: new evidence derived from the North East Melbourne Stroke Incidence Study (NEMESIS). *Stroke,* 40**,** 915-21.

CALLIER, S., MORISSETTE, M., GRANDBOIS, M., PELAPRAT, D. & DI PAOLO, T. (2001) Neuroprotective properties of 17beta-estradiol, progesterone, and raloxifene in MPTP C57Bl/6 mice. *Synapse,* 41**,** 131-8.

CALOF, A. L. (1995) Intrinsic and extrinsic factors regulating vertebrate neurogenesis. *Curr Opin Neurobiol,* 5**,** 19-27.

CARLONE, D. L. & RICHARDS, J. S. (1997) Evidence that functional interactions of CREB and SF-1 mediate hormone regulated expression of the aromatase gene in granulosa cells and constitutive expression in R2C cells. *J Steroid Biochem Mol Biol,* 61**,** 223-31.

CARMECI, C., THOMPSON, D. A., RING, H. Z., FRANCKE, U. & WEIGEL, R. J. (1997) Identification of a gene (GPR30) with homology to the G-protein-coupled receptor superfamily associated with estrogen receptor expression in breast cancer. *Genomics,* 45**,** 607-17.

CARMELIET, P. (2003) Angiogenesis in health and disease. *Nat Med,* 9**,** 653-60.

CARMICHAEL, S. T. (2003) Plasticity of cortical projections after stroke. *Neuroscientist,* 9**,** 64-75.

CARMICHAEL, S. T. (2005) Rodent models of focal stroke: size, mechanism, and purpose. *NeuroRx,* 2**,** 396-409.

CARSWELL, H. V., BINGHAM, D., WALLACE, K., NILSEN, M., GRAHAM, D. I., DOMINICZAK, A. F. & MACRAE, I. M. (2004) Differential effects of 17beta-estradiol upon stroke damage in stroke prone and normotensive rats. *J Cereb Blood Flow Metab,* 24**,** 298-304.

CARSWELL, H. V., DOMINICZAK, A. F. & MACRAE, I. M. (2000) Estrogen status affects sensitivity to focal cerebral ischemia in stroke-prone spontaneously hypertensive rats. *Am J Physiol Heart Circ Physiol,* 278**,** H290-4.

CARSWELL, H. V., MACRAE, I. M. & FARR, T. D. (2010) Complexities of oestrogen in stroke. *Clin Sci (Lond),* 118**,** 375-89.

CAULEY, J. A., NORTON, L., LIPPMAN, M. E., ECKERT, S., KRUEGER, K. A., PURDIE, D. W., FARRERONS, J., KARASIK, A., MELLSTROM, D., NG, K. W., STEPAN, J. J., POWLES, T. J., MORROW, M., COSTA, A., SILFEN, S. L., WALLS, E. L., SCHMITT, H., MUCHMORE, D. B., JORDAN, V. C. & STE-MARIE, L. G. (2001) Continued breast cancer risk reduction in postmenopausal

women treated with raloxifene: 4-year results from the MORE trial. Multiple outcomes of raloxifene evaluation. *Breast Cancer Res Treat,* 65**,** 125-34.

CENCI, M. A., WHISHAW, I. Q. & SCHALLERT, T. (2002) Animal models of neurological deficits: how relevant is the rat? *Nat Rev Neurosci,* 3**,** 574-9.

CHAKRAVARTHY, B., RASHID, A., BROWN, L., TESSIER, L., KELLY, J. & MENARD, M. (2008) Association of Gap-43 (neuromodulin) with microtubule-associated protein MAP-2 in neuronal cells. *Biochem Biophys Res Commun,* 371**,** 679-83.

CHEN, J., LI, Y., KATAKOWSKI, M., CHEN, X., WANG, L., LU, D., LU, M., GAUTAM, S. C. & CHOPP, M. (2003a) Intravenous bone marrow stromal cell therapy reduces apoptosis and promotes endogenous cell proliferation after stroke in female rat. *J Neurosci Res,* 73**,** 778-86.

CHEN, J., LI, Y., WANG, L., LU, M., ZHANG, X. & CHOPP, M. (2001a) Therapeutic benefit of intracerebral transplantation of bone marrow stromal cells after cerebral ischemia in rats. *J Neurol Sci,* 189**,** 49-57.

CHEN, J., SANBERG, P. R., LI, Y., WANG, L., LU, M., WILLING, A. E., SANCHEZ-RAMOS, J. & CHOPP, M. (2001b) Intravenous administration of human umbilical cord blood reduces behavioral deficits after stroke in rats. *Stroke,* 32**,** 2682-8.

CHEN, J., ZACHAREK, A., ZHANG, C., JIANG, H., LI, Y., ROBERTS, C., LU, M., KAPKE, A. & CHOPP, M. (2005) Endothelial nitric oxide synthase regulates brain-derived neurotrophic factor expression and neurogenesis after stroke in mice. *J Neurosci,* 25**,** 2366-75.

CHEN, J., ZHANG, Z. G., LI, Y., WANG, L., XU, Y. X., GAUTAM, S. C., LU, M., ZHU, Z. & CHOPP, M. (2003b) Intravenous administration of human bone marrow stromal cells induces angiogenesis in the ischemic boundary zone after stroke in rats. *Circ Res,* 92**,** 692-9.

CHEN, X., LI, Y., WANG, L., KATAKOWSKI, M., ZHANG, L., CHEN, J., XU, Y., GAUTAM, S. C. & CHOPP, M. (2002) Ischemic rat brain extracts induce human marrow stromal cell growth factor production. *Neuropathology,* 22**,** 275-9.

CHENG, H. L. & FELDMAN, E. L. (1998) Bidirectional regulation of p38 kinase and c-Jun N-terminal protein kinase by insulin-like growth factor-I. *J Biol Chem,* 273**,** 14560-5.

CIRIZA, I., CARRERO, P., AZCOITIA, I., LUNDEEN, S. G. & GARCIA-SEGURA, L. M. (2004) Selective estrogen receptor modulators protect hippocampal neurons from kainic acid excitotoxicity: differences with the effect of estradiol. *J Neurobiol,* 61**,** 209-21.

CLARK, W. M., LESSOV, N. S., DIXON, M. P. & ECKENSTEIN, F. (1997) Monofilament intraluminal middle cerebral artery occlusion in the mouse. *Neurol Res,* 19**,** 641-8.

CONNOLLY, E. S., JR., WINFREE, C. J., STERN, D. M., SOLOMON, R. A. & PINSKY, D. J. (1996) Procedural and strain-related variables significantly affect outcome in a murine model of focal cerebral ischemia. *Neurosurgery,* 38**,** 523-31; discussion 532.

COOK, M. N., BOLIVAR, V. J., MCFADYEN, M. P. & FLAHERTY, L. (2002) Behavioral differences among 129 substrains: implications for knockout and transgenic mice. *Behav Neurosci,* 116**,** 600-11.

CRAMER, S. C., NELLES, G., BENSON, R. R., KAPLAN, J. D., PARKER, R. A., KWONG, K. K., KENNEDY, D. N., FINKLESTEIN, S. P. & ROSEN, B. R. (1997) A functional MRI study of subjects recovered from hemiparetic stroke. *Stroke,* 28**,** 2518-27.

CUMMINGS, S. R., ECKERT, S., KRUEGER, K. A., GRADY, D., POWLES, T. J., CAULEY, J. A., NORTON, L., NICKELSEN, T., BJARNASON, N. H., MORROW, M., LIPPMAN, M. E., BLACK, D., GLUSMAN, J. E., COSTA, A. & JORDAN, V. C. (1999) The effect of raloxifene on risk of breast cancer in postmenopausal women: results from the MORE randomized trial. Multiple Outcomes of Raloxifene Evaluation. *JAMA,* 281**,** 2189-97.

DAS, A., DIKSHIT, M., SRIVASTAVA, S. R., SRIVASTAVA, U. K. & NATH, C. (2002) Effect of ovariectomy and estrogen supplementation on brain acetylcholinesterase activity and passive-avoidance learning in rats. *Can J Physiol Pharmacol,* 80**,** 907-14.

DE SIMONI, M. G., STORINI, C., BARBA, M., CATAPANO, L., ARABIA, A. M., ROSSI, E. & BERGAMASCHINI, L. (2003) Neuroprotection by complement (C1) inhibitor in mouse transient brain ischemia. *J Cereb Blood Flow Metab,* 23**,** 232-9.

DELANEY, J. A., OPATRNY, L., BROPHY, J. M. & SUISSA, S. (2007) Drug drug interactions between antithrombotic medications and the risk of gastrointestinal bleeding. *CMAJ,* 177**,** 347-51.

DELAUNAY, F., PETTERSSON, K., TUJAGUE, M. & GUSTAFSSON, J. A. (2000) Functional differences between the amino-terminal domains of estrogen receptors alpha and beta. *Mol Pharmacol,* 58**,** 584-90.

DEVRIES, A. C., NELSON, R. J., TRAYSTMAN, R. J. & HURN, P. D. (2001) Cognitive and behavioral assessment in experimental stroke research: will it prove useful? *Neurosci Biobehav Rev,* 25**,** 325-42.

DIENER, H. C., LEES, K. R., LYDEN, P., GROTTA, J., DAVALOS, A., DAVIS, S. M., SHUAIB, A., ASHWOOD, T., WASIEWSKI, W., ALDERFER, V., HARDEMARK, H. G. & RODICHOK, L. (2008) NXY-059 for the treatment of acute stroke: pooled analysis of the SAINT I and II Trials. *Stroke,* 39**,** 1751-8.

DIRNAGL, U., IADECOLA, C. & MOSKOWITZ, M. A. (1999) Pathobiology of ischaemic stroke: an integrated view. *Trends Neurosci,* 22**,** 391-7.

DONNAN, G. A., FISHER, M., MACLEOD, M. & DAVIS, S. M. (2008) Stroke. *Lancet,* 371**,** 1612-23.

DUAN, W. M., WIDNER, H. & BRUNDIN, P. (1995) Temporal pattern of host responses against intrastriatal grafts of syngeneic, allogeneic or xenogeneic embryonic neuronal tissue in rats. *Exp Brain Res,* 104**,** 227-42.

DUBAL, D. B., KASHON, M. L., PETTIGREW, L. C., REN, J. M., FINKLESTEIN, S. P., RAU, S. W. & WISE, P. M. (1998) Estradiol protects against ischemic injury. *J Cereb Blood Flow Metab,* 18**,** 1253-8.

DUBAL, D. B. & WISE, P. M. (2001) Neuroprotective effects of estradiol in middle-aged female rats. *Endocrinology,* 142**,** 43-8.

DUBAL, D. B., ZHU, H., YU, J., RAU, S. W., SHUGHRUE, P. J., MERCHENTHALER, I., KINDY, M. S. & WISE, P. M. (2001) Estrogen receptor alpha, not beta, is a critical link in estradiol-mediated protection against brain injury. *Proc Natl Acad Sci U S A,* 98**,** 1952-7.

DUENAS, M., TORRES-ALEMAN, I., NAFTOLIN, F. & GARCIA-SEGURA, L. M. (1996) Interaction of insulin-like growth factor-I and estradiol signaling pathways on hypothalamic neuronal differentiation. *Neuroscience,* 74**,** 531-9.

DUNAC, A., FRELIN, C., POPOLO-BLONDEAU, M., CHATEL, M., MAHAGNE, M. H. & PHILIP, P. J. (2007) Neurological and functional recovery in human stroke are associated with peripheral blood CD34+ cell mobilization. *J Neurol,* 254**,** 327-32.

DURUKAN, A. & TATLISUMAK, T. (2007) Acute ischemic stroke: overview of major experimental rodent models, pathophysiology, and therapy of focal cerebral ischemia. *Pharmacol Biochem Behav,* 87**,** 179-97.

EMERICH, D. F., DEAN, R. L., 3RD & BARTUS, R. T. (2002) The role of leukocytes following cerebral ischemia: pathogenic variable or bystander reaction to emerging infarct? *Exp Neurol,* 173**,** 168-81.

ENGLUND, U., BJORKLUND, A., WICTORIN, K., LINDVALL, O. & KOKAIA, M. (2002) Grafted neural stem cells develop into functional pyramidal neurons and integrate into host cortical circuitry. *Proc Natl Acad Sci U S A,* 99**,** 17089-94.

ENMARK, E., PELTO-HUIKKO, M., GRANDIEN, K., LAGERCRANTZ, S., LAGERCRANTZ, J., FRIED, G., NORDENSKJOLD, M. & GUSTAFSSON, J. A. (1997) Human estrogen receptor beta-gene structure, chromosomal localization, and expression pattern. *J Clin Endocrinol Metab,* 82**,** 4258-65.

ERDO, F., BUHRLE, C., BLUNK, J., HOEHN, M., XIA, Y., FLEISCHMANN, B., FOCKING, M., KUSTERMANN, E., KOLOSSOV, E., HESCHELER, J., HOSSMANN, K. A. & TRAPP, T. (2003) Host-dependent tumorigenesis of embryonic stem cell transplantation in experimental stroke. *J Cereb Blood Flow Metab,* 23**,** 780-5.

ERIKSSON, C., BJORKLUND, A. & WICTORIN, K. (2003) Neuronal differentiation following transplantation of expanded mouse neurosphere cultures derived from different embryonic forebrain regions. *Exp Neurol,* 184**,** 615-35.

FARR, T. D., CARSWELL, H. V., GALLAGHER, L., CONDON, B., FAGAN, A. J., MULLIN, J. & MACRAE, I. M. (2006a) 17beta-Estradiol treatment following permanent focal ischemia does not influence recovery of sensorimotor function. *Neurobiol Dis,* 23**,** 552-62.

FARR, T. D., CARSWELL, H. V., GSELL, W. & MACRAE, I. M. (2007) Estrogen receptor beta agonist diarylpropiolnitrile (DPN) does not mediate neuroprotection in a rat model of permanent focal ischemia. *Brain Res,* 1185**,** 275-82.

FARR, T. D., CARSWELL, H. V., MCCANN, D. J., SATO, M., BRYANT, H. U., DODGE, J. A. & MACRAE, I. M. (2008) The selective oestrogen receptor modulator, LY362321, is not neuroprotective in a rat model of transient focal ischaemia. *J Neuroendocrinol,* 20**,** 366-74.

FARR, T. D., LIU, L., COLWELL, K. L., WHISHAW, I. Q. & METZ, G. A. (2006b) Bilateral alteration in stepping pattern after unilateral motor cortex injury: a new test strategy for analysis of skilled limb movements in neurological mouse models. *J Neurosci Methods,* 153**,** 104-13.

FEIGIN, V. L., LAWES, C. M., BENNETT, D. A. & ANDERSON, C. S. (2003) Stroke epidemiology: a review of population-based studies of incidence, prevalence, and case-fatality in the late 20th century. *Lancet Neurol,* 2**,** 43-53.

FERREIRA, A. & CACERES, A. (1991) Estrogen-enhanced neurite growth: evidence for a selective induction of Tau and stable microtubules. *J Neurosci,* 11**,** 392-400.

FIEBACH, J. B., SCHELLINGER, P. D., JANSEN, O., MEYER, M., WILDE, P., BENDER, J., SCHRAMM, P., JUTTLER, E., OEHLER, J., HARTMANN, M., HAHNEL, S., KNAUTH, M., HACKE, W. & SARTOR, K. (2002) CT and diffusion-weighted MR imaging in randomized order: diffusion-weighted imaging results in higher accuracy and lower interrater variability in the diagnosis of hyperacute ischemic stroke. *Stroke,* 33**,** 2206-10.

FILARDO, E. J., QUINN, J. A., BLAND, K. I. & FRACKELTON, A. R., JR. (2000) Estrogen-induced activation of Erk-1 and Erk-2 requires the G protein-coupled receptor homolog, GPR30, and occurs via trans-activation of the epidermal growth factor receptor through release of HB-EGF. *Mol Endocrinol,* 14**,** 1649-60.

FISHER, B., COSTANTINO, J. P., WICKERHAM, D. L., REDMOND, C. K., KAVANAH, M., CRONIN, W. M., VOGEL, V., ROBIDOUX, A., DIMITROV, N., ATKINS, J., DALY, M., WIEAND, S., TAN-CHIU, E., FORD, L. & WOLMARK, N. (1998) Tamoxifen for prevention of breast cancer: report of the National Surgical Adjuvant Breast and Bowel Project P-1 Study. *J Natl Cancer Inst,* 90**,** 1371-88.

FISHER, M. (2008) Stroke and TIA: epidemiology, risk factors, and the need for early intervention. *Am J Manag Care,* 14**,** S204-11.

FISHER, M., FEUERSTEIN, G., HOWELLS, D. W., HURN, P. D., KENT, T. A., SAVITZ, S. I. & LO, E. H. (2009) Update of the stroke therapy academic industry roundtable preclinical recommendations. *Stroke,* 40**,** 2244-50.

FLAHERTY, M. L., KISSELA, B., WOO, D., KLEINDORFER, D., ALWELL, K., SEKAR, P., MOOMAW, C. J., HAVERBUSCH, M. & BRODERICK, J. P. (2007) The increasing incidence of anticoagulant-associated intracerebral hemorrhage. *Neurology,* 68**,** 116-21.

FLEMING, S. M., SALCEDO, J., FERNAGUT, P. O., ROCKENSTEIN, E., MASLIAH, E., LEVINE, M. S. & CHESSELET, M. F. (2004) Early and progressive sensorimotor anomalies in mice overexpressing wild-type human alpha-synuclein. *J Neurosci,* 24**,** 9434-40.

FLYNN, J. M., DIMITRIJEVICH, S. D., YOUNES, M., SKLIRIS, G., MURPHY, L. C. & CAMMARATA, P. R. (2008) Role of wild-type estrogen receptor-beta in mitochondrial cytoprotection of cultured normal male and female human lens epithelial cells. *Am J Physiol Endocrinol Metab,* 295**,** E637-47.

FOY, M. R., BAUDRY, M., DIAZ BRINTON, R. & THOMPSON, R. F. (2008) Estrogen and hippocampal plasticity in rodent models. *J Alzheimers Dis,* 15**,** 589-603.

FRIED, G., ANDERSSON, E., CSOREGH, L., ENMARK, E., GUSTAFSSON, J. A., AANESEN, A. & OSTERLUND, C. (2004) Estrogen receptor beta is expressed in

human embryonic brain cells and is regulated by 17beta-estradiol. *Eur J Neurosci,* 20**,** 2345-54.

FUNAKOSHI, T., YANAI, A., SHINODA, K., KAWANO, M. M. & MIZUKAMI, Y. (2006) G protein-coupled receptor 30 is an estrogen receptor in the plasma membrane. *Biochem Biophys Res Commun,* 346**,** 904-10.

GARCIA-OVEJERO, D., VEIGA, S., GARCIA-SEGURA, L. M. & DONCARLOS, L. L. (2002) Glial expression of estrogen and androgen receptors after rat brain injury. *J Comp Neurol,* 450**,** 256-71.

GARCIA-SEGURA, L. M., WOZNIAK, A., AZCOITIA, I., RODRIGUEZ, J. R., HUTCHISON, R. E. & HUTCHISON, J. B. (1999) Aromatase expression by astrocytes after brain injury: implications for local estrogen formation in brain repair. *Neuroscience,* 89**,** 567-78.

GARCIA, J. H., LIU, K. F. & HO, K. L. (1995) Neuronal necrosis after middle cerebral artery occlusion in Wistar rats progresses at different time intervals in the caudoputamen and the cortex. *Stroke,* 26**,** 636-42; discussion 643.

GARCIA, J. H., YOSHIDA, Y., CHEN, H., LI, Y., ZHANG, Z. G., LIAN, J., CHEN, S. & CHOPP, M. (1993) Progression from ischemic injury to infarct following middle cerebral artery occlusion in the rat. *Am J Pathol,* 142**,** 623-35.

GERRIETS, T., STOLZ, E., WALBERER, M., MULLER, C., KLUGE, A., BACHMANN, A., FISHER, M., KAPS, M. & BACHMANN, G. (2004) Noninvasive quantification of brain edema and the space-occupying effect in rat stroke models using magnetic resonance imaging. *Stroke,* 35**,** 566-71.

GERSTNER, B., LEE, J., DESILVA, T. M., JENSEN, F. E., VOLPE, J. J. & ROSENBERG, P. A. (2009) 17beta-estradiol protects against hypoxic/ischemic white matter damage in the neonatal rat brain. *J Neurosci Res,* 87**,** 2078-86.

GERSTNER, B., SIFRINGER, M., DZIETKO, M., SCHULLER, A., LEE, J., SIMONS, S., OBLADEN, M., VOLPE, J. J., ROSENBERG, P. A. & FELDERHOFF-MUESER, U. (2007) Estradiol attenuates hyperoxia-induced cell death in the developing white matter. *Ann Neurol,* 61**,** 562-73.

GIBBS, R. B. & GABOR, R. (2003) Estrogen and cognition: applying preclinical findings to clinical perspectives. *J Neurosci Res,* 74**,** 637-43.

GIRALDI-GUIMARAES, A., REZENDE-LIMA, M., BRUNO, F. P. & MENDEZ-OTERO, R. (2009) Treatment with bone marrow mononuclear cells induces functional recovery and decreases neurodegeneration after sensorimotor cortical ischemia in rats. *Brain Res*.

GOBEIL, F., FORTIER, A., ZHU, T., BOSSOLASCO, M., LEDUC, M., GRANDBOIS, M., HEVEKER, N., BKAILY, G., CHEMTOB, S. & BARBAZ, D. (2006) G-protein-coupled receptors signalling at the cell nucleus: an emerging paradigm. *Can J Physiol Pharmacol,* 84**,** 287-97.

GOODMAN, Y., BRUCE, A. J., CHENG, B. & MATTSON, M. P. (1996) Estrogens attenuate and corticosterone exacerbates excitotoxicity, oxidative injury, and amyloid beta-peptide toxicity in hippocampal neurons. *J Neurochem,* 66**,** 1836-44.

GORDON, K. B., MACRAE, I. M. & CARSWELL, H. V. (2005) Effects of 17beta-oestradiol on cerebral ischaemic damage and lipid peroxidation. *Brain Res,* 1036**,** 155-62.

GOULD, E., WOOLLEY, C. S., FRANKFURT, M. & MCEWEN, B. S. (1990) Gonadal steroids regulate dendritic spine density in hippocampal pyramidal cells in adulthood. *J Neurosci,* 10**,** 1286-91.

GRAY, J. A., GRIGORYAN, G., VIRLEY, D., PATEL, S., SINDEN, J. D. & HODGES, H. (2000) Conditionally immortalized, multipotential and multifunctional neural stem cell lines as an approach to clinical transplantation. *Cell Transplant,* 9**,** 153-68.

GRAY, J. A., HODGES, H. & SINDEN, J. (1999) Prospects for the clinical application of neural transplantation with the use of conditionally immortalized neuroepithelial stem cells. *Philos Trans R Soc Lond B Biol Sci,* 354**,** 1407-21.

GREEN, P. S., GORDON, K. & SIMPKINS, J. W. (1997) Phenolic A ring requirement for the neuroprotective effects of steroids. *J Steroid Biochem Mol Biol,* 63**,** 229-35.

GREEN, P. S., GRIDLEY, K. E. & SIMPKINS, J. W. (1998) Nuclear estrogen receptor-independent neuroprotection by estratrienes: a novel interaction with glutathione. *Neuroscience,* 84**,** 7-10.

GU, Q. & MOSS, R. L. (1996) 17 beta-Estradiol potentiates kainate-induced currents via activation of the cAMP cascade. *J Neurosci,* 16**,** 3620-9.

GUO, W., MASON, J. S., STONE, C. G., JR., MORGAN, S. A., MADU, S. I., BALDINI, A., LINDSAY, E. A., BIESECKER, L. G., COPELAND, K. C., HORLICK, M. N. & ET AL. (1995) Diagnosis of X-linked adrenal hypoplasia congenita by mutation analysis of the DAX1 gene. *JAMA,* 274**,** 324-30.

GURATES, B., AMSTERDAM, A., TAMURA, M., YANG, S., ZHOU, J., FANG, Z., AMIN, S., SEBASTIAN, S. & BULUN, S. E. (2003) WT1 and DAX-1 regulate SF-1-mediated human P450arom gene expression in gonadal cells. *Mol Cell Endocrinol,* 208**,** 61-75.

GURSOY-OZDEMIR, Y., CAN, A. & DALKARA, T. (2004) Reperfusion-induced oxidative/nitrative injury to neurovascular unit after focal cerebral ischemia. *Stroke,* 35**,** 1449-53.

GUSTAFSSON, J. A. (1999) Estrogen receptor beta--a new dimension in estrogen mechanism of action. *J Endocrinol,* 163**,** 379-83.

HAAS, S., WEIDNER, N. & WINKLER, J. (2005) Adult stem cell therapy in stroke. *Curr Opin Neurol,* 18**,** 59-64.

HABERMAN, S., CAPILDEO, R. & ROSE, F. C. (1981) Sex differences in the incidence of cerebrovascular disease. *J Epidemiol Community Health,* 35**,** 45-50.

HALVORSON, L. M., ITO, M., JAMESON, J. L. & CHIN, W. W. (1998) Steroidogenic factor-1 and early growth response protein 1 act through two composite DNA binding sites to regulate luteinizing hormone beta-subunit gene expression. *J Biol Chem,* 273**,** 14712-20.

HANLEY, N. A., RAINEY, W. E., WILSON, D. I., BALL, S. G. & PARKER, K. L. (2001) Expression profiles of SF-1, DAX1, and CYP17 in the human fetal adrenal gland: potential interactions in gene regulation. *Mol Endocrinol,* 15**,** 57-68.

HANNA, J., WERNIG, M., MARKOULAKI, S., SUN, C. W., MEISSNER, A., CASSADY, J. P., BEARD, C., BRAMBRINK, T., WU, L. C., TOWNES, T. M. & JAENISCH, R. (2007) Treatment of sickle cell anemia mouse model with iPS cells generated from autologous skin. *Science,* 318**,** 1920-3.

HARA, K., YASUHARA, T., MAKI, M., MATSUKAWA, N., MASUDA, T., YU, S. J., ALI, M., YU, G., XU, L., KIM, S. U., HESS, D. C. & BORLONGAN, C. V. (2008) Neural progenitor NT2N cell lines from teratocarcinoma for transplantation therapy in stroke. *Prog Neurobiol,* 85**,** 318-34.

HARMS, K. M., LI, L. & CUNNINGHAM, L. A. (2010) Murine neural stem/progenitor cells protect neurons against ischemia by HIF-1alpha-regulated VEGF signaling. *PLoS One,* 5**,** e9767.

HARRIS, R. J., SYMON, L., BRANSTON, N. M. & BAYHAN, M. (1981) Changes in extracellular calcium activity in cerebral ischaemia. *J Cereb Blood Flow Metab,* 1**,** 203-9.

HATA, R., MIES, G., WIESSNER, C., FRITZE, K., HESSELBARTH, D., BRINKER, G. & HOSSMANN, K. A. (1998) A reproducible model of middle cerebral artery occlusion in mice: hemodynamic, biochemical, and magnetic resonance imaging. *J Cereb Blood Flow Metab,* 18**,** 367-75.

HATCHER, J. P., VIRLEY, D., HADINGHAM, S. J., ROBERTS, J., HUNTER, A. J. & PARSONS, A. A. (2002) The behavioural effect of middle cerebral artery occlusion on apolipoprotein-E deficient mice. *Behav Brain Res,* 131**,** 139-49.

HAYASHI, J., TAKAGI, Y., FUKUDA, H., IMAZATO, T., NISHIMURA, M., FUJIMOTO, M., TAKAHASHI, J., HASHIMOTO, N. & NOZAKI, K. (2006) Primate embryonic stem cell-derived neuronal progenitors transplanted into ischemic brain. *J Cereb Blood Flow Metab,* 26**,** 906-14.

HE, Z., HE, Y. J., DAY, A. L. & SIMPKINS, J. W. (2002) Proestrus levels of estradiol during transient global cerebral ischemia improves the histological outcome of the hippocampal CA1 region: perfusion-dependent and-independent mechanisms. *J Neurol Sci,* 193**,** 79-87.

HEFTI, F. (1986) Nerve growth factor promotes survival of septal cholinergic neurons after fimbrial transections. *J Neurosci,* 6**,** 2155-62.

HENDRIX, S. L., WASSERTHEIL-SMOLLER, S., JOHNSON, K. C., HOWARD, B. V., KOOPERBERG, C., ROSSOUW, J. E., TREVISAN, M., ARAGAKI, A., BAIRD, A. E., BRAY, P. F., BURING, J. E., CRIQUI, M. H., HERRINGTON, D., LYNCH, J. K., RAPP, S. R. & TORNER, J. (2006) Effects of conjugated equine estrogen on stroke in the Women's Health Initiative. *Circulation,* 113**,** 2425-34.

HILL, R. A., CHUA, H. K., JONES, M. E., SIMPSON, E. R. & BOON, W. C. (2009) Estrogen deficiency results in apoptosis in the frontal cortex of adult female aromatase knockout mice. *Mol Cell Neurosci,* 41**,** 1-7.

HIRAI, H. (2002) Stem cells and regenerative medicine. *Hum Cell,* 15**,** 190-8.

HODGES, H., SOWINSKI, P., VIRLEY, D., NELSON, A., KERSHAW, T. R., WATSON, W. P., VEIZOVIC, T., PATEL, S., MORA, A., RASHID, T., FRENCH, S. J., CHADWICK, A., GRAY, J. A. & SINDEN, J. D. (2000a) Functional reconstruction of the hippocampus: fetal versus conditionally immortal neuroepithelial stem cell grafts. *Novartis Found Symp,* 231**,** 53-65; discussion 65-9.

HODGES, H., VEIZOVIC, T., BRAY, N., FRENCH, S. J., RASHID, T. P., CHADWICK, A., PATEL, S. & GRAY, J. A. (2000b) Conditionally immortal neuroepithelial stem cell grafts reverse age-associated memory impairments in rats. *Neuroscience,* 101**,** 945-55.

HOJO, Y., HATTORI, T. A., ENAMI, T., FURUKAWA, A., SUZUKI, K., ISHII, H. T., MUKAI, H., MORRISON, J. H., JANSSEN, W. G., KOMINAMI, S., HARADA, N., KIMOTO, T. & KAWATO, S. (2004) Adult male rat hippocampus synthesizes estradiol from pregnenolone by cytochromes P45017alpha and P450 aromatase localized in neurons. *Proc Natl Acad Sci U S A,* 101**,** 865-70.

HOLTER, E., KOTAJA, N., MAKELA, S., STRAUSS, L., KIETZ, S., JANNE, O. A., GUSTAFSSON, J. A., PALVIMO, J. J. & TREUTER, E. (2002) Inhibition of androgen receptor (AR) function by the reproductive orphan nuclear receptor DAX-1. *Mol Endocrinol,* 16**,** 515-28.

HORITA, Y., HONMOU, O., HARADA, K., HOUKIN, K., HAMADA, H. & KOCSIS, J. D. (2006) Intravenous administration of glial cell line-derived neurotrophic factor gene-modified human mesenchymal stem cells protects against injury in a cerebral ischemia model in the adult rat. *J Neurosci Res,* 84**,** 1495-504.

HOSSMANN, K. A. (2008) Cerebral ischemia: models, methods and outcomes. *Neuropharmacology,* 55**,** 257-70.

HUA, Y., SCHALLERT, T., KEEP, R. F., WU, J., HOFF, J. T. & XI, G. (2002) Behavioral tests after intracerebral hemorrhage in the rat. *Stroke,* 33**,** 2478-84.

HUANG, J., KIM, L. J., POISIK, A., PINSKY, D. J. & CONNOLLY, E. S., JR. (1998) Does poly-L-lysine coating of the middle cerebral artery occlusion suture improve infarct consistency in a murine model? *J Stroke Cerebrovasc Dis,* 7**,** 296-301.

HUNTER, A. J., HATCHER, J., VIRLEY, D., NELSON, P., IRVING, E., HADINGHAM, S. J. & PARSONS, A. A. (2000) Functional assessments in mice and rats after focal stroke. *Neuropharmacology,* 39**,** 806-16.

HUNTER, A. J., MACKAY, K. B. & ROGERS, D. C. (1998) To what extent have functional studies of ischaemia in animals been useful in the assessment of potential neuroprotective agents? *Trends Pharmacol Sci,* 19**,** 59-66.

HURN, P. D. & MACRAE, I. M. (2000) Estrogen as a neuroprotectant in stroke. *J Cereb Blood Flow Metab,* 20**,** 631-52.

HUSSAIN, M. S. & SHUAIB, A. (2007) Thrombolysis for acute ischemic stroke in India: overcoming the challenges. *Neurol India,* 55**,** 9-10.

IAFRATI, M. D., KARAS, R. H., ARONOVITZ, M., KIM, S., SULLIVAN, T. R., JR., LUBAHN, D. B., O'DONNELL, T. F., JR., KORACH, K. S. & MENDELSOHN, M. E. (1997) Estrogen inhibits the vascular injury response in estrogen receptor alpha-deficient mice. *Nat Med,* 3**,** 545-8.

IKEDA, Y., SWAIN, A., WEBER, T. J., HENTGES, K. E., ZANARIA, E., LALLI, E., TAMAI, K. T., SASSONE-CORSI, P., LOVELL-BADGE, R., CAMERINO, G. & PARKER, K. L. (1996) Steroidogenic factor 1 and Dax-1 colocalize in multiple cell lineages: potential links in endocrine development. *Mol Endocrinol,* 10**,** 1261-72.

IRRIBARRA, V., GERMAIN, A., CUEVAS, A., FAUNDEZ, L. & VALDES, G. (2000) [Endothelial dysfunction as a primary disorder in vascular diseases]. *Rev Med Chil,* 128**,** 659-70.

ISACSON, O., BRUNDIN, P., KELLY, P. A., GAGE, F. H. & BJORKLUND, A. (1984) Functional neuronal replacement by grafted striatal neurones in the ibotenic acid-lesioned rat striatum. *Nature,* 311**,** 458-60.

ITO, M., YU, R. & JAMESON, J. L. (1997) DAX-1 inhibits SF-1-mediated transactivation via a carboxy-terminal domain that is deleted in adrenal hypoplasia congenita. *Mol Cell Biol,* 17**,** 1476-83.

JACKSON, C. & SUDLOW, C. (2005) Are lacunar strokes really different? A systematic review of differences in risk factor profiles between lacunar and nonlacunar infarcts. *Stroke,* 36**,** 891-901.

JAENISCH, R. & YOUNG, R. (2008) Stem cells, the molecular circuitry of pluripotency and nuclear reprogramming. *Cell,* 132**,** 567-82.

JARLESTEDT, K., ROUSSET, C. I., FAIZ, M., WILHELMSSON, U., STAHLBERG, A., SOURKOVA, H., PEKNA, M., MALLARD, C., HAGBERG, H. & PEKNY, M. (2010) Attenuation of reactive gliosis does not affect infarct volume in neonatal hypoxic-ischemic brain injury in mice. *PLoS One,* 5**,** e10397.

JAT, P. S., NOBLE, M. D., ATALIOTIS, P., TANAKA, Y., YANNOUTSOS, N., LARSEN, L. & KIOUSSIS, D. (1991) Direct derivation of conditionally immortal cell lines from an H-2Kb-tsA58 transgenic mouse. *Proc Natl Acad Sci U S A,* 88**,** 5096-100.

JEZIERSKI, M. K. & SOHRABJI, F. (2003) Estrogen enhances retrograde transport of brain-derived neurotrophic factor in the rodent forebrain. *Endocrinology,* 144**,** 5022-9.

JIA, J., GUAN, D., ZHU, W., ALKAYED, N. J., WANG, M. M., HUA, Z. & XU, Y. (2009) Estrogen inhibits Fas-mediated apoptosis in experimental stroke. *Exp Neurol,* 215**,** 48-52.

JIANG, Y., JAHAGIRDAR, B. N., REINHARDT, R. L., SCHWARTZ, R. E., KEENE, C. D., ORTIZ-GONZALEZ, X. R., REYES, M., LENVIK, T., LUND, T., BLACKSTAD, M., DU, J., ALDRICH, S., LISBERG, A., LOW, W. C., LARGAESPADA, D. A. & VERFAILLIE, C. M. (2002) Pluripotency of mesenchymal stem cells derived from adult marrow. *Nature,* 418**,** 41-9.

JIN, K., ZHU, Y., SUN, Y., MAO, X. O., XIE, L. & GREENBERG, D. A. (2002) Vascular endothelial growth factor (VEGF) stimulates neurogenesis in vitro and in vivo. *Proc Natl Acad Sci U S A,* 99**,** 11946-50.

JUNG-TESTAS, I., RENOIR, M., BUGNARD, H., GREENE, G. L. & BAULIEU, E. E. (1992) Demonstration of steroid hormone receptors and steroid action in primary cultures of rat glial cells. *J Steroid Biochem Mol Biol,* 41**,** 621-31.

KAJTA, M., BUDZISZEWSKA, B., MARSZAL, M. & LASON, W. (2001) Effects of 17-beta estradiol and estriol on NMDA-induced toxicity and apoptosis in primary cultures of rat cortical neurons. *J Physiol Pharmacol,* 52**,** 437-46.

KAJTA, M., LASON, W., BIEN, E. & MARSZAL, M. (2002) Neuroprotective effects of estrone on NMDA-induced toxicity in primary cultures of rat cortical neurons are independent of estrogen receptors. *Pol J Pharmacol,* 54**,** 727-9.

KANDA, N. & WATANABE, S. (2003) 17beta-estradiol inhibits oxidative stress-induced apoptosis in keratinocytes by promoting Bcl-2 expression. *J Invest Dermatol,* 121**,** 1500-9.

KANDA, N. & WATANABE, S. (2004) 17beta-estradiol stimulates the growth of human keratinocytes by inducing cyclin D2 expression. *J Invest Dermatol,* 123**,** 319-28.

KANEMITSU, H., NAKAGOMI, T., TAMURA, A., TSUCHIYA, T., KONO, G. & SANO, K. (2002) Differences in the extent of primary ischemic damage between middle cerebral artery coagulation and intraluminal occlusion models. *J Cereb Blood Flow Metab,* 22**,** 1196-204.

KANG, S. K., LEE, D. H., BAE, Y. C., KIM, H. K., BAIK, S. Y. & JUNG, J. S. (2003) Improvement of neurological deficits by intracerebral transplantation of human adipose tissue-derived stromal cells after cerebral ischemia in rats. *Exp Neurol,* 183**,** 355-66.

KARAS, R. H., PATTERSON, B. L. & MENDELSOHN, M. E. (1994) Human vascular smooth muscle cells contain functional estrogen receptor. *Circulation,* 89**,** 1943-50.

KARHUNEN, H., VIRTANEN, T., SCHALLERT, T., SIVENIUS, J. & JOLKKONEN, J. (2003) Forelimb use after focal cerebral ischemia in rats treated with an alpha 2-adrenoceptor antagonist. *Pharmacol Biochem Behav,* 74**,** 663-9.

KATZENELLENBOGEN, B. S. & KATZENELLENBOGEN, J. A. (2002) Biomedicine. Defining the "S" in SERMs. *Science,* 295**,** 2380-1.

KAUFMANN, A. M., FIRLIK, A. D., FUKUI, M. B., WECHSLER, L. R., JUNGRIES, C. A. & YONAS, H. (1999) Ischemic core and penumbra in human stroke. *Stroke,* 30**,** 93-9.

KAWAMURA, S., YASUI, N., SHIRASAWA, M. & FUKASAWA, H. (1991) Rat middle cerebral artery occlusion using an intraluminal thread technique. *Acta Neurochir (Wien),* 109**,** 126-32.

KAWATO, S., HOJO, Y. & KIMOTO, T. (2002) Histological and metabolism analysis of P450 expression in the brain. *Methods Enzymol,* 357**,** 241-9.

KAWATO, S., YAMADA, M. & KIMOTO, T. (2003) Brain neurosteroids are 4th generation neuromessengers in the brain: cell biophysical analysis of steroid signal transduction. *Adv Biophys,* 37**,** 1-48.

KELLY, M. J. & LEVIN, E. R. (2001) Rapid actions of plasma membrane estrogen receptors. *Trends Endocrinol Metab,* 12**,** 152-6.

KELLY, S., BLISS, T. M., SHAH, A. K., SUN, G. H., MA, M., FOO, W. C., MASEL, J., YENARI, M. A., WEISSMAN, I. L., UCHIDA, N., PALMER, T. & STEINBERG, G. K. (2004) Transplanted human fetal neural stem cells survive, migrate, and differentiate in ischemic rat cerebral cortex. *Proc Natl Acad Sci U S A,* 101**,** 11839-44.

KERNAN, W. N., BRASS, L. M., VISCOLI, C. M., SARREL, P. M., MAKUCH, R. & HORWITZ, R. I. (1998) Estrogen after ischemic stroke: clinical basis and design of the Women's Estrogen for Stroke Trial. *J Stroke Cerebrovasc Dis,* 7**,** 85-95.

KHALFALLAH, O., ROULEAU, M., BARBRY, P., BARDONI, B. & LALLI, E. (2009) Dax-1 knockdown in mouse embryonic stem cells induces loss of pluripotency and multilineage differentiation. *Stem Cells,* 27**,** 1529-37.

KIDWELL, C. S., LIEBESKIND, D. S., STARKMAN, S. & SAVER, J. L. (2001) Trends in acute ischemic stroke trials through the 20th century. *Stroke,* 32**,** 1349-59.

KIM, H. J. & CASADESUS, G. (2010) Estrogen-mediated effects on cognition and synaptic plasticity: What do estrogen receptor knockout models tell us? *Biochim Biophys Acta,* 1800**,** 1090-3.

KIM, J. Y., KOH, H. C., LEE, J. Y., CHANG, M. Y., KIM, Y. C., CHUNG, H. Y., SON, H., LEE, Y. S., STUDER, L., MCKAY, R. & LEE, S. H. (2003) Dopaminergic neuronal differentiation from rat embryonic neural precursors by Nurr1 overexpression. *J Neurochem,* 85**,** 1443-54.

KIMELBERG, H. K., FEUSTEL, P. J., JIN, Y., PAQUETTE, J., BOULOS, A., KELLER, R. W., JR. & TRANMER, B. I. (2000) Acute treatment with tamoxifen reduces ischemic damage following middle cerebral artery occlusion. *Neuroreport,* 11**,** 2675-9.

KIMELBERG, H. K., JIN, Y., CHARNIGA, C. & FEUSTEL, P. J. (2003) Neuroprotective activity of tamoxifen in permanent focal ischemia. *J Neurosurg,* 99**,** 138-42.

KIMOTO, T., TSURUGIZAWA, T., OHTA, Y., MAKINO, J., TAMURA, H., HOJO, Y., TAKATA, N. & KAWATO, S. (2001) Neurosteroid synthesis by cytochrome p450-containing systems localized in the rat brain hippocampal neurons: N-methyl-D-aspartate and calcium-dependent synthesis. *Endocrinology,* 142**,** 3578-89.

KIPP, M. & BEYER, C. (2009) Impact of sex steroids on neuroinflammatory processes and experimental multiple sclerosis. *Front Neuroendocrinol,* 30**,** 188-200.

KISHI, Y., TAKAHASHI, J., KOYANAGI, M., MORIZANE, A., OKAMOTO, Y., HORIGUCHI, S., TASHIRO, K., HONJO, T., FUJII, S. & HASHIMOTO, N. (2005) Estrogen promotes differentiation and survival of dopaminergic neurons derived from human neural stem cells. *J Neurosci Res,* 79**,** 279-86.

KITAGAWA, K., MATSUMOTO, M., YANG, G., MABUCHI, T., YAGITA, Y., HORI, M. & YANAGIHARA, T. (1998) Cerebral ischemia after bilateral carotid artery occlusion and intraluminal suture occlusion in mice: evaluation of the patency of the posterior communicating artery. *J Cereb Blood Flow Metab,* 18**,** 570-9.

KLEIN, M., PIERI, I., UHLMANN, F., PFIZENMAIER, K. & EISEL, U. (1998) Cloning and characterization of promoter and 5'-UTR of the NMDA receptor subunit epsilon 2: evidence for alternative splicing of 5'-non-coding exon. *Gene,* 208**,** 259-69.

KLINGE, C. M., BLANKENSHIP, K. A., RISINGER, K. E., BHATNAGAR, S., NOISIN, E. L., SUMANASEKERA, W. K., ZHAO, L., BREY, D. M. & KEYNTON, R. S. (2005) Resveratrol and estradiol rapidly activate MAPK signaling through estrogen receptors alpha and beta in endothelial cells. *J Biol Chem,* 280**,** 7460-8.

KOFLER, J., HATTORI, K., SAWADA, M., DEVRIES, A. C., MARTIN, L. J., HURN, P. D. & TRAYSTMAN, R. J. (2004) Histopathological and behavioral characterization of a novel model of cardiac arrest and cardiopulmonary resuscitation in mice. *J Neurosci Methods,* 136**,** 33-44.

KOLOMINSKY-RABAS, P. L., WEBER, M., GEFELLER, O., NEUNDOERFER, B. & HEUSCHMANN, P. U. (2001) Epidemiology of ischemic stroke subtypes according to TOAST criteria: incidence, recurrence, and long-term survival in ischemic stroke subtypes: a population-based study. *Stroke,* 32**,** 2735-40.

KONDZIOLKA, D., WECHSLER, L., GOLDSTEIN, S., MELTZER, C., THULBORN, K. R., GEBEL, J., JANNETTA, P., DECESARE, S., ELDER, E. M., MCGROGAN, M., REITMAN, M. A. & BYNUM, L. (2000) Transplantation of cultured human neuronal cells for patients with stroke. *Neurology,* 55**,** 565-9.

KRUPINSKI, J., KALUZA, J., KUMAR, P., KUMAR, S. & WANG, J. M. (1994) Role of angiogenesis in patients with cerebral ischemic stroke. *Stroke,* 25**,** 1794-8.

KUHN, H. G., WINKLER, J., KEMPERMANN, G., THAL, L. J. & GAGE, F. H. (1997) Epidermal growth factor and fibroblast growth factor-2 have different effects on neural progenitors in the adult rat brain. *J Neurosci,* 17**,** 5820-9.

KUIPER, G. G., CARLSSON, B., GRANDIEN, K., ENMARK, E., HAGGBLAD, J., NILSSON, S. & GUSTAFSSON, J. A. (1997) Comparison of the ligand binding specificity and transcript tissue distribution of estrogen receptors alpha and beta. *Endocrinology,* 138**,** 863-70.

KUIPER, G. G. & GUSTAFSSON, J. A. (1997) The novel estrogen receptor-beta subtype: potential role in the cell- and promoter-specific actions of estrogens and anti-estrogens. *FEBS Lett,* 410**,** 87-90.

KUIPER, G. G., SHUGHRUE, P. J., MERCHENTHALER, I. & GUSTAFSSON, J. A. (1998) The estrogen receptor beta subtype: a novel mediator of estrogen action in neuroendocrine systems. *Front Neuroendocrinol,* 19**,** 253-86.

KUMAR, V., ABBAS, A. & FAUSTO, N. (2005) Robbins and Cotran Pathological Basis of Disease *Elsevier,* 7th edition p.1361

KYOSSEVA, S. V. (2004) Mitogen-activated protein kinase signaling. *Int Rev Neurobiol,* 59**,** 201-20.

LALLI, E., BARDONI, B., ZAZOPOULOS, E., WURTZ, J. M., STROM, T. M., MORAS, D. & SASSONE-CORSI, P. (1997) A transcriptional silencing domain in DAX-1 whose mutation causes adrenal hypoplasia congenita. *Mol Endocrinol,* 11**,** 1950-60.

LALLI, E., MELNER, M. H., STOCCO, D. M. & SASSONE-CORSI, P. (1998) DAX-1 blocks steroid production at multiple levels. *Endocrinology,* 139**,** 4237-43.

LALONDE, R., EYER, J., WUNDERLE, V. & STRAZIELLE, C. (2003) Characterization of NFH-LacZ transgenic mice with the SHIRPA primary screening battery and tests of motor coordination, exploratory activity, and spatial learning. *Behav Processes,* 63**,** 9-19.

LAMBERTSEN, K. L., CLAUSEN, B. H., BABCOCK, A. A., GREGERSEN, R., FENGER, C., NIELSEN, H. H., HAUGAARD, L. S., WIRENFELDT, M., NIELSEN, M., DAGNAES-HANSEN, F., BLUETHMANN, H., FAERGEMAN, N. J., MELDGAARD, M., DEIERBORG, T. & FINSEN, B. (2009) Microglia protect neurons against ischemia by synthesis of tumor necrosis factor. *J Neurosci,* 29**,** 1319-30.

LEBESGUE, D., TRAUB, M., DE BUTTE-SMITH, M., CHEN, C., ZUKIN, R. S., KELLY, M. J. & ETGEN, A. M. (2010) Acute administration of non-classical estrogen

receptor agonists attenuates ischemia-induced hippocampal neuron loss in middle-aged female rats. *PLoS One,* 5**,** e8642.

LEE, J. P., JEYAKUMAR, M., GONZALEZ, R., TAKAHASHI, H., LEE, P. J., BAEK, R. C., CLARK, D., ROSE, H., FU, G., CLARKE, J., MCKERCHER, S., MEERLOO, J., MULLER, F. J., PARK, K. I., BUTTERS, T. D., DWEK, R. A., SCHWARTZ, P., TONG, G., WENGER, D., LIPTON, S. A., SEYFRIED, T. N., PLATT, F. M. & SNYDER, E. Y. (2007) Stem cells act through multiple mechanisms to benefit mice with neurodegenerative metabolic disease. *Nat Med,* 13**,** 439-47.

LEE, R. M. (1995) Morphology of cerebral arteries. *Pharmacol Ther,* 66**,** 149-73.

LEE, S. T., CHU, K., JUNG, K. H., KIM, S. J., KIM, D. H., KANG, K. M., HONG, N. H., KIM, J. H., BAN, J. J., PARK, H. K., KIM, S. U., PARK, C. G., LEE, S. K., KIM, M. & ROH, J. K. (2008) Anti-inflammatory mechanism of intravascular neural stem cell transplantation in haemorrhagic stroke. *Brain,* 131**,** 616-29.

LEMIEUX, C., CLOUTIER, I. & TANGUAY, J. F. (2008) Estrogen-induced gene expression in bone marrow c-kit+ stem cells and stromal cells: identification of specific biological processes involved in the functional organization of the stem cell niche. *Stem Cells Dev,* 17**,** 1153-63.

LEPHART, E. D. (1996) A review of brain aromatase cytochrome P450. *Brain Res Brain Res Rev,* 22**,** 1-26.

LERANTH, C., SHANABROUGH, M. & REDMOND, D. E., JR. (2002) Gonadal hormones are responsible for maintaining the integrity of spine synapses in the CA1 hippocampal subfield of female nonhuman primates. *J Comp Neurol,* 447**,** 34-42.

LEWIS, J. S. & JORDAN, V. C. (2005) Selective estrogen receptor modulators (SERMs): mechanisms of anticarcinogenesis and drug resistance. *Mutat Res,* 591**,** 247-63.

LI, F., OMAE, T. & FISHER, M. (1999) Spontaneous hyperthermia and its mechanism in the intraluminal suture middle cerebral artery occlusion model of rats. *Stroke,* 30**,** 2464-70; discussion 2470-1.

LI, L., LUNDKVIST, A., ANDERSSON, D., WILHELMSSON, U., NAGAI, N., PARDO, A. C., NODIN, C., STAHLBERG, A., APRICO, K., LARSSON, K., YABE, T., MOONS, L., FOTHERINGHAM, A., DAVIES, I., CARMELIET, P., SCHWARTZ, J. P., PEKNA, M., KUBISTA, M., BLOMSTRAND, F., MARAGAKIS, N., NILSSON, M. & PEKNY, M. (2008) Protective role of reactive astrocytes in brain ischemia. *J Cereb Blood Flow Metab,* 28**,** 468-81.

LI, X., BLIZZARD, K. K., ZENG, Z., DEVRIES, A. C., HURN, P. D. & MCCULLOUGH, L. D. (2004) Chronic behavioral testing after focal ischemia in the mouse: functional recovery and the effects of gender. *Exp Neurol,* 187**,** 94-104.

LI, Y., CHEN, J., ZHANG, C. L., WANG, L., LU, D., KATAKOWSKI, M., GAO, Q., SHEN, L. H., ZHANG, J., LU, M. & CHOPP, M. (2005) Gliosis and brain remodeling after treatment of stroke in rats with marrow stromal cells. *Glia,* 49**,** 407-17.

LI, Y., JIANG, N., POWERS, C. & CHOPP, M. (1998) Neuronal damage and plasticity identified by microtubule-associated protein 2, growth-associated protein 43, and cyclin D1 immunoreactivity after focal cerebral ischemia in rats. *Stroke,* 29**,** 1972-80; discussion 1980-1.

LIAO, S. L., CHEN, W. Y. & CHEN, C. J. (2002) Estrogen attenuates tumor necrosis factor-alpha expression to provide ischemic neuroprotection in female rats. *Neurosci Lett,* 330**,** 159-62.

LINDNER, V., KIM, S. K., KARAS, R. H., KUIPER, G. G., GUSTAFSSON, J. A. & MENDELSOHN, M. E. (1998) Increased expression of estrogen receptor-beta mRNA in male blood vessels after vascular injury. *Circ Res,* 83**,** 224-9.

LINDVALL, O. & KOKAIA, Z. (2004) Recovery and rehabilitation in stroke: stem cells. *Stroke,* 35**,** 2691-4.

LINDVALL, O. & KOKAIA, Z. (2005) Stem cell therapy for human brain disorders. *Kidney Int,* 68**,** 1937-9.

LITTLETON-KEARNEY, M. T., AGNEW, D. M., TRAYSTMAN, R. J. & HURN, P. D. (2000) Effects of estrogen on cerebral blood flow and pial microvasculature in rabbits. *Am J Physiol Heart Circ Physiol,* 279**,** H1208-14.

LIU, G., WU, Y. S., BRENIN, D., YUE, W., AIYAR, S., GOMPEL, A., WANG, J. P., TEKMAL, R. R. & SANTEN, R. J. (2007) Development of a high sensitivity, nested Q-PCR assay for mouse and human aromatase. *Breast Cancer Res Treat*.

LLOYD-JONES, D., ADAMS, R. J., BROWN, T. M., CARNETHON, M., DAI, S., DE SIMONE, G., FERGUSON, T. B., FORD, E., FURIE, K., GILLESPIE, C., GO, A., GREENLUND, K., HAASE, N., HAILPERN, S., HO, P. M., HOWARD, V., KISSELA, B., KITTNER, S., LACKLAND, D., LISABETH, L., MARELLI, A., MCDERMOTT, M. M., MEIGS, J., MOZAFFARIAN, D., MUSSOLINO, M., NICHOL, G., ROGER, V. L., ROSAMOND, W., SACCO, R., SORLIE, P., THOM, T., WASSERTHIEL-SMOLLER, S., WONG, N. D. & WYLIE-ROSETT, J. (2010) Heart disease and stroke statistics--2010 update: a report from the American Heart Association. *Circulation,* 121**,** e46-e215.

LOH, Y. H., WU, Q., CHEW, J. L., VEGA, V. B., ZHANG, W., CHEN, X., BOURQUE, G., GEORGE, J., LEONG, B., LIU, J., WONG, K. Y., SUNG, K. W., LEE, C. W., ZHAO, X. D., CHIU, K. P., LIPOVICH, L., KUZNETSOV, V. A., ROBSON, P., STANTON, L. W., WEI, C. L., RUAN, Y., LIM, B. & NG, H. H. (2006) The Oct4 and Nanog transcription network regulates pluripotency in mouse embryonic stem cells. *Nat Genet,* 38**,** 431-40.

LONGA, E. Z., WEINSTEIN, P. R., CARLSON, S. & CUMMINS, R. (1989) Reversible middle cerebral artery occlusion without craniectomy in rats. *Stroke,* 20**,** 84-91.

LOUBINOUX, I., VOLK, A., BORREDON, J., GUIRIMAND, S., TIFFON, B., SEYLAZ, J. & MERIC, P. (1997) Spreading of vasogenic edema and cytotoxic edema assessed by quantitative diffusion and T2 magnetic resonance imaging. *Stroke,* 28**,** 419-26; discussion 426-7.

LOVE, S. (2003) Apoptosis and brain ischaemia. *Prog Neuropsychopharmacol Biol Psychiatry,* 27**,** 267-82.

MAKINEN, S., KEKARAINEN, T., NYSTEDT, J., LIIMATAINEN, T., HUHTALA, T., NARVANEN, A., LAINE, J. & JOLKKONEN, J. (2006) Human umbilical cord blood cells do not improve sensorimotor or cognitive outcome following transient middle cerebral artery occlusion in rats. *Brain Res,* 1123**,** 207-15.

MARIN-HUSSTEGE, M., MUGGIRONI, M., RABAN, D., SKOFF, R. P. & CASACCIA-BONNEFIL, P. (2004) Oligodendrocyte progenitor proliferation and maturation is

differentially regulated by male and female sex steroid hormones. *Dev Neurosci,* 26**,** 245-54.

MARTINS, R. S., DELOFFRE, L. A., MYLONAS, C. C., POWER, D. M. & CANARIO, A. V. (2007) Developmental expression of DAX1 in the European sea bass, Dicentrarchus labrax: lack of evidence for sexual dimorphism during sex differentiation. *Reprod Biol Endocrinol,* 5**,** 19.

MAY, T., WIRTH, D., HAUSER, H. & MUELLER, P. P. (2005) Transcriptionally regulated immortalization overcomes side effects of temperature-sensitive SV40 large T antigen. *Biochem Biophys Res Commun,* 327**,** 734-41.

MCAULEY, M. A. (1995) Rodent models of focal ischemia. *Cerebrovasc Brain Metab Rev,* 7**,** 153-80.

MCCOLL, B. W., CARSWELL, H. V., MCCULLOCH, J. & HORSBURGH, K. (2004) Extension of cerebral hypoperfusion and ischaemic pathology beyond MCA territory after intraluminal filament occlusion in C57Bl/6J mice. *Brain Res,* 997**,** 15-23.

MCCULLOUGH, L. D., BLIZZARD, K., SIMPSON, E. R., OZ, O. K. & HURN, P. D. (2003) Aromatase cytochrome P450 and extragonadal estrogen play a role in ischemic neuroprotection. *J Neurosci,* 23**,** 8701-5.

MCEWEN, B. (2002) Estrogen actions throughout the brain. *Recent Prog Horm Res,* 57**,** 357-84.

MCEWEN, B. S. (2001) Invited review: Estrogens effects on the brain: multiple sites and molecular mechanisms. *J Appl Physiol,* 91**,** 2785-801.

MCEWEN, B. S. & ALVES, S. E. (1999) Estrogen actions in the central nervous system. *Endocr Rev,* 20**,** 279-307.

MCILVOY, L. H. (2005) The effect of hypothermia and hyperthermia on acute brain injury. *AACN Clin Issues,* 16**,** 488-500.

MEDA, C., VEGETO, E., POLLIO, G., CIANA, P., PATRONE, C., PELLICCIARI, C. & MAGGI, A. (2000) Oestrogen prevention of neural cell death correlates with decreased expression of mRNA for the pro-apoptotic protein nip-2. *J Neuroendocrinol,* 12**,** 1051-9.

MELLODEW, K., SUHR, R., UWANOGHO, D. A., REUTER, I., LENDAHL, U., HODGES, H. & PRICE, J. (2004) Nestin expression is lost in a neural stem cell line through a mechanism involving the proteasome and Notch signalling. *Brain Res Dev Brain Res,* 151**,** 13-23.

MENDELSOHN, M. E. & KARAS, R. H. (1994) Estrogen and the blood vessel wall. *Curr Opin Cardiol,* 9**,** 619-26.

MENDEZ, P., AZCOITIA, I. & GARCIA-SEGURA, L. M. (2003) Estrogen receptor alpha forms estrogen-dependent multimolecular complexes with insulin-like growth factor receptor and phosphatidylinositol 3-kinase in the adult rat brain. *Brain Res Mol Brain Res,* 112**,** 170-6.

MERGENTHALER, P., DIRNAGL, U. & MEISEL, A. (2004) Pathophysiology of stroke: lessons from animal models. *Metab Brain Dis,* 19**,** 151-67.

MERMELSTEIN, P. G., BECKER, J. B. & SURMEIER, D. J. (1996) Estradiol reduces calcium currents in rat neostriatal neurons via a membrane receptor. *J Neurosci,* 16**,** 595-604.

METZ, G. A. & WHISHAW, I. Q. (2002) Cortical and subcortical lesions impair skilled walking in the ladder rung walking test: a new task to evaluate fore- and hindlimb stepping, placing, and co-ordination. *J Neurosci Methods,* 115**,** 169-79.

METZ, G. A. & WHISHAW, I. Q. (2009) The ladder rung walking task: a scoring system and its practical application. *J Vis Exp*.

MHAIRI MACRAE, I. (1992) New models of focal cerebral ischaemia. *Br J Clin Pharmacol,* 34**,** 302-8.

MIGLIACCIO, A., DI DOMENICO, M., CASTORIA, G., DE FALCO, A., BONTEMPO, P., NOLA, E. & AURICCHIO, F. (1996) Tyrosine kinase/p21ras/MAP-kinase pathway activation by estradiol-receptor complex in MCF-7 cells. *EMBO J,* 15**,** 1292-300.

MIKLYAEVA, E. I., CASTANEDA, E. & WHISHAW, I. Q. (1994) Skilled reaching deficits in unilateral dopamine-depleted rats: impairments in movement and posture and compensatory adjustments. *J Neurosci,* 14**,** 7148-58.

MILLER, R. H. (2006) The promise of stem cells for neural repair. *Brain Res,* 1091**,** 258-64.

MILNER, T. A., MCEWEN, B. S., HAYASHI, S., LI, C. J., REAGAN, L. P. & ALVES, S. E. (2001) Ultrastructural evidence that hippocampal alpha estrogen receptors are located at extranuclear sites. *J Comp Neurol,* 429**,** 355-71.

MINGER, S. L., EKONOMOU, A., CARTA, E. M., CHINOY, A., PERRY, R. H. & BALLARD, C. G. (2007) Endogenous neurogenesis in the human brain following cerebral infarction. *Regen Med,* 2**,** 69-74.

MIRANDA, R. C., SOHRABJI, F. & TORAN-ALLERAND, C. D. (1993a) Neuronal colocalization of mRNAs for neurotrophins and their receptors in the developing central nervous system suggests a potential for autocrine interactions. *Proc Natl Acad Sci U S A,* 90**,** 6439-43.

MIRANDA, R. C., SOHRABJI, F. & TORAN-ALLERAND, C. D. (1993b) Presumptive Estrogen Target Neurons Express mRNAs for both the Neurotrophins and Neurotrophin Receptors: A Basis for Potential Developmental Interactions of Estrogen with the Neurotrophins. *Mol Cell Neurosci,* 4**,** 510-25.

MIURA, M., MIURA, Y., PADILLA-NASH, H. M., MOLINOLO, A. A., FU, B., PATEL, V., SEO, B. M., SONOYAMA, W., ZHENG, J. J., BAKER, C. C., CHEN, W., RIED, T. & SHI, S. (2006) Accumulated chromosomal instability in murine bone marrow mesenchymal stem cells leads to malignant transformation. *Stem Cells,* 24**,** 1095-103.

MODO, M., BEECH, J. S., MEADE, T. J., WILLIAMS, S. C. & PRICE, J. (2009) A chronic 1 year assessment of MRI contrast agent-labelled neural stem cell transplants in stroke. *Neuroimage,* 47 Suppl 2**,** T133-42.

MODO, M., HOPKINS, K., VIRLEY, D. & HODGES, H. (2003) Transplantation of neural stem cells modulates apolipoprotein E expression in a rat model of stroke. *Exp Neurol,* 183**,** 320-9.

MODO, M., REZAIE, P., HEUSCHLING, P., PATEL, S., MALE, D. K. & HODGES, H. (2002a) Transplantation of neural stem cells in a rat model of stroke: assessment of short-term graft survival and acute host immunological response. *Brain Res,* 958**,** 70-82.

MODO, M., STROEMER, R. P., TANG, E., PATEL, S. & HODGES, H. (2002b) Effects of implantation site of stem cell grafts on behavioral recovery from stroke damage. *Stroke,* 33**,** 2270-8.

MODO, M., STROEMER, R. P., TANG, E., VEIZOVIC, T., SOWNISKI, P. & HODGES, H. (2000) Neurological sequelae and long-term behavioural assessment of rats with transient middle cerebral artery occlusion. *J Neurosci Methods,* 104**,** 99-109.

MONCADA, S. & HIGGS, A. (1993) The L-arginine-nitric oxide pathway. *N Engl J Med,* 329**,** 2002-12.

MOODY, S. A. (2005) Stem cells: cell and developmental biology in regenerative medicine. *Biol Cell,* 97**,** 111.

MOORADIAN, A. D. (1993) Antioxidant properties of steroids. *J Steroid Biochem Mol Biol,* 45**,** 509-11.

MORGANTI-KOSSMAN, M. C., LENZLINGER, P. M., HANS, V., STAHEL, P., CSUKA, E., AMMANN, E., STOCKER, R., TRENTZ, O. & KOSSMANN, T. (1997) Production of cytokines following brain injury: beneficial and deleterious for the damaged tissue. *Mol Psychiatry,* 2**,** 133-6.

MORIKAWA, E., MORI, H., KIYAMA, Y., MISHINA, M., ASANO, T. & KIRINO, T. (1998) Attenuation of focal ischemic brain injury in mice deficient in the epsilon1 (NR2A) subunit of NMDA receptor. *J Neurosci,* 18**,** 9727-32.

MORLEY, P., HOGAN, M. J. & HAKIM, A. M. (1994) Calcium-mediated mechanisms of ischemic injury and protection. *Brain Pathol,* 4**,** 37-47.

MORRISON, H., MCKEE, D. & RITTER, L. (2010) Systemic Neutrophil Activation in a Mouse Model of Ischemic Stroke and Reperfusion. *Biol Res Nurs*.

MULLER, F. J., SNYDER, E. Y. & LORING, J. F. (2006) Gene therapy: can neural stem cells deliver? *Nat Rev Neurosci,* 7**,** 75-84.

MURPHY, S., MCCULLOUGH, L., LITTLETON-KEARNEY, M. & HURN, P. (2003) Estrogen and selective estrogen receptor modulators: neuroprotection in the Women's Health Initiative era. *Endocrine,* 21**,** 17-26.

MUSCATELLI, F., STROM, T. M., WALKER, A. P., ZANARIA, E., RECAN, D., MEINDL, A., BARDONI, B., GUIOLI, S., ZEHETNER, G., RABL, W. & ET AL. (1994) Mutations in the DAX-1 gene give rise to both X-linked adrenal hypoplasia congenita and hypogonadotropic hypogonadism. *Nature,* 372**,** 672-6.

MUTHALIF, M. M., KARZOUN, N. A., BENTER, I. F., GABER, L., LJUCA, F., UDDIN, M. R., KHANDEKAR, Z., ESTES, A. & MALIK, K. U. (2002) Functional significance of activation of calcium/calmodulin-dependent protein kinase II in angiotensin II--induced vascular hyperplasia and hypertension. *Hypertension,* 39**,** 704-9.

NAFTOLIN, F., RYAN, K. J. & PETRO, Z. (1971) Aromatization of androstenedione by the diencephalon. *J Clin Endocrinol Metab,* 33**,** 368-70.

NELSON, T. J., MARTINEZ-FERNANDEZ, A., YAMADA, S., IKEDA, Y., PEREZ-TERZIC, C. & TERZIC, A. (2010) Induced pluripotent stem cells: advances to applications. *Stem Cells Cloning,* 3**,** 29-37.

NELSON, T. J., MARTINEZ-FERNANDEZ, A., YAMADA, S., PEREZ-TERZIC, C., IKEDA, Y. & TERZIC, A. (2009) Repair of acute myocardial infarction by human stemness factors induced pluripotent stem cells. *Circulation,* 120**,** 408-16.

NIAKAN, K. K., DAVIS, E. C., CLIPSHAM, R. C., JIANG, M., DEHART, D. B., SULIK, K. K. & MCCABE, E. R. (2006) Novel role for the orphan nuclear receptor Dax1 in embryogenesis, different from steroidogenesis. *Mol Genet Metab,* 88**,** 261-71.

NILSSON, S., MAKELA, S., TREUTER, E., TUJAGUE, M., THOMSEN, J., ANDERSSON, G., ENMARK, E., PETTERSSON, K., WARNER, M. & GUSTAFSSON, J. A. (2001) Mechanisms of estrogen action. *Physiol Rev,* 81**,** 1535-65.

NISHIGAYA, K., YOSHIDA, Y., SASUGA, M., NUKUI, H. & OONEDA, G. (1991) Effect of recirculation on exacerbation of ischemic vascular lesions in rat brain. *Stroke,* 22**,** 635-42.

O'DOWD, B. F., NGUYEN, T., MARCHESE, A., CHENG, R., LYNCH, K. R., HENG, H. H., KOLAKOWSKI, L. F., JR. & GEORGE, S. R. (1998) Discovery of three novel G-protein-coupled receptor genes. *Genomics,* 47**,** 310-3.

OLIFF, H. S., WEBER, E., MIYAZAKI, B. & MAREK, P. (1995) Infarct volume varies with rat strain and vendor in focal cerebral ischemia induced by transcranial middle cerebral artery occlusion. *Brain Res,* 699**,** 329-31.

ONAL, M. Z. & FISHER, M. (1997) Acute ischemic stroke therapy. A clinical overview. *Eur Neurol,* 38**,** 141-54.

ONYSZCHUK, G., AL-HAFEZ, B., HE, Y. Y., BILGEN, M., BERMAN, N. E. & BROOKS, W. M. (2007) A mouse model of sensorimotor controlled cortical impact: characterization using longitudinal magnetic resonance imaging, behavioral assessments and histology. *J Neurosci Methods,* 160**,** 187-96.

ORLIC, D., KAJSTURA, J., CHIMENTI, S., JAKONIUK, I., ANDERSON, S. M., LI, B., PICKEL, J., MCKAY, R., NADAL-GINARD, B., BODINE, D. M., LERI, A. & ANVERSA, P. (2001) Bone marrow cells regenerate infarcted myocardium. *Nature,* 410**,** 701-5.

OSBORNE, K. A., SHIGENO, T., BALARSKY, A. M., FORD, I., MCCULLOCH, J., TEASDALE, G. M. & GRAHAM, D. I. (1987) Quantitative assessment of early brain damage in a rat model of focal cerebral ischaemia. *J Neurol Neurosurg Psychiatry,* 50**,** 402-10.

PARK, C. K. & KANG, S. G. (2000) Effects of brain oedema in the measurement of ischaemic brain damage in focal cerebral infarction. *Acta Neurochir Suppl,* 76**,** 269-71.

PARK, I. H., LEROU, P. H., ZHAO, R., HUO, H. & DALEY, G. Q. (2008) Generation of human-induced pluripotent stem cells. *Nat Protoc,* 3**,** 1180-6.

PARK, K. I. (2000) Transplantation of neural stem cells: cellular & gene therapy for hypoxic-ischemic brain injury. *Yonsei Med J,* 41**,** 825-35.

PARK, K. I., TENG, Y. D. & SNYDER, E. Y. (2002) The injured brain interacts reciprocally with neural stem cells supported by scaffolds to reconstitute lost tissue. *Nat Biotechnol,* 20**,** 1111-7.

PATRONE, C., ANDERSSON, S., KORHONEN, L. & LINDHOLM, D. (1999) Estrogen receptor-dependent regulation of sensory neuron survival in developing dorsal root ganglion. *Proc Natl Acad Sci U S A,* 96**,** 10905-10.

PEDERSEN, A. T., LIDEGAARD, O., KREINER, S. & OTTESEN, B. (1997) Hormone replacement therapy and risk of non-fatal stroke. *Lancet,* 350**,** 1277-83.

PELLIGRINO, D. A., SANTIZO, R., BAUGHMAN, V. L. & WANG, Q. (1998) Cerebral vasodilating capacity during forebrain ischemia: effects of chronic estrogen depletion and repletion and the role of neuronal nitric oxide synthase. *Neuroreport,* 9**,** 3285-91.

PEREL, P., ROBERTS, I., SENA, E., WHEBLE, P., BRISCOE, C., SANDERCOCK, P., MACLEOD, M., MIGNINI, L. E., JAYARAM, P. & KHAN, K. S. (2007) Comparison of treatment effects between animal experiments and clinical trials: systematic review. *BMJ,* 334**,** 197.

PERRY, V. H., NICOLL, J. A. & HOLMES, C. (2010) Microglia in neurodegenerative disease. *Nat Rev Neurol,* 6**,** 193-201.

PETTERSSON, K., GRANDIEN, K., KUIPER, G. G. & GUSTAFSSON, J. A. (1997) Mouse estrogen receptor beta forms estrogen response element-binding heterodimers with estrogen receptor alpha. *Mol Endocrinol,* 11**,** 1486-96.

PLACHTA, N., BIBEL, M., TUCKER, K. L. & BARDE, Y. A. (2004) Developmental potential of defined neural progenitors derived from mouse embryonic stem cells. *Development,* 131**,** 5449-56.

PLATANIA, P., LAUREANTI, F., BELLOMO, M., GIUFFRIDA, R., GIUFFRIDA-STELLA, A. M., CATANIA, M. V. & SORTINO, M. A. (2003) Differential expression of estrogen receptors alpha and beta in the spinal cord during postnatal development: localization in glial cells. *Neuroendocrinology,* 77**,** 334-40.

PLUCHINO, S., QUATTRINI, A., BRAMBILLA, E., GRITTI, A., SALANI, G., DINA, G., GALLI, R., DEL CARRO, U., AMADIO, S., BERGAMI, A., FURLAN, R., COMI, G., VESCOVI, A. L. & MARTINO, G. (2003) Injection of adult neurospheres induces recovery in a chronic model of multiple sclerosis. *Nature,* 422**,** 688-94.

PLUCHINO, S., ZANOTTI, L., ROSSI, B., BRAMBILLA, E., OTTOBONI, L., SALANI, G., MARTINELLO, M., CATTALINI, A., BERGAMI, A., FURLAN, R., COMI, G., CONSTANTIN, G. & MARTINO, G. (2005) Neurosphere-derived multipotent precursors promote neuroprotection by an immunomodulatory mechanism. *Nature,* 436**,** 266-71.

POLLOCK, K., STROEMER, P., PATEL, S., STEVANATO, L., HOPE, A., MILJAN, E., DONG, Z., HODGES, H., PRICE, J. & SINDEN, J. D. (2006) A conditionally immortal clonal stem cell line from human cortical neuroepithelium for the treatment of ischemic stroke. *Exp Neurol,* 199**,** 143-55.

PROCKOP, D. J. (1997) Marrow stromal cells as stem cells for nonhematopoietic tissues. *Science,* 276**,** 71-4.

PROSSNITZ, E. R., OPREA, T. I., SKLAR, L. A. & ARTERBURN, J. B. (2008a) The ins and outs of GPR30: a transmembrane estrogen receptor. *J Steroid Biochem Mol Biol,* 109**,** 350-3.

PROSSNITZ, E. R., SKLAR, L. A., OPREA, T. I. & ARTERBURN, J. B. (2008b) GPR30: a novel therapeutic target in estrogen-related disease. *Trends Pharmacol Sci,* 29**,** 116-23.

RABB, C. H. (1996) Nylon monofilament for intraluminal middle cerebral artery occlusion in rats. *Stroke,* 27**,** 151.

RALEA, I. C., RIOUFOL, G., CAKMAK, S., DEREX, L. & NIGHOGHOSSIAN, N. (2009) Acute stroke and heart attack management within a four-hour time window. *J Stroke Cerebrovasc Dis,* 18**,** 167-70.

RAU, S. W., DUBAL, D. B., BOTTNER, M., GERHOLD, L. M. & WISE, P. M. (2003) Estradiol attenuates programmed cell death after stroke-like injury. *J Neurosci,* 23**,** 11420-6.

REGLODI, D., SOMOGYVARI-VIGH, A., MADERDRUT, J. L., VIGH, S. & ARIMURA, A. (2000) Postischemic spontaneous hyperthermia and its effects in middle cerebral artery occlusion in the rat. *Exp Neurol,* 163**,** 399-407.

REGLODI, D., TAMAS, A. & LENGVARI, I. (2003) Examination of sensorimotor performance following middle cerebral artery occlusion in rats. *Brain Res Bull,* 59**,** 459-66.

REVANKAR, C. M., CIMINO, D. F., SKLAR, L. A., ARTERBURN, J. B. & PROSSNITZ, E. R. (2005) A transmembrane intracellular estrogen receptor mediates rapid cell signaling. *Science,* 307**,** 1625-30.

REYNA-NEYRA, A., CAMACHO-ARROYO, I., FERRERA, P. & ARIAS, C. (2002) Estradiol and progesterone modify microtubule associated protein 2 content in the rat hippocampus. *Brain Res Bull,* 58**,** 607-12.

REYNOLDS, B. A. & WEISS, S. (1992) Generation of neurons and astrocytes from isolated cells of the adult mammalian central nervous system. *Science,* 255**,** 1707-10.

RICHARD GREEN, A., ODERGREN, T. & ASHWOOD, T. (2003) Animal models of stroke: do they have value for discovering neuroprotective agents? *Trends Pharmacol Sci,* 24**,** 402-8.

RIEK-BURCHARDT, M., HENRICH-NOACK, P., METZ, G. A. & REYMANN, K. G. (2004) Detection of chronic sensorimotor impairments in the ladder rung walking task in rats with endothelin-1-induced mild focal ischemia. *J Neurosci Methods,* 137**,** 227-33.

RINGLEB, P. A., SCHELLINGER, P. D., SCHRANZ, C. & HACKE, W. (2002) Thrombolytic therapy within 3 to 6 hours after onset of ischemic stroke: useful or harmful? *Stroke,* 33**,** 1437-41.

RONNEKLEIV, O. K., MALYALA, A. & KELLY, M. J. (2007) Membrane-initiated signaling of estrogen in the brain. *Semin Reprod Med,* 25**,** 165-77.

ROSELLI, C. F. (2007) Brain aromatase: roles in reproduction and neuroprotection. *J Steroid Biochem Mol Biol,* 106**,** 143-50.

ROSSBERG, M. I., MURPHY, S. J., TRAYSTMAN, R. J. & HURN, P. D. (2000) LY353381.HCl, a selective estrogen receptor modulator, and experimental stroke. *Stroke,* 31**,** 3041-6.

ROSSI, F., GIANOLA, S. & CORVETTI, L. (2007) Regulation of intrinsic neuronal properties for axon growth and regeneration. *Prog Neurobiol,* 81**,** 1-28.

ROSSOUW, J. E., ANDERSON, G. L., PRENTICE, R. L., LACROIX, A. Z., KOOPERBERG, C., STEFANICK, M. L., JACKSON, R. D., BERESFORD, S. A., HOWARD, B. V., JOHNSON, K. C., KOTCHEN, J. M. & OCKENE, J. (2002) Risks and benefits of estrogen plus progestin in healthy postmenopausal women: principal results From the Women's Health Initiative randomized controlled trial. *JAMA,* 288**,** 321-33.

ROTHWELL, P. M. (2001) The high cost of not funding stroke research: a comparison with heart disease and cancer. *Lancet,* 357**,** 1612-6.

ROUHL, R. P., VAN OOSTENBRUGGE, R. J., DAMOISEAUX, J., COHEN TERVAERT, J. W. & LODDER, J. (2008) Endothelial progenitor cell research in stroke: a potential shift in pathophysiological and therapeutical concepts. *Stroke,* 39**,** 2158-65.

ROY, N. S., CLEREN, C., SINGH, S. K., YANG, L., BEAL, M. F. & GOLDMAN, S. A. (2006) Functional engraftment of human ES cell-derived dopaminergic neurons enriched by coculture with telomerase-immortalized midbrain astrocytes. *Nat Med,* 12**,** 1259-68.

RUBIO, D., GARCIA-CASTRO, J., MARTIN, M. C., DE LA FUENTE, R., CIGUDOSA, J. C., LLOYD, A. C. & BERNAD, A. (2005) Spontaneous human adult stem cell transformation. *Cancer Res,* 65**,** 3035-9.

RUSA, R., ALKAYED, N. J., CRAIN, B. J., TRAYSTMAN, R. J., KIMES, A. S., LONDON, E. D., KLAUS, J. A. & HURN, P. D. (1999) 17beta-estradiol reduces stroke injury in estrogen-deficient female animals. *Stroke,* 30**,** 1665-70.

SAKA, O., MCGUIRE, A. & WOLFE, C. (2009) Cost of stroke in the United Kingdom. *Age Ageing,* 38**,** 27-32.

SAKAMOTO, H., MEZAKI, Y., SHIKIMI, H., UKENA, K. & TSUTSUI, K. (2003) Dendritic growth and spine formation in response to estrogen in the developing Purkinje cell. *Endocrinology,* 144**,** 4466-77.

SAMPEI, K., GOTO, S., ALKAYED, N. J., CRAIN, B. J., KORACH, K. S., TRAYSTMAN, R. J., DEMAS, G. E., NELSON, R. J. & HURN, P. D. (2000) Stroke in estrogen receptor-alpha-deficient mice. *Stroke,* 31**,** 738-43; discussion 744.

SANCHEZ-RAMOS, J., SONG, S., CARDOZO-PELAEZ, F., HAZZI, C., STEDEFORD, T., WILLING, A., FREEMAN, T. B., SAPORTA, S., JANSSEN, W., PATEL, N., COOPER, D. R. & SANBERG, P. R. (2000) Adult bone marrow stromal cells differentiate into neural cells in vitro. *Exp Neurol,* 164**,** 247-56.

SAPORTA, S., BORLONGAN, C. V. & SANBERG, P. R. (1999) Neural transplantation of human neuroteratocarcinoma (hNT) neurons into ischemic rats. A quantitative dose-response analysis of cell survival and behavioral recovery. *Neuroscience,* 91**,** 519-25.

SATO, K., MATSUKI, N., OHNO, Y. & NAKAZAWA, K. (2003) Estrogens inhibit l-glutamate uptake activity of astrocytes via membrane estrogen receptor alpha. *J Neurochem,* 86**,** 1498-505.

SAVER, J. L., ALBERS, G. W., DUNN, B., JOHNSTON, K. C. & FISHER, M. (2009) Stroke Therapy Academic Industry Roundtable (STAIR) recommendations for extended window acute stroke therapy trials. *Stroke,* 40**,** 2594-600.

SAVITZ, S. I., ROSENBAUM, D. M., DINSMORE, J. H., WECHSLER, L. R. & CAPLAN, L. R. (2002) Cell transplantation for stroke. *Ann Neurol,* 52**,** 266-75.

SAVITZ, S. L., MALHOTRA, S., GUPTA, G. & ROSENBAUM, D. M. (2003) Cell transplants offer promise for stroke recovery. *J Cardiovasc Nurs,* 18**,** 57-61.

SAWADA, H., IBI, M., KIHARA, T., URUSHITANI, M., HONDA, K., NAKANISHI, M., AKAIKE, A. & SHIMOHAMA, S. (2000) Mechanisms of antiapoptotic effects of estrogens in nigral dopaminergic neurons. *FASEB J,* 14**,** 1202-14.

SCHABITZ, W. R., KRUGER, C., PITZER, C., WEBER, D., LAAGE, R., GASSLER, N., ARONOWSKI, J., MIER, W., KIRSCH, F., DITTGEN, T., BACH, A., SOMMER, C. & SCHNEIDER, A. (2008) A neuroprotective function for the hematopoietic protein granulocyte-macrophage colony stimulating factor (GM-CSF). *J Cereb Blood Flow Metab,* 28**,** 29-43.

SCHABITZ, W. R. & SCHNEIDER, A. (2007) New targets for established proteins: exploring G-CSF for the treatment of stroke. *Trends Pharmacol Sci,* 28**,** 157-61.

SCHALLERT, T., FLEMING, S. M., LEASURE, J. L., TILLERSON, J. L. & BLAND, S. T. (2000) CNS plasticity and assessment of forelimb sensorimotor outcome in unilateral rat models of stroke, cortical ablation, parkinsonism and spinal cord injury. *Neuropharmacology,* 39**,** 777-87.

SCHALLERT, T., UPCHURCH, M., LOBAUGH, N., FARRAR, S. B., SPIRDUSO, W. W., GILLIAM, P., VAUGHN, D. & WILCOX, R. E. (1982) Tactile extinction: distinguishing between sensorimotor and motor asymmetries in rats with unilateral nigrostriatal damage. *Pharmacol Biochem Behav,* 16**,** 455-62.

SCHEFFLER, B., SCHMANDT, T., SCHRODER, W., STEINFARZ, B., HUSSEINI, L., WELLMER, J., SEIFERT, G., KARRAM, K., BECK, H., BLUMCKE, I., WIESTLER, O. D., STEINHAUSER, C. & BRUSTLE, O. (2003) Functional network integration of embryonic stem cell-derived astrocytes in hippocampal slice cultures. *Development,* 130**,** 5533-41.

SCHMID-ELSAESSER, R., ZAUSINGER, S., HUNGERHUBER, E., BAETHMANN, A. & REULEN, H. J. (1998) A critical reevaluation of the intraluminal thread model of focal cerebral ischemia: evidence of inadvertent premature reperfusion and subarachnoid hemorrhage in rats by laser-Doppler flowmetry. *Stroke,* 29**,** 2162-70.

SCHNEIDER, A., KRUGER, C., STEIGLEDER, T., WEBER, D., PITZER, C., LAAGE, R., ARONOWSKI, J., MAURER, M. H., GASSLER, N., MIER, W., HASSELBLATT, M., KOLLMAR, R., SCHWAB, S., SOMMER, C., BACH, A., KUHN, H. G. & SCHABITZ, W. R. (2005) The hematopoietic factor G-CSF is a neuronal ligand that counteracts programmed cell death and drives neurogenesis. *J Clin Invest,* 115**,** 2083-98.

SCHOEPP, D. D. & CONN, P. J. (1993) Metabotropic glutamate receptors in brain function and pathology. *Trends Pharmacol Sci,* 14**,** 13-20.

SCHWARTZ, R. E., REYES, M., KOODIE, L., JIANG, Y., BLACKSTAD, M., LUND, T., LENVIK, T., JOHNSON, S., HU, W. S. & VERFAILLIE, C. M. (2002) Multipotent adult progenitor cells from bone marrow differentiate into functional hepatocyte-like cells. *J Clin Invest,* 109**,** 1291-302.

SEBASTIAN, S. & BULUN, S. E. (2001) A highly complex organization of the regulatory region of the human CYP19 (aromatase) gene revealed by the Human Genome Project. *J Clin Endocrinol Metab,* 86**,** 4600-2.

SERAFINI, M., DYLLA, S. J., OKI, M., HEREMANS, Y., TOLAR, J., JIANG, Y., BUCKLEY, S. M., PELACHO, B., BURNS, T. C., FROMMER, S., ROSSI, D. J., BRYDER, D., PANOSKALTSIS-MORTARI, A., O'SHAUGHNESSY, M. J., NELSON-HOLTE, M., FINE, G. C., WEISSMAN, I. L., BLAZAR, B. R. & VERFAILLIE, C. M. (2007) Hematopoietic reconstitution by multipotent adult progenitor cells: precursors to long-term hematopoietic stem cells. *J Exp Med,* 204**,** 129-39.

SHAH, Z. A., NAMIRANIAN, K., KLAUS, J., KIBLER, K. & DORE, S. (2006) Use of an optimized transient occlusion of the middle cerebral artery protocol for the mouse stroke model. *J Stroke Cerebrovasc Dis,* 15**,** 133-8.

SHEN, C. C., LIN, C. H., YANG, Y. C., CHIAO, M. T., CHENG, W. Y. & KO, J. L. (2010) Intravenous implanted neural stem cells migrate to injury site, reduce infarct volume, and improve behavior after cerebral ischemia. *Curr Neurovasc Res,* 7**,** 167-79.

SHEN, L. H., LI, Y., CHEN, J., ZHANG, J., VANGURI, P., BORNEMAN, J. & CHOPP, M. (2006) Intracarotid transplantation of bone marrow stromal cells increases axon-myelin remodeling after stroke. *Neuroscience,* 137**,** 393-9.

SHI, J., PANICKAR, K. S., YANG, S. H., RABBANI, O., DAY, A. L. & SIMPKINS, J. W. (1998) Estrogen attenuates over-expression of beta-amyloid precursor protein messager RNA in an animal model of focal ischemia. *Brain Res,* 810**,** 87-92.

SHIGENO, T., MCCULLOCH, J., GRAHAM, D. I., MENDELOW, A. D. & TEASDALE, G. M. (1985) Pure cortical ischemia versus striatal ischemia. Circulatory, metabolic, and neuropathologic consequences. *Surg Neurol,* 24**,** 47-51.

SHIMAMURA, N., MATCHETT, G., YATSUSHIGE, H., CALVERT, J. W., OHKUMA, H. & ZHANG, J. (2006) Inhibition of integrin alphavbeta3 ameliorates focal cerebral ischemic damage in the rat middle cerebral artery occlusion model. *Stroke,* 37**,** 1902-9.

SHUGHRUE, P. J. & DORSA, D. M. (1993) Estrogen modulates the growth-associated protein GAP-43 (Neuromodulin) mRNA in the rat preoptic area and basal hypothalamus. *Neuroendocrinology,* 57**,** 439-47.

SHUGHRUE, P. J., SCRIMO, P. J. & MERCHENTHALER, I. (2000) Estrogen binding and estrogen receptor characterization (ERalpha and ERbeta) in the cholinergic neurons of the rat basal forebrain. *Neuroscience,* 96**,** 41-9.

SIMPKINS, J. W., RAJAKUMAR, G., ZHANG, Y. Q., SIMPKINS, C. E., GREENWALD, D., YU, C. J., BODOR, N. & DAY, A. L. (1997) Estrogens may reduce mortality and ischemic damage caused by middle cerebral artery occlusion in the female rat. *J Neurosurg,* 87**,** 724-30.

SINDEN, J. D., RASHID-DOUBELL, F., KERSHAW, T. R., NELSON, A., CHADWICK, A., JAT, P. S., NOBLE, M. D., HODGES, H. & GRAY, J. A. (1997) Recovery of spatial learning by grafts of a conditionally immortalized hippocampal neuroepithelial cell line into the ischaemia-lesioned hippocampus. *Neuroscience,* 81**,** 599-608.

SINGER, C. A., FIGUEROA-MASOT, X. A., BATCHELOR, R. H. & DORSA, D. M. (1999) The mitogen-activated protein kinase pathway mediates estrogen neuroprotection after glutamate toxicity in primary cortical neurons. *J Neurosci,* 19**,** 2455-63.

SINGER, C. A., ROGERS, K. L. & DORSA, D. M. (1998) Modulation of Bcl-2 expression: a potential component of estrogen protection in NT2 neurons. *Neuroreport,* 9**,** 2565-8.

SINGER, C. A., ROGERS, K. L., STRICKLAND, T. M. & DORSA, D. M. (1996) Estrogen protects primary cortical neurons from glutamate toxicity. *Neurosci Lett,* 212**,** 13-6.

SMITH, A. G. (2001) Embryo-derived stem cells: of mice and men. *Annu Rev Cell Dev Biol,* 17**,** 435-62.

SMITH, W. S. (2004) Pathophysiology of focal cerebral ischemia: a therapeutic perspective. *J Vasc Interv Radiol,* 15**,** S3-12.

SPRIGG, N., BATH, P. M., ZHAO, L., WILLMOT, M. R., GRAY, L. J., WALKER, M. F., DENNIS, M. S. & RUSSELL, N. (2006) Granulocyte-colony-stimulating factor mobilizes bone marrow stem cells in patients with subacute ischemic stroke: the Stem cell Trial of recovery EnhanceMent after Stroke (STEMS) pilot randomized, controlled trial (ISRCTN 16784092). *Stroke,* 37**,** 2979-83.

SQUIRE, L., ROBERTS, J, SPITZER N., ZIGMOND M., MCCONNELL S., BLOOM FLOYD E. (2003) Fundamental Neuroscience, Second edition, San Diego.

SRIBNICK, E. A., WINGRAVE, J. M., MATZELLE, D. D., RAY, S. K. & BANIK, N. L. (2003) Estrogen as a neuroprotective agent in the treatment of spinal cord injury. *Ann N Y Acad Sci,* 993**,** 125-33; discussion 159-60.

STARKEY, M. L., BARRITT, A. W., YIP, P. K., DAVIES, M., HAMERS, F. P., MCMAHON, S. B. & BRADBURY, E. J. (2005) Assessing behavioural function following a pyramidotomy lesion of the corticospinal tract in adult mice. *Exp Neurol,* 195**,** 524-39.

STREHLOW, K., WERNER, N., BERWEILER, J., LINK, A., DIRNAGL, U., PRILLER, J., LAUFS, K., GHAENI, L., MILOSEVIC, M., BOHM, M. & NICKENIG, G. (2003) Estrogen increases bone marrow-derived endothelial progenitor cell production and diminishes neointima formation. *Circulation,* 107**,** 3059-65.

STROEMER, R. P., KENT, T. A. & HULSEBOSCH, C. E. (1995) Neocortical neural sprouting, synaptogenesis, and behavioral recovery after neocortical infarction in rats. *Stroke,* 26**,** 2135-44.

STROM, J. O., THEODORSSON, A. & THEODORSSON, E. (2009) Dose-related neuroprotective versus neurodamaging effects of estrogens in rat cerebral ischemia: a systematic analysis. *J Cereb Blood Flow Metab,* 29**,** 1359-72.

STRUBLE, R. G., ROSARIO, E. R., KIRCHER, M. L., LUDWIG, S. M., MCADAMIS, P. J., WATABE, K., MCASEY, M. E., CADY, C. & NATHAN, B. P. (2003)

Regionally specific modulation of brain apolipoprotein E in the mouse during the estrous cycle and by exogenous 17beta estradiol. *Exp Neurol,* 183**,** 638-44.

SUAREZ, J. I., TARR, R. W. & SELMAN, W. R. (2006) Aneurysmal subarachnoid hemorrhage. *N Engl J Med,* 354**,** 387-96.

SUN, H., WANG, H. & HU, S. (2010) Effects of estrogen on diverse stem cells and relevant intracellular mechanisms. *Sci China Life Sci,* 53**,** 542-7.

SUN, N., PANETTA, N. J., GUPTA, D. M., WILSON, K. D., LEE, A., JIA, F., HU, S., CHERRY, A. M., ROBBINS, R. C., LONGAKER, M. T. & WU, J. C. (2009) Feeder-free derivation of induced pluripotent stem cells from adult human adipose stem cells. *Proc Natl Acad Sci U S A,* 106**,** 15720-5.

SUZUKI, S., GERHOLD, L. M., BOTTNER, M., RAU, S. W., DELA CRUZ, C., YANG, E., ZHU, H., YU, J., CASHION, A. B., KINDY, M. S., MERCHENTHALER, I., GAGE, F. H. & WISE, P. M. (2007) Estradiol enhances neurogenesis following ischemic stroke through estrogen receptors alpha and beta. *J Comp Neurol,* 500**,** 1064-75.

SVED, A. F., ITO, S. & YAJIMA, Y. (2002) Role of excitatory amino acid inputs to the rostral ventrolateral medulla in cardiovascular regulation. *Clin Exp Pharmacol Physiol,* 29**,** 503-6.

SVENDSEN, C. N., CLARKE, D. J., ROSSER, A. E. & DUNNETT, S. B. (1996) Survival and differentiation of rat and human epidermal growth factor-responsive precursor cells following grafting into the lesioned adult central nervous system. *Exp Neurol,* 137**,** 376-88.

SWAIN, A. & LOVELL-BADGE, R. (1997) A molecular approach to sex determination in mammals. *Acta Paediatr Suppl,* 423**,** 46-9.

SWANSON, R. A., MORTON, M. T., TSAO-WU, G., SAVALOS, R. A., DAVIDSON, C. & SHARP, F. R. (1990) A semiautomated method for measuring brain infarct volume. *J Cereb Blood Flow Metab,* 10**,** 290-3.

TAKAGI, Y., TAKAHASHI, J., SAIKI, H., MORIZANE, A., HAYASHI, T., KISHI, Y., FUKUDA, H., OKAMOTO, Y., KOYANAGI, M., IDEGUCHI, M., HAYASHI, H., IMAZATO, T., KAWASAKI, H., SUEMORI, H., OMACHI, S., IIDA, H., ITOH, N., NAKATSUJI, N., SASAI, Y. & HASHIMOTO, N. (2005) Dopaminergic neurons generated from monkey embryonic stem cells function in a Parkinson primate model. *J Clin Invest,* 115**,** 102-9.

TAKAHASHI, K., OKITA, K., NAKAGAWA, M. & YAMANAKA, S. (2007) Induction of pluripotent stem cells from fibroblast cultures. *Nat Protoc,* 2**,** 3081-9.

TAKIZAWA, S., HOGAN, M. & HAKIM, A. M. (1991) The effects of a competitive NMDA receptor antagonist (CGS-19755) on cerebral blood flow and pH in focal ischemia. *J Cereb Blood Flow Metab,* 11**,** 786-93.

TAMURA, A., GRAHAM, D. I., MCCULLOCH, J. & TEASDALE, G. M. (1981) Focal cerebral ischaemia in the rat: 1. Description of technique and early neuropathological consequences following middle cerebral artery occlusion. *J Cereb Blood Flow Metab,* 1**,** 53-60.

TANAPAT, P., HASTINGS, N. B. & GOULD, E. (2005) Ovarian steroids influence cell proliferation in the dentate gyrus of the adult female rat in a dose- and time-dependent manner. *J Comp Neurol,* 481**,** 252-65.

TANAPAT, P., HASTINGS, N. B., REEVES, A. J. & GOULD, E. (1999) Estrogen stimulates a transient increase in the number of new neurons in the dentate gyrus of the adult female rat. *J Neurosci,* 19**,** 5792-801.

TEGTMEYER, P. (1975) Function of simian virus 40 gene A in transforming infection. *J Virol,* 15**,** 613-8.

TEMPLE, S. (2001) The development of neural stem cells. *Nature,* 414**,** 112-7.

THANVI, B. & ROBINSON, T. (2006) Sporadic cerebral amyloid angiopathy--an important cause of cerebral haemorrhage in older people. *Age Ageing,* 35**,** 565-71.

THOMAS, P., PANG, Y., FILARDO, E. J. & DONG, J. (2005) Identity of an estrogen membrane receptor coupled to a G protein in human breast cancer cells. *Endocrinology,* 146**,** 624-32.

THRIFT, A. G., DEWEY, H. M., MACDONELL, R. A., MCNEIL, J. J. & DONNAN, G. A. (2001) Incidence of the major stroke subtypes: initial findings from the North East Melbourne stroke incidence study (NEMESIS). *Stroke,* 32**,** 1732-8.

TIWARI-WOODRUFF, S., MORALES, L. B., LEE, R. & VOSKUHL, R. R. (2007) Differential neuroprotective and antiinflammatory effects of estrogen receptor (ER)alpha and ERbeta ligand treatment. *Proc Natl Acad Sci U S A,* 104**,** 14813-8.

TOLAR, J., NAUTA, A. J., OSBORN, M. J., PANOSKALTSIS MORTARI, A., MCELMURRY, R. T., BELL, S., XIA, L., ZHOU, N., RIDDLE, M., SCHROEDER, T. M., WESTENDORF, J. J., MCIVOR, R. S., HOGENDOORN, P. C., SZUHAI, K., OSETH, L., HIRSCH, B., YANT, S. R., KAY, M. A., PEISTER, A., PROCKOP, D. J., FIBBE, W. E. & BLAZAR, B. R. (2007) Sarcoma derived from cultured mesenchymal stem cells. *Stem Cells,* 25**,** 371-9.

TOMAS-CAMARDIEL, M., VENERO, J. L., HERRERA, A. J., DE PABLOS, R. M., PINTOR-TORO, J. A., MACHADO, A. & CANO, J. (2005) Blood-brain barrier disruption highly induces aquaporin-4 mRNA and protein in perivascular and parenchymal astrocytes: protective effect by estradiol treatment in ovariectomized animals. *J Neurosci Res,* 80**,** 235-46.

TORAN-ALLERAND, C. D. (2004a) Estrogen and the brain: beyond ER-alpha and ER-beta. *Exp Gerontol,* 39**,** 1579-86.

TORAN-ALLERAND, C. D. (2004b) Minireview: A plethora of estrogen receptors in the brain: where will it end? *Endocrinology,* 145**,** 1069-74.

TORAN-ALLERAND, C. D., ELLIS, L. & PFENNINGER, K. H. (1988) Estrogen and insulin synergism in neurite growth enhancement in vitro: mediation of steroid effects by interactions with growth factors? *Brain Res,* 469**,** 87-100.

TORAN-ALLERAND, C. D., MIRANDA, R. C., BENTHAM, W. D., SOHRABJI, F., BROWN, T. J., HOCHBERG, R. B. & MACLUSKY, N. J. (1992) Estrogen receptors colocalize with low-affinity nerve growth factor receptors in cholinergic neurons of the basal forebrain. *Proc Natl Acad Sci U S A,* 89**,** 4668-72.

TOUNG, T. J., TRAYSTMAN, R. J. & HURN, P. D. (1998) Estrogen-mediated neuroprotection after experimental stroke in male rats. *Stroke,* 29**,** 1666-70.

TOUZANI, O., BOUTIN, H., LEFEUVRE, R., PARKER, L., MILLER, A., LUHESHI, G. & ROTHWELL, N. (2002) Interleukin-1 influences ischemic brain damage in the mouse independently of the interleukin-1 type I receptor. *J Neurosci,* 22**,** 38-43.

TRANQUE, P. A., SUAREZ, I., OLMOS, G., FERNANDEZ, B. & GARCIA-SEGURA, L. M. (1987) Estradiol--induced redistribution of glial fibrillary acidic protein immunoreactivity in the rat brain. *Brain Res,* 406**,** 348-51.

TREMBLAY, G. B., TREMBLAY, A., COPELAND, N. G., GILBERT, D. J., JENKINS, N. A., LABRIE, F. & GIGUERE, V. (1997) Cloning, chromosomal localization, and functional analysis of the murine estrogen receptor beta. *Mol Endocrinol,* 11**,** 353-65.

TROPEL, P., PLATET, N., PLATEL, J. C., NOEL, D., ALBRIEUX, M., BENABID, A. L. & BERGER, F. (2006) Functional neuronal differentiation of bone marrow-derived mesenchymal stem cells. *Stem Cells,* 24**,** 2868-76.

TSUCHIYA, D., HONG, S., KAYAMA, T., PANTER, S. S. & WEINSTEIN, P. R. (2003) Effect of suture size and carotid clip application upon blood flow and infarct volume after permanent and temporary middle cerebral artery occlusion in mice. *Brain Res,* 970**,** 131-9.

TUREYEN, K., VEMUGANTI, R., SAILOR, K. A. & DEMPSEY, R. J. (2004) Infarct volume quantification in mouse focal cerebral ischemia: a comparison of triphenyltetrazolium chloride and cresyl violet staining techniques. *J Neurosci Methods,* 139**,** 203-7.

UNTERBERG, A. W., STOVER, J., KRESS, B. & KIENING, K. L. (2004) Edema and brain trauma. *Neuroscience,* 129**,** 1021-9.

VAN DER WORP, H. B. & VAN GIJN, J. (2007) Clinical practice. Acute ischemic stroke. *N Engl J Med,* 357**,** 572-9.

VEGETO, E., BELCREDITO, S., ETTERI, S., GHISLETTI, S., BRUSADELLI, A., MEDA, C., KRUST, A., DUPONT, S., CIANA, P., CHAMBON, P. & MAGGI, A. (2003) Estrogen receptor-alpha mediates the brain antiinflammatory activity of estradiol. *Proc Natl Acad Sci U S A,* 100**,** 9614-9.

VEGETO, E., BENEDUSI, V. & MAGGI, A. (2008) Estrogen anti-inflammatory activity in brain: a therapeutic opportunity for menopause and neurodegenerative diseases. *Front Neuroendocrinol,* 29**,** 507-19.

VEGETO, E., BONINCONTRO, C., POLLIO, G., SALA, A., VIAPPIANI, S., NARDI, F., BRUSADELLI, A., VIVIANI, B., CIANA, P. & MAGGI, A. (2001) Estrogen prevents the lipopolysaccharide-induced inflammatory response in microglia. *J Neurosci,* 21**,** 1809-18.

VEGETO, E., SHAHBAZ, M. M., WEN, D. X., GOLDMAN, M. E., O'MALLEY, B. W. & MCDONNELL, D. P. (1993) Human progesterone receptor A form is a cell- and promoter-specific repressor of human progesterone receptor B function. *Mol Endocrinol,* 7**,** 1244-55.

VEIZOVIC, T., BEECH, J. S., STROEMER, R. P., WATSON, W. P. & HODGES, H. (2001) Resolution of stroke deficits following contralateral grafts of conditionally immortal neuroepithelial stem cells. *Stroke,* 32**,** 1012-9.

VENKOV, C. D., RANKIN, A. B. & VAUGHAN, D. E. (1996) Identification of authentic estrogen receptor in cultured endothelial cells. A potential mechanism for steroid hormone regulation of endothelial function. *Circulation,* 94**,** 727-33.

VERGOUWEN, M. D., ANDERSON, R. E. & MEYER, F. B. (2000) Gender differences and the effects of synthetic exogenous and non-synthetic estrogens in focal cerebral ischemia. *Brain Res,* 878**,** 88-97.

VILHARDT, F. (2005) Microglia: phagocyte and glia cell. *Int J Biochem Cell Biol,* 37**,** 17-21.

VIRLEY, D., RIDLEY, R. M., SINDEN, J. D., KERSHAW, T. R., HARLAND, S., RASHID, T., FRENCH, S., SOWINSKI, P., GRAY, J. A., LANTOS, P. L. & HODGES, H. (1999) Primary CA1 and conditionally immortal MHP36 cell grafts restore conditional discrimination learning and recall in marmosets after excitotoxic lesions of the hippocampal CA1 field. *Brain,* 122 (Pt 12)**,** 2321-35.

VISCOLI, C. M., BRASS, L. M., KERNAN, W. N., SARREL, P. M., SUISSA, S. & HORWITZ, R. I. (2001) A clinical trial of estrogen-replacement therapy after ischemic stroke. *N Engl J Med,* 345**,** 1243-9.

VON KUMMER, R., FORSTING, M., WILDEMANN, B. & SARTOR, K. (1993) [Thrombolysis in acute cerebral ischemia]. *Aktuelle Radiol,* 3**,** 351-5.

WAHLSTEN, D., METTEN, P. & CRABBE, J. C. (2003) A rating scale for wildness and ease of handling laboratory mice: results for 21 inbred strains tested in two laboratories. *Genes Brain Behav,* 2**,** 71-9.

WALBERER, M., STOLZ, E., MULLER, C., FRIEDRICH, C., ROTTGER, C., BLAES, F., KAPS, M., FISHER, M., BACHMANN, G. & GERRIETS, T. (2006) Experimental stroke: ischaemic lesion volume and oedema formation differ among rat strains (a comparison between Wistar and Sprague-Dawley rats using MRI). *Lab Anim,* 40**,** 1-8.

WANG, G., BHATTACHARYYA, N., WILKERSON, C., RAMSAMMY, R. A., EATMAN, E. & ANDERSON, W. A. (1994) Estrogen induced peroxidase secretion from the endometrial epithelium: a possible function for the luminal enzyme. *J Submicrosc Cytol Pathol,* 26**,** 405-14.

WANG, J., GREEN, P. S. & SIMPKINS, J. W. (2001a) Estradiol protects against ATP depletion, mitochondrial membrane potential decline and the generation of reactive oxygen species induced by 3-nitroproprionic acid in SK-N-SH human neuroblastoma cells. *J Neurochem,* 77**,** 804-11.

WANG, Q., SANTIZO, R., BAUGHMAN, V. L., PELLIGRINO, D. A. & IADECOLA, C. (1999) Estrogen provides neuroprotection in transient forebrain ischemia through perfusion-independent mechanisms in rats. *Stroke,* 30**,** 630-7.

WANG, X., TSUJI, K., LEE, S. R., NING, M., FURIE, K. L., BUCHAN, A. M. & LO, E. H. (2004) Mechanisms of hemorrhagic transformation after tissue plasminogen activator reperfusion therapy for ischemic stroke. *Stroke,* 35**,** 2726-30.

WANG, Z. J., JEFFS, B., ITO, M., ACHERMANN, J. C., YU, R. N., HALES, D. B. & JAMESON, J. L. (2001b) Aromatase (Cyp19) expression is up-regulated by targeted disruption of Dax1. *Proc Natl Acad Sci U S A,* 98**,** 7988-93.

WASSERTHEIL-SMOLLER, S., HENDRIX, S. L., LIMACHER, M., HEISS, G., KOOPERBERG, C., BAIRD, A., KOTCHEN, T., CURB, J. D., BLACK, H., ROSSOUW, J. E., ARAGAKI, A., SAFFORD, M., STEIN, E., LAOWATTANA, S. & MYSIW, W. J. (2003) Effect of estrogen plus progestin on stroke in postmenopausal women: the Women's Health Initiative: a randomized trial. *JAMA,* 289**,** 2673-84.

WATTERS, J. J., CAMPBELL, J. S., CUNNINGHAM, M. J., KREBS, E. G. & DORSA, D. M. (1997) Rapid membrane effects of steroids in neuroblastoma cells: effects of estrogen on mitogen activated protein kinase signalling cascade and c-fos immediate early gene transcription. *Endocrinology,* 138**,** 4030-3.

WECHSLER, L. R. (2004) Stem cell transplantation for stroke. *Cleve Clin J Med,* 71 Suppl 1**,** S40-1.

WECHSLER, L. R. & KONDZIOLKA, D. (2003) Cell therapy: replacement. *Stroke,* 34**,** 2081-2.

WERNIG, M., BENNINGER, F., SCHMANDT, T., RADE, M., TUCKER, K. L., BUSSOW, H., BECK, H. & BRUSTLE, O. (2004) Functional integration of embryonic stem cell-derived neurons in vivo. *J Neurosci,* 24**,** 5258-68.

WERNIG, M., ZHAO, J. P., PRUSZAK, J., HEDLUND, E., FU, D., SOLDNER, F., BROCCOLI, V., CONSTANTINE-PATON, M., ISACSON, O. & JAENISCH, R. (2008) Neurons derived from reprogrammed fibroblasts functionally integrate into the fetal brain and improve symptoms of rats with Parkinson's disease. *Proc Natl Acad Sci U S A,* 105**,** 5856-61.

WHISHAW, I. Q., LI, K., WHISHAW, P. A., GORNY, B. & METZ, G. A. (2003) Distinct forelimb and hind limb stepping impairments in unilateral dopamine-depleted rats: use of the rotorod as a method for the qualitative analysis of skilled walking. *J Neurosci Methods,* 126**,** 13-23.

WHITE, M. M., ZAMUDIO, S., STEVENS, T., TYLER, R., LINDENFELD, J., LESLIE, K. & MOORE, L. G. (1995a) Estrogen, progesterone, and vascular reactivity: potential cellular mechanisms. *Endocr Rev,* 16**,** 739-51.

WHITE, R. E., DARKOW, D. J. & LANG, J. L. (1995b) Estrogen relaxes coronary arteries by opening BKCa channels through a cGMP-dependent mechanism. *Circ Res,* 77**,** 936-42.

WIDMANN, R., KUROIWA, T., BONNEKOH, P. & HOSSMANN, K. A. (1991) [14C]leucine incorporation into brain proteins in gerbils after transient ischemia: relationship to selective vulnerability of hippocampus. *J Neurochem,* 56**,** 789-96.

WILLING, A. E., VENDRAME, M., MALLERY, J., CASSADY, C. J., DAVIS, C. D., SANCHEZ-RAMOS, J. & SANBERG, P. R. (2003) Mobilized peripheral blood cells administered intravenously produce functional recovery in stroke. *Cell Transplant,* 12**,** 449-54.

WISDEN, W. & SEEBURG, P. H. (1993) Mammalian ionotropic glutamate receptors. *Curr Opin Neurobiol,* 3**,** 291-8.

WISE, P. M., DUBAL, D. B., WILSON, M. E., RAU, S. W. & BOTTNER, M. (2001) Minireview: neuroprotective effects of estrogen-new insights into mechanisms of action. *Endocrinology,* 142**,** 969-73.

WONG, A. M., HODGES, H. & HORSBURGH, K. (2005) Neural stem cell grafts reduce the extent of neuronal damage in a mouse model of global ischaemia. *Brain Res,* 1063**,** 140-50.

WONG, M. & MOSS, R. L. (1992) Long-term and short-term electrophysiological effects of estrogen on the synaptic properties of hippocampal CA1 neurons. *J Neurosci,* 12**,** 3217-25.

WOOLLEY, C. S., GOULD, E., FRANKFURT, M. & MCEWEN, B. S. (1990) Naturally occurring fluctuation in dendritic spine density on adult hippocampal pyramidal neurons. *J Neurosci,* 10**,** 4035-9.

WOOLLEY, C. S., WEILAND, N. G., MCEWEN, B. S. & SCHWARTZKROIN, P. A. (1997) Estradiol increases the sensitivity of hippocampal CA1 pyramidal cells to NMDA receptor-mediated synaptic input: correlation with dendritic spine density. *J Neurosci,* 17**,** 1848-59.

WURMSER, A. E., NAKASHIMA, K., SUMMERS, R. G., TONI, N., D'AMOUR, K. A., LIE, D. C. & GAGE, F. H. (2004) Cell fusion-independent differentiation of neural stem cells to the endothelial lineage. *Nature,* 430**,** 350-6.

WYCKOFF, M. H., CHAMBLISS, K. L., MINEO, C., YUHANNA, I. S., MENDELSOHN, M. E., MUMBY, S. M. & SHAUL, P. W. (2001) Plasma membrane estrogen receptors are coupled to endothelial nitric-oxide synthase through Galpha(i). *J Biol Chem,* 276**,** 27071-6.

XU, D., ALIPIO, Z., FINK, L. M., ADCOCK, D. M., YANG, J., WARD, D. C. & MA, Y. (2009) Phenotypic correction of murine hemophilia A using an iPS cell-based therapy. *Proc Natl Acad Sci U S A,* 106**,** 808-13.

YAMASHITA, T., KAWAI, H., TIAN, F., OHTA, Y. & ABE, K. Tumorigenic Development of Induced Pluripotent Stem Cells in Ischemic Mouse Brain. *Cell Transplant*.

YAMASHITA, T., NINOMIYA, M., HERNANDEZ ACOSTA, P., GARCIA-VERDUGO, J. M., SUNABORI, T., SAKAGUCHI, M., ADACHI, K., KOJIMA, T., HIROTA, Y., KAWASE, T., ARAKI, N., ABE, K., OKANO, H. & SAWAMOTO, K. (2006) Subventricular zone-derived neuroblasts migrate and differentiate into mature neurons in the post-stroke adult striatum. *J Neurosci,* 26**,** 6627-36.

YANG, G., KITAGAWA, K., MATSUSHITA, K., MABUCHI, T., YAGITA, Y., YANAGIHARA, T. & MATSUMOTO, M. (1997) C57BL/6 strain is most susceptible to cerebral ischemia following bilateral common carotid occlusion among seven mouse strains: selective neuronal death in the murine transient forebrain ischemia. *Brain Res,* 752**,** 209-18.

YENARI, M. A., KAUPPINEN, T. M. & SWANSON, R. A. (2010) Microglial activation in stroke: therapeutic targets. *Neurotherapeutics,* 7**,** 378-91.

YIHUA AN, K. K. S. T. A. H. Z. (2006) Potential of stem cell based therapy and tissue engineering in the regeneration of the central nervous system. *Biomed. Mater.,* 1 R38–R44.

YOON, Y. S., WECKER, A., HEYD, L., PARK, J. S., TKEBUCHAVA, T., KUSANO, K., HANLEY, A., SCADOVA, H., QIN, G., CHA, D. H., JOHNSON, K. L., AIKAWA, R., ASAHARA, T. & LOSORDO, D. W. (2005) Clonally expanded

novel multipotent stem cells from human bone marrow regenerate myocardium after myocardial infarction. *J Clin Invest,* 115**,** 326-38.

YOUMAN, P., WILSON, K., HARRAF, F. & KALRA, L. (2003) The economic burden of stroke in the United Kingdom. *Pharmacoeconomics,* 21 Suppl 1**,** 43-50.

YU, J., VODYANIK, M. A., SMUGA-OTTO, K., ANTOSIEWICZ-BOURGET, J., FRANE, J. L., TIAN, S., NIE, J., JONSDOTTIR, G. A., RUOTTI, V., STEWART, R., SLUKVIN, II & THOMSON, J. A. (2007) Induced pluripotent stem cell lines derived from human somatic cells. *Science,* 318**,** 1917-20.

ZAMANI, M. R., LEVY, W. B. & DESMOND, N. L. (2004) Estradiol increases delayed, N-methyl-D-aspartate receptor-mediated excitation in the hippocampal CA1 region. *Neuroscience,* 129**,** 243-54.

ZAZOPOULOS, E., LALLI, E., STOCCO, D. M. & SASSONE-CORSI, P. (1997) DNA binding and transcriptional repression by DAX-1 blocks steroidogenesis. *Nature,* 390**,** 311-5.

ZHANG, H., THOMSEN, J. S., JOHANSSON, L., GUSTAFSSON, J. A. & TREUTER, E. (2000) DAX-1 functions as an LXXLL-containing corepressor for activated estrogen receptors. *J Biol Chem,* 275**,** 39855-9.

ZHANG, Y. Q., SHI, J., RAJAKUMAR, G., DAY, A. L. & SIMPKINS, J. W. (1998) Effects of gender and estradiol treatment on focal brain ischemia. *Brain Res,* 784**,** 321-4.

ZHANG, Z. G., ZHANG, L., JIANG, Q. & CHOPP, M. (2002) Bone marrow-derived endothelial progenitor cells participate in cerebral neovascularization after focal cerebral ischemia in the adult mouse. *Circ Res,* 90**,** 284-8.

ZHAO, C., TORESSON, G., XU, L., KOEHLER, K. F., GUSTAFSSON, J. A. & DAHLMAN-WRIGHT, K. (2005) Mouse estrogen receptor beta isoforms exhibit differences in ligand selectivity and coactivator recruitment. *Biochemistry,* 44**,** 7936-44.

ZHAO, L. R., DUAN, W. M., REYES, M., KEENE, C. D., VERFAILLIE, C. M. & LOW, W. C. (2002) Human bone marrow stem cells exhibit neural phenotypes and ameliorate neurological deficits after grafting into the ischemic brain of rats. *Exp Neurol,* 174**,** 11-20.

ZWAIN, I. H. & YEN, S. S. (1999) Neurosteroidogenesis in astrocytes, oligodendrocytes, and neurons of cerebral cortex of rat brain. *Endocrinology,* 140**,** 3843-52.